

# ULRR

## Cloning and expression of *Zymobacter palmae* pyruvate decarboxylase for enhanced ethanol production in the cyanobacterium *Synechocystis* sp. PCC 6803

Item Type	Thesis
Authors	Quinn, Lorraine
Download date	2026-05-20 14:23:43
Item License	<a href="https://creativecommons.org/licenses/by-nc-sa/1.0/">https://creativecommons.org/licenses/by-nc-sa/1.0/</a>
Link to Item	<a href="https://hdl.handle.net/10344/6116">https://hdl.handle.net/10344/6116</a>



**UNIVERSITY of LIMERICK**

**OLLSCOIL LUIMNIGH**

**Cloning and Expression of *Zymobacter palmae* pyruvate  
decarboxylase for enhanced ethanol production in the  
cyanobacterium *Synechocystis* sp. PCC 6803**

**Lorraine Quinn B.Sc.**

**Project supervised by Prof. J. Tony Pembroke, Dr. Patricia Armshaw, Prof.  
Tewfik Soulimane and Dr. Con Sheahan.**

A thesis submitted to the University of Limerick in candidature for the degree of  
Masters of Science. Submitted to the University of Limerick.



## Abstract

### **Cloning and Expression of *Zymobacter palmae* pyruvate decarboxylase for enhanced ethanol production in the cyanobacterium *Synechocystis* sp. PCC 6803.**

Lorraine Quinn

Recently, photoautotrophic cyanobacteria have gained much attention due to their ability to convert carbon dioxide using light energy into carbon metabolites, some with potential biofuel applications. This is significant due to the sustainable nature of production and the global limitation of fossil fuels in the future. Model organisms such as *Synechocystis* sp. PCC 6803 have been described as “cell factories” for this reason and can be genetically modified and manipulated to produce compounds such as ethanol. It was decided to construct a recombinant strain of *Synechocystis* 6803 expressing a *Zymomonas mobilis* pyruvate decarboxylase (*pdh*) and an alcohol dehydrogenase (*adh*) native to *Synechocystis* 6803 which is capable of autotrophic conversion of pyruvate to ethanol.

In an attempt to improve ethanol yield it was hypothesised that utilising a PDC with a reported lower  $K_m$  might improve flux to ethanol and have identified and utilised a novel *pdh* gene from *Zymobacter palmae* in this respect.

A pET22b (+) expression vector with a strong T7 promoter was primarily used to overexpress the ZpPDC for enzymatic analysis and purification purposes for potential structural studies. The *pdh* gene from *Zymobacter palmae* was amplified and a codon optimised version was also synthesised. Two constructs were created which contained the native/codon optimised Zppdh and the *adh* native to *Synechocystis* 6803 under the control of the strong light driven pPSBII promoter. These cassette constructs were transformed into wildtype *Synechocystis* 6803 and integration of the cassettes into the polyploidy chromosome at the PSBII neutral site was confirmed via DNA sequencing and PCR screening. Strains confirmed as verified recombinants were then characterised for growth, biomass and ethanol productivity relative to UL004 (expressing the *Zymomonas mobilis pdh*).

Unfortunately and to our surprise, no increase in ethanol production was observed in the fully segregated strains in comparison to UL004, the original production strain expressing the ZmPDC despite testing a number of different segregants and utilising repeated assays. Although there may in fact be several reasons for this it was hypothesised that the ZpPDC may be less compatible than the ZmPDC in terms of its pH optimum, functional linkage to the native ADH or just sensitivity to ethanol. Going forward, it may be worthwhile focusing on other PDC enzymes from organisms such as *Gluconacetobacter diazotrophicus* or *Gluconobacter oxydans* which have recently been reported to display even lower  $K_m$  values than the PDC from *Zymobacter palmae*.

## **Declaration**

I hereby declare that the work detailed in this thesis is the results of my own investigations. No part of this work has been or is being submitted in candidature for any other degree.

---

Lorraine Quinn

---

Date

## List of Publications

- Armshaw, P., Carey, D., Quinn, L., Sheahan, C. and Pembroke, J.T. (2015) 'Optimisation of ethanol production in *Synechocystis* PCC 6803, the DEMA approach.', in *1st International Solar Fuels Conference (ISF-1)*, Uppsala, Sweden, April 26th-May 1st 2015, University of Limerick.
- Carey, D., Armshaw, P., Quinn, L., Sheahan, C. and Pembroke, J.T. (2015) 'Phenotypical analysis of different strains of *Synechocystis* sp. PCC 6803 for determination of the optimal strain for ethanol production', in *Society for General Microbiology: Irish Division Meeting: Microbial Interfaces*, NUIG, Galway, 17th-19th June 2015, University of Limerick.
- Manuscript in preparation for *Biotechnology Letters*, 'The pyruvate decarboxylase from *Zymomonas mobilis* out performs that of *Zymobacter palmae* for ethanol production in metabolic engineered *Synechocystis* sp. PCC 6803', Quinn, L., Armshaw, P., Soulimane, T., Sheahan, C. and Pembroke, J.T.
- Pembroke, J.T., Quinn, L., O' Riordan, H. and Armshaw, P. (2017) 'Ethanol Production in Cyanobacteria: Impact of Omics of the Model Organism *Synechocystis* on Yield Enhancement' in Los, D. A., ed., *Cyanobacteria: Omics and Manipulation*, Norfolk, UK: Caister Academic Press, 200-217.
- Quinn, L., Armshaw, P., Carey, D., Sheahan, C. and Pembroke, J.T. (2015) 'Kinetic optimisation of the pyruvate decarboxylase from *Zymomonas mobilis* to maximise ethanol productivity in the cyanobacterium *Synechocystis* sp. PCC 6803', in *Society for General Microbiology: Irish Division Meeting: Microbial Interfaces*, NUIG, Galway, 17-19th of June 2015, University of Limerick.

## **Acknowledgements**

First of all I would like to sincerely thank Dr. Patricia Armshaw for her continued support and guidance over the last two years as both a supervisor and friend. Without her help and patience the completion of this work would not have been possible. I am eternally grateful.

To Professor Tony Pembroke for his words of wisdom and supervision throughout this project and my undergraduate degree. Words cannot express how thankful I am and I will always remember the anecdotes as well as the advice.

To Professor Tewfik Soulimane for his advice and help as I progressed from strength to strength (I think) in my knowledge of proteins and also in my undergraduate years. For his persistence in convincing me to continue in research and for the belief that I could achieve something great. For that I thank you.

To Dr. Michael Ryan for all his help and guidance at the final hurdle. The finishing touches made all the difference and I can be truly proud of what I've written thanks to your knowledge and expertise.

To all of the staff in the CES department who assisted me with my work throughout the years, notably Sinéad, Brian, Ciara, Miriam and Maria. Your continued support will never be forgotten. Also a huge thank you to Dr. Fintan Bracken in the UL Glucksman Library for all his help in the final stages.

I too would like to gratefully thank Dr. Con Sheahan and all in the DEMA consortium with a special word of thanks to Davide Montesarchio for all his help and advice. Also to DEMA for funding my research.

To all in L2-007. Not all of us may have worked together but I still looked on you as my science family. Wishing you all the best in the future wherever it may take you and I hope we can stay in contact and continue to socialise as the years move on.

To my fellow lab friends Kevin and Helen. Where would I be without your friendship and support? I truly wish you both the very best of luck as you continue with your studies and I know that you will do great! I'll never forget the craic and banter of A2-005. Memories forever.

To my close Industrial Biochemistry friend Michael. For all your help throughout the past six years, I cannot thank you enough. Never were you too busy to lend a hand when I was in need of advice or a miracle. Wishing you luck and success in the years ahead.

To my parents Margaret and Liam and my sister Rachel. Thank you for all the love and support over the past six years, for putting up with the mood swings and tantrums. I don't think I was as bad for the second degree but then again I could be wrong. All that you have done will never be forgotten.

# Table of Contents

<b>Abstract</b> .....	iii
<b>Declaration</b> .....	iv
<b>List of Publications</b> .....	v
<b>Acknowledgements</b> .....	vi
<b>Table of Contents</b> .....	viii
<b>List of Figures</b> .....	xiii
<b>List of Tables</b> .....	xvii
<b>List of Abbreviations</b> .....	xix
<b>Units of Measurement</b> .....	xxii
<b>Chapter 1: Introduction</b> .....	2
1.1 Biofuel necessity.....	3
1.1.1 First, second and third generation biofuels .....	3
1.2 Cyanobacteria: Model organisms .....	5
1.2.1 <i>Synechocystis</i> sp. PCC 6803 .....	7
1.2.2 Ploidy levels.....	8
1.2.3 Cultivation.....	9
1.3 Ethanol Production Pathway.....	10
1.4 Pyruvate decarboxylase enzyme (PDC).....	14
1.4.1 PDC mechanism of action .....	15
1.4.2 PDC cofactor: ThDp .....	15
1.4.3 <i>Zymomonas mobilis</i> PDC.....	16
1.4.4 Other PDC enzymes.....	19
1.5 <i>Zymomonas mobilis</i> alcohol dehydrogenase enzyme (ADH).....	22
1.5.1 <i>Synechocystis</i> sp. PCC 6803 native ADH.....	23
1.6 Methods to enhance ethanol production in cyanobacteria .....	25
1.6.1 Gene Dosage .....	25
1.6.2 Utilising small native plasmids.....	26
1.6.3 Pyruvate diversion towards ethanol pathway .....	27
1.6.4 Pathway knock out.....	27
1.6.5 Promoters .....	28
1.6.6 Fusion of <i>pdh</i> and <i>adh</i> genes.....	29
1.6.7 Increase in carbon uptake.....	30

1.7 Ethanol tolerance .....	30
1.8 Pembroke Lab Strains .....	31
1.8.1 UL004.....	32
1.8.2 UL030.....	33
<b>1.9 Aim of this study.....</b>	<b>35</b>
<b>Chapter 2: Materials and Methods.....</b>	<b>37</b>
2.1 Media and bacterial strains.....	38
2.2 Plates, overnight cultures, bacterial stocks and antibiotics .....	38
2.3 Cloning Methods .....	39
2.3.1 Template preparation.....	39
2.3.2 Traditional Cloning .....	39
2.3.2.1 Restriction Analysis .....	40
2.3.3 Clontech In-Fusion Cloning.....	40
2.3.4 Agarose gels for DNA analysis .....	41
2.3.5 Plasmid extraction and PCR clean-up .....	41
2.3.6 DNA sequencing .....	41
2.4 Transformation .....	41
2.4.1 Transformation into <i>E.coli</i> .....	41
2.4.2 Transformation into <i>Synechocystis</i> sp. PCC 6803.....	42
2.5 Ethanol Determination .....	44
2.6 Expression and Purification of <i>Zymobacter palmae</i> PDC.....	45
2.6.1 Expression .....	45
2.6.2 ZpPDC Purification.....	45
2.6.2.1 Preparation of column .....	46
2.6.2.2 IMAC purification.....	46
2.6.3 SDS-PAGE gel and Western blot analysis.....	46
2.6.3.1 SDS-PAGE.....	46
2.6.3.2 Western blots.....	47
2.6.4 Dialysis.....	48
2.6.5 Protein concentration.....	48
2.6.6 Regeneration of the column .....	48
2.7 Crystallisation trials.....	49
2.7.1 Initial crystallisation trials .....	49
2.7.2 Follow on crystallisation trials .....	50

2.7.3 Homology Modelling.....	51
2.7.3.1 Other programs used as part of this project .....	52
2.8 OD <sub>730nm</sub> and enzyme activity determination.....	53
2.9 Activity assays .....	53
2.9.1 Activity assay with <i>Saccharomyces cerevisiae</i> PDC.....	54
2.9.2 Preparation of <i>E.coli</i> CFE with Zm/ZpPDCs .....	55
2.9.2.1 Activity assay to determine a fixed protein concentration for future assays using <i>E.coli</i> CFE with ZmPDC.....	55
2.9.2.2 Activity assay using a fixed protein concentration of <i>E.coli</i> CFE with Zm and ZpPDC.....	56
2.9.3 Activity assay with <i>Synechocystis</i> sp. PCC 6803 CFE.....	58
2.9.3.1 Lysis analysis of <i>Synechocystis</i> sp. PCC 6803 cells prior to activity assay .....	58
2.9.3.2 Activity assay with <i>Synechocystis</i> sp. PCC 6803 CFE at different pH values .....	59
<b>Chapter 3: Results and Discussion .....</b>	<b>60</b>
3.1 Choosing a different PDC.....	61
3.2 Cloning into the pET22b (+) vector.....	64
3.2.1 Creation of pULLQ1: <i>Zmpdc</i> in pET22b (+) .....	64
3.2.2 Creation of pULLQ2: <i>Zppdc</i> in pET22b (+).....	66
3.2.3 Creation of pULLQ3: <i>ZpOpdc</i> in pET22b (+).....	71
3.3 Activity assays .....	71
3.3.1 Activity assay with <i>Saccharomyces cerevisiae</i> PDC.....	72
3.3.2 Activity assay to determine a fixed [protein] for future assays using <i>E.coli</i> CFE with ZmPDC.....	74
3.3.3 Activity assay using a fixed [protein] of <i>E.coli</i> CFE with Zm and ZpPDC .....	75
3.3.3.1 <i>E.coli</i> CFE with ZmPDC .....	76
3.3.3.2 <i>E.coli</i> CFE with ZpPDC .....	79
3.4 Cloning into the PSBAII vector.....	84
3.4.1 Creation of pUL101: <i>Zppdc</i> in PSBAII.....	84
3.4.2 Creation of pUL102: <i>ZpOpdc</i> in PSBAII .....	85
3.5 Transformation into <i>Synechocystis</i> sp. PCC 6803 .....	87
3.5.1 PCR screening to verify fully segregated strains.....	89
3.5.2 DNA sequencing to verify fully segregated strains .....	101
3.6 Ethanol Determination.....	101

3.6.1 Strains tested for ethanol production .....	104
3.6.2 OD <sub>730nm</sub> and ethanol results for tested strains .....	108
3.7 Activity assay with <i>Synechocystis</i> sp. PCC 6803 CFE .....	115
3.7.1 Lysis analysis of <i>Synechocystis</i> sp. PCC 6803 cells prior to activity assay .....	115
3.8 Purification of <i>Zymobacter palmae</i> PDC .....	121
3.8.1 Protein visualisation .....	122
3.8.2 Dialysis .....	126
3.8.3 Concentration .....	127
3.8.4 SEC.....	128
3.9 Crystallisation trials.....	128
3.9.1 Initial trials .....	129
3.9.2 Follow on trials.....	129
3.9.3 Published data.....	130
3.10 Homology Modelling .....	131
3.11 Activity assay with purified ZpPDC .....	134
3.11.1 Activity assay to determine a fixed [protein] of purified ZpPDC for future assays.....	134
3.11.2 Activity assay using a fixed [protein] of purified ZpPDC at different pH values.....	134
<b>Conclusion</b> .....	139
<b>Bibliography</b> .....	142
<b>Appendices</b> .....	161
<b>Appendix I</b> .....	161
<b>Appendix I A</b> .....	161
<b>Appendix I B</b> .....	161
<b>Appendix II</b> .....	163
<b>Appendix III</b> .....	165
<b>Appendix III A</b> .....	165
<b>Appendix III B</b> .....	166
<b>Appendix III C</b> .....	166
<b>Appendix III D</b> .....	167
<b>Appendix III E</b> .....	168

<b>Appendix IV</b> .....	169
<b>Appendix IV A</b> .....	169
<b>Appendix IV B</b> .....	170

## List of Figures

<b>Figure 1.1:</b> Summary of First Generation Biofuels.....	4
<b>Figure 1.2:</b> Summary of Second Generation Biofuels .....	4
<b>Figure 1.3:</b> Summary of Third Generation Biofuels .....	5
<b>Figure 1.4:</b> Metabolically engineered pathways in cyanobacteria .....	13
<b>Figure 1.5:</b> Overview of the major metabolic pathways in cyanobacteria.....	27
<b>Figure 1.6:</b> Flow diagram of pUL004 .....	32
<b>Figure 1.7:</b> pUL004 .....	33
<b>Figure 1.8:</b> pUL030 .....	34
<b>Figure 1.9:</b> Summary diagram representing the nature of the cassette constructs in the constructed strains UL004 and UL030.....	35
<b>Figure 2.1:</b> Example of the plate set up used for the Initial Index Screen (initial trials).....	50
<b>Figure 2.2:</b> Example of the plate set up used for the Optimised Index Screen (follow on trials).....	51
<b>Figure 3.1:</b> Clustal alignment of the <i>Zymobacter palmae</i> and <i>Zymomonas mobilis</i> PDC enzymes .....	62
<b>Figure 3.2:</b> Clustal alignment of the 6 bacterial PDC enzymes in Sv, Go, Zm, Gd, Zp and Ap.....	63
<b>Figure 3.3:</b> pULLQ1.....	66
<b>Figure 3.4:</b> BLAST n alignment of the <i>Zppdc</i> sequencing results showing the first mutation .....	68
<b>Figure 3.5:</b> BLAST n alignment of the <i>Zppdc</i> sequencing results showing the second mutation.....	68
<b>Figure 3.6:</b> pULLQ2.....	69
<b>Figure 3.7:</b> Diagrammatic representation of the Clontech In-Fusion® HD cloning protocol.....	70
<b>Figure 3.8:</b> pULLQ3.....	71
<b>Figure 3.9:</b> Michaelis-Menten graph for the <i>Saccharomyces cerevisiae</i> PDC activity assay, plate 1 (all blank wells and all test wells together).....	73

<b>Figure 3.10:</b> Michaelis-Menten graph for the <i>Saccharomyces cerevisiae</i> PDC activity assay, plate 2 (alternating blank and test wells).....	74
<b>Figure 3.11:</b> Michaelis-Menten graph for <i>E.coli</i> CFE with ZmPDC.....	77
<b>Figure 3.12:</b> Lineweaver-Burk plot for <i>E.coli</i> CFE with ZmPDC.....	78
<b>Figure 3.13:</b> Michaelis-Menten graph for <i>E.coli</i> CFE with ZpPDC.....	80
<b>Figure 3.14:</b> Lineweaver-Burk plot for <i>E.coli</i> CFE with ZpPDC.....	81
<b>Figure 3.15:</b> pUL101.....	85
<b>Figure 3.16:</b> pUL102.....	86
<b>Figure 3.17:</b> 1% SYBR® safe stained DNA agarose gel from PCR assays of screened UL070 strains (containing <i>Zmpdc</i> ) with 1% glucose and under high light conditions (HL).....	89
<b>Figure 3.18:</b> 1% SYBR® safe stained DNA agarose gel from PCR assays of screened UL071 strains (containing <i>Zppdc</i> ) with 1% glucose and under high light conditions (HL).....	89
<b>Figure 3.19:</b> 1% SYBR® safe stained DNA agarose gel from PCR assays of screened UL072 strains (containing <i>ZpOpdc</i> ) with 1% glucose and under high light conditions (HL).....	90
<b>Figure 3.20:</b> 1% SYBR® safe stained DNA agarose gel from PCR assays of screened UL070 strains (containing <i>Zmpdc</i> ) with 1% glucose and under low light conditions (LL) .....	90
<b>Figure 3.21:</b> 1% SYBR® safe stained DNA agarose gel from PCR assays of screened UL071 strains (containing <i>Zppdc</i> ) with 1% glucose and under low light conditions (LL) .....	91
<b>Figure 3.22:</b> 1% SYBR® safe stained DNA agarose gel from PCR assays of screened UL072 strains (containing <i>ZpOpdc</i> ) with 1% glucose and under low light conditions (LL).....	91
<b>Figure 3.23:</b> Gel 1: 1% SYBR® safe stained DNA agarose gel from PCR assays of screened strains which had previously shown to be fully segregated but reverted back to a semi-segregated state.....	92
<b>Figure 3.24:</b> Gel 2: 1% SYBR® safe stained DNA agarose gel from PCR assays of screened strains which had previously been shown to be fully segregated but reverted back to a semi-segregated state.....	94
<b>Figure 3.25:</b> 1% SYBR® safe stained DNA agarose gel from PCR assays of screened samples with no glucose under high and low light conditions .....	95

<b>Figure 3.26:</b> Gel 1: 1% SYBR® safe stained DNA agarose gel from PCR assays of fully segregated strains which were brought back from a semi-segregated state .....	96
<b>Figure 3.27:</b> Gel 2: 1% SYBR® safe stained DNA agarose gel from PCR assays of fully segregated strains which were brought back from a semi-segregated state .....	97
<b>Figure 3.28:</b> Gel 3: 1% SYBR® safe stained DNA agarose gel from PCR assays of fully segregated strains which were brought back from a semi-segregated state .....	98
<b>Figure 3.29:</b> Gel 4: 1% SYBR® safe stained DNA agarose gel from PCR assays of fully segregated strains which were brought back from a semi-segregated state .....	99
<b>Figure 3.30:</b> Principle of the ethanol assay kit .....	101
<b>Figure 3.31:</b> Cultures of wildtype <i>Synechocystis</i> 6803 and UL004 .....	104
<b>Figure 3.32:</b> Independent isolates of UL070 strains .....	105
<b>Figure 3.33:</b> Independent isolates of UL071 strains .....	106
<b>Figure 3.34:</b> Independent isolates of UL072 strains .....	107
<b>Figure 3.35:</b> Flask 1: Independent isolate of a UL070 strain. Flasks 2 and 3: Independent isolates of UL072 strains .....	107
<b>Figure 3.36:</b> Bar chart representation of the OD <sub>730nm</sub> readings of WT, UL070, UL071 and UL072 strains tested for ethanol production .....	110
<b>Figure 3.37:</b> Bar chart representation of ethanol levels in g/L/OD <sub>730nm</sub> for tested WT, UL070, UL071 and UL072 strains on days 0, 3, 7 and 11 .....	113
<b>Figure 3.38:</b> 12% SDS-PAGE gel stained with Instant Blue showing samples of <i>Synechocystis</i> 6803 (WT, UL070, UL071 and UL072) lysed with heat .....	116
<b>Figure 3.39:</b> 12% SDS-PAGE gel stained with Instant Blue showing samples of <i>Synechocystis</i> 6803 (WT, UL070, UL071 and UL072) lysed via bead beating (time variation) and freeze/thaw .....	117
<b>Figures 3.40 and 3.41:</b> Samples 1 and 2 showing lysed WT <i>Synechocystis</i> 6803 and a UL070 strain respectively .....	118
<b>Figures 3.42 and 3.43:</b> Samples 3 and 4 showing lysed UL071 and UL072 strains respectively .....	119

<b>Figure 3.44:</b> 12% SDS-PAGE gel stained with Instant Blue showing samples of <i>Synechocystis</i> 6803 (WT, UL070, UL071 and UL072) lysed via bead beating for 1.5 hours and freeze/thaw for the activity assay .....	120
<b>Figure 3.45:</b> Gel 1: 12% SDS-PAGE gel stained with Instant Blue showing fractions collected during the purification of the ZpPDC.....	122
<b>Figure 3.46:</b> Blot 1: Western blot showing fractions collected during the purification of ZpPDC .....	123
<b>Figure 3.47:</b> Gel 2: 12% SDS-PAGE gel stained with Instant blue showing fractions collected during the purification of the ZpPDC.....	124
<b>Figure 3.48:</b> Blot 2: Western blot showing fractions collected during the purification of the ZpPDC .....	125
<b>Figure 3.49:</b> Chromatogram of the purification process as shown by the Primeview software with the Akta™ prime plus purification system .....	126
<b>Figure 3.50:</b> Dialysis tubing sealed with dialysis tubing clips .....	127
<b>Figure 3.51:</b> Crystals obtained under index screen number 75 (attempt number 1, initial trials).....	129
<b>Figure 3.52:</b> Slightly larger crystals were seen at 1 mg.ml-1 ZpPDC and in the range of 20-25% PEG 3350 (attempt number two, follow on trials).....	130
<b>Figure 3.53:</b> A monomer from the Zm and ZpPDC enzymes superimposed on one another.....	133
<b>Figure 3.54:</b> Active site and surrounding amino acid residues (labelled according to the ZmPDC) in a monomer of the Zm and ZpPDC enzymes superimposed on one another.....	133
<b>Figure 3.55:</b> Close up of the active site and surrounding amino acid residues (labelled according to the ZmPDC) in a monomer of the Zm and ZpPDC enzymes superimposed on one another.....	134
<b>Figure 3.56:</b> Michaelis-Menten graph using purified ZpPDC at pH 6.0 .....	137
<b>Figure 3.57:</b> Michaelis-Menten graph using purified ZpPDC at pH 7.8 .....	137
<b>Figure 3.58:</b> Michaelis-Menten graph using purified ZpPDC at pH 8.2 .....	138

## List of Tables

<b>Table 1.1:</b> Different methods of ethanol production and the amount produced in gal per acre per year .....	6
<b>Table 1.2:</b> Amount of biofuels produced by modified cyanobacteria .....	12
<b>Table 1.3:</b> Characteristics of bacterial PDCs.....	21
<b>Table 2.1:</b> SDS-PAGE gel recipe. ....	47
<b>Table 3.1:</b> Data produced from the assay using <i>E.coli</i> CFE with ZmPDC. ....	76
<b>Table 3.2:</b> Data used to create a Michaelis-Menten graph for <i>E.coli</i> CFE with ZmPDC.....	76
<b>Table 3.3:</b> Data used to create a Lineweaver-Burk graph for <i>E.coli</i> CFE with ZmPDC.....	78
<b>Table 3.4:</b> Data produced from the assay using <i>E.coli</i> CFE with ZpPDC. ....	79
<b>Table 3.5:</b> Data used to create a Michaelis-Menten graph for <i>E.coli</i> CFE with ZpPDC.....	80
<b>Table 3.6:</b> Data used to create a Lineweaver-Burk plot for <i>E.coli</i> CFE with ZpPDC.....	81
<b>Table 3.7:</b> Vmax and Km results for both the Zm and ZpPDCs in <i>E.coli</i> CFE. ...	83
<b>Table 3.8:</b> Constructs used in this study and the created strains. ....	87
<b>Table 3.9:</b> Strains used in ethanol tests. ....	102
<b>Table 3.10:</b> OD <sub>730nm</sub> readings for wildtype <i>Synechocystis</i> 6803 on days 0, 3, 7 and 11.....	108
<b>Table 3.11:</b> OD <sub>730nm</sub> readings for independent isolates of UL070 strains on days 0, 3, 7 and 11 as well as the average readings and standard deviation.....	108
<b>Table 3.12:</b> OD <sub>730nm</sub> readings for independent isolates of UL071 strains on days 0, 3, 7 and 11 as well as the average readings and standard deviation.....	108
<b>Table 3.13:</b> OD <sub>730nm</sub> readings for independent isolates of UL072 strains on days 0, 3, 7 and 11 as well as the average readings and standard deviation.....	109
<b>Table 3.14:</b> Combined OD <sub>730nm</sub> readings for wildtype <i>Synechocystis</i> 6803 and UL070, UL071 and UL072 strains (average readings) as well as standard deviation. ....	109

<b>Table 3.15:</b> Ethanol levels in g/L/OD <sub>730nm</sub> for independent isolates of UL070 strains on days 0, 3, 7 and 11 as well as average levels, standard deviation and 90% confidence intervals (CI). .....	111
<b>Table 3.16:</b> Ethanol levels in g/L/OD <sub>730nm</sub> for independent isolates of UL071 strains on days 0, 3, 7 and 11 as well as average levels, standard deviation and 90% confidence intervals (CI). .....	111
<b>Table 3.17:</b> Ethanol levels in g/L/OD <sub>730nm</sub> for independent isolates of UL072 strains on days 0, 3, 7 and 11 as well as average levels, standard deviation and 90% confidence intervals (CI). .....	111
<b>Table 3.18:</b> Combined ethanol levels in g/L/OD <sub>730nm</sub> for wildtype <i>Synechocystis</i> 6803 and strains UL070, UL071 and UL072 (average readings) as well as standard deviation. ....	112
<b>Table 3.19:</b> Active site and surrounding amino acid residues in one monomer of the Zm and ZpPDC enzymes. ....	132
<b>Table 3.20:</b> Data gathered from the activity assay using a buffer at three different pH values: 6.0, 7.8 and 8.2.....	136

## List of Abbreviations

aa	amino acid
<i>adhA</i> (slr1192)	alcohol dehydrogenase gene native to <i>Synechocystis</i> 6803
<i>adhII/B</i>	alcohol dehydrogenase gene from <i>Zymomonas mobilis</i>
ADH	Alcohol dehydrogenase protein from <i>Synechocystis</i> 6803
ADHII	Alcohol dehydrogenase protein from <i>Zymomonas mobilis</i>
ADP	Adenosine diphosphate
Al-DH	Aldehyde dehydrogenase
Ap	<i>Acetobacter pasteurianus</i>
ATCC	American Type Culture Collection
ATP	Adenosine triphosphate
BG-11 media	blue green media
BLAST	Basic Local Alignment Search Tool
Ca	calcium
CCM	Carbon Concentrating Mechanism
CFE	cell free extract
CI	Confidence Interval
CO <sub>2</sub>	carbon dioxide
CV	column volume
Δ	delta
DIC	dissolved inorganic carbon
DMSO	dimethyl sulfoxide
DSMZ	Deutsche Sammlung von Mikroorganismen und Zellkulturen GmbH
DNA	deoxyribonucleic acid
DNase	deoxyribonucleic acid nuclease
dNTP	deoxynucleotide triphosphate
EPA	Environmental Protection Agency
Gd	<i>Gluconacetobacter diazotrophicus</i>
Go	<i>Gluconobacter oxydans</i>
GT	glucose tolerant
HCl	hydrochloric acid
HEPES	4-(2-hydroxyethyl)-1-piperazineethanesulfonic acid

HF	high fidelity
HRP	horse radish peroxidase enzyme
ICE	Integrative Conjugative Element
IDT	Integrated DNA Technologies
INC	Inconclusive
IP	Intellectual property
IPTG	isopropyl $\beta$ -D-thiogalactopyranoside
IMAC	Immobilised Metal Affinity Chromatography
KEGG	Kyoto Encyclopaedia of Genes and Genomes
LB	Luria-Bertani
Mg	Magnesium
M-M	Michaelis-Menten
MOPS	3-( <i>N</i> -morpholino) propanesulfonic acid
MSC	Medical Supply Company
MQ	MilliQ water
N <sub>2</sub>	nitrogen
NAD <sup>+</sup> /NADH	Nicotinamide adenine dinucleotide
NaOH	sodium hydroxide
NEB	New England Biolabs
NCBI	National Centre for Biotechnology Information
NMWL	Nominal Molecular Weight Limit
O <sub>2</sub>	oxygen
OAA	oxaloacetate
OD	optical density
OPP	oxidative pentose phosphate pathway
PBR	photobioreactor
PCC	Pasteur Culture Collection
PCR	Polymerase Chain Reaction
PDB	Protein Data Bank
<i>pdv</i>	pyruvate decarboxylase gene
PDC	pyruvate decarboxylase protein
PEG	polyethylene glycol
PEP	phosphoenolpyruvate
<i>phaA</i>	polyhydroxyalkanoate-specific $\beta$ -ketothiolase

<i>phaB</i>	polyhydroxyalkanoate-specific acetoacetyl-CoA reductase
PHB	poly- $\beta$ -hydroxybutyrate
pk	pyruvate kinase
ppc	phosphoenolpyruvate carboxylase
SACII	restriction enzyme
SDS-PAGE	sodium dodecyl sulfate polyacrylamide gel electrophoresis
SEC	Size Exclusion Chromatography
Sv	<i>Sarcina ventriculi</i>
TBS	tris buffered saline
TEMED	Tetramethylethylenediamine
TES	<i>N</i> -[Tris (hydroxymethyl) methyl]-2-aminoethanesulfonic acid
ThDp	Thiamine diphosphate
TMB	3, 3', 5, 5' tetramthylbenzidine
Tris	tris (hydroxymethyl) aminomethane
U.S	United States
UL	University of Limerick
UV	ultraviolet
UvA	University of Amsterdam
WT	wildtype
YFP	Yellow Fluorescent Protein
Zm	<i>Zymomonas mobilis</i>
Zp	native <i>Zymobacter palmae</i>
ZpO	codon optimised <i>Zymobacter palmae</i>

## Units of Measurement

°C	degrees Celsius
bps	base pairs
Da	daltons
g.L <sup>-1</sup>	grams per litre
hrs	hours
kDa	kilodaltons
L	litre
lb.in <sup>-2</sup>	pounds per square inch
mg	milligram
ml	millilitre
ml.min <sup>-1</sup>	millilitre per minute
ml <sup>-1</sup>	per millilitre
M	Molar
mM	millimolar
mM.min <sup>-1</sup>	mM per minute
mM.sec <sup>-1</sup>	mM per second
ng	nanogram
nm	nanometre
rpm	revolutions per minute
μE	microeinsteins
μE.m <sup>-2</sup> .s <sup>-1</sup>	microeinsteins per square metre per second
μg	microgram
μg.ml <sup>-1</sup>	microgram per millilitre
μl	microlitre



## **Chapter 1: Introduction**

## **1.1 Biofuel necessity**

### **1.1.1 First, second and third generation biofuels**

For centuries, much time, money and effort has been invested in the exploitation of fossil feed stocks to produce fuels such as coal, natural gas and petroleum. These feed stocks were in the past readily available and abundant in nature with the added advantage of being relatively cheap to exploit (Bender 2000; Demirbas 2006). These resources however are dwindling with use and global warming has become a major problem in the last number of years with the combustion of fossil fuels being reported as the main contributor to increasing levels of carbon dioxide (CO<sub>2</sub>) in the atmosphere, a greenhouse gas which has been shown to be directly linked to this environmental issue (Shell 2016). As well as this, fossil fuel resources are unsustainable and the stocks are running out. There have also been major fluctuations in the price of oil over the last ten years (Naik *et al.* 2010). Therefore, to meet the energy demands of an ever increasing population, other avenues needed to be investigated to search for more environmentally friendly, sustainable and viable sources of energy which is why renewable biofuels, produced from organic waste and plants have attracted much attention in recent times (Mabee *et al.* 2005).

Producing biofuels from biomass for example can contribute to stemming the global warming crisis by reducing dependence on oil and utilising and reducing CO<sub>2</sub> levels via biomass photosynthesis (Osamu and Carl 1989). With research and application of biomass for biofuel production, various stages have occurred in their development such that first, second and third generation biofuels are introduced as drivers towards this sustainability. These generations have been summarised in Figures 1.1, 1.2 and 1.3 below.

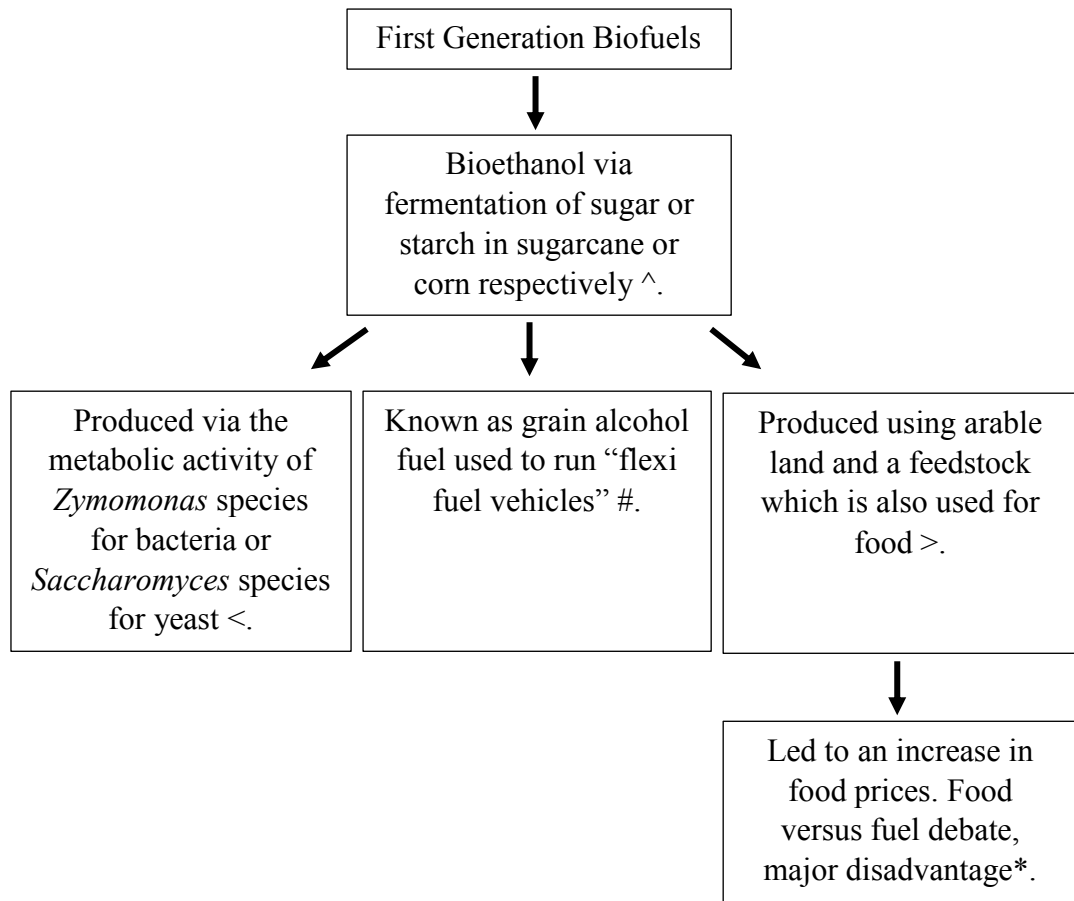


**Figure 1.1: Summary of First Generation Biofuels.**

\* (Laursen 2005) # (Balat 2006) ^ (Minteer 2016) < (Speight 2007)  
> (Shell 2016)

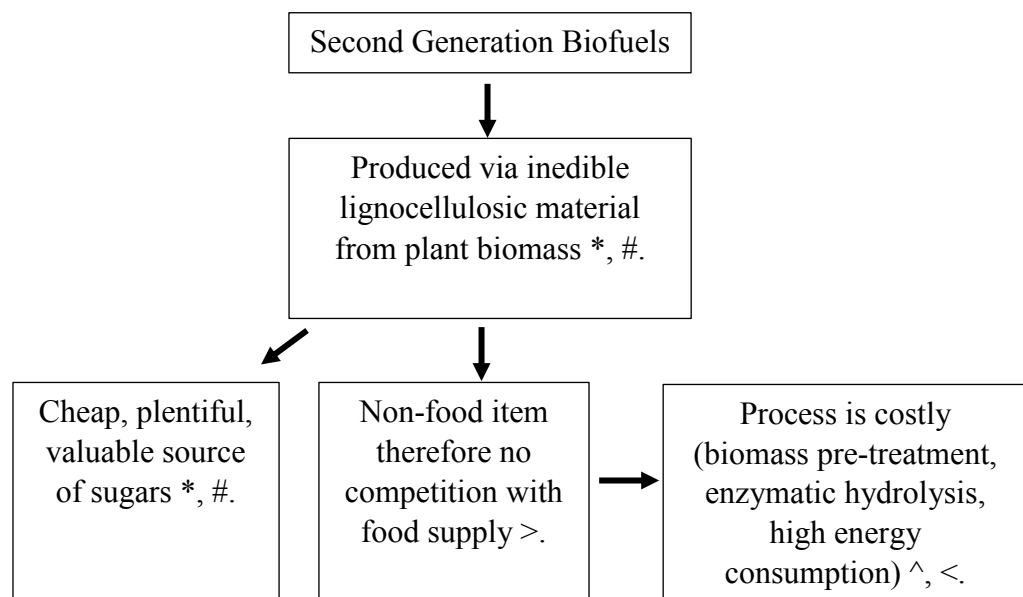


**Figure 1.2: Summary of Second Generation Biofuels.**

^ (Minteer 2016) < (Speight 2007) \* (Gomez *et al.* 2008) > (Shell 2016)  
# (Zabaniotou *et al.* 2008)

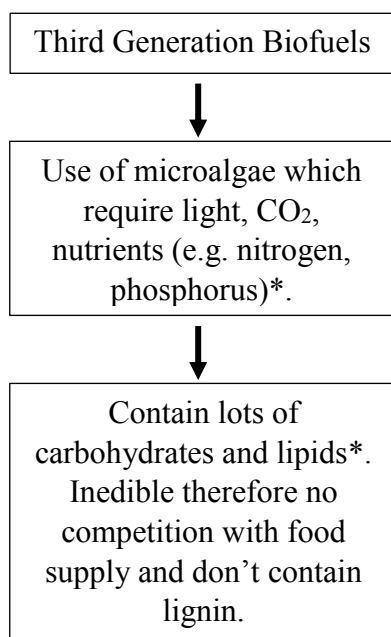


**Figure 1.3: Summary of Third Generation Biofuels.**

\* (Osamu and Carl 1989)

## 1.2 Cyanobacteria: Model organisms

Cyanobacteria (cyanophyta) or blue green algae are a group of prokaryotic photosynthetic microorganisms which contain the chlorophyll *a* and  $\beta$  carotene pigments (Stanier *et al.* 1971). They can carry out oxygenic photosynthesis in a way similar to plants (Rippka *et al.* 1979) and are found in fresh, marine and estuarine waters in the U.S (US Environmental Protection Agency 2016). Like other microbial groups cyanobacteria have ‘model’ members that are utilised as examples which include *Synechococcus elongatus* sp. Pasteur Culture Collection (PCC) 7942 and *Synechocystis* sp. PCC 6803. Cyanobacteria as a group have the ability to use light energy from the sun and via fixation through the Calvin cycle convert carbon dioxide into organic carbon metabolites (Angermayr *et al.* 2009) as well as generating chemical energy in the form of adenosine triphosphate (ATP) and liberating oxygen ( $O_2$ ) (Brennan and Owende 2010). To grow cyanobacteria in culture the growth media must contain the necessary inorganic compounds such as phosphorus and nitrogen. Phosphates do tend to bind with any metal ions present and so phosphorus needs to be added in excess to account for this occurrence (Chisti 2007) while the best nitrogen source has been found to be urea as it gives the highest

growth yields and causes smaller changes in pH during the growth phase. Nitrogen supplied as nitrate (NO<sub>3</sub><sup>-</sup>) however is a sufficient source (Shi *et al.* 2000). As well as needing adequate amounts of macronutrients like nitrogen and phosphorus and ions such as calcium and magnesium, metals like iron, zinc and copper also need to be included (Sunda *et al.* 2005). The BG-11 (blue green) media used to cultivate cyanobacteria (see appendix I B) ensures that all the necessary components are present.

In addition to having simple growth requirements and being able to use inorganic compounds efficiently, cyanobacteria can grow to relatively high densities, are non-pathogenic and high in nutrients. Therefore, not only are they suitable for the production of valuable commodities but can also be used for food (Radmer 1996). It is also possible to manipulate model members to produce different types of biofuels including ethanol via the metabolic conversion of carbon metabolites generated by photosynthesis through a single biological system (Gao *et al.* 2012). Thus cyanobacteria have received attention as potential cell factories (Pembroke *et al.* 2017) for the production of ethanol as a biofuel. Theoretical calculations have been carried out to show the amount of ethanol which could potentially be produced by different methods in gal per acre per year which can be seen in Table 1.1 below with the photosynthetic organism clearly having the potential to produce the most ethanol [\* (Angermayr *et al.* 2009) # (Budny and Sotero 2007) ^ (Sanderson 2006)].

**Table 1.1: Different methods of ethanol production and the amount produced in gal per acre per year (Gao *et al.* 2012).**

Ethanol producer	Ethanol produced in gal/acre/year
*Photosynthetic organism	~5,280
#Corn	321
#Sugar cane	727
^Switchgrass	330-810
^Corn stover	290-580

\* (Angermayr *et al.* 2009) # (Budny and Sotero 2007) ^ (Sanderson 2006)

### 1.2.1 *Synechocystis* sp. PCC 6803

*Synechocystis* sp. PCC 6803 (hereafter *Synechocystis* 6803) is a unicellular and freshwater cyanobacterium which has been utilised as a model organism for studying processes in this group. *Synechocystis* 6803 can undergo natural transformation and take up DNA. It can be described as a spherical or coccoid bacterium (Ikeuchi and Tabata 2001) with a circular chromosome (KEGG genome 2016) which does not possess a sheath or any gas vesicles and divides by binary fission (Ikeuchi and Tabata 2001). It follows the lineage of bacteria, cyanobacteria, synechococcales, merismopediaceae and *synechocystis* (KEGG genome 2016). The GC content of *Synechocystis* 6803 also places it in a “high GC group” which is one of three groups into which *Synechocystis* 6803 can be classified. Members of this group naturally utilise glucose and were mostly isolated from fresh water (Rippka *et al.* 1979). Others include the marine group and the low GC group (Ikeuchi and Tabata 2001). The original PCC strain was isolated from freshwater by R. Kunisawa in California (Stanier *et al.* 1971) in 1968 (Yu *et al.* 2013). This was placed in the Pasteur Culture Collection (PCC) as PCC 6803 and the American Type Culture Collection (ATCC) as ATCC 27184 strain (Pembroke *et al.* 2017). The Kazusa Research Institute in Japan received a glucose tolerant (GT) strain which was isolated from the ATCC strain (Williams 1988) and this resulted in sequencing the first *Synechocystis* genome (Kaneko *et al.* 1996). Its entire genome of 3,573,470 bps (KEGG genome 2016) is contained within several copies of a single chromosome and was fully sequenced in 1996 (Kaneko *et al.* 1996) encoding more than 3,000 genes. *Synechocystis* 6803 also contains four large native plasmids (Yu *et al.* 2013): pSYSG (44kb), pSYSM (120kb), pSYSA (103kb) and pSYSX (106kb), whose nucleotide sequences were resolved by Kaneko *et al.* (2003) as well as three smaller plasmids: pCC5.2 (5.2kb), pCA2.4 (2.4kb) and pCB2.4 (2.3kb) (Labarre *et al.* 1989; Kaneko *et al.* 2003). These plasmids appear to be maintained stably in all strains.

Over the years, many sub strains have also developed including the GT strain which allows glucose addition and is often beneficial in isolating recombinants (Williams 1988; Nordling *et al.* 2002), the PCC, ATCC and the Kazusa strain (Ikeuchi and Tabata 2001), a Vermaas strain (Vermaas 1998), a ‘China’ strain (Dexter and Fu

2009) and an ‘Amsterdam’ strain (Angermayr *et al.* 2014) to list a few. All of these strains differ in various ways which may be beneficial when using this model organism as a cell factory (Pembroke *et al.* 2017).

### **1.2.2 Ploidy levels**

The genome of *Synechocystis* 6803 is polyploid. Studies carried out by Griese *et al.* (2011) using real time PCR showed that that the motile ‘Moscow strain’ contained up to 58 genome copies per cell at stationary phase while the GT ‘Vermass strain’ contained somewhat less with 42 copies during the same time period. Further studies showed that respectively these strains contained 218 and 142 genome copies per cell during the exponential phase of growth (Griese *et al.* 2011). The higher copy number during this phase of growth has also been observed in several archaeal and bacterial species (Hildenbrand *et al.* 2011; Pecoraro *et al.* 2011). These copy numbers are also the highest numbers recorded for any of the cyanobacterial species and of any ‘normal’ prokaryote (Griese *et al.* 2011). Earlier work carried out by Mori *et al.* (1996) showed that *Synechococcus elongatus* sp. PCC 7942 (hereafter *Synechococcus* 7942) and *Synechococcus* WH7803 were oligoploid with only 3-4 copies of the genome per cell (Mori *et al.* 1996). Overall this clearly shows that the ploidy level is extremely high based on these results and is growth regulated (Griese *et al.* 2011).

Other workers using the ‘Kazusa WT strain’ and a similar method showed it to contain only 12 copies of the genome in each cell during stationary phase (Labarre *et al.* 1989). This difference could be due to technical reasons in measurement or due to mutations affecting ploidy (Griese *et al.* 2011). However, it is difficult to stay if these high levels naturally occur in nature or if they are due to continuous cultivation over the years. To answer this question, fresh *Synechocystis* 6803 samples as well as frozen isolates would need to be examined (Griese *et al.* 2011). Either way the polyploidy nature of the organism may be a response to combatting high levels of potential UV mutagenesis with its growth in light environments but in addition must put metabolic strain on the organism to cope with multiple genome copies. This could have a large effect on the productivity of components when utilising the organism as a cell factory.

### 1.2.3 Cultivation

Photoautotrophic *Synechocystis* 6803 is capable of carrying out oxygenic photosynthesis with the release of O<sub>2</sub> and the fixation of CO<sub>2</sub> via the Calvin cycle with the enzyme RuBisCo (Ribulose-1, 5-bisphosphate carboxylase, an intermediate of the cycle) catalysing the primary step of this process. There is an issue however with this protein as it is sensitive to oxygen. Therefore to combat this problem, *Synechocystis* 6803 has adapted and produced an organelle which does not allow oxygen to pass through its membrane. This carboxysome will however allow the diffusion of bicarbonate ions by active transport to facilitate growth for biomass production (Pierce *et al.* 1989). With RuBisCo enclosed in this area away from oxygen, photorespiration (the oxidation of RuBisCo by oxygen) is kept at a minimum during the growth phase (Young *et al.* 2011). Also, in the event of low inorganic carbon levels, *Synechocystis* 6803 can activate a mechanism to concentrate CO<sub>2</sub> which allows it to grow and survive even in very low concentrations (Battchikova *et al.* 2010).

*Synechocystis* 6803 can also grow photoheterotrophically by using glucose via the glycolytic and oxidative pentose phosphate (OPP) pathways. With conditions of optimal light under photoautotrophic growth, the maximum doubling time is between 7 and 10 hours while it increases to 3.5 days if using glucose via the above pathways (Williams 1988; Bartsevich and Pakrasi 1995; Ikeuchi and Tabata 2001; Yoshikawa *et al.* 2013). *Synechocystis* 6803 is usually grown at 30°C in BG-11 media which maintains the pH between ~7 and 8 (Kim *et al.* 2011). The cultures are irradiated with light and supplied with CO<sub>2</sub> and gentle shaking to allow for aeration.

In addition to this, cyanobacteria also require inorganic compounds like nitrogen (N<sub>2</sub>) and phosphorus. *Synechocystis* 6803 however is unable to naturally use N<sub>2</sub> due to the lack of the enzyme nitrogenase but by producing cyanophycin, a unique polypeptide structure which is rich in aspartate and arginine residues, it has the ability to overcome this problem. Cyanophycinase (a hydrolytic enzyme) is used to degrade this polymer under low nitrogen conditions (Richter *et al.* 1999). *Synechocystis* 6803 can also take up and store polyphosphate within the cell where

deprivation can lead to the slow generation of nucleotide sugars and energy as well as having a negative impact on the photosynthetic machinery (Fuszard *et al.* 2013). Overall, a lack of nitrogen and phosphorus has a detrimental effect on the cyanobacterium resulting in the down regulation of photosynthesis and chlorosis (Collier and Grossman 1992).

Studies have also shown that RuBisCo is not the rate limiting step when it comes to the growth of cells but is due to the reduction of phosphoglycerate, an intermediate molecule in the Calvin cycle and glycolysis caused by the lack of ATP and nicotinamide adenine dinucleotide phosphate (NADPH) (Marcus *et al.* 2011). It is also impossible for cyanobacteria to absorb all light which they are exposed to for reasons such as scattering, reflection and being caught in the shade. As well as that, not all photons of light taken in by the bacteria's antennae can be converted into energy (Beckmann *et al.* 2009) and so efforts have been made to improve the efficiency of light uptake by shortening these appendages. This uptake of light however is still considered the rate limiting step due to no improvement in the production of biomass by the alternation of the antennae (Page *et al.* 2012).

### **1.3 Ethanol Production Pathway**

To utilise *Synechocystis* 6803 as a cell factory and source of a biotechnology product, such as the biofuel ethanol, an understanding of its central metabolism is necessary.

In *Synechocystis* 6803 RuBisCo is used to fix carbon dioxide to 3-phosphoglycerate. This can be converted to phosphoenolpyruvate (PEP) from 2-phosphoglycerate via enolase (Pepper *et al.* 2010) or travel back through the Calvin cycle. Pyruvate kinase (PK) is then used to convert PEP to pyruvate (see Figure 1.4 below). This component can be used in several ways during metabolism to make for e.g. lactate, isobutanol or acetate from acetyl-CoA (Yu *et al.* 2013; Dexter *et al.* 2015).

Studies on the potential for ethanol production started with the introduction of heterologous genes from *Zymomonas mobilis* (Zm) in the late 1980s where Ingram

*et al.* (1987) showed ethanol production in *Escherichia coli* (hereafter *E. coli*) with the heterologous expression of *pdc* (pyruvate decarboxylase, see appendix III A) and *adhII* (alcohol dehydrogenase) genes from *Zymomonas mobilis*. The introduction of these genes created a novel ethanol producing bacterium (Ingram *et al.* 1987). PDC works by catalysing the non-oxidative decarboxylation of the pyruvate substrate to produce acetaldehyde and CO<sub>2</sub> (Montenecourt 1986) using thiamine diphosphate (ThDp) and the divalent cation magnesium (Mg<sup>2+</sup>) as cofactors (Reid and Fewson 1994). This intermediate is converted to ethanol by the enzyme ADH (Montenecourt 1986) which is much more common in nature than PDC. ADH uses the cofactor NAD or NADP (which undergoes oxidation) (Reid and Fewson 1994) depending on the enzyme source which will be discussed in more detail at a later stage in Section 1.5.1. Many prokaryotes can produce small amounts of ethanol but *Zymomonas mobilis* is an organism which produces ethanol as its prevalent product (Montenecourt 1986). The PDC enzyme (see appendix III B) makes up ~5% of the soluble proteins in the cell overall (Algar and Scopes 1985) while ADH is present in two isomeric forms, ADHI and ADHII with the latter being present in larger amounts (Hoppner and Doelle 1983; Neale *et al.* 1986).

Because of their photoautotrophic lifestyle there has been an impetus to determine if cyanobacteria could be utilised as a cell factory for biofuel production for some time. Although some cyanobacteria do produce small amounts of ethanol under heterotrophic conditions during anaerobic metabolism in the dark (Heyer and Krumbein 1991), ethanol production photoautotrophically has not been observed. The unicellular, freshwater bacterium *Synechococcus elongatus* 7942 was the first to be metabolically engineered for ethanol production by Deng and Coleman (Deng and Coleman 1999). This strain was transformed with the *pdc* and *adhII* genes from *Zymomonas mobilis* (similar constructs to Ingram *et al.* 1987) which were expressed under the *rbcLS* promoter. The total amount of ethanol produced was ~ 5 mM or 0.23 g L<sup>-1</sup> (Deng and Coleman 1999). This cyanobacterium was also used to produce #1-butanol (Lan and Liao 2011), ~isobutanol and <isobutyraldehyde (Atsumi *et al.* 2009) (see Table 1.2 below). The year after, Lagarde *et al.* (2000) used the PSBAII neutral site to overexpress genes involved in carotenoid biosynthesis (Lagarde *et al.* 2000; Dexter *et al.* 2015). These sites are areas in the genome where insertions would result in no phenotypic alterations (Varman *et al.*

2013a). Integration of genes into this site by recombinant insertion results in the deletion of the gene which codes for the D1 protein in photosystem II which also allows for the use of the strong, native, light driven pPSBII promoter. By using this site, phenotypic changes have not been reported probably due to the expression of the PSBAIII gene which compensates for the deletion of the PSBII gene (Mohamed and Jansson 1989). Shortly after, Dexter and Fu in 2009 showed that *Synechocystis* 6803 could also be used to produce ethanol with a final yield of ~10 mM or 0.46 g L<sup>-1</sup>, double that of Deng and Coleman using the same *pdh* and *adh* genes but under the pPSBII promoter mentioned above and in the same neutral site as Lagarde *et al.* 2000 (Dexter and Fu 2009). Work also carried out by Liu *et al.* (2000) showed the production of fatty acids in a genetically altered strain of *Synechocystis* 6803 which resulted in 197 mg L<sup>-1</sup> (Liu *et al.* 2011) while Gao *et al.* (2012) produced alkanes and fatty alcohols whilst also using an altered version of the same strain (Gao *et al.* 2012). Other products produced by metabolically engineered strains include \*isoprene (Lindberg *et al.* 2010) and ^ethylene (Sakai *et al.* 1997) (see Table 1.2).

**Table 1.2: Amount of biofuels produced by modified cyanobacteria (Gao *et al.* 2012).**

Type of biofuel	Amount
*Isoprene	0.05 mg per g dry cell per day
^Ethylene	37 mg L <sup>-1</sup>
#1-butanol	14.5 mg L <sup>-1</sup>
~Isobutanol	450 mg L <sup>-1</sup>
<Isobutyraldehyde	1100 mg L <sup>-1</sup>

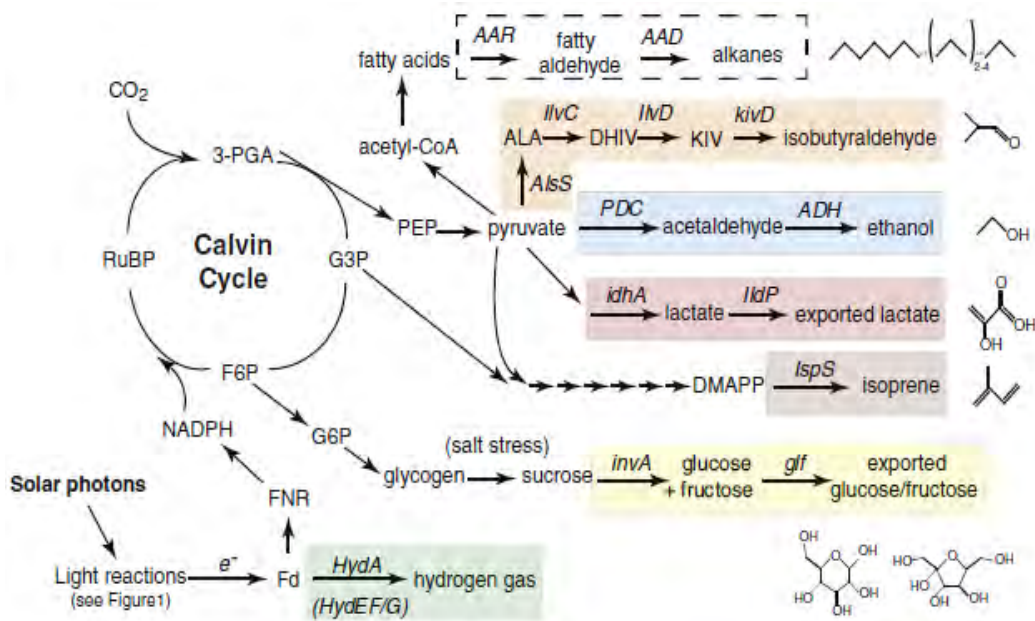


**Figure 1.4: Metabolically engineered pathways in cyanobacteria.** Main pathways in processes associated with photosynthesis are shown in black. Highlighted pathways show the production of various compounds with reaction enzymes in italics. Main abbreviations: PDC pyruvate decarboxylase, ADH alcohol dehydrogenase II, *ldhA* lactate dehydrogenase, *IlvC* acetohydroxy acid isomeroreductase, *IlvD* dihydroxy-acid dehydratase, *AAD* aldehyde decarbonylase, ALA 2-acetolactate, *AlsS* acetolactate synthase, PEP phosphoenolpyruvate, 3-PGA 3-phosphoglycerate, DHIV 2,3-dihydroxyisovalerate (Ducat *et al.* 2011). (Licence permission received from Elsevier publishers for the use of this image).

US biofuel companies such as Algenol Biofuels and Joule Unlimited have made quite an impression using these photoautotrophic bacteria for ethanol production. Algenol were granted intellectual property (IP) for the earlier work carried out by Deng and Coleman relating to *Synechococcus* 7942 (publication no: US6306639B1; filing date: 20/02/1998) (Woods *et al.* 2001). They also obtained the patent for work performed by Dexter and Fu with *Synechocystis* 6803 (publication no: US8372613B2; filing date: 16/01/2007) (Fu and Dexter 2013). By using the same *pdh* but an *adh* native to *Synechocystis* 6803 (*slr1192*), Algenol Biofuels demonstrated that ethanol levels could be increased via the overexpression of an *adh* other than *adhII* from *Zymomonas mobilis* (Dexter *et al.* 2015). This showed a total amount of ~3.6 g L<sup>-1</sup> of ethanol in the medium after 38 days of cultivation (publication no: US8163516B2; filing date: 09/02/2009) (Dehring *et al.* 2012). Gao *et al.* (2012) created many ethanol producing strains using different

genes, neutral sites and promoters but it was the third generation ethanol producing strain that surpassed ethanol levels achieved by Algenol biofuels. By using two copies of the *Zmpdc* and the endogenous *slr1192 adh* at two different sites in the chromosome: *slr0168* and the sites for the polyhydroxyalkanoate-specific  $\beta$ -ketothiolase (*phaA*) and polyhydroxyalkanoate-specific acetoacetyl-CoA reductase (*phaB*) genes along with the *prbc* promoter, 5.50 g L<sup>-1</sup> of ethanol was reached over 26 days of cultivation (Gao *et al.* 2012) in comparison to Algenol's 3.6 g L<sup>-1</sup> after 38 days. To develop commercial processes it is important to maximise production levels in order to make ethanol production procedures economically comparable with other biofuel production systems (corn or lignocellulose processes). However as these reported ethanol production levels in cyanobacteria are far below the expected economic levels, research and development is needed to increase the productivity of such organisms.

The strategies mentioned above which have utilised heterologous *pdc* and *adh* genes have shown promising results in the production of ethanol as a biofuel using this cyanobacterial cell factory. However, in carrying out such metabolic engineering it should be realised that as pyruvate is also a key component in the production of essential intermediates such as lipids, nucleotides, amino acids and biomass within *Synechocystis* 6803, diverting pyruvate away from this pathway towards ethanol production may have a negative effect on the health status of the cyanobacterial strain due to a decrease in biomass yields (Pembroke *et al.* 2017).

## 1.4 Pyruvate decarboxylase enzyme (PDC)

PDC (pyruvate decarboxylase EC 4.1.1.1, PDB ID IZPD) (Dobritzsch *et al.* 1998) is an important cytosolic enzyme in alcohol fermentation which requires ThDp and Mg<sup>2+</sup> as cofactors for catalytic activity (Bringer-Meyer *et al.* 1986; Reid and Fewson 1994). Several other enzymes also require these cofactors to function and it is believed that each of them use a similar mechanism of action (Kern *et al.* 1997). PDC can be found in fungi, plants and yeast (Ullrich 1982) but is very rare in bacteria (Scrutton 1971; Finn *et al.* 1984). Through cloning and purification, PDC has been characterised well in only a few bacteria: *Zymomonas mobilis* (Hoppner and Doelle 1983; Bräu and Sahm 1986; Bringer-Meyer *et al.* 1986; T. Conway *et*

*al.* 1987; Neale *et al.* 1987a; Neale *et al.* 1987b), *Acetobacter pasteurianus* (Raj *et al.* 2001), *Sarcina ventriculi* (Lowe and Zeikus 1992; Talarico *et al.* 2001) and *Zymobacter palmae* (Raj *et al.* 2002). Only PDCs from bacteria can be expressed in *E.coli* at high enough levels to give active recombinant products (T. Conway *et al.* 1987; Neale *et al.* 1987a; Raj *et al.* 2001; Talarico *et al.* 2001) and therefore these are of potential use in metabolic engineering applications in bacterial systems (Raj *et al.* 2002). As well as that, PDC is also quite stable, simple to purify and study (Schenk *et al.* 1997). Other reported PDC's from the *Acetobacteraceae* genera include *Gluconobacter oxydans* (GoPDC) and *Gluconacetobacter diazotrophicus* (GdPDC) (Van Zyl *et al.* 2014) which have also been investigated.

#### **1.4.1 PDC mechanism of action**

The exact reaction mechanism for enzymes requiring ThDP has not been fully elucidated. However it is thought that atom C2 on the thiazolium ring of ThDP is deprotonated to form a carbanion or ylide (Meyer *et al.* 2013). The carbonyl group of the pyruvate substrate undergoes a nucleophilic attack by the ylide entity to give an intermediate: C2- $\alpha$ -lactylthiamine diphosphate (Kern *et al.* 1997; Zhang *et al.* 2004). The way in which PDC binds to ThDP allows for the atom N4' of the aminopyrimidine ring to be in close proximity to atom C2. With the aminopyrimidine ring in its imino tautomeric state, atom N4' can act as a strong base which allows for the deprotonation of atom C2 and the activation of the cofactor. The lactyl intermediate is then decarboxylated to produce an enamine intermediate with the release of CO<sub>2</sub>. The intermediate is protonated to form a hydroxyethyl ThDP adduct along with the generation of acetaldehyde which allows for the renewal of the ylide (Baykal *et al.* 2006).

#### **1.4.2 PDC cofactor: ThDp**

Enzymes that are dependent on ThDP as a cofactor are generally oligomeric and are arranged as either homodimers, homotetramers or heterotetramers (Pei *et al.* 2010). Because ThDP is utilised in many cellular reactions, incorporating a highly expressed PDC for metabolic engineering purposes will affect levels of the cofactor within the cell and result in competition unless extra can be provided. As *Synechocystis* 6803 does not contain a ThDp transporter (Tajima *et al.* 2011), steps

may need to be taken to increase cellular cofactor concentrations. Ways to overcome this may involve overexpression of the *thiC* (phosphomethylpyrimidine synthase) gene which is involved in the production of ThDp or adding a specific transport system. Proteome analysis of an ethanol producing *Synechocystis* 6803 strain suggested that overexpression of *thiC* was a feature of the cellular response to ethanol tolerance with the up-regulation of the *thiC* gene being observed (Borirak *et al.* 2015). Other potential methods to supply thiamine exogenously may be by ultrasonic intensification to allow diffusion of added thiamine into the cell (Naveena *et al.* 2015).

### **1.4.3 *Zymomonas mobilis* PDC**

Understanding the nature of heterologous enzymes expressed in heterologous hosts such as *Synechocystis* 6803 is important to optimise metabolic engineering protocols. The PDC from *Zymomonas mobilis* (ZmPDC), an obligate fermentative Gram negative bacteria has been well studied (Bringer-Meyer *et al.* 1986). Its crystal structure has been determined at a resolution of 1.9 Å (PDB ID 1ZPD, (Dobritzsch *et al.* 1998). When in solution, PDC is present as four identical monomeric subunits, each consisting of 568 amino acids with a combined molecular mass of ~240 kDa and a gene size of ~1.7 kb (Bringer-Meyer *et al.* 1986; Neale *et al.* 1987a). The optimum pH for activity is pH 6.0 (Bringer-Meyer *et al.* 1986; Diefenbach and Duggleby 1991) but the PDC structure is actually stabilised by the cofactors from a pH of 4.5 to 8.5, which is important given the slightly alkaline growth conditions of *Synechocystis* 6803. An increase in alkalinity however will cause the cofactors to separate which leads to loss of activity (Pohl *et al.* 1995).

The quaternary structure of ZmPDC has a size of ~85 X 98 X 118 Å with each monomer containing three domains: PYR, PP and R (Dobritzsch *et al.* 1998). It can be described as a dimer of dimers with interactions including salt bridges and hydrogen bonds. In narrow pockets at the interface of the two dimers there are also a large number of water molecules. The cofactors bind to ZmPDC in a similar way to the *Saccharomyces cerevisiae* PDC in a tight but non covalent manner and interactions are also tighter between the monomer interfaces than between the two dimers (Koenig *et al.* 1992; Dyda *et al.* 1993) with 19% of the overall surface area

being hidden in the interface between both monomers (Dobritsch *et al.* 1998). ZmPDC additionally possesses more interactions between both dimers than *Saccharomyces cerevisiae* PDC. The area between both monomers is approximately 4,400 Å<sup>2</sup> which correlates to 12% of the surface of the dimer. Angle x-ray scattering studies support these results which showed that the ZmPDC forms a compact tetramer when in solution in comparison to other PDCs (Konig 1998). In contrast however, a common feature amongst PDCs is “allosteric activation” by the substrate molecule. In *Saccharomyces cerevisiae*, molecules such as pyruvamide which is similar to pyruvate, can start the activation process by working as activators where the PDC experiences a considerable change in conformation (Hübner *et al.* 1978). This does not occur in ZmPDC (Bringer-Meyer *et al.* 1986; Sun *et al.* 1995).

Conformational changes however need and do take place during catalysis in ZmPDC with the helix at the C terminus having to move out of the way of the pyruvate substrate to allow it access to the active site of the enzyme. Once it is bound, it is thought that the active site might be closed by the helix to create a hydrophobic environment which would allow the conversion of pyruvate to acetaldehyde. ZmPDC activity is higher than that of *Saccharomyces cerevisiae* PDC by ~3 fold and so this could be related to the varied conformational changes that take place in both PDC enzymes (Bringer-Meyer *et al.* 1986). The binding site for the substrate is speculated to be within a pocket located a short distance from ThDP’s thiazolium ring. It has previously been shown that the intermediates formed during the catalytic reaction can position themselves quite well into this cavity (Lobell and Crout 1996). At this location, pyruvate atoms are enclosed by the side chains of various amino acids: Asp<sup>27</sup>, Glu<sup>473</sup>, His<sup>113</sup>, His<sup>114</sup>, Thr<sup>388</sup> and Tyr<sup>290</sup>, all of which are conserved in *Saccharomyces cerevisiae* PDC with the exception of the latter residue. It is possible that these may be involved in the binding of the substrate and catalytic activity. Modelling studies have proposed that the glutamate amino acid at position 473 in ZmPDC and 477 in *Saccharomyces cerevisiae* has an important role to play in the decarboxylation of the substrate which leads to the formation of the hydroxyethyl ThDP. This in turn leads to this molecule being protonated and the acetaldehyde product being released. Once the substrate’s thiazolium carbanion has been nucleophilically attacked, a dianion is created which

is thought to be stabilised by Glu<sup>477</sup> in *Saccharomyces cerevisiae* PDC by use of a hydrogen bond (Lobell and Crout 1996). As well as this, in ZmPDC another amino acid also seems to aid in stabilisation. Tyr<sup>290</sup>'s hydroxyl group is in a position to make a hydrogen bond with 2-(2-hydroxyldroxypropionyl) ThDP's carboxyl group to help stabilise its negative charge (Dobritsch *et al.* 1998).

Carboligase activity is a secondary reaction that occurs which is also catalysed by PDC (Bringer-Meyer 1988). Another aldehyde particle is formed when the acetaldehyde product that is joined to the cofactor is condensed. This type of reaction is of great interest in industry due to its use in the synthesis of (R)-1-hydroxy-1-phenylpropan-2-one which is an intermediate created during the formation of L-ephedrine. Even though the carboligase activity of PDC in *Saccharomyces cerevisiae* is higher than that of ZmPDC (by ~20 fold) (Bringer-Meyer 1988), it would be more useful to increase the activity in the latter organism due to its greater stability. Steric hindrance is more than likely the reason behind the differences in activity between the two PDCs (Bruhn *et al.* 1995). Studies have shown that there is a pocket at the active site of *Saccharomyces cerevisiae* PDC which can be easily accessed which in turn allows the second aldehyde particle to bind. This however is not the case in ZmPDC as the cavity is occupied by amino acids like Trp<sup>392</sup> and Tyr<sup>290</sup> which have large awkward side chains. Mutation of tryptophan to alanine which has a much smaller side chain led to an increase in the activity by ~5 fold in the PDC from Zm (Zang *et al.* 2007). Expanding the size of this area at the active site by replacing side chains of other amino acids may result in another increase in the carboligase activity (Dobritsch *et al.* 1998).

Due to the tetrameric structure of PDC, there are four binding sites for the cofactors and substrate. The binding site for the ThDP is located quite a distance from the surface of the protein (~15 Å) and is found within cavities which are created by the PP domain of one monomer and the PYR domain of another (Dobritsch *et al.* 1998).

As with other enzymes which require ThDP (such as *Saccharomyces cerevisiae*), the cofactor binds in a V type arrangement (Dyda *et al.* 1993) where its pyrimidine ring comes into contact with the PYR domain in one monomer and its residual component in the PP domain in another. The diphosphate segment of the cofactor

is attached to the protein by the  $Mg^{2+}$  where an “octahedral coordination sphere” containing oxygen atoms belonging to the cofactor’s diphosphate group and amino acids Asp<sup>440</sup>, Asn<sup>467</sup> and Gly<sup>469</sup> along with a water molecule is formed. The binding site for the ThDP cofactor in ZmPDC shares high similarity with that in *Saccharomyces cerevisiae* PDC (Dobritsch *et al.* 1998).

#### 1.4.4 Other PDC enzymes

When comparing the bacterial PDCs there are many similarities as well as differences as was the case between ZmPDC and the *Saccharomyces cerevisiae* PDC. Raj *et al.* (2002) examined the four bacterial PDCs as mentioned above: *Zymomonas mobilis*, *Zymobacter palmae*, *Acetobacter pasteurianus* and *Sarcina ventriculi*. By aligning the amino acid sequences of these PDCs (see Figures A and B, Section 3.1), it was found that the PDC from *Zymobacter palmae* (ZpPDC) shared 72% identity with the PDC from *Acetobacter pasteurianus* (ApPDC) but only 62/63% to ZmPDC (Raj *et al.* 2002; Buddrus *et al.* 2016). These Gram negative PDCs seemed to be more closely related to PDCs from plants. The Gram positive PDC from *Sarcina ventriculi* (SvPDC) however associated more with PDCs from fungi and yeast and only shared 30-31% identity with the Gram negative PDCs. All of the enzymes had a similar number of amino acids ranging from 552-568 as well as their mass which was in the region of 59,830 to 61,809 daltons. It was also found that the percentage of alanine in the Gram negative PDCs was comparable at 13.1% but it was ~2 fold less in the Gram positive *Sarcina ventriculi* PDC at 6.9% (Raj *et al.* 2002).

With regards to structure, the regions involved in cofactor binding were maintained in each of the bacterial PDCs by using the crystal structures of ZmPDC and *Saccharomyces cerevisiae* PDC as a guide. It is also thought that the percentage of alanine is linked to thermostability as heating cell lysates containing ZmPDC and its cofactors to 60°C does not affect the activity (T. Conway *et al.* 1987). The activity of other PDCs was investigated at various temperatures with cofactors added in excess and it was found that the PDCs from the Gram negative organisms still showed a high level of activity (60-100%) once the cell lysate was heated for 30 minutes at 60°C. The Gram positive PDC however lost all activity at a

temperature of 50°C or more (Raj *et al.* 2002). It is possible that the increased levels of alanine in the Gram negative PDCs resulted in the development of helical structures which formed a solid core thus stabilising the proteins at elevated temperatures (Raj *et al.* 2002).

An important factor in characterising PDCs of different origins is whether they possess contrasting kinetics. In metabolic engineering applications in *Synechocystis* 6803, a key issue is to have a  $K_m$  that will remove as much pyruvate as possible from the central metabolic pathway to channel this to ethanol. Comparison of kinetic parameters as seen in Table 1.3 below indicates for example that the ZpPDC and the GoPDC may have some potential in this respect to enhance ethanol productivity over the ZmPDC, based on their lower  $K_m$  values.

**Table 1.3: Characteristics of bacterial PDCs.**

PDC	ZmPDC	ZpPDC	ApPDC	SvPDC	GoPDC	GdPDC
PDB entry	1ZPD	5EUJ	2VBI	N/A	N/A	4COK
GenBank gene	M15393.2	AF474145	AF368435.1	AAL18557.1	KF650839.1	KJ746104.1
GenBank protein	AAA27696.2	AAM49566.1	AAM21208.1	AF354297.1	AHB37781.1	AIG13066.1
Gram status	*Negative	*Negative	*Negative	*Positive	*Negative	*Negative
Amino acid identity %	*62/^63	Reference	^73	^31	^67	^71
Kinetics	*M-M	*M-M	*M-M	*Sigmoidal	*M-M	*M-M
Km mM (pH)	*0.43 (6.0) 0.94 (7.0)	*0.24 (6.0) 0.71 (7.0)	*0.39 (5.0) 5.1 (7.0)	*5.7 (6.5) 4.0 (7.0)	#0.12 (5.0) 1.2 (6.5) 2.8 (7.0)	#0.06 (5.0) 0.6 (6.0) 1.2 (7.0)
Optimum temperature °C	*60	*55	*65	N/A	#53	#45-50
Optimum pH	*6.0	*5.5-6.0	*5.0-5.5	*6.3-6.7	#4.5-5.0	#5.0-5.5

PDB entries obtained from the PDB (Protein Data Bank) website.

PDB ID: 1ZPD, (Dobritzsch *et al.* 1998)

PDB ID: 5EUJ, (Buddrus *et al.* 2016)

PDB ID: 2VBI, (Gocke *et al.* 2008)

PDB ID: 4COK, (Van Zyl *et al.* 2014)

\*(Raj *et al.* 2002) # (Van Zyl *et al.* 2014) ^ (Buddrus *et al.* 2016)

M-M: Michaelis-Menten

## **1.5 *Zymomonas mobilis* alcohol dehydrogenase enzyme (ADH)**

Two ADH (alcohol dehydrogenase) isozymes are known to be present within the genome of *Zymomonas mobilis*, ADH I and ADH II (EC 1.1.1.1, PDB ID 3OWO/3OX4) (Moon 2011). Both of these enzymes along with PDC and others involved in glycolysis make up to ~30 - 50 % of the soluble proteins present in *Zymomonas mobilis* (Pawluk *et al.* 1986; Osman *et al.* 1987). ADH II is smaller in size than ADH I and is present as a tetramer, with each monomer having a molecular weight of between 31 and 38 kDa (Wills *et al.* 1981; Hoppner and Doelle 1983; Scopes 1983; Kinoshita *et al.* 1985; Neale *et al.* 1986). Both enzymes appear to take part in the fermentation process (Kinoshita *et al.* 1985; Neale *et al.* 1986). ADH I contains zinc at its active site, similar to ADH IV from *Saccharomyces cerevisiae* (Lutstorf and Megnet 1968; Ciriacy 1975; Wills *et al.* 1981; Neale *et al.* 1986) but ADH II unusually contains iron with each subunit binding a single ferrous ion (Neale *et al.* 1986; Tse *et al.* 1988). It is also completely inactivated by the addition of zinc and during purification, ferrous or cobaltous ions need to be added to preserve activity (Neale *et al.* 1986). The *adhB* gene which codes for the ADH II isozyme contains 1,149 bps within a single open reading frame. In total, 383 amino acids make up this protein which includes the methionine at the N terminus (T Conway *et al.* 1987). Both enzymes have been purified and polypeptide sequencing has confirmed both sequences of the N terminus (Neale *et al.* 1986) which are entirely different for each isozyme. Studies have also shown that the *adhB* gene is present as a single copy but that there is no discernible homologous regions between it and the gene which codes for ADH I (Neale *et al.* 1986). For the latter enzyme, the reduction of acetaldehyde to ethanol and the oxidation of nicotinamide adenine dinucleotide (NADH) to NAD<sup>+</sup> works best at a pH of 6.5 with its V<sub>max</sub> 2.2 times faster than for the oxidation of ethanol to acetaldehyde. In

contrast, the optimum pH for ADH II is 8.5 where ethanol oxidation takes place at a much faster rate than acetaldehyde reduction (Neale *et al.* 1986). ADH II is also stimulated by ethanol build up whereas the activity of ADH I is hindered (Mackenzie *et al.* 1989). ADH II however is present in larger amounts and is responsible for most of the activity in *Zymomonas mobilis* (Wills *et al.* 1981; Kinoshita *et al.* 1985; Neale *et al.* 1986). Hence, ADH II was initially selected as the enzyme of choice for metabolic engineering of ethanol production in heterologous systems such as cyanobacteria (Dexter and Fu 2009).

### **1.5.1 *Synechocystis* sp. PCC 6803 native ADH**

The *adhA* (slr1192) gene of *Synechocystis* 6803 encodes a member of the medium chain alcohol dehydrogenase/reductase superfamily which catalyses the reversible oxidation of alcohols to aldehydes or ketones in a NADP dependent manner (Jornvall *et al.* 1987; Persson *et al.* 1994; Riveros-Rosas *et al.* 2003). The gene product is a tetrameric 140 kDa zinc-dependent enzyme which exhibits broad alcohol dehydrogenase activity on aromatic and aliphatic alcohols and aldehydes (Vidal *et al.* 2009). It shows no activity however on secondary alcohols or ketones but demonstrates efficient catalytic activity towards aldehyde reduction as opposed to alcohol oxidation (Vidal *et al.* 2009).

*Synechocystis* 6803 unusually has been reported to contain multiple hypothetical *adh* genes of its own even though it does not contain a *pdh* gene and so does not natively produce ethanol (Pembroke *et al.* 2017). This suggests that the slr1192 gene product may play another yet unknown metabolic role in *Synechocystis* 6803. *adhA* can be induced by osmotic (Mikami *et al.* 2002) or salt stress (Shoumskaya *et al.* 2005) which is often regulated by two component regulatory systems. In this case, the histidine kinase (Hik34) and a response regulator (Rre1) can induce or repress *adhA* expression in response to environmental stress (Murata and Suzuki 2006). Once activated, it auto-phosphorylates a conserved histidine residue and then transfers the phosphate to an aspartate residue in the response regulator, Rre1 (Murata and Suzuki 2006). The Rre1 response regulator has been shown to then bind specifically to the promoter region of the *adhA* gene with two repeated

palindromic GTTG sequences being the suspected binding site (Vidal *et al.* 2009), resulting in gene activation.

In addition to this, medium-chain dehydrogenases/reductases in cyanobacteria are considered the main scavengers of lipid-derived reactive carbonyls. Reactive carbonyls are widespread species in living organisms and are mainly known for their damaging effects, with the most abundant reactive carbonyl species derived from oxidation of carbohydrates, lipids and amino acids. Reactive carbonyls such as methylglyoxal and acrolein have a toxic effect on the photosynthetic activity of cyanobacteria (Shimakawa *et al.* 2014). These toxic effects are unique to photosynthetic organisms indicating that scavenging systems are thus essential for cyanobacterial survival. The aldo-keto reductase and the glyoxalase systems mainly scavenge sugar-derived reactive carbonyls. The 2-alkenal reductases and alkenal/alkenone reductase catalyse the reduction of lipid-derived reactive carbonyls while medium-chain dehydrogenases/reductases are the main scavengers of these carbonyl types (Shimakawa *et al.* 2014). This suggests another possible role for the *adhA* in *Synechocystis* 6803.

In another study, it was demonstrated that *adhA* enhanced odd-chain fatty alcohol production which may point to yet another function. Such fatty alcohols are produced for purposes of buoyancy, as a source of metabolic water and for energy purposes (Cao *et al.* 2015).

With regards to metabolic engineering experiments *adhA* has been used to produce ethanol in *Synechocystis* 6803 in lieu of *adhII* from *Zymomonas mobilis* (Gao *et al.* 2012). Studies carried out by Gao *et al.* (2012) showed that construction of a strain using *Zmpdc* and *adhA* (slr1192) resulted in a 50% increase in ethanol yields in comparison to those produced by a strain using *Zmpdc* and *ZmadhII*. This result was an indication that the alcohol dehydrogenase used plays an important role in ethanol production and yield. Therefore, to investigate this further, nine *adh* genes in total were chosen from different cyanobacteria with all expressing ethanol. However, expression of the PDC from *Zm* and one copy of the slr1192 from *Synechocystis* 6803 still gave the highest ethanol levels overall (Gao *et al.* 2012).

He also found that by using NADPH as a cofactor and acetaldehyde as a substrate, there was up to a 74,000 fold difference in the *slr1192* activity (showing a  $K_m$  of 1.56 mM) in comparison to others (Gao *et al.* 2012). Naturally, the concentration of NADPH in cyanobacteria is ~10 fold higher compared to NADH levels due to electrons being released from water in the cell membranes (Pembroke *et al.* 2017). However, the activity for *ZmadhII* was 94 fold higher than the *slr1192* when NADH was used as a cofactor and acetaldehyde as a substrate which resulted in a  $K_m$  of 2.73 mM, demonstrating the importance of using the correct cofactors. Thus when manipulating the *adh* genes for metabolic engineering, depending on which one is expressed, the cofactor requirements may differ and so there may be merit in expressing both. This huge difference in activity observed by Gao *et al.* (2012) is also an indication that the pyruvate decarboxylation may possibly be the rate limiting step in this ethanol production pathway. Using the *adh* native to *Synechocystis* 6803 only resulted in a 50% increase in ethanol levels even though its activity is considerably higher than ZmADHII under the optimal conditions for both (Gao *et al.* 2012).

## **1.6 Methods to enhance ethanol production in cyanobacteria**

To enhance ethanol productivity a combination of genetic and production strategies would be needed to enhance and optimise levels to an economically viable status. A number of such strategies are discussed.

### **1.6.1 Gene Dosage**

As mentioned above in Section 1.3, Gao *et al.* (2012) created a strain of *Synechocystis* 6803 which consisted of two copies of the *Zmpdc* and *slr1192 adh* in two separate areas of the chromosome (a double cassette strain). This resulted in ethanol levels of 5.50 g L<sup>-1</sup> over 26 days which was 4.9 and 3.7 fold higher in comparison to strains they had previously created using a single copy of each gene in the *slr0168* and *phaAB* sites respectively. This was an indication that the idea of gene dosage may have potential to increase ethanol production (Gao *et al.* 2012). However, one can only presume that this might only work to a certain extent even though no reports have been made on its upper limitations as yet (Pembroke *et al.*

2017). The principle was also applied to the production of lactate (lactic acid) from pyruvate using LDH (lactate dehydrogenase) in *Synechocystis* 6803 (Niederholtmeyer *et al.* 2010; Angermayr *et al.* 2012; Varman *et al.* 2013b). Various strains were constructed which contained different copy numbers of the LDH enzyme: one copy versus two which showed double the lactic acid production than the strain with just one copy of LDH (Angermayr *et al.* 2014). However there would have to ultimately be an upper limit to gene dosage as diverting too much pyruvate away from central metabolism would have an effect on biomass and other essential processes. Equally, gene dosage of similar cassettes would potentially lead to genetic instability and recombination which would potentially mitigate against stable production strains.

### **1.6.2 Utilising small native plasmids**

Genomic analysis has determined that PCC 6803 contains a number of plasmids which appear to be highly stable (Yang and McFadden 1993; Yang and McFadden 1994; Kaneko *et al.* 1996; Xu and McFadden 1997; Kaneko *et al.* 2003) and these have been used to insert heterologous genes to examine stability and gene dosage (Berla and Pakrasi 2012). One of these plasmids, pCA2.4 is stably and consistently maintained in PCC 6803 at a copy number of ~7 per genome under mixotrophic conditions during the stationary phase of growth (Berla and Pakrasi 2012) and it is believed to replicate via a rolling circle mechanism (Yang and McFadden 1993). Recently it was used in this laboratory to express a gene which coded for a yellow fluorescent protein (YFP) (Armshaw *et al.* 2015) with results suggesting that this plasmid could possibly be used as a neutral site to enhance gene expression in PCC 6803 due to the fluorescence (as measured as an expression quantity) from YFP in pCA2.4 being 20 fold higher on average in comparison to its fluorescence when integrated into a single chromosomal site. The integration into pCA2.4 was also shown to be relatively stable due to no loss of fluorescence with or without a selective antibiotic pressure over multiple generations and culture trials (Armshaw *et al.* 2015).

### 1.6.3 Pyruvate diversion towards ethanol pathway

Other methods associated with the production of lactic acid (Angermayr *et al.* 2012; Angermayr *et al.* 2014) which could potentially lead to increased ethanol titres have also been investigated. Pyruvate is the precursor to ethanol as well as lactate and is produced via the conversion of PEP by pyruvate kinase. This occurs via the transfer of a phosphate group to ADP (adenosine diphosphate) which in turn generates one molecule of pyruvate and ATP. Studies have shown that by coupling a highly expressed LDH enzyme with a correct pyruvate kinase led to an increase in lactic acid production, with more carbon partitioned towards the product (Angermayr *et al.* 2014). The same idea could be applied to ethanol levels in PCC 6803 to increase the flux towards pyruvate by overexpressing pyruvate kinase (see Figure 1.5 below).

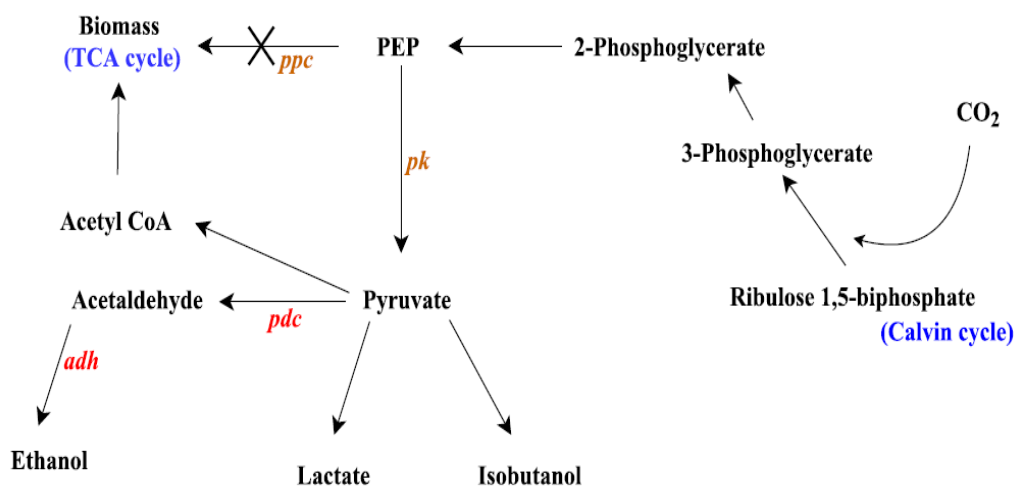


**Figure 1.5: Overview of the major metabolic pathways in cyanobacteria.** The Calvin cycle fixes CO<sub>2</sub> from the atmosphere to 2-phosphoglycerate which is converted to PEP (phosphoenolpyruvate) via enolase and subsequently to pyruvate via pyruvate kinase (PK). Pyruvate can be diverted to many products such as lactate, isobutanol or acetate via acetyl CoA. With the introduction however of *pdh* and *adh* it can be converted to ethanol. Methods such as increasing expression levels of pyruvate kinase or decreasing levels of PPC (phosphoenolpyruvate carboxylase) may lead to improved pyruvate concentrations for enhanced ethanol production (Pembroke *et al.* 2017).

### 1.6.4 Pathway knock out

Knocking out or blocking competitive pathways have also been investigated to increase product levels. When carbon is not limited, PEP is converted to OAA

(oxaloacetate), an intermediate of the TCA (tricarboxylic acid) cycle via PPC (phosphoenolpyruvate carboxylase) which depletes the flux towards pyruvate and hence ethanol/lactic acid production. Angermayr *et al.* (2014) created strains with a slight reduction in PPC which showed lactic acid levels similar to those produced by strains with highly expressed LDH (Angermayr *et al.* 2014). Gao *et al.* (2012) also constructed an ethanol producing strain by integrating the genes for *Zmpdc* and the native *adh* into the sites for the *phaA* and *phaB* genes which are involved in the PHB (poly- $\beta$ -hydroxybutyrate) pathway, a major storage pathway to store excess light energy for potential usage during dark metabolism. The production of PHB potentially channels carbon away from ethanol production and so it was hypothesised that by generating a pathway knockout an increase in ethanol levels would be observed. However to their surprise, by only blocking the PHB pathway alone there was no increase in ethanol levels in comparison to using the native *slr1192 adh* in lieu of *adhII* from *Zymomonas mobilis* (see Section 1.5.1). Within the cell, pyruvate is controlled by many other pathways and just interrupting PHB production was not enough to increase pyruvate levels (Gao *et al.* 2012).

However, as already mentioned above in Section 1.6.1, this construct was transformed into a previously constructed strain which already contained one copy of the *Zmpdc* and native *adh* in the *slr0168* neutral site. This created strain surpassed Algenol's ethanol production levels which could be contributed to both gene dosage and the pathway knockout.

### 1.6.5 Promoters

Currently, there are a shortage of promoters available for use in *Synechocystis* 6803 and limitations associated with existing promoters (Huang and Lindblad 2013). The systems generally used for the expression and over expression of genes are centred on the *tac* and *trc* promoters which are LacI regulated (Ng *et al.* 2000; Nair *et al.* 2002; Mutsuda *et al.* 2003; Kim *et al.* 2009). Non-native promoters such as the strong *P<sub>trc</sub>* promoter which does function in both *Synechocystis* 6803 (Huang *et al.* 2010) and *Synechococcus* 7942 causes “leaky repressed activity” and its regulation range is also very narrow. Other promoters such as  $\lambda P_R$ ,  $\lambda P_L$  and  $\lambda P_{lac}$  derived promoters do not function in *Synechocystis* 6803 even though they have been

characterised in *E.coli* (Nair *et al.* 2002; Mutsuda *et al.* 2003). Some promoters that do naturally exist in *Synechocystis* can be induced by the dark like *IrtA* (Imamura *et al.* 2004), by the light *psA* (Eriksson *et al.* 2000), *psB* (Muramatsu and Hihara 2007), *secA* (Mazouni *et al.* 1998), by nitrate/nitrite (*nirA*) (Ivanikova *et al.* 2005), copper ions (*petE*) (Briggs *et al.* 1990) or heavy metal ions (Peca *et al.* 2008) all of which can be classified as type I, II or III (Imamura and Asayama 2009). The native pPSBAII promoter mentioned above in Section 1.3 is a strong inducible promoter which exhibits higher activity under high light conditions (Mohamed and Jansson 1989) but the inducible system of the nickel *nrsB* promoter may be more advantageous, helping to integrate genes which could have a damaging effect on the host by keeping expression low until induction takes place. Studies carried out by Englund *et al.* (2015) also showed that using this promoter may help with genetic instability (Englund *et al.* 2015). In order to improve ethanol production by focusing on promoter variation however, Huang and Lindblad (2013) worked towards developing highly inducible and fully repressed promoters (Huang and Lindblad 2013) which can be used to drive the expression of genes in the ethanol production pathway and in others areas of metabolic engineering and synthetic biology (Huang and Lindblad 2013).

### **1.6.6 Fusion of *pdh* and *adh* genes**

Lewicka *et al.* (2014) showed that the fusion of the *pdh* and *adhII* genes from *Zymomonas mobilis* resulted in a protein exhibiting both PDC and ADH activity which increased ethanol levels in *E.coli*. Cultures expressing the fusion protein showed much higher levels of specific ethanol production (22.6 mM/OD) and cell densities in comparison to those with the unfused protein (8.6 mM/OD) after a 24 hour incubation period. These cultures were normalised to OD at 600 nm which suggested that the increased ethanol levels were not simply due to more cells. They hypothesised that this was due to decreased amounts of the toxic acetaldehyde intermediate and substrate channelling. Even though levels produced in this study were lower than in previous reports, the idea may be utilised in a more realistic setting to investigate if ethanol levels can be improved (Lewicka *et al.* 2014).

### **1.6.7 Increase in carbon uptake**

As photoautotrophic organisms, cyanobacteria take up “dissolved inorganic carbon (DIC)” in the form of bicarbonate ions ( $\text{HCO}_3^-$ ) (Price 2011) through  $\text{HCO}_3^-/\text{Na}^+$  transport mechanisms as well as by the diffusion of carbon dioxide from the surrounding environment (Price and Howitt 2010; Ramanan *et al.* 2012). *Synechocystis* 6803 has three bicarbonate transporters as part of the carbon concentrating mechanism (CCM): SbtA which is an inducible symport with a high affinity and low flux for  $\text{HCO}_3^-/\text{Na}^+$ , BicA which is a constitutive symport with a low affinity and high flux for the above and BCT1 which is a high affinity, inducible uniport. SbtA and BicA are both single-component transporters while BCT1 is a multi-component transporter dependent on ATP (Daley *et al.* 2012).

Work carried out by Kamennaya *et al.* (2015) focused on increasing the uptake of carbon by *Synechocystis* 6803. Strains were constructed with an extra copy of the native BicA transporter and were cultured under various  $\text{CO}_2$  concentrations. It was found that the strains grew nearly twice as fast and produced almost double the amount of biomass in comparison to the wildtype control strain. Even at 0.5 or 5%  $\text{CO}_2$  levels, the new strains still created more biomass than the control although they did grow more slowly and their turbidity levels were also similar to the appearance of the wildtype control (Kamennaya *et al.* 2015).

In the Pembroke Lab, similar strains were created but with BicA replaced with the SbtA transporter to investigate if this would give similar or better results than those achieved above. Work is ongoing to investigate if either transporter would lead to an increase in ethanol levels in this ethanol producing strain (O’Riordan, personal communication, unpublished data).

### **1.7 Ethanol tolerance**

There is also another factor to consider when trying to increase ethanol levels within such a cell factory. Ethanol is not naturally produced by *Synechocystis* 6803 (Pembroke *et al.* 2017) and so one must ask the question: how tolerant is this organism to ethanol? High levels of such a product may impose a stress response from the organism with certain genes being up or down regulated as a sort of coping

mechanism. Changes such as the diversion of carbon away from the usual metabolic pathways as mentioned above will have a negative effect on the cell with regards to growth rate and biomass production (Borirak *et al.* 2015). Ethanol tolerant strains therefore may need to be developed if this process is to become economical. Proteomic analysis as a result is of utmost importance to understand the organism's response to the ethanol product. This will give us further insight into what needs to be done with regards to the overexpression of upregulated genes or knock out of down regulated genes during times of stress due to ethanol build up (Qiao *et al.* 2012). Borirak *et al.* (2015) carried out realistic studies using a glucose tolerant *Synechocystis* 6803 strain which supplied a carbon pool for ethanol production and mimics what would happen during the normal process to produce the biofuel product. It was found that between 60 and 70% of carbon was diverted away from biomass production to product formation with a 71% reduction in growth rate in comparison to the wildtype (WT) strain. Upregulated genes included those involved in the Calvin cycle, in mechanisms to concentrate carbon and the RuBisCo enzyme for carbon fixation. Genes involved in the production of ribosomal and photosynthetic antennae proteins were down regulated more than likely due to the reduction in growth with the majority of carbon diverted towards ethanol formation. As mentioned earlier in Section 1.4.2, the *thiC* gene was up regulated to assist the PDC enzyme during the production process (Borirak *et al.* 2015).

## 1.8 Pembroke Lab Strains

Because of IP issues associated with ethanol cassettes and strains the Pembroke Lab have made a number of isogenic novel ethanol constructs utilising the *Zmpdc* gene, the ICE (Integrative Conjugative Element) R391 *kan* resistance determinant and either *Zmadh* or the native *adh* gene controlled by the pPSBAII promoter in either single or double construct strains which were stably integrated and selected in *Synechocystis* 6803. This work was carried out as part on an EU funded FP7 project termed DEMA (Direct Ethanol from Microalgae). These strains and recombinant constructs provided a source of tester strains to modify and attempt to improve.

The following constructs and strains were created and kindly provided by Dr. Patricia Armshaw (personal communication, unpublished data) in the Pembroke Molecular Biochemistry Lab, University of Limerick, Limerick, Ireland. (For a clarified explanation on all constructs and strains used in this project, see appendix IV A and B).

### 1.8.1 UL004

UL004 is an ethanol producing strain which consists of a pUC18 backbone, the pPSBAII light promoter from *Synechocystis* 6803, the native *slr1192 adh* gene, the *pdc* gene from *Zymomonas mobilis* and the *kanamycin* resistance gene from ICE R391 (Armshaw and Pembroke 2013). All is located in the PSBAII neutral site in the *Synechocystis* 6803 chromosome with the construct created via homologous recombination (see Section 3.2.2 and Figure 1.6 below). The glucose tolerant strain of wildtype *Synechocystis* 6803 was obtained with gratitude from Professor Klass Hellingwerf, UvA, Amsterdam.

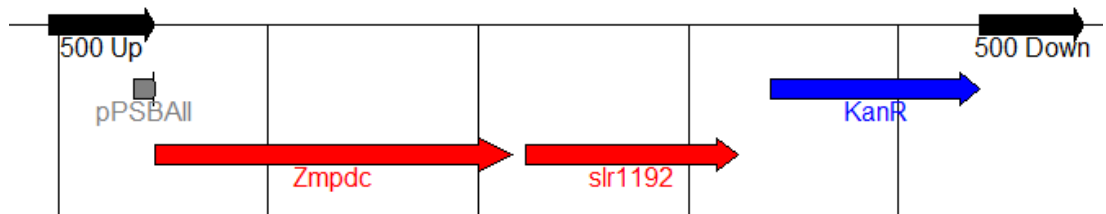


**Figure 1.6: Flow diagram of pUL004** (constructed in GENTle, see Section 2.7.3.1) explained in more detail in Figure 1.7 below.

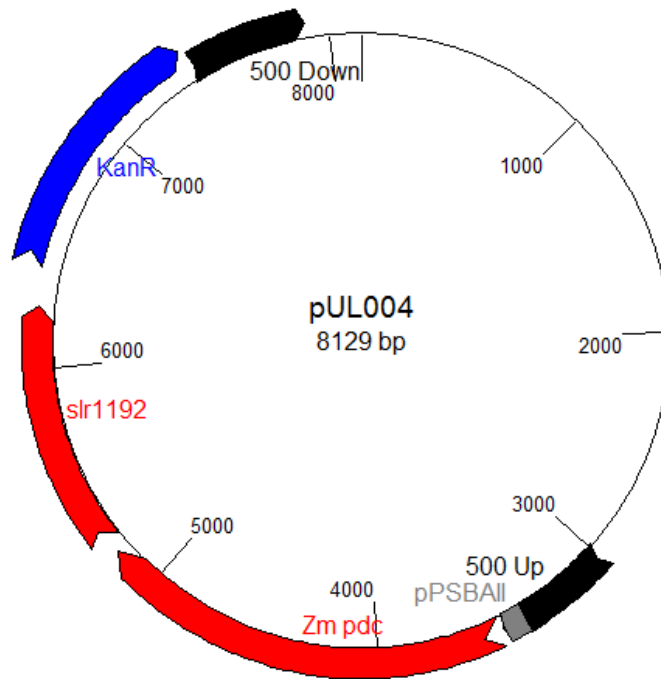


**Figure 1.7: pUL004.** (Constructed in GENTle, see Section 2.7.3.1). This construct shows the pPSBII promoter of *Synechocystis* 6803 amplified and fused to the *Zymomonas mobilis pdc* (*Zmpdc*) and linked to the native *Synechocystis* 6803 *adh* (*slr1192*) and *kanamycin* resistance gene (a gene encoding kanamycin phosphotransferase which was amplified from the enterobacterial ICE R391). This construct which was verified by sequencing contained two 500 bp flanking regions which were homologous to the PSBII neutral site in *Synechocystis* 6803. It was now suitable for transformation and incorporation into this site. Transformants were initially screened for kanamycin resistance and the level of kanamycin then gradually increased (as per Section 3.5) to allow for screening and selection for full segregation into the polyploidy genome of *Synechocystis* 6803. Primer sets spanning the PSBII site were designed to differentiate between full incorporation of this construct into every copy of the chromosome, partial non segregated incorporation and no incorporation.

## 1.8.2 UL030

UL030 was also created in the Pembroke Lab which consisted of a UL004 backbone (as described above) but contained two copies of a modified cassette for the purpose of gene dosage as mentioned earlier. However, because the PSBII neutral site was already occupied by the UL004 construct in its transformed host, a new site for the second cassette had to be chosen. This was based on work carried out by Gao *et al.* (2012) in which the *phaA* and *phaB* genes involved in the PHB pathway were deleted by the incorporation of the *Zmpdc* and native *adh* into these sites (Gao *et al.* 2012). The same pPSBII promoter controlling the expression of *pdc* and *adh* was used but a *zeocin* resistance gene from the pcDNA3.1+ plasmid

(Armshaw and Pembroke 2013) replaced kanamycin for the second cassette and the 500 bp regions were homologous to the *phaA* and *phaB* genes to drive integration of the second cassette into this site. The constructed strain, UL030, therefore contained two copies of the *Zmpdc* and two copies of the native *adh* as well as the copy of this *adh* gene already contained within the chromosome. It also used a different neutral site (PHB vs PSBAII) and resistance gene (*zeocin* vs *kanamycin*) compared to that used in the construction of UL004. The created vector pUL030 can be seen below in Figure 1.8.

The constructed strains (UL004 and UL030) using pUL004 and pUL030 respectively are compared in Figure 1.9.

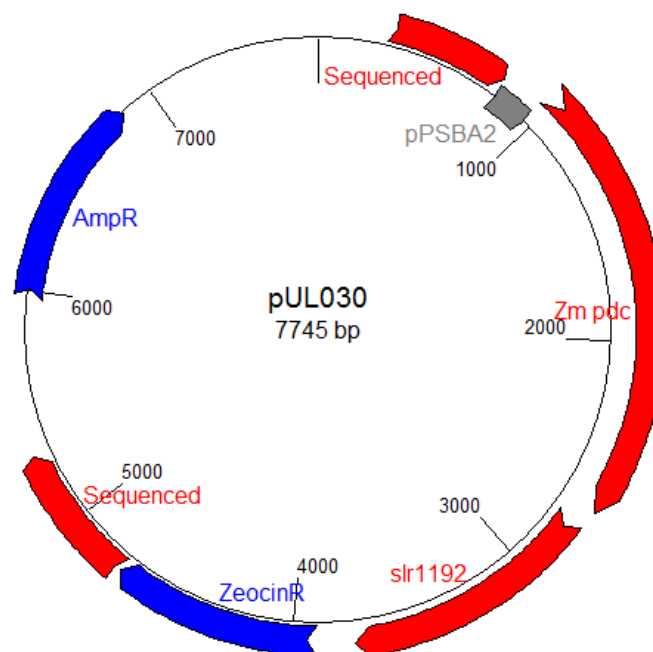


**Figure 1.8: pUL030.** (Constructed in GENTle, see Section 2.7.3.1). This construct shows the pPSBAII promoter of *Synechocystis* 6803 amplified and fused to the *Zymomonas mobilis pdc* (*Zmpdc*) and linked to the native *Synechocystis* 6803 *adh* (*slr1192*) and *kanamycin* resistance gene (a gene encoding kanamycin phosphotransferase which was amplified from the enterobacterial ICE R391). This construct which was verified by sequencing contained two 500 bp flanking regions which were homologous to the *phaA* and *phaB* genes in *Synechocystis* 6803. It was now suitable for transformation and incorporation into this site. Transformants were initially screened for zeocin resistance and the level of zeocin gradually increased (as per Section 3.5) to allow for screening and selection for full segregation into the polyploidy genome of *Synechocystis* 6803. Primer sets spanning the *phaAB* site were designed to differentiate between full incorporation of this construct into every copy of the chromosome, partial non segregated incorporation and no incorporation.

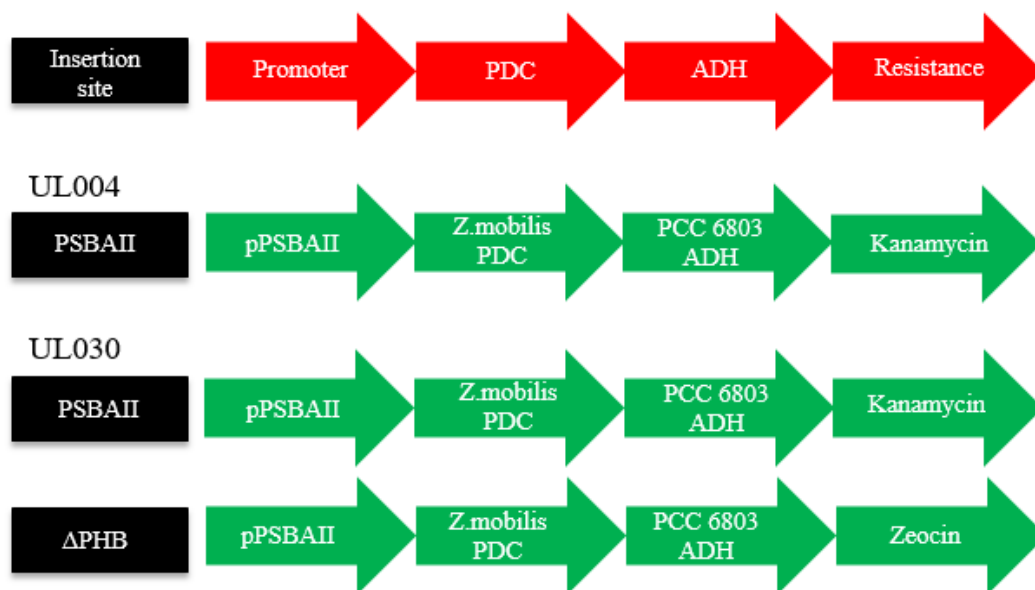


**Figure 1.9: Summary diagram representing the nature of the cassette constructs in the constructed strains UL004 and UL030 illustrating the insertion site PSBAII and PHB, the pPSBAII promoter utilised to express the cassette constructs, the genes expressed and the resistant determinant utilised.**

## 1.9 Aim of this study

The focus on utilising the photoautotrophic cyanobacterium *Synechocystis* 6803 as a model organism cell factory to examine the production of biofuels, in this case ethanol, ultimately requires maximum productivity of the biofuel product. As described earlier this might be achieved in several ways including increased gene dosage via improved or regulated promoters, via pathway knockouts to increase flux to pyruvate or via enhancement of enzymes or cofactors to increase carbon flux into the cell.

During this project, the following hypothesis was examined: could ethanol productivity be enhanced by substitution of an alternative PDC (reported to possess a lower  $K_m$  from *Zymobacter palmae*, see appendix III D) to the traditional ZmPDC? In order to test this hypothesis the following steps were taken:

- The *Zppdc* gene from *Zymobacter palmae* was amplified (see appendix III C) and used to construct a new cassette where the *Zppdc* gene was substituted for that of the *Zmpdc* to generate a new strain UL071.

- The *Zppdc* gene sequence was codon optimised (see appendix III E) to minimise the effect of codon bias in limiting expression in the heterologous host giving UL072.
- Expression of the ZpPDC was carried out following transformation, integration into the PSBAII neutral site (chosen to allow genetic comparison), selection and full segregation.
- To examine the ZpPDC more thoroughly the protein was his-tagged and overexpressed, purified to homogeneity and crystallisation trials were initiated as a preliminary step to determine more information on its activity and structure.

## **Chapter 2: Materials and Methods**

## 2.1 Media and bacterial strains

Unless otherwise stated, all media (e.g. broth, agar) and reagents (e.g. restriction enzymes, PCR reagents, vectors etc.) were purchased from Sigma Aldrich Ireland Ltd. (Arklow, Wicklow, Ireland), Thermo Fisher Scientific (Ballycoolin, Dublin 15, Ireland) or New England Biolabs® Inc. (Hitchin, SG4 0TY, United Kingdom).

Media was prepared by dissolving the correct amount of powder in distilled water (or adding the correct reagents) and autoclaving for 15 minutes at 15 lb.in<sup>-2</sup> pressure at 121°C for sterilisation. Any filter sterilisation was carried out using a Filtropur S 0.2 µm filter from Sarstedt (51588 Numbrecht, Germany).

Rehydration of the *Zymobacter palmae* was carried out as per the information leaflet from DSMZ. The strain was cultured using the specified media (see appendix I B). Other strains used include: BL21 (DE3)\* expression strain of *E.coli* from Thermo Fisher Scientific (Ballycoolin, Dublin 15, Ireland), wildtype *Synechocystis* sp. PCC 6803 from Professor Klass Hellingwerf, UvA, Amsterdam and UL004, ethanol producing strain of altered wildtype *Synechocystis* sp. PCC 6803 from Dr. Patricia Armshaw (personal communication, unpublished data), Pembroke Molecular Biochemistry Lab, UL, Limerick, Ireland.

## 2.2 Plates, overnight cultures, bacterial stocks and antibiotics

Agar plates were incubated at 30°C for the appropriate length of time. They were also used to inoculate (overnight) broth cultures which were incubated at the appropriate temperature (usually between 30 and 37°C), 200 revolutions per minute (rpm) agitation with the correct antibiotics.

Bacterial stocks were prepared in Luria-Bertani (LB) broth with 50% glycerol (for *E.coli*) or 50% BG-11 media containing 5% (v/v) methanol (for *Synechocystis* 6803) and stored at -80°C.

Antibiotics were prepared in the correct solvent at 1000X concentration, filter sterilised and aliquoted to 1 ml amounts. These were stored at -20°C. Antibiotics

used: streptomycin 100  $\mu\text{g.ml}^{-1}$ , ampicillin 100  $\mu\text{g.ml}^{-1}$ , kanamycin 50  $\mu\text{g.ml}^{-1}$  and zeocin 20  $\mu\text{g.ml}^{-1}$ .

## 2.3 Cloning Methods

### 2.3.1 Template preparation

Template for Polymerase Chain Reaction (PCR): For plasmid, a 1/10 dilution was made in DNase/RNase free water and 1  $\mu\text{l}$  used in the reaction while for the amplification of a gene, a small amount of culture (*E.coli* or *Synechocystis* 6803) was placed in 30  $\mu\text{l}$  of DNase/RNase free water as well as some acid washed glass beads of  $<106 \mu\text{m}$ , vortexed for  $\sim 30$  secs with the vortex 2 genie, scientific industries from VWR (Ballycoolin, Dublin 15, Ireland) and centrifuged at 13,400 rpm for 1 minute in a super mini desktop centrifuge from Medical Supply Company Ltd. (MSC, Dublin 15, Ireland). 1  $\mu\text{l}$  of the supernatant was used in the reaction.

### 2.3.2 Traditional Cloning

PCR mix for amplification of the insert contained DNase/RNase free water, GC buffer with  $\text{MgCl}_2$ , the appropriate primers as described in appendix II, dNTPs, template DNA prepared as per Section 2.3.1, 3% DMSO and Phusion™ HF DNA polymerase. An extension time of 15-30 secs/kb is recommended for this polymerase. The cycling conditions were as follows with the PCR carried out using a 2720 Applied Biosystems Thermal Cycler from Thermo Fisher Scientific (Ballycoolin, Dublin 15, Ireland):

Initial denaturation	98°C, 1 minute
Denaturation	98°C, 10 seconds
Annealing	50°C, 20 seconds
Extension	72°C, 1 minute (30 secs/kb for $\sim 2\text{kb}$ gene)
Final extension	72°C, 5 minutes
Hold	4°C, hold

35 cycles

The PCR product was purified from a 1% agarose gel as per Section 2.3.5. The following mixes were then used for the restriction digests of the insert and the

empty pET22b (+) vector: DNase/RNase free water, buffer, NdeI and NotI restriction enzymes (see appendix I A) and amplified insert/vector. 37°C, ~2.5 hours. The digested plasmid was also purified from a 1% agarose gel as per the same section above. The ligation ratios were varied for insert: vector (e.g. 1:1, 3:1, 7:1) with the mixes containing the correct amount of insert and vector, DNase/RNase free water, ligation buffer and ligase. Samples were left to ligate at 22°C for ~3 hours using the Eppendorf® Mastercycler personal Thermal Cycler from Sigma Aldrich (Arklow, Wicklow, Ireland).

### **2.3.2.1 Restriction Analysis**

A single digest was carried out to verify the insertion of the *Zppdc* into the pET22b (+) vector. Reaction mixture contained plasmid DNA with the *Zm* or *Zppdc*, buffer, water and the SacII enzyme. 37°C, 2 hours. Samples were analysed on a 1% agarose gel as per Section 2.3.5.

### **2.3.3 Clontech In-Fusion Cloning**

PCR mixes for the amplification of an insert and the linearisation of a vector contained PCR premix (reaction buffer, dNTPS, MgCl<sub>2</sub>, DNA polymerase), the appropriate primers as described in appendix II, template DNA prepared as per Section 2.3.1 and DNase/RNase free water. The appropriate cycling times and reagent quantities were used as per the In-Fusion® HD cloning kit user manual (Clontech Laboratories Inc. 2014) from Takara Bio Company, Mountain view, California, USA. PCR products were purified as per Section 2.3.5. The enzyme reaction contained amplified insert, linearised vector, enzyme premix and DNase/RNase free water. Heated for 15 minutes at 50°C. Transformed into stellar cells via heat shock as per the ClonTech instruction manual and spread on two LB agar plates with 100 µg.ml<sup>-1</sup> ampicillin/100 µg.ml<sup>-1</sup> kanamycin depending on the construct requirements. Incubated at 30°C for ~20 hours.

### **2.3.4 Agarose gels for DNA analysis**

Agarose gels for DNA analysis were prepared to the appropriate percentage by dissolving the correct amount of genetic analysis grade agarose powder in 50 ml of 1X TAE buffer prepared from a 50X stock solution. Gels for DNA analysis were always run with a 1 kb DNA ladder from NEB (New England Biolabs® Inc. (Hitchin, SG4 0TY, United Kingdom)) with samples in 6X purple gel loading dye in a horizontal electrophoresis tank filled with 1X TAE buffer prepared as above.

### **2.3.5 Plasmid extraction and PCR clean-up**

Plasmid extraction was carried out using the Qiagen QIAprep Spin Miniprep plasmid extraction kit (Fleming Way, Crawley, West Sussex, RH10, 9NQ, UK) as per the instruction manual (Qiagen 2013) while the Promega Wizard® SV Gel and PCR Clean-Up System from MSC was used to purify PCR products from agarose gels or directly from the reaction also according to the instruction manual (Promega Corporation 2016).

### **2.3.6 DNA sequencing**

When necessary, DNA sequencing was carried out by Source BioScience (Tramore, Waterford, Ireland) and Eurofins Genomics (Anzingerstr. 7a, 85560 Ebersberg, Germany) using the appropriate primers as per appendix II. Samples were prepared according to the company's requirements as outlined on the respective websites (Eurofins Genomics 2016; Source Bioscience 2016).

Sequencing results were analysed using the nucleotide Basic Local Alignment Search tool (BLAST n) from the NCBI (National Centre for Biotechnology Information) which can be reached here:

[https://blast.ncbi.nlm.nih.gov/Blast.cgi?PROGRAM=blastn&PAGE\\_TYPE=BlastSearch&LINK\\_LOC=blasthome](https://blast.ncbi.nlm.nih.gov/Blast.cgi?PROGRAM=blastn&PAGE_TYPE=BlastSearch&LINK_LOC=blasthome).

## **2.4 Transformation**

### **2.4.1 Transformation into *E.coli***

Electrocompetent cells were prepared as per (Murphy 1998). For a (i) ligation, 25 µl of DNA was added to 70 µl of electrocompetent cells while for a (ii) plasmid, 1 µl of DNA was added to 50 µl of electrocompetent cells. The reaction mixture was

placed in appropriate cuvettes and the cells were electroporated using the Easyject prima™ equibio electroporator from MSC. The cells were added to LB broth and left to recover for ~45 minutes at 150/175 rpm agitation and 30-37°C. The reactions were subsequently plated on two LB agar plates with the appropriate antibiotics (100 µg.ml<sup>-1</sup> of streptomycin and ampicillin for Top 10 cells/100 µg.ml<sup>-1</sup> of ampicillin for BL21 (DE3)\* cells) and incubated at 30°C for ~17 hours.

## 2.4.2 Transformation into *Synechocystis* sp. PCC 6803

Steps involved in the transformation of the following constructs into wildtype *Synechocystis* sp. PCC 6803:

-pUL004: *Zmpdc*, *slr1192* (native *adh*) and *kanamycin* resistant gene in the PSBAII neutral site under the control of the pPSBAII light promoter.

-pUL101: *Zppdc*, *slr1192* (native *adh*) and *kanamycin* resistant gene in the PSBAII neutral site under the control of the pPSBAII light promoter.

-pUL102: *ZpOpdc*, *slr1192* (native *adh*) and *kanamycin* resistant gene in the PSBAII neutral site under the control of the pPSBAII light promoter.

**Note:** the transformation of pUL004 had already been undertaken (see Section 1.8.1) and resulted in the creation of UL004.

*Synechocystis* 6803 cells were cultured to mid exponential phase optical density (OD) 730nm 0.6-1.2 at 2% CO<sub>2</sub>, 150 rpm agitation, 30°C and ~80-100 µE m<sup>-2</sup> s<sup>-1</sup> of white light illumination in a Multitron Pro, Infors HT incubator. **Note:** growth of cultures sometimes varied and so if the OD<sub>730nm</sub> was too high i.e. above 1.2, dilutions were made in order to reduce it to an acceptable OD<sub>730nm</sub>. In brief, 20 ml of cells were centrifuged at 4,000 rpm for 10 minutes. The supernatant was removed taking great care not to disturb the pellet which could be quite loose. The cells were washed with 20 ml of BG-11 + HEPES and centrifuged again. The supernatant was removed in the same way as above and the pellet was re-suspended in 1 ml of BG-11 + HEPES to give an approximate OD<sub>730nm</sub> of 10. **Note:** Another centrifugation step was sometimes necessary if the pellet became dislodged and a dilution was made if the OD<sub>730nm</sub> was too high. Natural transformation was carried out as per Zang *et al.* (2007) (Zang *et al.* 2007) but with some modifications: 50 µl of cells were placed in 6 sterile 1.5 ml tubes. 1 µl of 20% glucose (filter sterilised

before use) was added to 3 of the tubes while 10  $\mu\text{l}$  of the correct DNA construct in the range of 100-300  $\text{ng}\cdot\mu\text{l}^{-1}$  (PSBAII constructs containing *Zm*, *Zp*, *ZpOpdc*) was added to the 6 tubes.

Overall, there was the following:

<i>Zmpdc</i> +/- glucose	<i>Zppdc</i> +/- glucose	<i>ZpOpdc</i> +/- glucose	
2 tubes (control)	2 tubes	2 tubes	= 6 tubes in total

The 6 tubes were placed on a tray, covered with one layer of tissue paper to receive low/medium light intensity ( $\sim 20\text{-}40 \mu\text{E m}^{-2} \text{s}^{-1}$ ) and placed in the 30°C incubator for  $\sim 16$  hours. The following day, 12 BG-11 agar plates were made with 5  $\mu\text{g}\cdot\text{ml}^{-1}$  kanamycin and +/- 20 mM glucose. The transformants were spread on the 12 plates with 6 placed under low light intensity ( $\sim 20\text{-}40 \mu\text{E m}^{-2} \text{s}^{-1}$ , LL low light) and 6 under high light intensity ( $\sim 80\text{-}100 \mu\text{E m}^{-2} \text{s}^{-1}$ , HL high light) and allowed to grow for  $\sim 5\text{-}10$  days.

<i>Zmpdc</i> + glucose, high light	<i>Zmpdc</i> + glucose, low light
<i>Zmpdc</i> - glucose, high light	<i>Zmpdc</i> - glucose, low light
<i>Zppdc</i> + glucose, high light	<i>Zppdc</i> + glucose, low light
<i>Zppdc</i> - glucose, high light	<i>Zppdc</i> - glucose, low light
<i>ZpOpdc</i> + glucose, high light	<i>ZpOpdc</i> + glucose, low light
<i>ZpOpdc</i> - glucose, high light	<i>ZpOpdc</i> - glucose, low light
6 plates	6 plates

As many colonies as possible were then streaked onto BG-11 agar plates with the same conditions as above but with increasing antibiotic pressure (5, 25, 50, 100  $\mu\text{g}\cdot\text{ml}^{-1}$  kanamycin) to allow for integration into the polyploid genome and eventually result in full segregation. PCR screening was used to check and verify for full segregation of the construct into the PSBAII site and fully segregated colonies were verified using PCR and DNA sequencing of the *Zm*, *Zp* or *ZpOpdc* PCR product.

### PCR screening conditions:

A PCR mastermix was made depending on the number of colonies to be screened. The mix included DNase/RNase free water, HF buffer, the appropriate primers as per appendix II, dNTPS, Phusion™ HF DNA polymerase and template prepared as per Section 2.3.1. The following conditions were used to screen for a ~4 kb product (the pPSBAII promoter, *pdc*, *adh*, kanamycin).

Initial Denaturation:	98°C, 1 minute
Denaturation:	98°C, 10 seconds
Annealing:	65°C, 20 seconds
Extension:	72°C, 2 minutes (30secs/kb for ~4 kb area)
Final extension:	72°C, 5 minutes
Hold	4°C
35 cycles	

## 2.5 Ethanol Determination

Ethanol determination was carried out using the Yellow line kit: UV-method for the determination of ethanol in foodstuffs and other materials from R-Biopharm AG (Darmstadt, Germany). The chosen strains were cultured to mid exponential phase as per Section 2.4.2, adjusted to OD<sub>730nm</sub> of 0.4 and assayed for ethanol three days later as per the instruction manual (R-Biopharm AG 2014) but with some modifications: 1 ml instead of 3 ml cuvettes were used in this study therefore volumes had to be adjusted.

Calculations were carried out as follows:

B<sub>0</sub>: First blank.      B<sub>1</sub>: Second blank.

A<sub>0</sub>: First sample reading.      A<sub>1</sub>: Second sample reading.

$$\Delta A = A_1 - A_0 - (B_1 - B_0).$$

**Note:** Multiply  $\Delta A$  by your dilution factor before working out the next calculations.

$$\text{Ethanol (g.L}^{-1}\text{)} = \Delta A \times 0.115174.$$

$$\text{Ethanol (g/L/OD}_{1730\text{nm}}\text{)} = (\Delta A \times 0.115174) / \text{OD}_{730\text{nm}}.$$

Cultures were assayed for ethanol on days 3, 7 and 11. Samples were diluted 1/10, 1/20 and 1/40 so as not to surpass the detection limit of the kit.

## **2.6 Expression and Purification of *Zymobacter palmae* PDC**

### **2.6.1 Expression**

The *Zymobacter palmae* PDC (ZpPDC) was expressed as per Gao *et al.* (2012) using the *E.coli* BL21 (DE3)\* expression strain transformed with the pULLQ2 plasmid (Figure 3.4) (Gao *et al.* 2012) with minor modifications. Following induction and harvesting of the cells, a sample of the supernatant and the cell pellet were taken to analyse later and were stored in the -20°C freezer. Depending on the number of cells they were washed with 5-10 ml of binding buffer (20 mM Tris-HCl, 50 mM NaCl, pH 7.9, minus 5 mM imidazole). The supernatant was removed and the appropriate amount of binding buffer (plus 5 mM imidazole) was added to each tube to re-suspend the cells which were subsequently placed into a beaker. 1 mg.ml<sup>-1</sup> of lysozyme was added to the combined cells and left to stir on the bench for 1 hour. A tip of DNase and MgCl<sub>2</sub> was added to a concentration of 5 mM and the cells were left to stir for 1 hour in the fridge. The beaker of cells was placed on ice and sonicated using a Sjia lab ultrasonic cell crusher sonicator for 10 minutes at 15% amplitude, 0.3 second pulse on and 3 second pulse off. Cells were left to rest for 30 minutes and the process was repeated. Cells were centrifuged at 24,500 g for 1 hour at 4°C using a Sorvall RC 6+ centrifuge from Thermo Fisher. The clarified cell lysate was placed in a pre-chilled 50 ml tube and held at 4°C. Samples of the cell pellet and lysate were also taken and stored in the -20°C freezer as before.

### **2.6.2 ZpPDC Purification**

Due to the presence of the 6X histidine tag, the ZpPDC was purified using a nickel resin (Sepharose 6 fast flow resin from GE healthcare, Carrigtwohill, Cork, Ireland) and IMAC (Immobilised Metal Affinity Chromatography) according to Gao *et al.* (2012) with minor modifications (Gao *et al.* 2012). An XK column from GE healthcare was used for the initial purification and was prepared in the following way:

### **2.6.2.1 Preparation of column**

For equilibration, the 5 ml column was washed with a large amount of MilliQ (MQ) water, ~4-5 column volumes (CV) of 200 mM NiSO<sub>4</sub> to generate the column, ~5 CVs of binding buffer with imidazole and more MQ water. The clarified cell lysate was applied to the column overnight at a speed of 1 ml.min<sup>-1</sup> using a Watson Marlow pump from Lennox (Dublin 12, Ireland).

### **2.6.2.2 IMAC purification**

The flow through was collected in a 100 ml cup. The column was then connected to the Akta prime™ plus purification system from GE healthcare which was used to purify the PDC. It was washed with 30 mls (6 CVs) of 20, 60, 100 and 150 mM wash buffers to elute loosely bound unwanted proteins (binding buffer as above in Section 2.6.1 and the appropriate amount of imidazole) and 15 ml fractions were collected and stored at 4°C. Samples were taken for sodium dodecyl sulfate polyacrylamide gel electrophoresis (SDS-PAGE) and Western blot analysis. The column was then washed with 30 mls (6 CVs) of the 250, 350, 500 and 1000 mM elution buffers (same as above) and 5 ml fractions were collected and stored. Samples were also taken as above.

### **2.6.3 SDS-PAGE gel and Western blot analysis**

The collected samples were run on a 12% SDS-PAGE gel (see Section 2.6.3.1) to establish what fraction(s) the PDC protein was located. A Western blot was also carried out to ensure the identified protein was the PDC (see Section 2.6.3.2).

#### **2.6.3.1 SDS-PAGE**

SDS-PAGE gels were made as outlined by Bio-Rad 2016 (Bio-Rad 2016) using Bio rad equipment distributed by Fannin Scientific (Dublin 18, Ireland) and were run using the Mini-PROTEAN Tetra cell vertical gel electrophoresis unit and a basic powerpac. A PageRuler™ plus pre-stained protein ladder was run on every gel. A 12% resolving gel and 4.5% stacking gel were used throughout the project and were made via the following recipes in Table 2.1:

**Table 2.1: SDS-PAGE gel recipe.**

	4.5% stacking gel	12% resolving gel
MQ water	3.6 ml	6.3 ml
40% acrylamide	640 $\mu$ l	4.5 ml
1 M Tris-HCl pH 6.8/8.8	630 $\mu$ l	3.9 ml
10% SDS	50 $\mu$ l	150 $\mu$ l
10% APS	50 $\mu$ l	150 $\mu$ l
TEMED	6 $\mu$ l	6 $\mu$ l

1X SDS-PAGE running buffer was made from a 5X stock (Tris, glycine, SDS, distilled/MQ water) and the tank was filled to the two or four gel mark. Cell pellet samples were prepared by boiling for ~10 minutes at 98-100°C in 80  $\mu$ l of 1X SDS loading dye and using 10  $\mu$ l of the supernatant once centrifuged. Supernatant samples were used directly. 2  $\mu$ l of 5X SDS loading dye was added to both preparations prior to loading onto the gel to give a total volume of 12  $\mu$ l. One gel was run for ~1 hour at 28 mA and was visualised by staining with Instantblue protein stain from Expedeon, distributed by MyBio (St Kieran's College Road, Kilkenny, Ireland). The gels were subsequently destained in MQ water, scanned and stored short term at 4°C.

### 2.6.3.2 Western blots

For the Western blot, a sandwich was prepared and assembled as outlined by Thermo Fisher Scientific 2015 (Thermo Fisher Scientific 2015). Any bubbles were removed and the blot was run for ~70 minutes at 80 mA using a semi-dry HORIZEBLOT 2M-R blotter from Gentaur (London N20 9BH, United Kingdom). Once the contents of the gel had transferred over to the membrane, the gel was discarded and the membrane was soaked in a 1% skim milk solution overnight (to block any unoccupied sites) which was made in 1X TBS (Tris buffered saline) buffer from a 10X stock (1 M Tris-HCl pH 7.4, 5 M NaCl and MQ water). The milk solution was removed the following day and three fifteen minute washes were performed with 1X TBST prepared by adding 10% tween solution to 1X TBS to achieve a concentration of 0.2% tween. The membrane was then covered in the

antibody solution (BSA, 1X TBST, 5 µl aliquot of the anti his-tag HRP (horse radish peroxidase conjugated antibody) and left to rock for ~2 hours. One more fifteen minute wash with 1X TBST was carried out once the 2 hours had elapsed and the blot was stained with 1-2 mls of TMB (3,3',5,5' tetramethylbenzidine) substrate in order to visualise the protein of interest due to a colour development caused by an enzymatic reaction. The blot was scanned and discarded.

#### **2.6.4 Dialysis**

From the results of both the gel and blot, it was decided what fractions to pool. BioDesign Dialysis Tubing™ (D106) with an 8,000 MWCO (molecular weight cut-off) point and dialysis tubing clips both from Thermo Fisher were used to dialyse the protein into 30 mM Tris-HCl buffer pH 7.9 to remove the imidazole. Three two hour 30:1 washes were carried out in the fridge at 4°C with constant stirring.

#### **2.6.5 Protein concentration**

The dialysed protein was concentrated to 1 ml amounts using an Amicon® ultra-15 centrifugal filter from Merck Millipore (Carrigtwohill, Cork, Ireland) with a 50 kDa NMWL (nominal molecular weight limit) at 2,200 g and 4°C. The concentration of the protein was checked on the Nanodrop spectrophotometer ND-1000, aliquoted and stored in liquid nitrogen in the -80°C freezer.

#### **2.6.6 Regeneration of the column**

The IMAC column was then stripped by washing with a large quantity of MQ water followed by 0.5 CVs of 200 mM EDTA, 500 mM NaCl pH 7.0. Any residual EDTA was removed with 2-3 CVs of 500 mM NaCl. The column was quickly washed with 1-2 CVs of 500 mM NaOH and then with at least 2 CVs of MQ water. As before, the column would be regenerated with ~4-5 CVs of 200 mM NiSO<sub>4</sub> and then washed with ~5 CVs of binding buffer with imidazole for equilibration and finally with more MQ water.

## **2.7 Crystallisation trials**

### **2.7.1 Initial crystallisation trials**

For the initial trials to crystallise the ZpPDC using the Hampton Research Index Screen HR2-144 from Hampton Research (CA 92656-3317, USA) the plates were set up in the following way (see Figure 2.1): Only one plate was opened at a time so as to avoid any contamination. The lid was removed and the plate was labelled with the reservoir solution number, the type and concentration of protein, initials and date. 250  $\mu\text{l}$  of the 96 reservoir solutions were used to fill each well over the four plates. The 50  $\text{mg}\cdot\text{ml}^{-1}$  protein was diluted to 5  $\text{mg}\cdot\text{ml}^{-1}$  as a starting protein concentration. 1  $\mu\text{l}$  of the protein was mixed with 1  $\mu\text{l}$  of each of the 96 reservoir solutions on the corresponding stage. This was mixed gently to avoid the formation of bubbles which could interfere with crystal growth. Two columns of each plate were filled at a time and then sealed as opposed to filling the entire plate all at once. This was done to prevent evaporation of the small amounts of liquid. The plates were sealed with crystal clear sealing tape from Hampton Research (CA 92656-3317, USA) and covered with the supplied lid (Hampton Research 2006b).

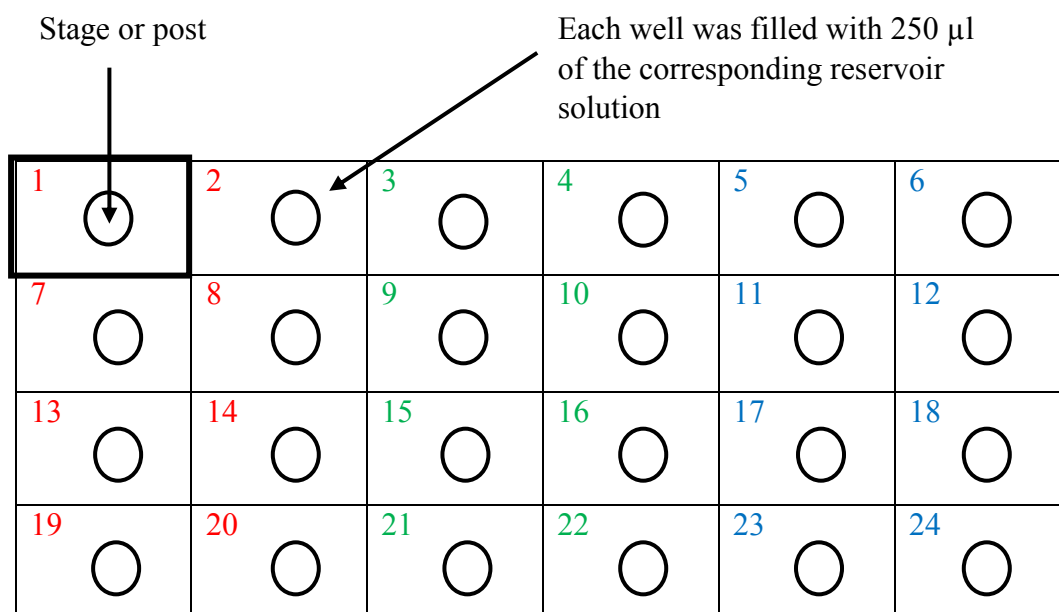


**Figure 2.1: Example of the plate set up used for the Initial Index Screen (initial trials).** Colours indicate the fill of two columns at a time. Each square represents a reservoir and the circle a stage or post.

-Condition number 75 from the Hampton Research Index Screen: 0.2 M lithium sulphate, 0.1 M BIS-TRIS pH 6.5 and 35% PEG 3350.

-Condition number 88 from the Hampton Research Index Screen: 0.2 M ammonium citrate tribasic pH 7.0 and 20% PEG 3350. (Not pursued but for reference).

### 2.7.2 Follow on crystallisation trials

1 M concentrations of lithium sulphate and BIS-TRIS pH 6.5 were prepared as per the Hampton Research Index Fundamentals guide (Hampton Research 2006a) to prepare condition number 75. The appropriate amounts were used to achieve 0.2 M and 0.1 M concentrations of each reagent respectively. A 50% stock of PEG 3350 was prepared by dissolving 5 g of PEG in 5 ml of MQ water at 50°C and 180 rpm. The appropriate amount was added to the lithium sulphate and BIS-TRIS to achieve the following percentages: 15, 17, 20, 22.5 and 30%. Screen number 75 with 25% PEG 3350 was used as a control. The ZpPDC protein was varied at 1, 2, 5 and 10 mg.ml<sup>-1</sup> by diluting the stock of 50 mg.ml<sup>-1</sup> with the buffer it was dialysed into i.e. 30 mM Tris-HCl pH 7.9. Only one plate was needed for the optimised conditions and was filled in the same way as above (see Figure 2.2) with the exception of using 400 µl of reservoir solution rather than 250 µl:

	PEG 3350				Screen 75	
[PDC] mg.ml <sup>-1</sup>	30	22.5	20	17	15	25
10	1 ○	2 ○	3 ○	4 ○	5 ○	6 ○
5	7 ○	8 ○	9 ○	10 ○	11 ○	12 ○
2	13 ○	14 ○	15 ○	16 ○	17 ○	18 ○
1	19 ○	20 ○	21 ○	22 ○	23 ○	24 ○

**Figure 2.2: Example of the plate set up used for the Optimised Index Screen (follow on trials).** Colours indicate the fill of two columns at a time. Each square represents a reservoir and the circle a stage or post. PDC protein concentration varied vertically while PEG 3350 concentration varied horizontally.

### 2.7.3 Homology Modelling

Figures 3.53, 3.54 and 3.55 were constructed using Swiss PDB Viewer Version 4.1.0. The amino acid sequence of ZpPDC was obtained from the NCBI website which can be found here:

<https://www.ncbi.nlm.nih.gov/protein/21359680?report=fasta>

This sequence was copy and pasted to a notepad in FASTA format and was loaded into Swiss PDB Viewer by carrying out the following steps: in the program click on swiss model and then load raw sequence from amino acids. Here the saved ZpPDC amino acid sequence was selected. The ZpPDC was modelled against the PDC from *Zymomonas mobilis* (the template) and so the PDB file for this enzyme (1ZPD) was downloaded from the PDB website which can be found here:

<http://www.rcsb.org/pdb/explore/explore.do?structureId=1ZPD>

This was also loaded into the Swiss PDB Viewer by clicking file, open PDB file and selecting 1ZPD.

The following steps were taken in order to thread the amino acid sequence of ZpPDC through the ZmPDC structure to create a model: click select and all. Then fit and magic fit. Centre the final image by using the buttons on the toolbar. Then

click window, layers info and colour by layer to differentiate between the Zm and ZpPDC. The receptor (ZpPDC) will be in yellow and the model (ZmPDC) in blue. One can toggle between the two by clicking on the grey line at the top of the control panel. Because the Zm and ZpPDCs are tetramers, there were four chains visible in the control panel: A, B, E and F. When comparing the two PDCs, only one monomer was selected for each for simplicity. A table was made (Table 3.20) in order to show the amino acid residues in the active site and vicinity of the active site in the PDC for both Zm and Zp and to highlight any differences. Using the control panel only these amino acid residues were made visible. Labels were added using the control panel and the buttons on the toolbar were used to zoom in and out and to rotate the model. Images were captured using the snipping tool and presented in Section 3.10.

### **2.7.3.1 Other programs used as part of this project:**

- Microsoft Excel was used to create any Michaelis-Menten graphs and Lineweaver-Burk plots by collating and highlighting the desired data and selecting scatterplot. The appropriate legends were applied in each instance along with any trendlines and other labels.
- Microsoft Excel was also used to create bar charts for optical density and ethanol measurements. The same steps as above were taken but bar chart was selected instead of scatterplot.
- Microsoft Word was used to create any images or tables throughout the project.
- Clustal alignments of amino acid sequences were created using the CLUSTAL Omega Algorithm which can be reached here: <http://www.ebi.ac.uk/Tools/msa/clustalo/>  
Sequences to be aligned were presented in FASTA format in a word document, one following the other and with the > symbol in front of each title. The sequences were copy and pasted into the tool and the output format was selected as GCG/MSF which is the format required by GENEDOC to read the output file and display the alignment. Run was selected to put through the request and the resulting file was downloaded. The GENEDOC tool was opened and the downloaded file was selected by clicking file, open

and selecting the correct file. The toolbar was used to change the appearance of the alignment. Images were captured by clicking “edit” and “select blocks to copy”. The desired areas were highlighted and edit was selected again followed by “copy selected blocks to bitmap” and “copy 256 colour DIB”.

- GENTle was used to create any vector maps throughout this study. DNA sequences for the desired vector was entered into GENTle by downloading the DNA sequence in plain format from Addgene, clicking file and enter sequence. The sequence was manipulated by adding features such as desired genes, promoters etc. by right clicking anywhere on the screen, selecting edit sequence, features and add feature. Restriction enzymes could also be added here by selecting the “restriction enzymes” tab at the top of the dialog box. The created vector could be viewed in circular or linear format and the snipping tool was used to capture these images.
- BLAST n, which can be found here:  
[https://blast.ncbi.nlm.nih.gov/Blast.cgi?PAGE\\_TYPE=BlastSearch](https://blast.ncbi.nlm.nih.gov/Blast.cgi?PAGE_TYPE=BlastSearch)  
was used to align any DNA sequencing results throughout the project. The two sequences were entered, one as a query and the other as a subject in FASTA format. The database and program selection were chosen and the query was run. Images of the alignments were captured using the snipping tool.

## **2.8 OD<sub>730nm</sub> and enzyme activity determination**

Optical density measurements were taken using a Cary UV-Vis spectrophotometer from Agilent (Cork, Ireland) and Sarstedt polystyrene cuvettes at either 600nm for *E.coli* or 730nm for *Synechocystis* sp. PCC 6803.

Readings for the enzyme activity assays were taken using the Biotek plate reader from Mason Technology (Dublin 8, Ireland) at 340nm using a UV-vis 96 well plate.

## **2.9 Activity assays**

Reagents required for the reaction include:

100 mM Tris-HCl buffer pH 7.8 (Sigma-Aldrich 2010)

20 mM ThDp (Sigma-Aldrich 2015c)

15 mM MgCl<sub>2</sub>.6H<sub>2</sub>O (Sigma-Aldrich 2016)  
1 mg.ml<sup>-1</sup> stock of ADH (Sigma-Aldrich 2015a)  
0.5 mM NADH (Sigma-Aldrich 2012)

PDC protein (from *Saccharomyces cerevisiae* (Sigma-Aldrich 2015b), CFE-cell free extract from *E.coli* or *Synechocystis* 6803 or purified protein (both this study)).  
MilliQ water up to 200 µl

Sodium pyruvate (Thermo Fisher Scientific 2013) concentrations varied depending on assay type.

Stock solutions were made as appropriate.

### **2.9.1 Activity assay with *Saccharomyces cerevisiae* PDC**

All reagents used in the assay were made according to the information supplied by the safety data and product information sheets (see references above). Two plates were set up:

Plate 1-All blank wells together on one side of the plate and all test wells together on the other side.

Plate 2-The blank and corresponding test well one after the other.

The blank wells contained all the reagents in Section 2.9 above minus the cell free extract (CFE) to act as controls while the test wells contained all the reagents plus the CFE. A fixed amount of *Saccharomyces cerevisiae* PDC from Sigma Aldrich (Arklow, Wicklow, Ireland) was used at 0.5 units.ml<sup>-1</sup>. Different concentrations of sodium pyruvate in triplicate data were used: 10, 8, 7, 5, 4, 3, 2, 1, 0.5 and 0.25 mM based on the Km of the *Saccharomyces cerevisiae* PDC. The assay was allowed to run at 30°C and 340 nm for 30 minutes with shaking for 5 seconds to allow for equilibration. Once finished the sodium pyruvate substrate was added to the wells of the plates and the assay was run again with the same parameters as above but a measurement was taken straight away and then every 2 minutes.

For the results, the triplicate data for the blank and test wells for each substrate concentration was laid out in an excel document and the average was calculated. The average of the blank wells for each substrate concentration was subtracted from its corresponding test average. These values were plotted on a scatterplot with time

on the x axis in minutes and absorbance on the y axis at 340nm. A trendline was added to each line from which the slope (m) was noted. These values in mM.min<sup>-1</sup> were plotted on the y axis against their corresponding substrate concentrations in mM on the x axis to form a Michaelis-Menten graph from which V<sub>max</sub> (max rate of the reaction) and K<sub>m</sub> (substrate concentration [S] when V<sub>max</sub> is half) were calculated.

### **V<sub>max</sub> and K<sub>m</sub> calculations:**

#### **Section 3.3.1, Figure 3.9.**

V<sub>max</sub> = 0.047 mM.min<sup>-1</sup> (max rate of the reaction where the line on the graph levels off, read from the y axis).

Half V<sub>max</sub> = 0.024 mM.min<sup>-1</sup> (0.047/2).

K<sub>m</sub> = 0.5 mM (The substrate concentration when V<sub>max</sub> is half. A line is drawn from half V<sub>max</sub> on the y axis to the graph line and dropped down to the x axis).

#### **Section 3.3.1, Figure 3.10.**

V<sub>max</sub> = 0.038 mM.min<sup>-1</sup> ((max rate of the reaction where the line on the graph levels off, read from the y axis).

Half V<sub>max</sub> = 0.019 mM.min<sup>-1</sup> (0.038/2).

K<sub>m</sub> = 0.5 mM (The substrate concentration when V<sub>max</sub> is half. A line is drawn from half V<sub>max</sub> on the y axis to the graph line and dropped down to the x axis).

## **2.9.2 Preparation of *E.coli* CFE with Zm/ZpPDCs**

Zm/ZpPDC proteins were expressed in the same way as Section 2.6.1 but with modifications: 50 ml cultures were prepared and cells were induced at 20°C for 4 hours. After centrifugation, cells were re-suspended in 100 mM Tris-HCl pH 7.8 assay buffer. The clarified cell lysate was placed into a pre-chilled 50 ml tube and stored short term at 4°C as before.

### **2.9.2.1 Activity assay to determine a fixed protein concentration for future assays using *E.coli* CFE with ZmPDC**

The total protein concentration of the CFE was determined using the Nanodrop spectrophotometer ND-1000. Dilutions of this CFE were made using the assay

buffer in order to achieve protein concentrations at 0.2, 0.5, 1, 3, 5, 7, 9, 11, 13 and 15  $\mu\text{g}$  in 200  $\mu\text{l}$ . Plates were arranged in such a way to test the above CFE concentrations in triplicate data along with the appropriate blanks. The blank wells contained all the reagents minus the CFE to act as controls while the test wells contained all the reagents plus the CFE as in Section 2.9 above. Once the equilibration time had elapsed at 30°C and with shaking for 5 seconds, the fixed amount of sodium pyruvate at 125 mM was added to each well and the reaction ran for 30 minutes, with a reading taken straight away at 340nm and every 30 seconds thereafter in order to gather a relatively large amount of data.

### **2.9.2.2 Activity assay using a fixed protein concentration of *E.coli* CFE with Zm and ZpPDC**

The total protein concentrations for the Zm and ZpPDC CFEs were measured as described above in Section 2.9.2.1. The appropriate dilutions were made to achieve a concentration of 11  $\mu\text{g}$  of protein in the 200  $\mu\text{l}$  wells. The assay was allowed to equilibrate as per Section 2.9.1. Once the sodium pyruvate was added to achieve the following concentrations: 3.2, 3.0, 2.8, 2.4, 2.0, 1.6, 1.2, 0.8 and 0.4 mM, a reading was taken straight away and then every 30 seconds only over the course of 5 minutes, as from previous results, it could be seen that the reaction had terminated after 30 minutes.

The data was collated in the usual manner and a scatterplot for each substrate concentration was made with time in seconds on the x axis and absorbance at 340nm on the y axis. Three lines were present on each graph due to having triplicate data for each [S]. With the addition of a trendline, the slope (m) for each replicate was established. This data was plotted on a scatterplot with [S] in mM on the x axis and the rate (slope  $V_o$ ) in  $\text{mM}\cdot\text{sec}^{-1}$  on the y axis to form a Michaelis-Menten graph from which  $V_{\text{max}}$  and  $K_m$  were calculated. The average of the slopes for each [S] were also calculated as well as the standard deviations, with this data plotted for clarity on another scatterplot with the addition of error bars. The reciprocal of these x and y values were calculated and plotted in the same way as above to form the Lineweaver-Burk plot which is a more accurate representation of the data. The point at which the line crosses the y axis is  $1/V_{\text{max}}$  therefore  $V_{\text{max}}$  was calculated

from this and the point at which it crosses the x axis is  $-1/K_m$  which was used to calculate the  $K_m$  value.  $V_{max}$  and  $K_m$  were again calculated and compared to the above results from the previous graph.

### **$V_{max}$ and $K_m$ calculations: ZmPDC**

#### **Section 3.3.3.1, Figure 3.11, Michaelis-Menten graph.**

$V_{max} = 0.0023 \text{ mM}\cdot\text{sec}^{-1}$  (max rate of the reaction where the line on the graph levels off, read from the y axis).

Half  $V_{max} = 0.0012 \text{ mM}\cdot\text{sec}^{-1}$  ( $0.0023/2$ ).

$K_m = 0.5 \text{ mM}$  (The substrate concentration when  $V_{max}$  is half. A line is drawn from half  $V_{max}$  on the y axis to the graph line and dropped down to the x axis).

#### **Section 3.3.3.1, Figure 3.12, Lineweaver-Burk plot.**

$V_{max}$  calculated in the following way:

$1/V_{max}$  = the value when the graph line crosses the y axis.

$$1/V_{max} = 380/1$$

$$(V_{max}) (380) = (1) (1)$$

$$V_{max} = 1/380$$

$$V_{max} = 0.0026 \text{ mM}\cdot\text{sec}^{-1}$$

$K_m$  was calculated in the following way:

$-1/K_m$  = the value when the graph line crosses the x axis.

$$-1/K_m = -2.2/1$$

$$(K_m) (-2.2) = (1) (-1)$$

$$K_m = -1/-2.2$$

$$K_m = 0.45 \text{ mM}$$

### **$V_{max}$ and $K_m$ calculations: ZpPDC**

#### **Section 3.3.3.1, Figure 3.13 (Michaelis-Menten graph) and Figure 3.14 (Lineweaver-Burk plot)**

Both inconclusive

### **2.9.3 Activity assay with *Synechocystis* sp. PCC 6803 CFE**

Selected strains were cultured to mid exponential phase as per Section 2.4.2. 20 ml of cells were centrifuged at 4,000 rpm at 4°C for 30 minutes. The supernatant was removed and the cell pellets were re-suspended in ~400 µl of 100 mM Tris-HCl buffer pH 7.8. Each of the four re-suspended pellets were transferred to 1.5 ml tubes and a spatula tip of the same beads as above were added. Each tube was vortexed for 1.5 hours and freeze/thawed in the same way as before. The samples were also centrifuged as above and the same blue/purple colour was observed. Samples of each lysate were taken to run later on an SDS-PAGE gel (see Section 3.7.1, Figure 3.44) with the remaining lysate for each strain placed in pre-chilled tubes on ice in the fridge at 4°C to be used in the assay.

#### **2.9.3.1 Lysis analysis of *Synechocystis* sp. PCC 6803 cells prior to activity assay**

The selected recombinant strains were cultured as described in Section 2.4.2 to an OD<sub>730nm</sub> of 1-2. Each of the strains were adjusted to OD<sub>730nm</sub> 1 with the resulting amount of each culture placed in a 1.5 ml tube and centrifuged at 6,100 rpm for 10 mins. ~80 µl of 1X SDS loading buffer was added to each tube and they were heated at 100°C for ~1 hour. The samples were centrifuged and the supernatant was run on an SDS-PAGE gel as per Section 2.6.3.1 which can be viewed in Section 3.7.1, Figure 3.38. This lysis method was solely based on heat which is a routine method to prepare *E.coli* samples for SDS-PAGE analysis (Qiagen 2016) but based on the results of the gel, perhaps not enough for *Synechocystis* 6803.

Therefore, according to a bead beating method developed at UvA, Amsterdam by Davide Montesarchio (personal communication) the same procedure as above was followed up until the addition of the 1X SDS loading buffer which was replaced with 50 µl of DNase/RNase free water with the addition of some acid washed glass beads. The four tubes were bead beat using a vortex 2 genie at high speed for 30 minutes, 1 hour, 1.5 and 2 hours respectively to investigate if time had an effect on the lysis efficiency. Each tube was freeze/thawed 4 times in the -20°C freezer and then centrifuged at 13,400 rpm for 30 minutes. Samples were taken and prepared as before for SDS-PAGE analysis (see Section 3.7.1, Figure 3.39).

### **2.9.3.2 Activity assay with *Synechocystis* sp. PCC 6803 CFE at different pH values**

1 L of BG-11 liquid media was prepared as per appendix I B. To achieve a 1X concentration, 1 g of HEPES was weighed out and dissolved in ~900 ml of BG-11. The pH was adjusted to 6.0/7.8/8.2 dropwise with 1 M HCl and checked using a Hanna pH 20 pH meter from Lennox. Distilled water was used to fill up to the 1 L mark and the overall pH was checked again. Each buffer was filter sterilised in a Safemate 1.2 Bioair Laminar flow hood using a 1 L 0.2 µm Nalgene filter from Thermo Fisher and a VCP 130 pump (vacuum/pressure) from VWR and were stored in the fridge at 4°C.

### **2.9.3.3 Activity assay to determine a fixed protein concentration of purified ZpPDC for future assays**

The ZpPDC protein was purified to a concentration of 50 mg.ml<sup>-1</sup> and so it was decided to make several dilutions to achieve the following concentrations: 1, 2, 5, 10, 15 and 20 µg per 200 µl well. The sodium pyruvate remained constant at 125 mM as per Sections 2.9.1 and 2.9.2.1 and the previously used Tris-HCl pH 7.8 buffer was also used.

## **Chapter 3: Results and Discussion**

### 3.1 Choosing a different PDC

As previously discussed in Section 1.4, PDCs have been characterised in few bacteria: *Zymomonas mobilis*, *Zymobacter palmae*, *Acetobacter pasteurianus*, *Sarcina ventriculi* as well as *Gluconobacter oxydans* and *Gluconacetobacter diazotrophicus* in the *Acetobacteraceae* genera which have received little attention. Therefore, when deciding on what PDC could replace the enzyme currently in use from *Zymomonas mobilis*, the obvious choice at the time was the PDC from *Zymobacter palmae* due to it sharing 62/63% identity with the ZmPDC (which can be seen in Figure 3.1 below via an alignment of the two PDCs), being well characterised and showing a lower  $K_m$  for pyruvate than ZmPDC: 0.24 mM at pH 6.0 in comparison to 0.43 mM for ZmPDC at the same pH (Table 1.3, Section 1.4.4). Figure 3.2 below also shows an alignment of the PDCs mentioned in Section 1.4.4 and Table 1.3 in the same section.

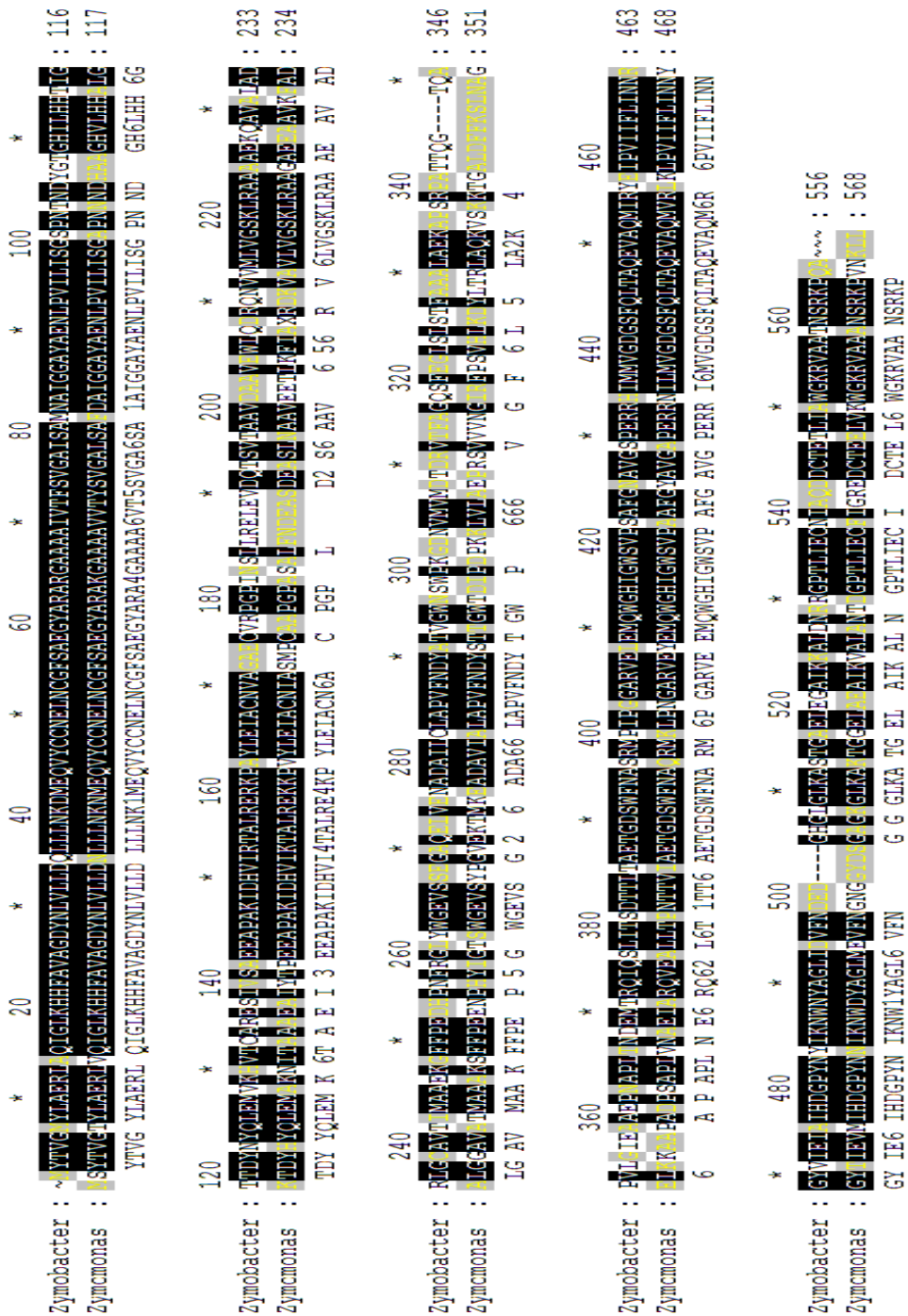


**Figure 3.1: Clustal alignment of the *Zymobacter palmae* and *Zymomonas mobilis* PDC enzymes.** ZpPDC shares 62/63% amino acid identity with ZmPDC as per Table 1.3, Section 1.4.4. Highly conserved regions shown in black, viewed in GENEDOC and constructed using the CLUSTAL Omega Algorithm (which can be reached here: <https://www.ebi.ac.uk/Tools/msa/clustalo/>) as part of this project (see Section 2.7.3.1).

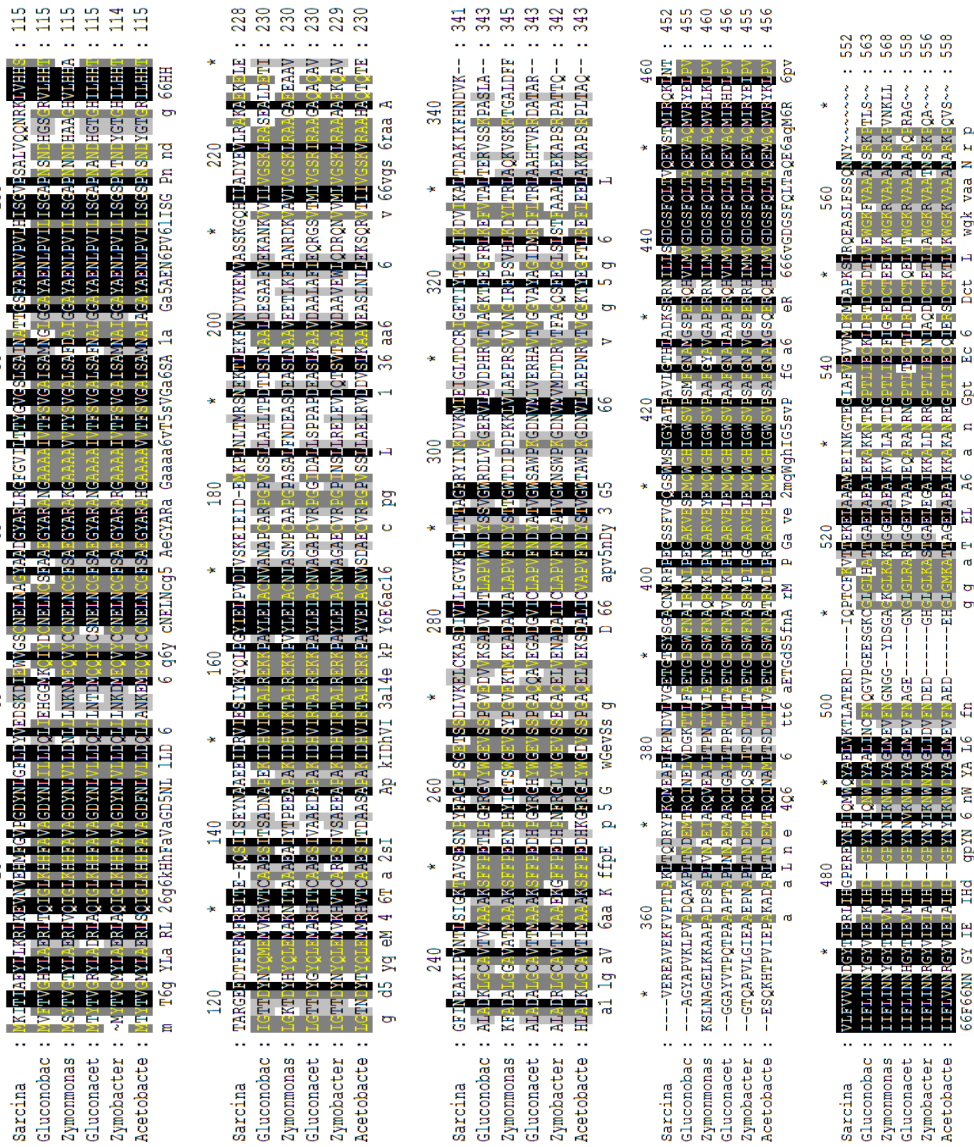


**Figure 3.2: Clustal alignment of the 6 bacterial PDC enzymes in Sv, Go, Zm, Gd, Zp and Ap.** Amino acid identities with reference to ZpPDC can be seen in Table 1.3, Section 1.4.4. Highly conserved regions shown in black, viewed in GENEDOC and constructed using the CLUSTAL Omega Algorithm as part of this project (see Section 2.7.3.1). (Sv: *Sarcina ventriculi*, Go: *Gluconobacter oxydans*, Zm: *Zymomonas mobilis*, Gd: *Gluconacetobacter diazotrophicus*, Zp: *Zymobacter palmae*, Ap: *Acetobacter pasteurianus*).

The *Zymobacter palmae* T109 strain was obtained from DSMZ: The German Collection of Microorganisms and Cell Cultures and was received as a dried pellet. The pellet was rehydrated as per the information leaflet and the strain was cultured in media specified for the strain: 753 MY broth and on 753 MY agar plates (see appendix I B) as per Section 2.1.

To examine, purify and ultimately characterise the *Zymobacter palmae* PDC, it was decided to create a construct (pULLQ2, Figure 3.6, Section 3.2.2) using the pET22b (+) expression vector. These expression systems, which originated from the pBR322 plasmid, are used extensively to clone and express recombinant proteins in *E.coli* (Agilent Technologies Inc. 2015) and contain the strong bacteriophage T7 promoter and *ampicillin* resistance gene. This T7 system allows for elevated expression levels due to the high selectivity of the T7 RNA polymerase for its corresponding T7 promoter sequence (Agilent Technologies Inc. 2015) and is suitable for the expression of recombinant soluble and non-toxic proteins in *E.coli* (Thermo Fisher Scientific 2015) (Thermo Fisher Scientific 2015). Using this system ensures that the host RNA polymerase will not recognise the T7 promoter sequence and so the gene will remain silent unless induced. Upon induction with IPTG (isopropyl  $\beta$ -D-thiogalactopyranoside) the gene of the protein of interest cloned downstream from the T7 promoter will be the only gene to undergo highly efficient transcription with T7 RNA polymerase which is expressed from the lacUV5 promoter, a variant of the *E.coli* lac promoter. This is usually carried out in an expression strain of *E.coli* (Agilent Technologies Inc. 2015) such as BL21 (DE3)\* which is the strain used in this project. Once purified it was planned that the ZpPDC would be used for enzyme activity assays and characterisation studies later on in this study. A construct using the *Zmpdc* was also created to act as a control (pULLQ1, Figure 3.3, Section 3.2.1). In addition to this it was speculated that using a *pdc* from *Zymobacter palmae* in *Synechocystis* 6803 may give rise to some incompatibility issues with regards to codon usage. Therefore to account for this possibility, the gene sequence for *Zppdc* was sent to IDT (Integrated DNA Technologies) to be codon optimised for *Synechocystis* 6803 and a third construct was created (pULLQ3, see Figure 3.8, Section 3.2.3) using this codon optimised *Zymobacter palmae* *pdc* gene (*ZpOpdc*).

## **3.2 Cloning into the pET22b (+) vector**

### **3.2.1 Creation of pULLQ1: *Zmpdc* in pET22b (+)**

pULLQ1 (Figure 3.3) was created using the traditional cloning method with digestion and ligation as per Section 2.3.2. PCR was used to amplify the *Zppdc*

insert from the *Zymobacter palmae* T109 genomic DNA. Primers which were designed to add a 6X histidine tag to the C terminus of the protein to allow for IMAC purification later on in the project were used and the resulting amplified PCR product was subsequently digested with restriction enzymes NdeI and NotI. The pET22b (+) plasmid was also digested with these restriction enzymes and ligation ratios of 1:1, 3:1 and 7:1 (insert: vector) were used. The DNA was then transformed into electrocompetent Top 10 *E.coli* cells as per Section 2.4.1 which were then spread on two LB agar plates with 100 µg.ml<sup>-1</sup> of streptomycin and ampicillin. These were incubated at 30°C for ~17 hours. Once colonies had appeared, overnight cultures and subsequently glycerol stocks were made as per Section 2.2. These were placed in both the -20°C and -80°C freezers.

Plasmid DNA was extracted from overnight cultures and sent away to be sequenced as per Section 2.3.5 and 2.3.6 respectively.

Results were aligned with plasmid map sequences created by GENTle software with gene sequences obtained from the NCBI's GenBank which can be viewed here: <https://www.ncbi.nlm.nih.gov/genbank/>. Any mutations in the form of deletions, insertions etc. could quickly and easily be seen.

Upon doing so, it was found that the clones with the 3:1 ligation ratio contained the *Zmpdc* insert with a correct gene sequence. Therefore, this ratio was pursued while the others were discarded.

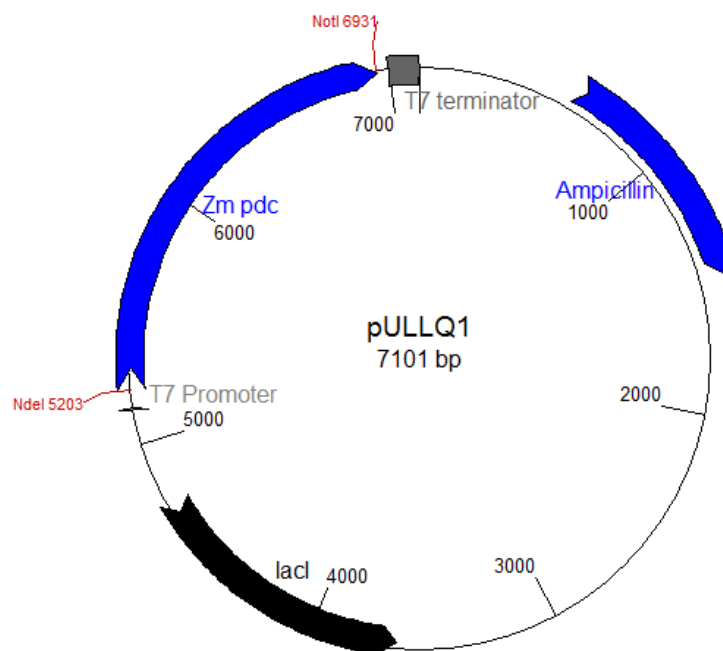


**Figure 3.3: pULLQ1.** (Constructed in GENTle, see Section 2.7.3.1). This construct shows the T7 promoter, *Zymomonas mobilis pdc* (*Zmpdc*), *ampicillin* resistance gene and NdeI and NotI restriction sites which were used to clone the *Zmpdc* gene into the pET22b (+) vector. Sequencing verified the insertion of the gene into this vector which was then transformed into competent Top 10 *E.coli* cells and later on into the BL21 (DE3)\* expression strain of *E.coli* for enzyme kinetic studies.

### 3.2.2 Creation of pULLQ2: *Zppdc* in pET22b (+)

pULLQ1 (*Zmpdc* in pET22b (+)) was used as a template to create a novel construct with the *pdc* from *Zymobacter palmae* (Figure 3.6). This was carried out as per Section 2.3.3. The *Zppdc* insert was amplified by preparing and using template from an overnight culture while the vector was linearised to remove only the *Zmpdc*, both with the appropriate primers as per appendix II. The insert and linearised vector had 15 bp homologous overlaps at both ends which were complementary to each other and annealed during the enzymatic reaction to form the recombinant circular construct which was then transformed into competent stellar cells. The reaction was spread on two LB agar plates with 100  $\mu\text{g}\cdot\text{ml}^{-1}$  of ampicillin which were incubated at 30°C for ~20 hours (see Figure 3.7). The same steps were taken as per Section 3.2.1 above once colonies had appeared on the plates.

To quickly check if the *Zppdc* insert was present, a single digest was carried out as per Section 2.3.2.1 using a S<sub>AC</sub>II restriction enzyme (see appendix I) which was expected to cut the *Zppdc* in two places but was a non-cutter in *Zmpdc*. This was therefore used as a control. Clones digested with this enzyme showed two bands on a 1% DNA gel (data not shown) made as per Section 2.3.4. Undigested samples and the control (*Zmpdc*) showed no evidence of digestion as expected.

The clones were also sequenced and results analysed in the same way as in Section 3.2.1 above with the appropriate sequencing primers as per appendix II. Two mutations were found towards the beginning of the *Zppdc* gene upon analysis of the sequencing results (see Figures 3.4 and 3.5). These were at base pairs 400-402 which changed a CGT arginine (R) to a GCT aliphatic non polar alanine (A) and at base pairs 733-735 which changed a GAA glutamic acid (E) also to a GCA alanine (A). It was originally thought that the selected clones had simply picked up random mutations. Therefore, another clone was selected and sequenced but the same mutations were observed again. Attention then turned to the *Zymobacter palmae* strain which had been used as a source of genomic DNA for the *pdC* gene. It was questioned whether the mutations might in fact have been present in the genomic DNA of the received strain. The *Zppdc* was amplified as before and the product itself was sequenced. Upon analysis the mutations were still in the same positions of the gene and so it was concluded that they did not come from the cloning procedure but from the *Zppdc* gene in the original strain. Little thought was given to this until Buddrus *et al.* (2016) reported the same mutations in the *Zppdc* gene during their attempt to solve the protein's crystal structure. They also found upon sequencing the gene that the arginine at amino acid position 134 and the glutamic acid at amino acid position 245 were both alanines and that the GenBank gene and protein entries of AF474145 and AAM49566.1 respectively were incorrect (Buddrus *et al.* 2016). This fortunately did not materially affect the creation of the constructs in this study due to using the genomic DNA as template for the *Zppdc* which was correct in comparison to using the GenBank sequences which were incorrect (see appendix III C and D).

```

TTACCTGCGCACGTGAAAGCATCGTTTCTGCCGAAGAAGCACCGGCAAAAATCGACCACG
|||||
TTACCTGCGCACGTGAAAGCATCGTTTCTGCCGAAGAAGCACCGGCAAAAATCGACCACG

TCATCCGTACGGCTCTACGTGAACGCAAACCGGCTTATCTGGAAATCGCATGCAACGTCG
|||||
TCATCCGTACGGCTCTACGTGAACGCAAACCGGCTTATCTGGAAATCGCATGCAACGTCG

```

**Figure 3.4: BLAST n alignment of the *Zppdc* sequencing results showing the first mutation.** The alignment above shows the sequencing results as the subject on the bottom line while the gene sequence of the same *pdC* from GenBank and the sequence used to make the GENTle plasmid maps appear as the query on the top line. Note the mutation of CG to GC at base pair positions 400 and 401 which changed a positively charged arginine (R, codon CGT) to an aliphatic non polar alanine (A, codon GCT). Accession number: AF474145. Created using BLAST n, see Section 2.7.3.1).

```

GCTGTCACGATCATGGCTGCCGAAAAGGCTTCTTCCCGGAAGATCATCCGAACTTCCGC
|||||
GCTGTCACGATCATGGCTGCCGAAAAGGCTTCTTCCCGGAAGATCATCCGAACTTCCGC

GGCCTGTACTGGGGTGAAGTCAGCTCCGAAGGTGCACAGGAACTGGTTGAAAACGCCGAT
|||||
GGCCTGTACTGGGGTGAAGTCAGCTCCGAAGGTGCACAGGAACTGGTTGAAAACGCCGAT

```

**Figure 3.5: BLAST n alignment of the *Zppdc* sequencing results showing the second mutation.** The alignment above shows the sequencing results as the subject on the bottom line while the gene sequence of the same *pdC* from GenBank and the sequence used to make the GENTle plasmid maps appear as the query on the top line. Note the mutation of A to C at base pair position 734 which changed a negatively charged glutamic acid (E, codon GAA) to an aliphatic non polar alanine (A, codon GCA). Accession number: AF474145. Created using BLAST n, see Section 2.7.3.1).

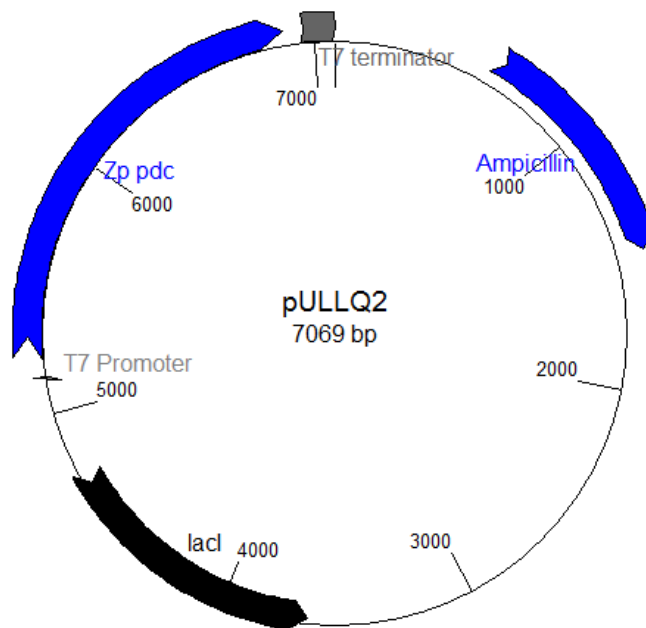


**Figure 3.6: pULLQ2.** (Constructed in GENTle, see Section 2.7.3.1). This construct shows the T7 promoter, native *Zymobacter palmae pdc* (*Zppdc*) and *ampicillin* resistance gene. Homologous recombination via the In-Fusion® HD cloning kit was used to insert the *Zppdc* gene into the pET22b (+) vector. Sequencing verified the insertion of the gene into this vector which was then transformed into competent Stellar *E.coli* cells and later on into the BL21 (DE3)\* expression strain of *E.coli* for expression and purification of the ZpPDC protein for enzyme kinetic and characterisation studies.

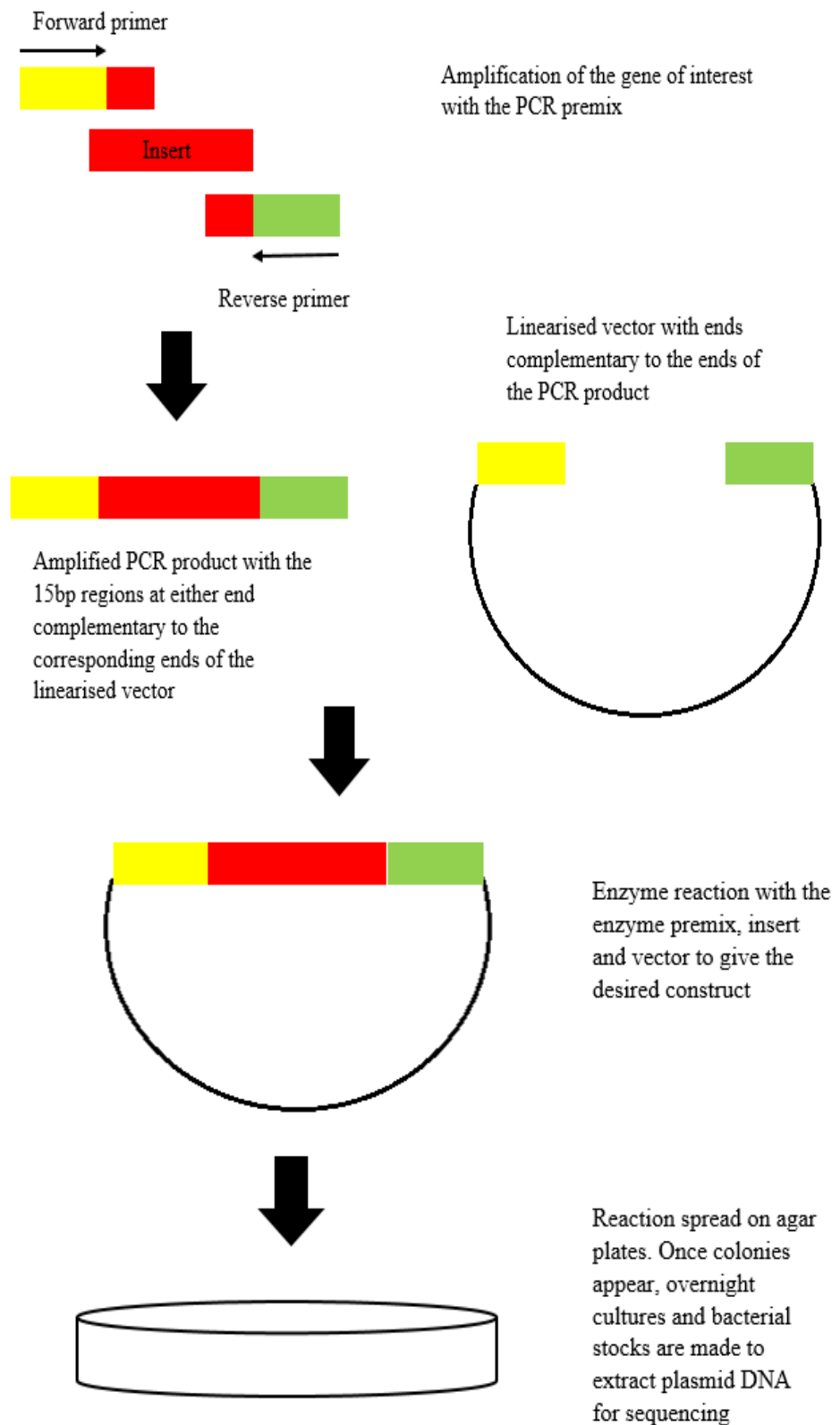


**Figure 3.7: Diagrammatic representation of the Clontech In-Fusion® HD cloning protocol (Takara Bio USA 2016).**

### 3.2.3 Creation of pULLQ3: ZpOpdc in pET22b (+)

pULLQ3 (Figure 3.8) was created in the same way as pULLQ2 above with the exception of primers used (see appendix II). Bacterial stocks were made and clones were sequenced as before (using the appropriate sequencing primers) with analysis of sequencing results showing no mutations within the *ZpOpdc* insert.

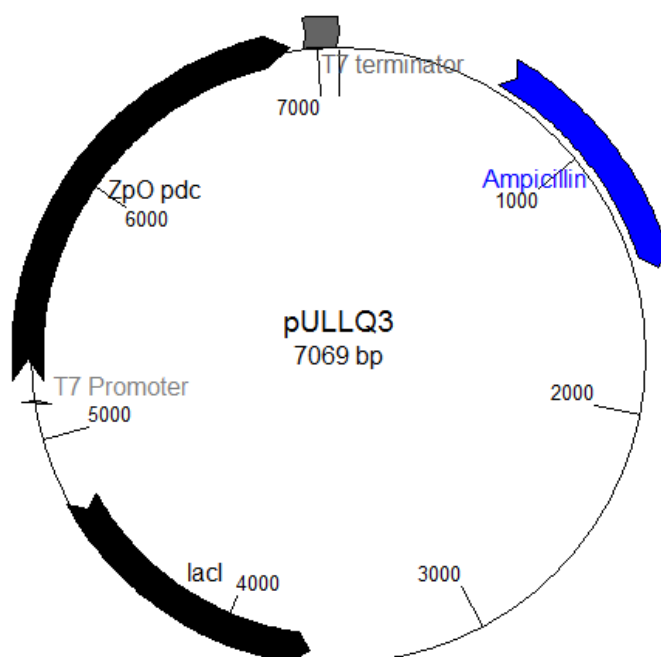


**Figure 3.8: pULLQ3.** (Constructed in GENTle, see Section 2.7.3.1). This construct shows the T7 promoter, codon optimised *Zymobacter palmae pdc* (*ZpOpdc*) and *ampicillin* resistance gene. Homologous recombination via the In-Fusion® HD cloning kit was used to insert the *Zppdc* gene into the pET22b (+) vector. Sequencing verified the insertion of the gene into this vector which was then transformed into competent Stellar *E.coli* cells.

Once the three constructs were completely verified by sequencing, each were transformed into the BL21 (DE3)\* expression strain of *E.coli* via electroporation as per Section 2.4.1 for expression, purification, kinetic and characterisation studies. All three proteins contained a 6X histidine tag on the C terminus.

## 3.3 Activity assays

According to the literature, the PDC from *Zymobacter palmae* displays a lower  $K_m$  (Raj *et al.* 2002) thus demonstrating improved enzyme kinetics compared to the

*Zymomonas mobilis* PDC. At a pH of 6.0, the  $K_m$  of the PDC from Zp is almost half that of the ZmPDC at 0.24 mM compared to 0.43 mM at the same pH. Even at an increased pH of 7.0, its  $K_m$  is still lower at 0.71 mM as opposed to 0.94 mM (Raj *et al.* 2002). Therefore to investigate this, the Zm and ZpPDCs were overexpressed under control of the strong T7 promoter in the BL21 (DE3)\* expression strain of *E.coli* containing the pULLQ1 and pULLQ2 constructs. Below is the layout of the assay used to investigate any PDC activity throughout the course of this study, details of which can be found in Section 2.9. It is a modified procedure developed and kindly provided by Davide Montesarchio (personal communication) from UvA, Amsterdam.

The principle of the assay is an indirect assay used to measure PDC activity by the measurement of NADH oxidation at 340nm which is the cofactor of the ADH in the ethanol pathway. Measurements were taken as per Section 2.8.

During the assay, a steady decrease in absorbance should be observed. Should the reaction go too quick a sudden drop will be seen and the graph will begin to level off. This may be an indication that there is too much enzyme present and that a dilution needs to be made. If so this is done in the same buffer used in the assay. If on the other hand no significant decrease is seen then this may indicate little to no activity. This applies to any activity assay carried out during the project.

### **3.3.1 Activity assay with *Saccharomyces cerevisiae* PDC**

Prior to investigating the PDC activity of Zm and Zp, the assay was used to look quickly at and validate the procedure using the PDC from *Saccharomyces cerevisiae* which possesses a  $K_m$  of ~1.1-1.3 mM (Boiteux and Hess 1970) and could be purchased in an ammonium sulphate suspension at 6.4 units/mg of 14 mg.ml<sup>-1</sup> protein. Therefore, it was known how much was being added to the assay and could determine if it was working correctly. It was also decided to investigate if there was any plate bias i.e. does plate arrangement affect the outcome of the assay. Two UV plates were set up as per Section 2.9.1 to ensure the measurements were consistent and the results were also analysed as per the same section.

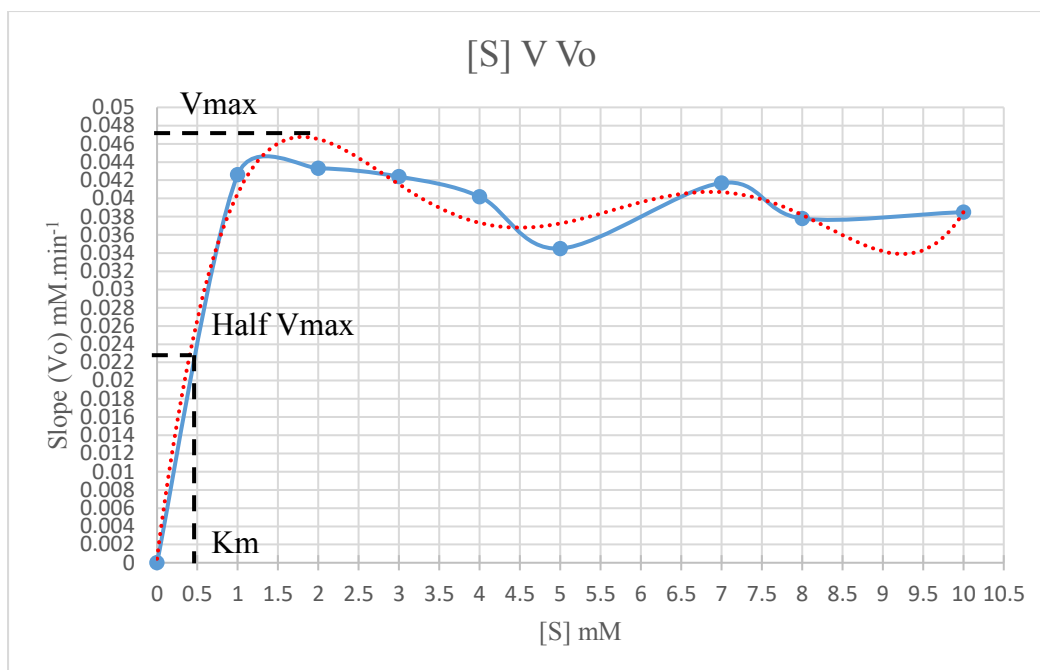


**Figure 3.9: Michaelis-Menten graph for the *Saccharomyces cerevisiae* PDC activity assay, plate 1 (all blank wells and all test wells together).** Slope in mM.min<sup>-1</sup> on the y axis and substrate concentration [S] in mM on the x axis. The V<sub>max</sub>, half V<sub>max</sub> and K<sub>m</sub> are noted.

The graph above in Figure 3.9 shows that the V<sub>max</sub> and half V<sub>max</sub> respectively are ~0.047 and ~0.024 mM.min<sup>-1</sup> which results in a K<sub>m</sub> value of ~0.5 mM (see Section 2.9.1 for calculations).

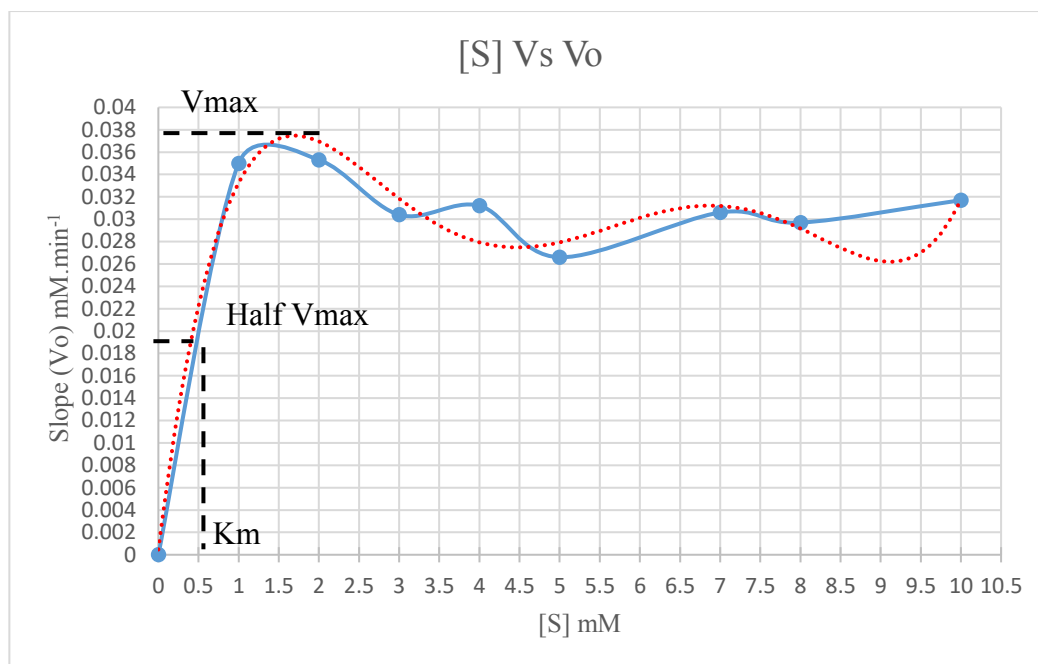


**Figure 3.10: Michaelis-Menten graph for the *Saccharomyces cerevisiae* PDC activity assay, plate 2 (alternating blank and test wells).** Slope in  $\text{mM}\cdot\text{min}^{-1}$  on the y axis and substrate concentration [S] in mM on the x axis. The  $V_{\text{max}}$ , half  $V_{\text{max}}$  and  $K_{\text{m}}$  are noted.

The graph above in Figure 3.10 shows that the  $V_{\text{max}}$  and half  $V_{\text{max}}$  respectively are  $\sim 0.038$  and  $\sim 0.019 \text{ mM}\cdot\text{min}^{-1}$  which results in a  $K_{\text{m}}$  value of  $\sim 0.5 \text{ mM}$  (see Section 2.9.1 for calculations).

Both plate layouts produced similar results for the  $V_{\text{max}}$  and  $K_{\text{m}}$  which gave good reason to believe that the assay was working well under the conditions used and that plate layout didn't actually affect the outcome. Therefore no plate bias was observed.

### 3.3.2 Activity assay to determine a fixed [protein] for future assays using *E.coli* CFE with ZmPDC

Having completed the control experiment using the purchased *Saccharomyces cerevisiae* PDC, attention returned to the Zm and ZpPDCs. As previously mentioned, the expression strains with the pULLQ1 and pULLQ2 constructs were used to overexpress these proteins. PDC activity could be measured using the above assay and CFE (crude extract) as a source for the PDC. This method was also demonstrated by Gao *et al.* (2012) albeit in *Synechocystis* 6803 (Gao *et al.* 2012).

A CFE concentration in the range of 0.2 to 15  $\mu\text{g}$  was recommended (Montesarchio, personal communication) but to select a fixed concentration, a brief assay was carried out using CFE containing ZmPDC. The CFE was prepared as per Section 2.9.2 while the assay was carried out as per Section 2.9.2.1. The resulting concentration was 1.7  $\text{mg}\cdot\text{ml}^{-1}$  determined as per the same section.

From the results of this assay, a steady decrease in absorbance as described above was observed for 11  $\mu\text{g}$  of CFE. Therefore, it was decided to use this total protein concentration as a guideline for future assays.

### **3.3.3 Activity assay using a fixed [protein] of *E.coli* CFE with Zm and ZpPDC**

Now that a fixed total protein concentration had been determined, it was possible to look at the activity of the Zm and ZpPDC in CFE overexpressed by *E.coli*. As mentioned earlier it has been reported that the PDC from Zp possesses a lower  $K_m$  than that from Zm which would imply superior enzymatic kinetics and possibly the ability to produce more ethanol in *Synechocystis* 6803 if incorporated into the ethanol cassette. To assay the activity of both these enzymes, the same reagents as previously described in Section 2.9 were used (for both the blank (control) and test wells). The CFE was also prepared in the same way as per Section 2.9.2 with the concentration of the ZmPDC determined at 1.83  $\text{mg}\cdot\text{ml}^{-1}$  and the ZpPDC at 1.95  $\text{mg}\cdot\text{ml}^{-1}$  as per Section 2.9.2.1. The assay was carried out as per Section 2.9.2.2 and data was analysed as per the same section.

### 3.3.3.1 *E.coli* CFE with ZmPDC

**Table 3.1: Data produced from the assay using *E.coli* CFE with ZmPDC.**

[S] mM	Slope (Vo) mM.sec <sup>-1</sup>			Average	Standard Deviation
	1	2	3		
3.2	0.002	0.0022	0.0023	0.0022	0
3	0.0023	0.0023	0.0023	0.0023	0
2.8	0.0022	0.0023	0.0023	0.0023	0
2.4	0.0022	0.0022	0.0021	0.0022	0
2	0.0022	0.0022	0.0022	0.0022	0
1.6	0.0021	0.0021	0.0021	0.0021	0
1.2	0.0019	0.0019	0.002	0.0019	0
0.8	0.0017	0.0017	0.0017	0.0017	0
0.4	0.0013	0.0013	0.0011	0.0012	0
0	0	0	0	0	0

Triplicate slope (Vo) data in mM.sec<sup>-1</sup> for each substrate concentration in mM used to assay the activity of the ZmPDC in CFE from *E.coli* showing the rates, average and standard deviation.

**Table 3.2: Data used to create a Michaelis-Menten graph for *E.coli* CFE with ZmPDC.**

[S] mM	Average slope (Vo) mM.sec <sup>-1</sup>	Standard Deviation
3	0.0023	0
2.8	0.0023	0
2.4	0.0022	0
2	0.0022	0
1.6	0.0021	0
1.2	0.0019	0
0.8	0.0017	0
0	0	0

Substrate concentration values in mM on the x axis and the average rate (slope Vo) for each substrate concentration value in mM.sec<sup>-1</sup> on the y axis along with the standard deviation used to make a Michaelis-Menten graph. The 3.2 and 0.4 substrate concentration values were omitted to allow for a better fit.

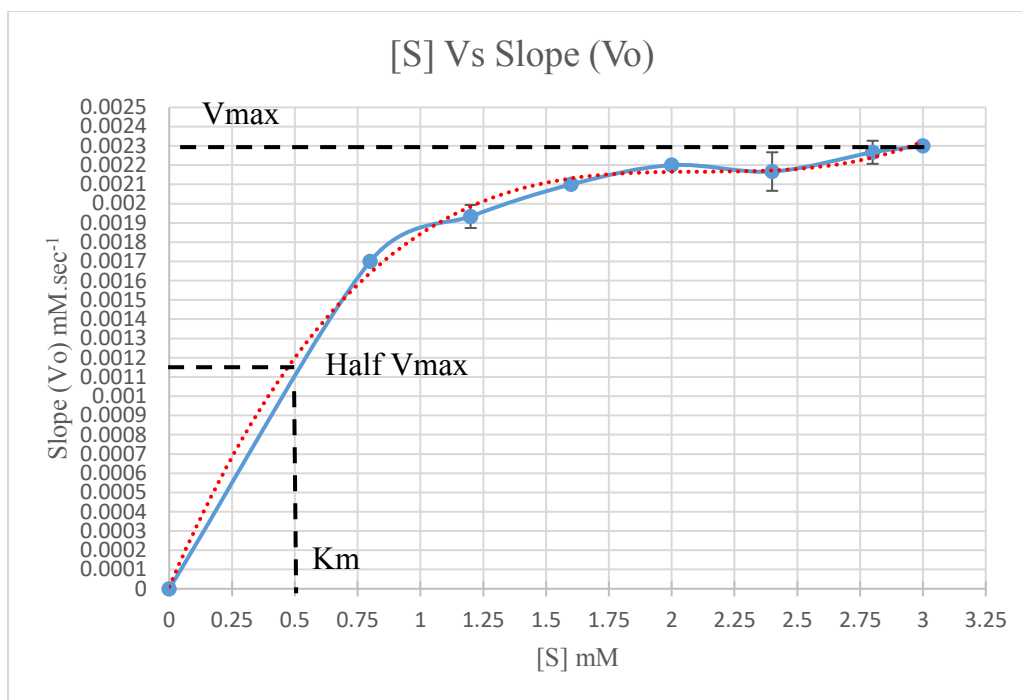


**Figure 3.11: Michaelis-Menten graph for *E.coli* CFE with ZmPDC.** Produced from the data in Table 3.2 above with the substrate concentration values in mM on the x axis and the average rate (slope  $V_o$ ) for each substrate concentration value in  $\text{mM}\cdot\text{sec}^{-1}$  on the y axis along with the addition of error bars.

Table 3.2 above shows the average slope values in  $\text{mM}\cdot\text{sec}^{-1}$  for the selected substrate concentration values ranging from 0.8 to 3 mM. The slope values steadily increased from  $0.0017 \text{ mM}\cdot\text{sec}^{-1}$  at 0.8 mM to  $0.0023 \text{ mM}\cdot\text{sec}^{-1}$  at 3 mM. An increase in the amount of substrate resulted in an increase in the rate of the reaction up to the point of saturation (2.8-3 mM) where the reaction ended due to the saturation of the enzyme's catalytic sites with substrate. At this point,  $V_{\text{max}}$  was reached. A calculated standard deviation of 0 shows that the triplicate data for the slope in  $\text{mM}\cdot\text{sec}^{-1}$  for each substrate concentration (shown in Table 3.1) was consistent and showed little fluctuation.

From the graph in Figure 3.11, an arrow drawn to the y axis at the max rate of the reaction shows  $V_{\text{max}}$  to be  $\sim 0.0023 \text{ mM}\cdot\text{sec}^{-1}$  with a  $K_m$  of  $\sim 0.5 \text{ mM}$  (see Section 2.9.2.2 for calculations). This isn't the same as the exact value stated in the literature at 0.43 mM (Raj *et al.* 2002) but taking everything into consideration such as the assay being carried out under a different set of conditions, using our own

equipment in a dissimilar laboratory setting, the results obtained are in the same region as the published data.

**Table 3.3: Data used to create a Lineweaver-Burk graph for *E.coli* CFE with ZmPDC.**

1/[S] mM	Average slope (Vo) mM.sec <sup>-1</sup>	Standard Deviation
0.3333	434.78	0
0.3571	441.37	11.41
0.4167	461.76	12.49
0.5	454.55	0
0.625	476.19	0
0.8333	517.54	15.19
1.25	588.24	0

The reciprocal of the data in Table 3.2. The substrate concentration values are in mM on the x axis while the average rate (slope Vo) for each substrate concentration value is in mM.sec<sup>-1</sup> on the y axis along with the standard deviation, used to make a Lineweaver-Burk plot.

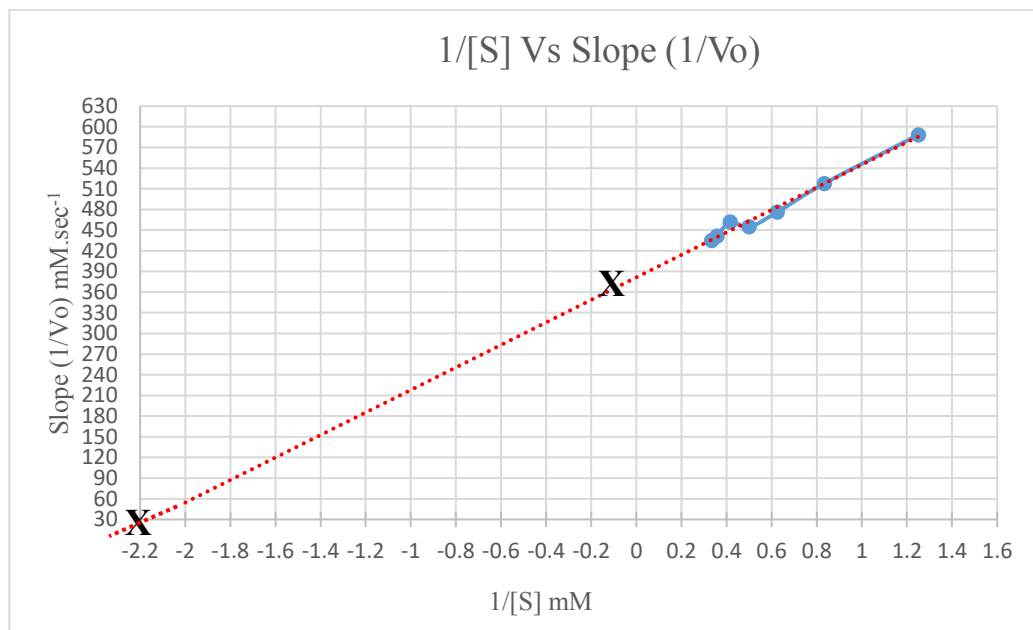


**Figure 3.12: Lineweaver-Burk plot for *E.coli* CFE with ZmPDC.** Produced from the data in Table 3.3 with the reciprocal of the substrate concentration values in mM on the x axis and the reciprocal of the average rate (slope Vo) for each substrate concentration value in mM.sec<sup>-1</sup> on the y axis.

The Lineweaver-Burk plot above in Figure 3.12 is a much more accurate representation of the Michaelis-Menten graph shown earlier in Figure 3.9. The  $V_{max}$  and  $K_m$  values are indicated on the graph where the line crosses the y and x axis respectively to give values of  $\sim 0.0026 \text{ mM}\cdot\text{sec}^{-1}$  for  $V_{max}$  and  $\sim 0.45 \text{ mM}$  for  $K_m$  (see Section 2.9.2.2 for calculations) which are within  $\pm 15\%$  of the corresponding  $V_{max}$  and  $K_m$  values calculated earlier in Figure 3.11.

### 3.3.3.2 *E.coli* CFE with ZpPDC

**Table 3.4: Data produced from the assay using *E.coli* CFE with ZpPDC.**

[S] mM	Slope ( $V_o$ ) $\text{mM}\cdot\text{sec}^{-1}$			Average	Standard Deviation
	1	2	3		
3	0.001	0.001	0.0011	0.001	0
2.8	0.0012	0.0012	0.0012	0.0012	0
2.4	0.0012	0.0012	0.0012	0.0012	0
2	0.0011	0.0011	0.0011	0.0011	0
1.6	0.0012	0.0012	0.0012	0.0012	0
1.2	0.0011	0.0012	0.0011	0.0011	0
0.8	0.0011	0.0011	0.0011	0.0011	0
0	0	0	0	0	0

Triplicate slope ( $V_o$ ) data in  $\text{mM}\cdot\text{sec}^{-1}$  for each substrate concentration in mM used to assay the activity of the ZpPDC in CFE from *E.coli* showing the rates, average and standard deviation.

**Table 3.5: Data used to create a Michaelis-Menten graph for *E.coli* CFE with ZpPDC.**

[S] mM	Average slope (Vo) mM.sec <sup>-1</sup>	Standard Deviation
3	0.0010	0
2.8	0.0012	0
2.4	0.0012	0
2	0.0011	0
1.6	0.0012	0
1.2	0.0011	0
0.8	0.0011	0
0	0	0

Substrate concentration values in mM on the x axis and the average rate (slope Vo) for each substrate concentration value in mM.sec<sup>-1</sup> on the y axis along with the standard deviation.

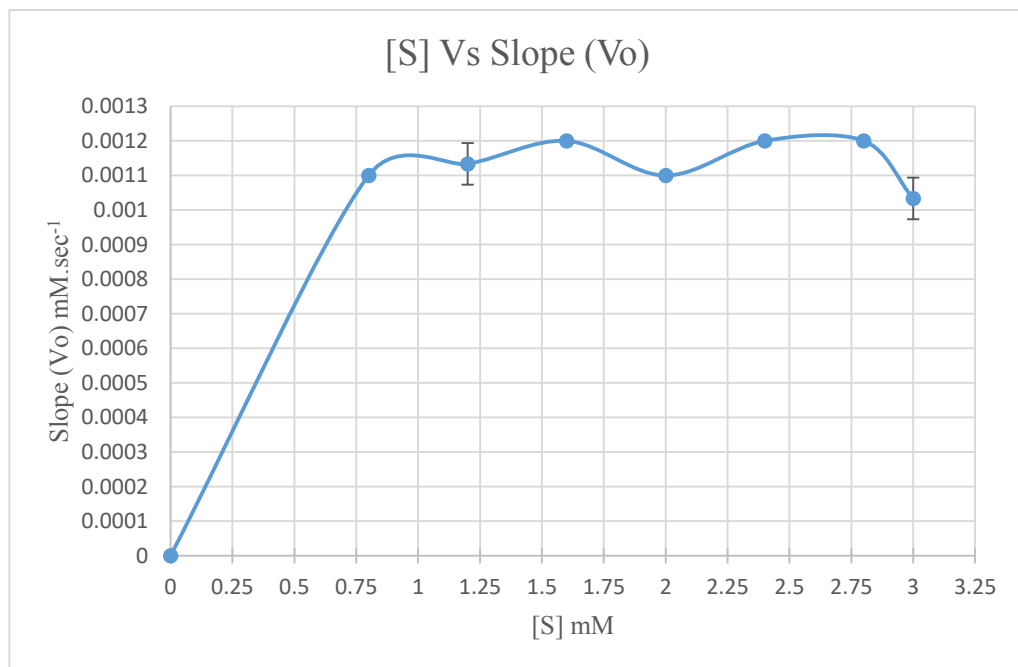


**Figure 3.13: Michaelis-Menten graph for *E.coli* CFE with ZpPDC.** Produced from the data in Table 3.5 above with substrate concentration values in mM on the x axis and the average rate (slope Vo) for each substrate concentration value in mM.sec<sup>-1</sup> on the y axis along with the addition of error bars.

**Table 3.6: Data used to create a Lineweaver-Burk plot for *E.coli* CFE with ZpPDC.**

1/[S] mM	Average slope (Vo) mM.sec <sup>-1</sup>	Standard Deviation
0.3333	969.70	52.49
0.3571	833.33	0
0.4167	833.33	0
0.5	909.09	0
0.625	833.33	0
0.8333	883.84	43.74
1.25	909.09	0

The reciprocal of the data in Table 3.5. The substrate concentration values are in mM on the x axis while the average rate (slope Vo) for each substrate concentration value is in mM.sec<sup>-1</sup> on the y axis along with the standard deviation, used to make a Lineweaver-Burk plot.

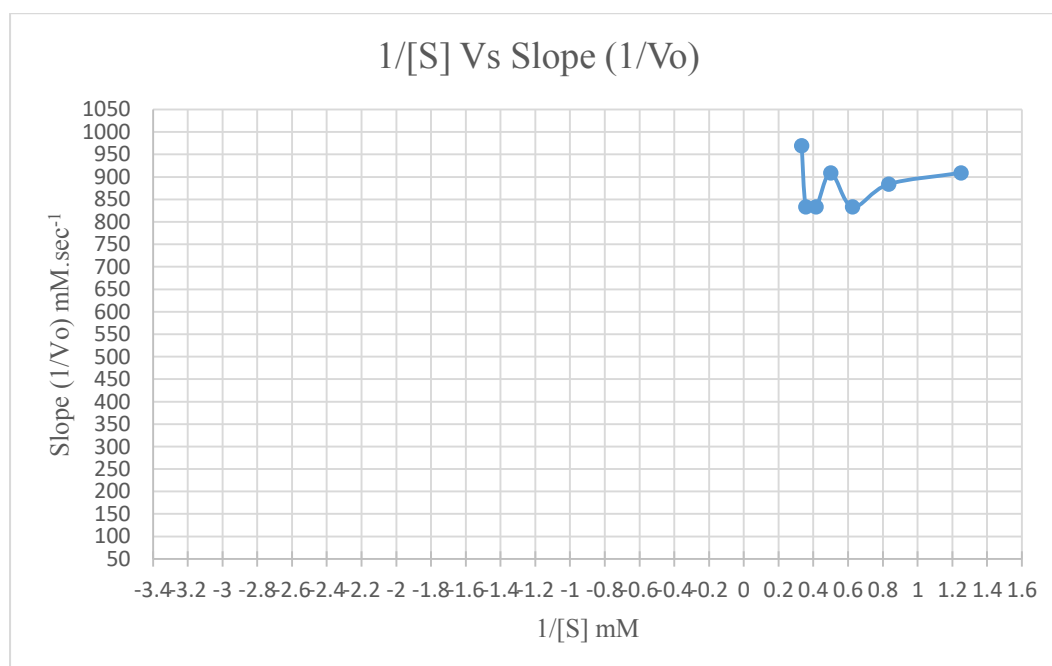


**Figure 3.14: Lineweaver-Burk plot for *E.coli* CFE with ZpPDC.** Produced from the data in Table 3.6 with the reciprocal of the substrate concentration values in mM on the x axis and reciprocal of the average rate (slope Vo) for each substrate concentration value in mM.sec<sup>-1</sup> on the y axis.

From the Michaelis-Menten graph above in Figure 3.13 and the Lineweaver-Burk plot in Figure 3.14, it was not possible to draw any firm conclusions with regards to the kinetic behaviour of the ZpPDC enzyme under the conditions used therefore

the attempt was not made to apply a line of best fit to either graph. The overall data in Table 3.4 used to make both graphs did not show any significant or detectable change in the slope with the values rising only slightly from 0.0011 mM.sec<sup>-1</sup> at 0.8 mM to 0.0012 mM.sec<sup>-1</sup> at 2.8 mM with a fall to 0.001 mM.sec<sup>-1</sup> seen at 3 mM. The absorbance readings from the raw data also showed no significant decrease over the course of the time period used in the assay. This may have been because the ZpPDC was inactive or less efficient at the pH used (7.8) in comparison to its optimum pH of 6.0. Previous studies have shown that the optimum pH for ZmPDC is 6.0 resulting in a Km value of 0.43 mM (Raj *et al.* 2002), 0.4 mM (Bringer-Meyer *et al.* 1986) and 0.31 mM (Meyer *et al.* 2010). At pH 7.0, the Km increased to 0.94, over double the value calculated at pH 6.0 (Raj *et al.* 2002). Due to the fact that the Zm and ZpPDCs share 62/63% identity (Raj *et al.* 2002; Buddrus *et al.* 2016), the effect that pH has on the ZmPDC may be a possible reason to reinforce the hypothesis that the ZpPDC is also pH dependent. The optimum pH for ZpPDC is between 5.5 and 6.0 (Raj *et al.* 2002) with a Km of 0.24 mM at pH 6.0 and 0.71 mM at pH 7.0. Buddrus *et al.* (2016) also quoted a Km value of 0.67 for ZpPDC at pH 6.5 which is a large increase for such a small difference of 0.5 units (Buddrus *et al.* 2016). Examples given for both Zm and ZpPDC show that the Km values are much lower at the optimum pH for both enzymes and that this value increases as the pH increases towards a more alkaline region and moves away from the optimum range. Meyer *et al.* (2010) also looked at varying a conserved glutamate residue in ZmPDC which had an effect on the steady state kinetics. Changing the glutamate residue to aspartate (Glu473Asp) and to a glutamine (Glu473Gln) had an effect on the resulting Km values at pH 6.0. It was calculated that the Km value for the wildtype ZmPDC was 0.31 mM (mentioned above) while the Glu473Gln variant had a similar Km value of 0.4 mM at the same pH. The resulting value for Glu473Asp was half that of the wildtype at 0.15 mM. However, it was noted in the study that in each instance “the Km constant for pyruvate increases at alkaline pH” (Meyer *et al.* 2010) which reinforces what has been discussed above. However, the ZmPDC can possibly operate at the more alkaline pH of 7.8 because its pH range is broader than the ZpPDC and it’s more tolerant to changes in the pH of the environment. No change in the slope may also have been due to the fast acting nature of the ZpPDC which may have caused the reaction to terminate before any measurements were taken. The opposite could be said for the ZmPDC because it is

reported to be a slower working enzyme. Either way, it has previously been reported that the ZpPDC does possess a lower  $K_m$  to the ZmPDC and so justified the decision to use this *pdC* in the ethanol cassette.

Overall, the results obtained during both assays are outlined below in Table 3.7:

**Table 3.7:  $V_{max}$  and  $K_m$  results for both the Zm and ZpPDCs in *E.coli* CFE.**

Source	ZmPDC $V_{max}$	$K_m$ (pH 6.0)	ZpPDC $V_{max}$	$K_m$ (pH 6.0)
Literature		0.43		0.24
Graph 1 (Michaelis- Menten)	~0.0023	~0.5	INC	INC
Graph 2 (Lineweaver- Burk)	~0.0026	~0.45	INC	INC

As depicted by the Michaelis-Menten and Lineweaver-Burk plots in addition to values found in the literature. (INC: Inconclusive).

As can be seen from Table 3.7 above, again it was not possible to definitively confirm that the ZpPDC has a lower  $K_m$  than the ZmPDC possibly due to the reasons discussed above. It has however been previously reported therefore work continued with this chosen *pdC*. Results obtained for the ZmPDC did not entirely match those quoted in the literature possibly due to the pH at which the assay was performed. This was not the optimum pH for the ZmPDC which may be a possible reason for this discrepancy. Looking at Table 1.3 in Section 1.4.4, five out of the six PDCs mentioned show an increased  $K_m$  value for an increase in pH (Raj *et al.* 2002; Van Zyl *et al.* 2014) which does imply that this enzyme is possibly pH dependent. The preferred pH of *Synechocystis* 6803 has been reported to be between 7 and 8.5 (Heidorn *et al.* 2010) and so this was the reason for using the higher pH value during the assay. Nevertheless, the reported lower  $K_m$  of the ZpPDC indicates the possibility of greater substrate conversion and flux away from pyruvate.

Thus it was hypothesised that the ZpPDC with its lower Km could prove better in ethanol production in metabolically engineered *Synechocystis* 6803 if its gene was incorporated into the ethanol cassette. To support this hypothesis, constructs were created with the native and codon optimised *Zymobacter palmae pdc* to allow for transformation into wildtype *Synechocystis* 6803. The pUL004 construct containing the pPSBAII promoter, *Zmpdc*, *slr1192 adh* and *kanamycin* resistance gene in the PSBAII neutral site (see Section 1.8.1) has already been transformed into wildtype *Synechocystis* 6803 to create UL004. This strain was reconstructed as part of this study by transforming pUL004 into wildtype *Synechocystis* 6803 again to act as a control strain for comparison.

### **3.4 Cloning into the PSBAII vector**

#### **3.4.1 Creation of pUL101: *Zppdc* in PSBAII**

pUL101 (Figure 3.15) was created using pUL004 from UL004 as a template. The only difference between the two constructs was the use of a different *pdc* gene: *Zppdc* vs *Zmpdc*. The construct was created in a similar way to pULLQ2 and 3 (Figures 3.6 and 3.8) using the Clontech In-Fusion® HD cloning kit as described in Section 3.2.2 and Section 3.2.3 above. The appropriate primers were used and can be found in appendix II.

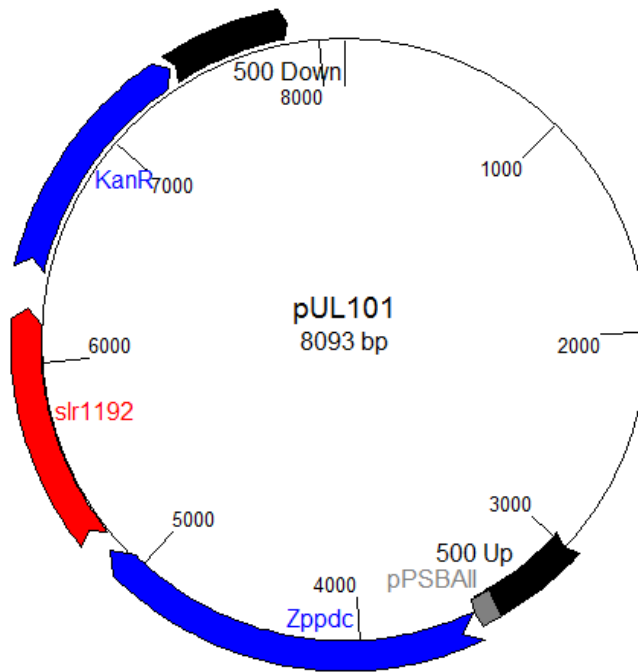


**Figure 3.15: pUL101.** (Constructed in GENTle, see Section 2.7.3.1). This construct shows the pPSBAlI promoter of *Synechocystis* 6803 amplified and fused to the native *Zymobacter palmae* *pdC* (*Zppdc*) and linked to the native *Synechocystis* 6803 *adh* (*slr1192*) and *kanamycin* resistance gene (a gene encoding kanamycin phosphotransferase which was amplified from the enterobacterial ICE R391). This construct which was verified by sequencing contained two 500 bp flanking regions which were homologous to the PSBAlI neutral site in *Synechocystis* 6803. It was now suitable for transformation and incorporation into this site. Transformants were initially screened for kanamycin resistance with the level of kanamycin gradually increased (as per Section 3.5) to allow for screening and selection for full segregation into the polyploidy genome of *Synechocystis* 6803. Primer sets spanning the PSBAlI site were designed to differentiate between full incorporation of this construct into every copy of the chromosome, partial non segregated incorporation and no incorporation.

### 3.4.2 Creation of pUL102: *ZpOpdc* in PSBAlI

The final construct created was pUL102 (Figure 3.16) which replaced the *Zm/Zppdc* with the codon optimised version (*ZpOpdc*). The same template as above in Section 3.4.1 was used to swap out the *pdC* from *Zymomonas mobilis* and insert the *ZpOpdc*. The same cloning technique was also used and the same steps were taken as in the creation of pUL101 above in the same section.

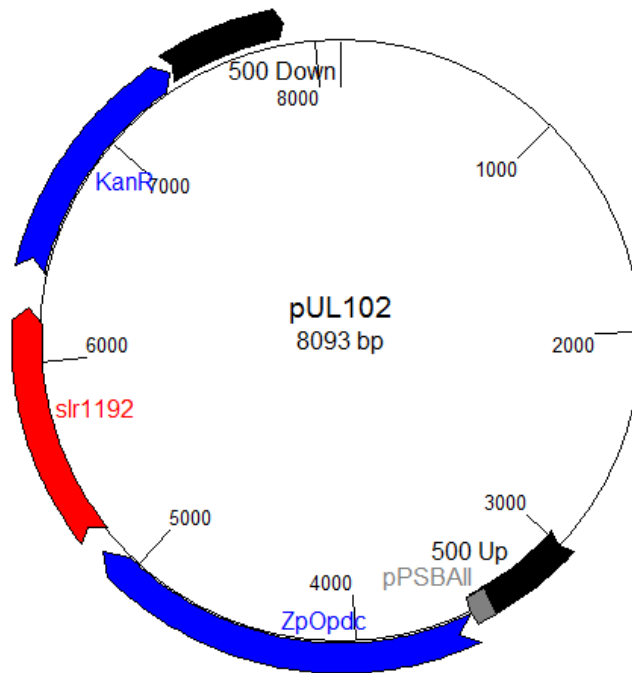


**Figure 3.16: pUL102.** (Constructed in GENTle, see Section 2.7.3.1). This construct shows the pPSBII promoter of *Synechocystis* 6803 amplified and fused to the codon optimised *Zymobacter palmae pdc* (*ZpOpdc*) and linked to the native *Synechocystis* 6803 *adh* (*slr1192*) and *kanamycin* resistance gene (a gene encoding kanamycin phosphotransferase which was amplified from the enterobacterial ICE R391). This construct which was verified by sequencing contained two 500 bp flanking regions which were homologous to the PSBII neutral site in *Synechocystis* 6803. It was now suitable for transformation and incorporation into this site. Transformants were initially screened for kanamycin resistance with the level of kanamycin gradually increased (as per Section 3.5) to allow for screening and selection for full segregation into the polyploidy genome of *Synechocystis* 6803. Primer sets spanning the PSBII site were designed to differentiate between full incorporation of this construct into every copy of the chromosome, partial non segregated incorporation and no incorporation.

Bacterial stocks for pUL101 and pUL102 were made as per Section 2.2. Sequencing was also carried out in the same manner as with previous clones (Section 2.3.6) using the correct sequencing primers (appendix II) and analysis of results showed no mutations in the inserted gene sequences for *Zppdc* or *ZpOpdc*.

A summary of the constructs created and those provided can be seen in Table 3.8 below which also shows their transformation strain.

**Table 3.8: Constructs used in this study and the created strains.**

Construct	In
pULLQ1: pET22b (+), T7 promoter, <i>Zmpdc</i> , ampicillin resistance. (This study). Figure 3.3	Top 10 and BL21 (DE3) * <i>E.coli</i> cells to create ULLQ1.
pULLQ2: pET22b (+), T7 promoter, <i>Zppdc</i> , ampicillin resistance. (This study). Figure 3.6	Stellar and BL21 (DE3)* <i>E.coli</i> cells to create ULLQ2.
pULLQ3: pET22b (+), T7 promoter, <i>ZpOpdc</i> , ampicillin resistance. (This study). Figure 3.8	Stellar and BL21 (DE3) * <i>E.coli</i> cells to create ULLQ3.
pUL004: PSBAII, pPSBAII, <i>Zmpdc</i> , slr1192 <i>adh</i> , kanamycin resistance. (Provided). Figure 1.7	Top 10 cells and wildtype <i>Synechocystis</i> sp. PCC 6803 to create UL004/UL070.
pUL004: PSBAII, pPSBAII, <i>Zmpdc</i> , slr1192 <i>adh</i> , kanamycin resistance + pUL030: ΔPHB, <i>Zmpdc</i> , slr1192 <i>adh</i> , zeocin resistance (Provided). Figure 1.8	Top 10 cells and wildtype <i>Synechocystis</i> sp. PCC 6803 to create UL030.
pUL101: PSBAII, pPSBAII, <i>Zppdc</i> , slr1192 <i>adh</i> , kanamycin resistance. (This study). Figure 3.15	Stellar cells and wildtype <i>Synechocystis</i> sp. PCC 6803 to create UL071.
pUL102: PSBAII, pPSBAII, <i>ZpOpdc</i> , slr1192 <i>adh</i> , kanamycin resistance. (This study). Figure 3.16	Stellar cells and wildtype <i>Synechocystis</i> sp. PCC 6803 to create UL072.

A more comprehensive list of the constructs and strains can be found in appendix IV A and IV B.

### 3.5 Transformation into *Synechocystis* sp. PCC 6803

pUL004, pUL101 and pUL102 were transformed via natural transformation into wildtype *Synechocystis* 6803 as per Section 2.4.2 to create strains UL070 (UL004), UL071 and UL072 which contained the *Zm*, *Zp* and *ZpOpdc*s respectively. Full

segregation of the constructs into the chromosome were confirmed as per the same section via PCR screening. Samples were run on a 1% DNA gel prepared as described in Section 2.3.4 for ~35 minutes and at 110 volts. Only one band was observed if the construct failed to insert itself into the correct location where the primers merely amplified the empty PSBAII neutral site to give a product of ~1.1 kb. This strain was therefore considered to be wildtype. A fully segregated strain also showed one band but at a size of ~4 kb which implied the integration of the cassette (pPSBAII light promoter, *pdv*, *adh* (slr1192) and *kanamycin* genes) into the neutral site. Finally a combination of the two bands indicated a semi-segregated strain where the construct was not yet fully taken up by all the copies of the polyploid chromosome. The wildtype strain of *Synechocystis* 6803 was therefore always run as a control to verify the segregation status of the transformed strains.

Clones which showed semi-segregation at 50  $\mu\text{g.ml}^{-1}$  kanamycin were transferred onto BG-11 agar plates with a higher selective antibiotic pressure of 100  $\mu\text{g.ml}^{-1}$  kanamycin to try and select for full segregation. The clones which remained semi-segregated even at this antibiotic pressure were not pursued and were discarded as were clones which failed to segregate. Clones which showed full segregation were re-streaked to fresh 50  $\mu\text{g.ml}^{-1}$  kanamycin plates. The 1% DNA gels below (Figures 3.15-3.20) which were stained with SYBR® safe and visualised using a UV transilluminator show some of the screened samples with the *Zm*, *Zp* or *ZpOpdv* under conditions of high or low light, +/- 1% glucose which either failed to segregate or were semi or fully segregated into the PSBAII neutral site in *Synechocystis* 6803.

### 3.5.1 PCR screening to verify fully segregated strains

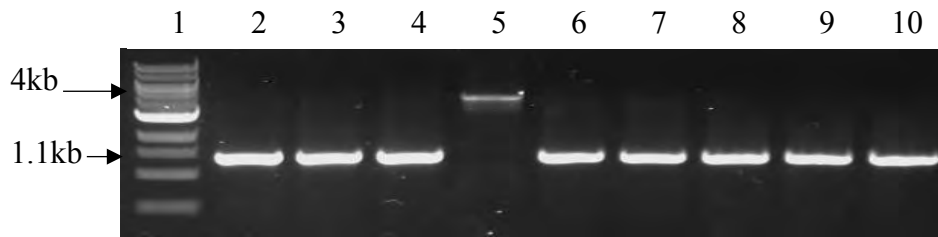


**Figure 3.17: 1% SYBR® safe stained DNA agarose gel from PCR assays of screened UL070 strains (containing *Zmpdc*) with 1% glucose and under high light conditions (HL).**

Lane 1: NEB (New England Biolabs®, Inc.) 1 kb DNA ladder.

Lane 2: WT *Synechocystis* 6803 control shows the empty PSBAII neutral site at ~1.1 kb.

Lanes 3 and 4: UL070 strains which failed to segregate, bands at ~1.1 kb show the empty PSBAII neutral site.

Lane 5: Fully segregated UL070 strain, band at ~4 kb shows the insertion of the pPSBAII promoter, *Zmpdc*, *adh* and *kanamycin* genes.

Lanes 6-10: UL070 strains which failed to segregate, bands at ~1.1 kb show the empty PSBAII neutral site.

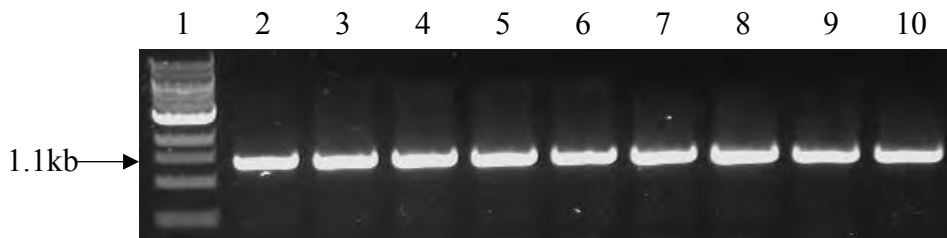


**Figure 3.18: 1% SYBR® safe stained DNA agarose gel from PCR assays of screened UL071 strains (containing *Zppdc*) with 1% glucose and under high light conditions (HL).**

Lane 1: NEB 1 kb DNA ladder.

Lane 2: WT *Synechocystis* 6803 control shows the empty PSBAII neutral site at ~1.1 kb.

Lanes 3-10: UL071 strains which failed to segregate, bands at ~1.1 kb show the empty PSBAII neutral site.

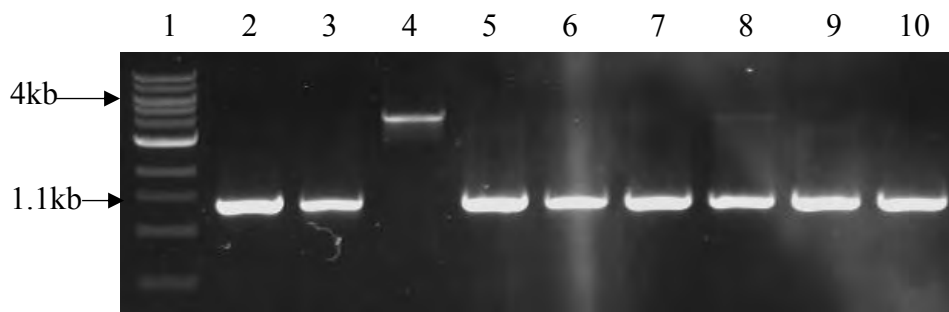


**Figure 3.19: 1% SYBR® safe stained DNA agarose gel from PCR assays of screened UL072 strains (containing *ZpOpdc*) with 1% glucose and under high light conditions (HL).**

Lane 1: NEB 1 kb DNA ladder.

Lane 2: WT *Synechocystis* 6803 control shows the empty PSBAII neutral site at ~1.1 kb.

Lane 3: UL072 strain which failed to segregate, band at ~1.1 kb shows the empty PSBAII neutral site.

Lane 4: Fully segregated UL072 strain, band at ~4 kb shows the insertion of the pPSBAII promoter, *ZpOpdc*, *adh* and *kanamycin* genes.

Lanes 5-10: UL072 strains which failed to segregate, bands at ~1.1 kb show the empty PSBAII neutral site.

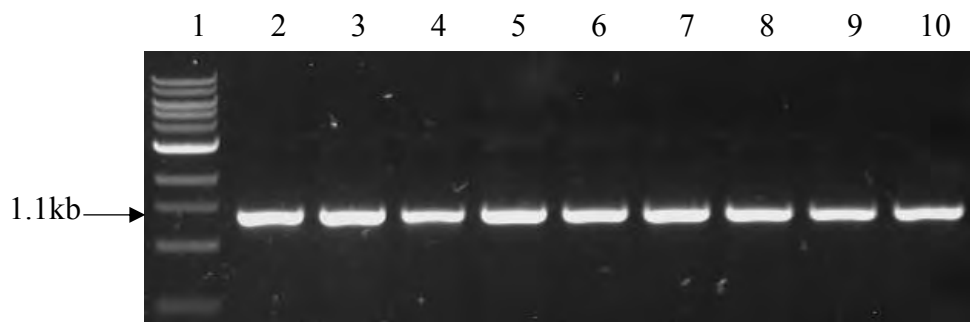


**Figure 3.20: 1% SYBR® safe stained DNA agarose gel from PCR assays of screened UL070 strains (containing *Zmpdc*) with 1% glucose and under low light conditions (LL).**

Lane 1: NEB 1 kb DNA ladder.

Lane 2: WT *Synechocystis* 6803 control shows the empty PSBAII neutral site at ~1.1 kb.

Lanes 3-10: UL070 strains which failed to segregate, bands at ~1.1 kb show the empty PSBAII neutral site.

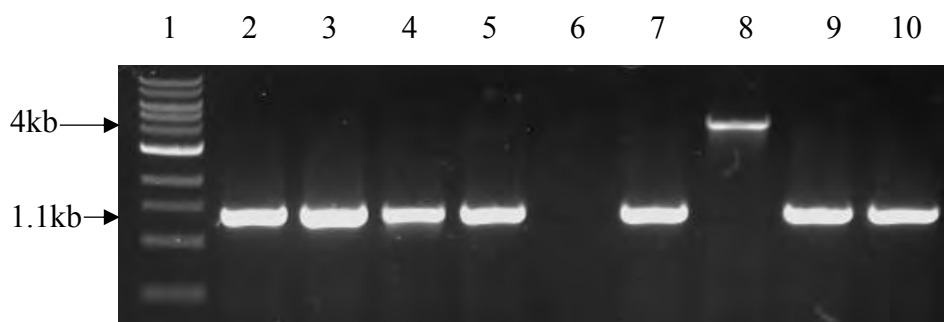


**Figure 3.21: 1% SYBR® safe stained DNA agarose gel from PCR assays of screened UL071 strains (containing *Zppdc*) with 1% glucose and under low light conditions (LL).**

Lane 1: NEB 1 kb DNA ladder.

Lane 2: WT *Synechocystis* 6803 control shows the empty PSBAII neutral site at ~1.1 kb.

Lanes 3-5: UL071 strains which failed to segregate, bands at ~1.1 kb show the empty PSBAII neutral site.

Lane 6: Empty due to poor template preparation.

Lane 7: UL071 strain which failed to segregate, band at ~1.1 kb shows the empty PSBAII neutral site.

Lane 8: Fully segregated UL071 strain, band at ~4 kb shows the insertion of the pPSBAII promoter, *Zppdc*, *adh* and *kanamycin* genes.

Lanes 9 and 10: UL071 strains which failed to segregate, bands at ~1.1 kb show the empty PSBAII neutral site.

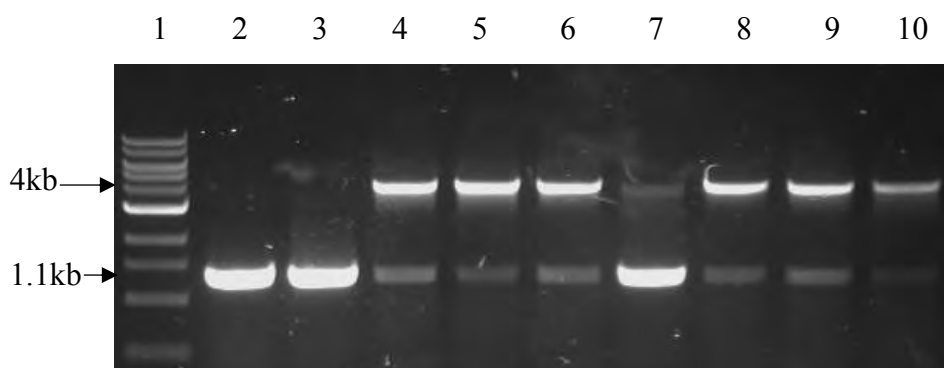


**Figure 3.22: 1% SYBR® safe stained DNA agarose gel from PCR assays of screened UL072 strains (containing *ZpOpdc*) with 1% glucose and under low light conditions (LL).**

Lane 1: NEB 1 kb DNA ladder.

Lane 2: WT *Synechocystis* 6803 control shows the empty PSBAII neutral site at ~1.1 kb.

Lanes 3: UL072 strain which failed to segregate, band at ~1.1 kb shows the empty PSBAII neutral site.

Lanes 4-10: Semi-segregated UL072 strains, the faint but still visible band at ~1.1 kb in lanes 4,5,6,7,8,9 and 10 shows the empty PSBAII neutral site while the second band at ~4 kb in the same lanes shows the insertion of the pPSBAII promoter, *ZpOpdc*, *adh* and *kanamycin* genes.

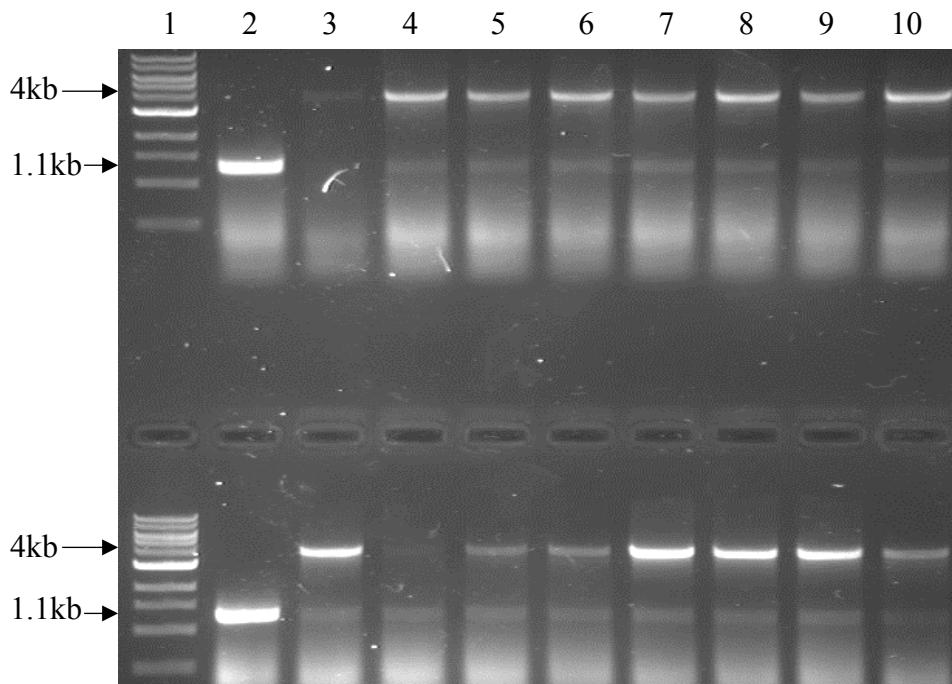


**Figure 3.23: Gel 1: 1% SYBR® safe stained DNA agarose gel from PCR assays of screened strains which had previously shown to be fully segregated but reverted back to a semi-segregated state.** (All gels showing this are not shown due to dispersal of strains throughout a large number of gels).

**Top of gel:**

Lane 1: NEB 1 kb DNA ladder.

Lane 2: WT *Synechocystis* 6803 control shows the empty PSBAII neutral site at ~1.1 kb.

Lane 3: Semi-segregated UL070 + glucose high light strains, low intensity band at ~1.1 kb shows the empty PSBAII neutral site while the band at ~4 kb shows the insertion of the pPSBAII promoter, *Zmpdc*, *adh* and *kanamycin* genes. The low intensity was due to poor template preparation.

Lanes 4 and 5: Semi-segregated UL070 + glucose high light strains, bands at ~1.1 kb show the empty PSBAII neutral site and bands at ~4 kb show the insertion of the pPSBAII promoter, *Zmpdc*, *adh* and *kanamycin* genes.

Lanes 6 and 7: Semi-segregated UL070 + glucose low light strains, bands at ~1.1 kb show the empty PSBAII neutral site and bands at ~4 kb show the insertion of the pPSBAII promoter, *Zmpdc*, *adh* and *kanamycin* genes.

Lanes 8-10: Semi-segregated UL071 + glucose high light strains, bands at ~1.1 kb show the empty PSBAII neutral site and bands at ~4 kb show the insertion of the pPSBAII promoter, *Zppdc*, *adh* and *kanamycin* genes.

**Bottom of gel:**

Lane 1: NEB 1 kb DNA ladder.

Lane 2: WT *Synechocystis* 6803 control shows the empty PSBAII neutral site at ~1.1 kb.

Lane 3: Semi-segregated UL071 + glucose high light strain, the band at ~1.1 kb shows the empty PSBAII neutral site while the band at ~4 kb shows the insertion of the pPSBAII promoter, *Zppdc*, *adh* and *kanamycin* genes.

Lanes 4-10: Semi-segregated UL071 + glucose low light strains, bands at ~1.1 kb show the empty PSBAII neutral site and bands at ~4 kb show the insertion of the pPSBAII promoter, *Zppdc*, *adh* and *kanamycin* genes.

Strains were rescreened to confirm full segregation before being tested for ethanol production. As can be seen above, all of the samples reverted back to a semi-segregated state showing a faint albeit visible band at ~1.1 kb. This may have been due to a reduction of the antibiotic pressure in the agar plates which kept the strains (that had a natural tendency to lose such an inserted non selected cassette) fully segregated. Once plate cultures were fully grown, they were usually placed at 4°C and re-streaked a number of days later depending on the strain stability i.e. its ability to keep the construct in the multiple copies of the chromosome. In this case, the fully segregated strains had only been streaked onto 50 µg.ml<sup>-1</sup> kanamycin plates once and left in the fridge for greater than a week. Therefore, the strains went from being fully to semi-segregated. Therefore to produce a strain which was homogeneous and genetically recombinant, transformed colonies needed to be continuously streaked onto plates with an increasing antibiotic selective pressure to achieve permanent full segregation of the DNA into all copies of the chromosome (Yu *et al.* 2013).

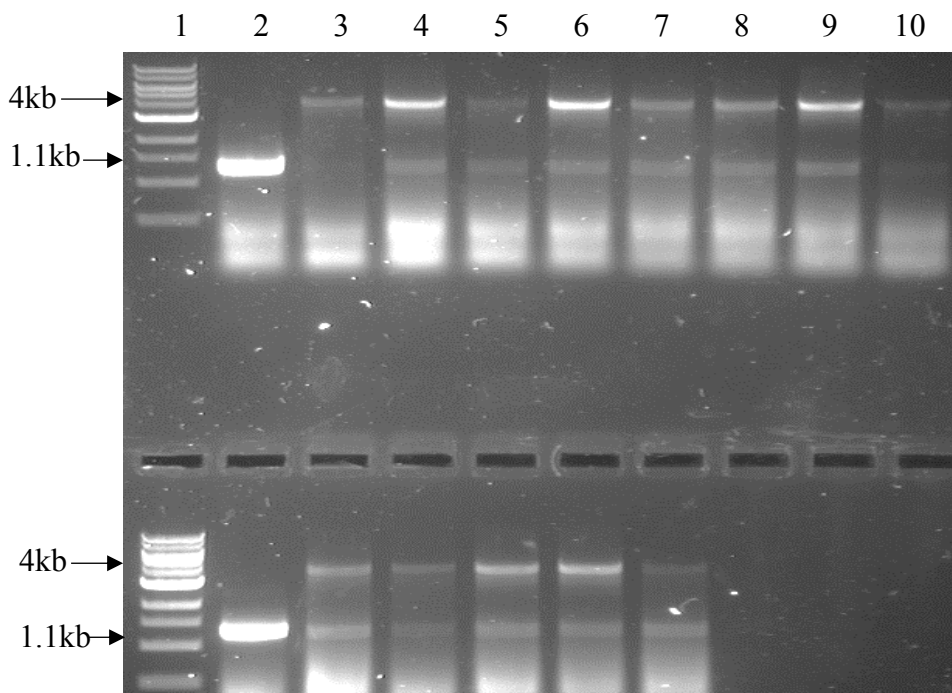


**Figure 3.24: Gel 2: 1% SYBR® safe stained DNA agarose gel from PCR assays of screened strains which had previously been shown to be fully segregated but reverted back to a semi-segregated state. (As explained above).**

**Top of gel:**

Lane 1: NEB 1 kb DNA ladder.

Lane 2: WT *Synechocystis* 6803 control shows the empty PSBAII neutral site at ~1.1 kb.

Lane 3: Semi-segregated UL071 + glucose low light strain, the band at ~1.1 kb shows the empty PSBAII neutral site while the band at ~4 kb shows the insertion of the pPSBAII promoter, *Zppdc*, *adh* and *kanamycin* genes.

Lanes 4-9: Semi-segregated UL072 + glucose high light strains, bands at ~1.1 kb show the empty PSBAII neutral site and bands at ~4 kb show the insertion of the pPSBAII promoter, *ZpOpdc*, *adh* and *kanamycin* genes.

Lane 10: Semi-segregated UL072 + glucose low light strain, the band at ~1.1 kb shows the empty PSBAII neutral site while the band at ~4 kb shows the insertion of the pPSBAII promoter, *ZpOpdc*, *adh* and *kanamycin* genes.

**Bottom of gel:**

Lane 1: NEB 1 kb DNA ladder.

Lane 2: WT *Synechocystis* 6803 control shows the empty PSBAII neutral site at ~1.1 kb.

Lanes 3-7: Semi-segregated UL072 + glucose low light strains, bands at ~1.1 kb show the empty PSBAII neutral site and bands at ~4 kb show the insertion of the pPSBAII promoter, *ZpOpdc*, *adh* and *kanamycin* genes.

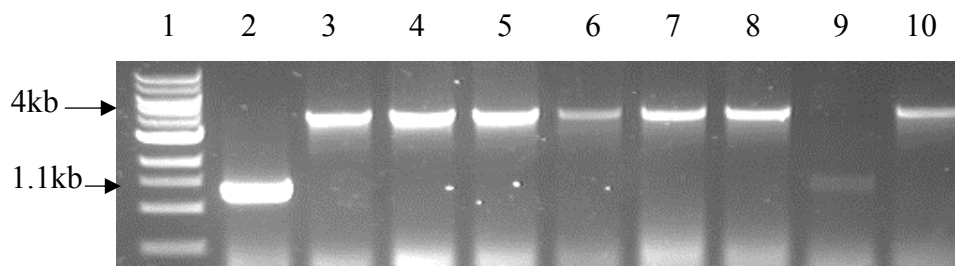


**Figure 3.25: 1% SYBR® safe stained DNA agarose gel from PCR assays of screened samples with no glucose under high and low light conditions.**

Lane 1: NEB 1 kb DNA ladder.

Lane 2: WT *Synechocystis* 6803 control shows the empty PSBAII neutral site at ~1.1 kb.

Lanes 3: Fully segregated UL070 – glucose high light strain, band at ~4 kb shows the insertion of the pPSBAII promoter, *Zmpdc*, *adh* and *kanamycin* genes.

Lanes 4 and 5: Fully segregated UL071 – glucose high light strains, bands at ~4 kb show the insertion of the pPSBAII promoter, *Zppdc*, *adh* and *kanamycin* genes.

Lanes 6-8: Fully segregated UL072 – glucose high light strains, bands at ~4 kb show the insertion of the pPSBAII promoter, *ZpOpdc*, *adh* and *kanamycin* genes.

Lane 9: Semi-segregated UL072 – glucose high light strain, the band at ~1.1 kb shows the empty PSBAII neutral site while the bands at ~4 kb show the insertion of the pPSBAII promoter, *ZpOpdc*, *adh* and *kanamycin* genes.

Lane 10: Fully segregated UL071 – glucose low light strain, band at ~4 kb shows the insertion of the pPSBAII promoter, *Zppdc*, *adh* and *kanamycin* genes.

The strains in Figures 3.23 and 3.24 were streaked onto both 50 and 100  $\mu\text{g.ml}^{-1}$  kanamycin plates in order to push them back to full segregation and increase their stability. This was done a total of four times for all of these strains and also for those in Figure 3.25.

The strains were re-screened (100  $\mu\text{g.ml}^{-1}$  plates only as this pressure was sure to force them back to full segregation) and the results can be seen below in Figures 3.26 to 3.29.

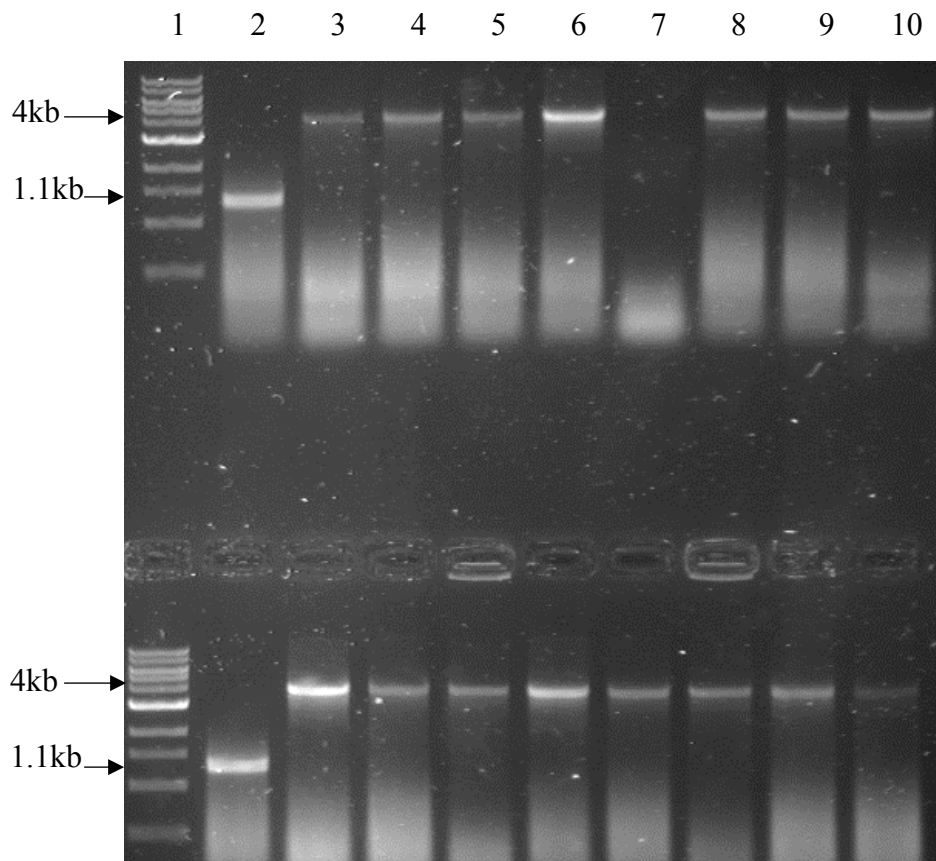


**Figure 3.26: Gel 1: 1% SYBR® safe stained DNA agarose gel from PCR assays of fully segregated strains which were brought back from a semi-segregated state.**

Re-screen to determine if several streaks of clones onto 100  $\mu\text{g}\cdot\text{ml}^{-1}$  kanamycin plates forced the clones back to full segregation.

Note the absence of the  $\sim 1.1$  kb band indicative of semi-segregation in all the strains.

**Top of gel:**

Lane 1: NEB 1 kb DNA ladder.

Lane 2: WT *Synechocystis* 6803 control shows the empty PSBII neutral site at  $\sim 1.1$  kb.

Lanes 3-5: Fully segregated UL070 + glucose high light strains, bands at  $\sim 4$  kb show the insertion of the pPSBII promoter, *Zmpdc*, *adh* and *kanamycin* genes.

Lane 6: Fully segregated UL070 + glucose low light strain, band at  $\sim 4$  kb shows the insertion of the pPSBII promoter, *Zmpdc*, *adh* and *kanamycin* genes.

Lane 7: Empty due to poor template preparation.

Lanes 8-10: Fully segregated UL071 + glucose high light strains, bands at  $\sim 4$  kb show the insertion of the pPSBII promoter, *Zppdc*, *adh* and *kanamycin* genes.

**Bottom of gel:**

Lane 1: NEB 1 kb DNA ladder.

Lane 2: WT *Synechocystis* 6803 control shows the empty PSBII neutral site at  $\sim 1.1$  kb.

Lane 3: Fully segregated UL071 + glucose high light strain, band at ~4 kb shows the insertion of the pPSBAII promoter, *Zppdc*, *adh* and *kanamycin* genes.  
Lanes 4-10: Fully segregated UL071 + glucose low light strains, bands at ~4 kb show the insertion of the pPSBAII promoter, *Zppdc*, *adh* and *kanamycin* genes.

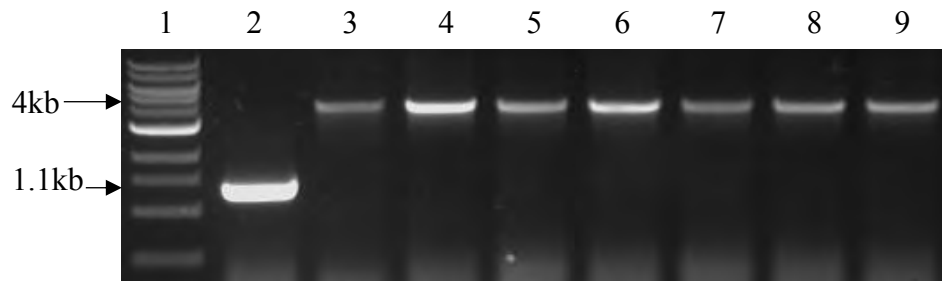


**Figure 3.27: Gel 2: 1% SYBR® safe stained DNA agarose gel from PCR assays of fully segregated strains which were brought back from a semi-segregated state.**

Re-screen to determine if repeated plating onto 100  $\mu\text{g}\cdot\text{ml}^{-1}$  kanamycin plates forced the clones back to full segregation.

Lane 1: NEB 1 kb DNA ladder.

Lane 2: WT *Synechocystis* 6803 control shows the empty PSBAII neutral site at ~1.1 kb.

Lane 3: Fully segregated UL071 + glucose low light strain, band at ~4 kb shows the insertion of the pPSBAII promoter, *Zppdc*, *adh* and *kanamycin* genes.

Lanes 4-9: Fully segregated UL072 + glucose high light strains, bands at ~4 kb show the insertion of the pPSBAII promoter, *ZpOpdc*, *adh* and *kanamycin* genes.

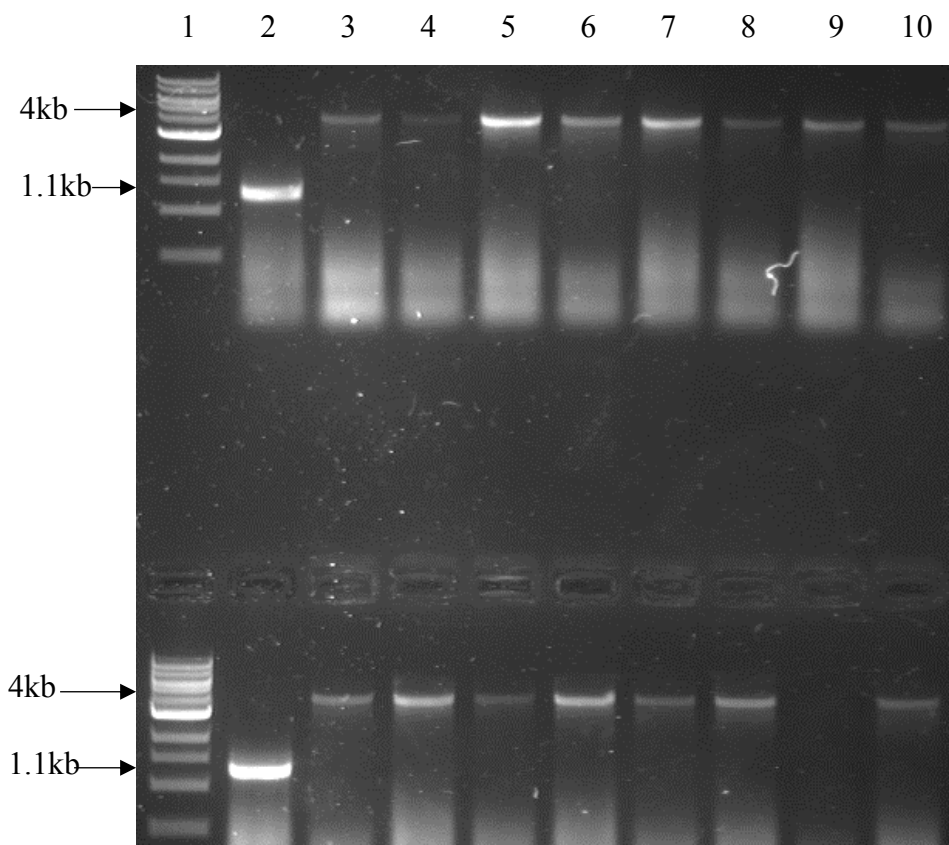


**Figure 3.28: Gel 3: 1% SYBR® safe stained DNA agarose gel from PCR assays of fully segregated strains which were brought back from a semi-segregated state.**

Re-screen to determine if repeated plating onto 100  $\mu\text{g.ml}^{-1}$  kanamycin plates forced the clones back to full segregation.

**Top of gel:**

Lane 1: NEB 1 kb DNA ladder.

Lane 2: WT *Synechocystis* 6803 control shows the empty PSBII neutral site at ~1.1 kb.

Lanes 3-8: Fully segregated UL072 + glucose low light strains, bands at ~4 kb show the insertion of the pPSBII promoter, *ZpOpc*, *adh* and *kanamycin* genes.

Lane 9: Fully segregated UL070 – glucose high light strain, band at ~4 kb shows the insertion of the pPSBII promoter, *Zmpdc*, *adh* and *kanamycin* genes.

Lane 10: Fully segregated UL071 – glucose high light strain, band at ~4 kb shows the insertion of the pPSBII promoter, *Zppdc*, *adh* and *kanamycin* genes.

**Bottom of gel:**

Lane 1: NEB 1 kb DNA ladder.

Lane 2: WT *Synechocystis* 6803 control shows the empty PSBII neutral site at ~1.1 kb.

Lane 3: Fully segregated UL071 – glucose high light strain, band at ~4 kb shows the insertion of the pPSBII promoter, *Zppdc*, *adh* and *kanamycin* genes.

Lanes 4-6: Fully segregated UL071 – glucose low light strains, bands at ~4 kb show the insertion of the pPSBII promoter, *Zppdc*, *adh* and *kanamycin* genes.

Lanes 7 and 8: Fully segregated UL072 – glucose high light strains, bands at ~4 kb show the insertion of the pPSBII promoter, *ZpOpdc*, *adh* and *kanamycin* genes.

Lane 9: Empty due to poor template preparation.

Lane 10: Fully segregated UL072 – glucose low light strain, band at ~4 kb shows the insertion of the pPSBII promoter, *ZpOpdc*, *adh* and *kanamycin* genes.

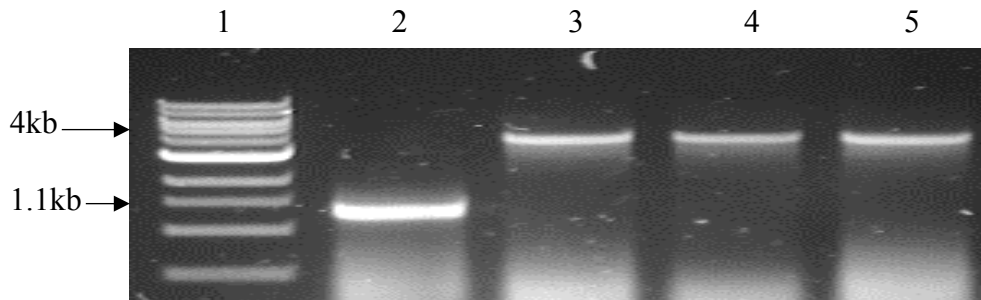


**Figure 3.29: Gel 4: 1% SYBR® safe stained DNA agarose gel from PCR assays of fully segregated strains which were brought back from a semi-segregated state.**

Re-screen to determine if repeated plating onto 100  $\mu\text{g.ml}^{-1}$  kanamycin plates forced the clones back to full segregation.

Lane 1: NEB 1 kb DNA ladder.

Lane 2: WT *Synechocystis* 6803 control shows the empty PSBII neutral site at ~1.1 kb.

Lane 3-5: Fully segregated UL072 – glucose low light strains, bands at ~4 kb show the insertion of the pPSBII promoter, *ZpOpdc*, *adh* and *kanamycin* genes.

When the recombinant strains were confirmed to be once again fully segregated, they were continuously streaked onto fresh 50 and 100  $\mu\text{g.ml}^{-1}$  kanamycin plates once per week. To re-streak them weekly at this stage was acceptable as passing them four times onto antibiotic resistant plates increased the stability of the strains and decreased the likelihood of them reverting back again to a semi-segregated state (confirmed by our repeated analysis).

However, in spite of this effort to increase the stability of the strains, this could be a possible reason as to why the created strains produced little to no ethanol (as discussed at a later stage in Section 3.6.1). It has previously been shown that ethanol has been produced successfully in *E.coli* (Ingram *et al.* 1987; Dien *et al.* 2000) using *Zmpdc* and the same ethanol synthesis pathway which was used in *Synechocystis* 6803. The same cannot be said for ethanol production in lactic acid

bacteria which is very low (Gold *et al.* 1996; Nichols *et al.* 2003). Liu *et al.* (2005) decided to use *Zppdc* in a study to rectify this problem and increase ethanol production in lactic acid bacteria (Liu *et al.* 2005). The *Zppdc* was chosen for the same reasons as outlined in this project: it's thermostable, possesses the lowest  $K_m$  for pyruvate and has the highest specific activity amongst all the bacterial PDCs (Raj *et al.* 2002). By using acid inducible and highly conserved constitutive promoters with the *Zppdc*, Liu *et al.* (2005) discovered that the acetaldehyde levels produced by the recombinant strains were 8 fold higher in comparison to the control strain but that there was no significant increase in ethanol levels. It was hypothesised that the native *adh* gene was not enough in order to convert the acetaldehyde to ethanol and by incorporating an *adh* gene directly after the *Zppdc* may be helpful. Overall however some ethanol albeit not an increased amount was produced (Liu *et al.* 2005). In this study, the recombinant strains possess two copies of the *adh* -the native gene and the gene included in the transformed construct. However, the inability of the *adh genes* to cope with the amount of acetaldehyde produced could be a possible reason for no ethanol production. In addition to this, the host organism could be why strains are more stable in other systems such as *E.coli* or *Lactococcus lactis* in comparison to *Synechocystis* 6803 possibly due to the complexity of the organism with regards to how its genome is contained (Labarre *et al.* 1989; Kaneko *et al.* 2003).

Recombinant strains containing the *Zm*, *Zp* and *ZpOpdcs* which were grown in the presence of glucose and under high or low light conditions were chosen to determine if any were producing ethanol. Those grown on the 100  $\mu\text{g.ml}^{-1}$  kanamycin plates were used and were re-screened nearer the time to ensure they were still fully segregated. Full segregation was confirmed via 1% SYBR® safe stained DNA agarose gels as before (data not shown). Recombinant strains grown in the absence of glucose did not grow as well as those which did contain glucose and so could not be checked for ethanol production due to the lack of biomass to set up an ethanol test.

From these results it can be seen that a large number of clones needed to be screened to obtain fully segregated strains for future use.

### 3.5.2 DNA sequencing to verify fully segregated strains

Fully segregated strains of UL070, UL071 and UL072 were also verified by DNA sequencing as per Section 2.3.6 using the appropriate primers as per appendix II. The sequencing was analysed in the same way as before (Section 3.2.1) using the BLAST n and CLUSTAL Omega Algorithm. No mutations were observed with the exception of those discussed in Section 3.2.2, Figures 3.2 and 3.3: the arginine and glutamic acid to alanine residues in the *Zppdc* from the genomic DNA but this was to be expected.

### 3.6 Ethanol Determination

The verified recombinant strains were cultured and assayed for ethanol production (Section 2.5) using the Yellow line kit: UV-method for the determination of ethanol in foodstuffs and other materials from R-Biopharm AG (Darmstadt, Germany).

Ethanol determination was based on the following principle (Figure 3.28): Nicotinamide-adenine dinucleotide (NAD) oxidises ethanol to acetaldehyde using alcohol dehydrogenase (ADH). Usually, equilibrium favours the left hand side of the reaction with the NAD and ethanol (i) but under alkaline conditions, this can be shifted to the right, trapping any acetaldehyde formed. In the presence of aldehyde dehydrogenase (Al-DH), acetaldehyde is oxidised to acetic acid while NAD<sup>+</sup> is reduced to NADH (ii). Its presence is determined by measuring the absorbance (R-Biopharm AG 2014) at 340nm using Sarstedt acrylic cuvettes and a Cary UV-Vis spectrophotometer.



**Figure 3.30: Principle of the ethanol assay kit.**

**Table 3.9: Strains used in ethanol tests.**

Strain used	Description
Wildtype <i>Synechocystis</i> 6803	No construct present (Control).
UL070.2	pPSBAII light promoter, <i>Zmpdc</i> , slr1192 (native <i>adh</i> ), kanamycin (this study).
UL070.4	pPSBAII light promoter, <i>Zmpdc</i> , slr1192 (native <i>adh</i> ), kanamycin (this study).
UL071.6	pPSBAII light promoter, <i>Zppdc</i> , slr1192 (native <i>adh</i> ), kanamycin (this study).
UL071.7	pPSBAII light promoter, <i>Zppdc</i> , slr1192 (native <i>adh</i> ), kanamycin (this study).
UL071.9	pPSBAII light promoter, <i>Zppdc</i> , slr1192 (native <i>adh</i> ), kanamycin (this study).
UL072.6	pPSBAII light promoter, <i>ZpOpdc</i> , slr1192 (native <i>adh</i> ), kanamycin (this study).
UL072.7	pPSBAII light promoter, <i>ZpOpdc</i> , slr1192 (native <i>adh</i> ), kanamycin (this study).

UL070, UL071 and UL072 indicate the strains with the *pdC* variation. The number after the decimal point for each indicates an independent isolate for that strain.

Only two strains containing the *Zm* and *ZpOpdc* were tested while three strains containing the *Zppdc* were used (Table 3.9). This was due to bleaching which was observed occasionally and therefore resulted in the loss of some cultures. It was hypothesised that because the *Zp/ZpOPDC* possessed a lower *K<sub>m</sub>* than the *PDC* from *Zymomonas mobilis* (Raj *et al.* 2002) more pyruvate may have been removed from the pathway involved in biomass production and hence, cultures were

becoming stressed and began to “bleach out”. This observation is also consistent with Borirak *et al.* (2015) where it was stated that diverting carbon towards product and away from central metabolism is a “key stress issue” which would in turn have an effect on the growth rate and hence the production of biomass (Borirak *et al.* 2015). This may also explain the colour change of the cultures from a dark healthy green to a pale, light and sometimes almost white/clear colour. In addition to this, a change in appearance was also seen by Takahama *et al.* (2003) due to metabolically engineering *Synechococcus elongatus* PCC 7942 to produce ethylene. This resulted in the growth of strains with a “yellow-green appearance” while strains that did not produce ethylene possessed a “healthy green-blue” colour (Takahama *et al.* 2003). Cultures throughout the project would also occasionally visibly clump together which again may suggest stress or metabolic shock due to the above. Another possibility may be the over production of acetaldehyde which is known for its toxic effects. As suggested by Dexter *et al.* (2015), this issue may be improved by titrating the PDC and ADH levels in a more optimised manner (Dexter *et al.* 2015). During the determinations it was reasoned that the change in culture appearance may very well have been due to a combination of these reasons.

Figure 3.31 below illustrates two *Synechocystis* 6803 cultures: Berkeley wildtype on the left and UL004 on the right. By comparing the two flasks, it can clearly be seen that the wildtype culture appears as a much darker, robust culture while UL004 (the ethanol producer) is much lighter in colour. Both strains were cultured from the same starting  $OD_{730nm}$  of 0.4. This recombinant UL004 strain produces  $\sim 0.1$  g/L/ $OD_{730nm}$  of ethanol (Armshaw, personal communication, unpublished data) following an  $OD_{730nm}$  adjustment to 0.4 and cultivation for three days. It was hypothesised that the strains created in this work could potentially produce a great deal more than that due to the use of the ZpPDC with its lower  $K_m$  (Raj *et al.* 2002).

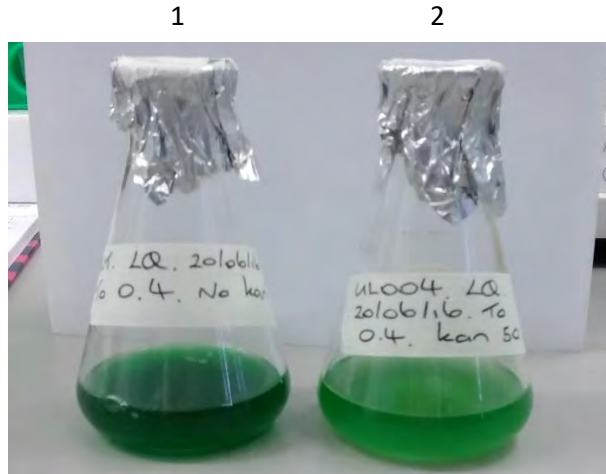


**Figure 3.31: Cultures of wildtype *Synechocystis* 6803 and UL004.** (On the left and right respectively). A difference in colour can clearly be seen. WT *Synechocystis* 6803 does not contain any construct while UL004 contains pUL004 which consists of the pPSBII light promoter, the *Zmpdc*, the slr1192 native *adh* and the *kanamycin* resistance gene in the PSBII neutral site.

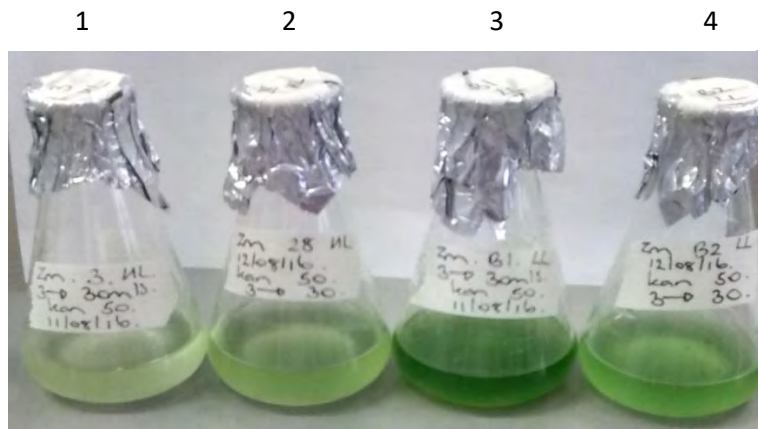
### 3.6.1 Strains tested for ethanol production

Below are some examples of the strains created during this project and cultured for ethanol determination (Section 2.5).

Figure 3.32 shows UL070 strains with the two cultures on the left grown from transformants which were held under high light conditions and the two on the right under low light conditions. Those exposed to high light are clearly much lighter in colour and seem to be bleaching as described earlier while those under low light appear to be slightly healthier, especially flask number 3 with its rich dark green appearance. It was expected upon completion of an ethanol test to find that cultures which looked like those in flasks 1, 2 and 4 would be producing a greater amount of ethanol than UL004 in Figure 3.31 due to the possible reasons mentioned above.

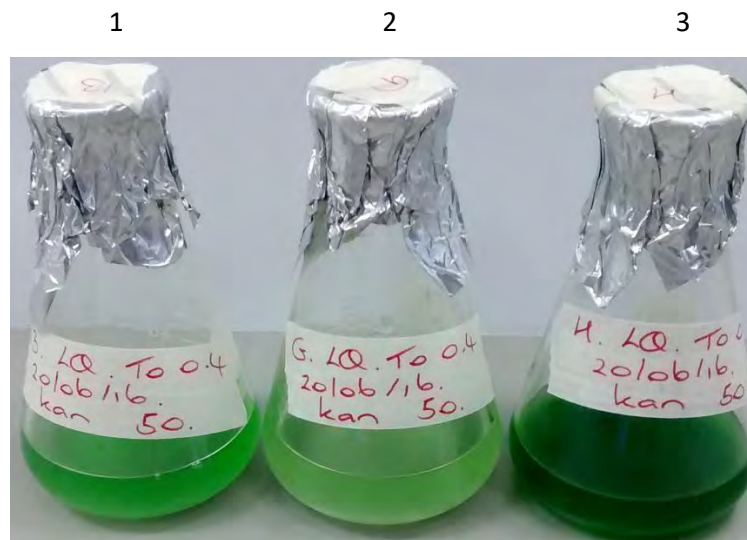
These cultures are much lighter in colour than the UL004 culture which looks somewhat more like flask 3. One could also assume that this flask would produce in or around the same amount of ethanol as UL004. It is also imperative to point out that judging how much ethanol may be produced by looking at the colour of the

culture is merely observational and in reality there was not always a connection between the two as results will later show.



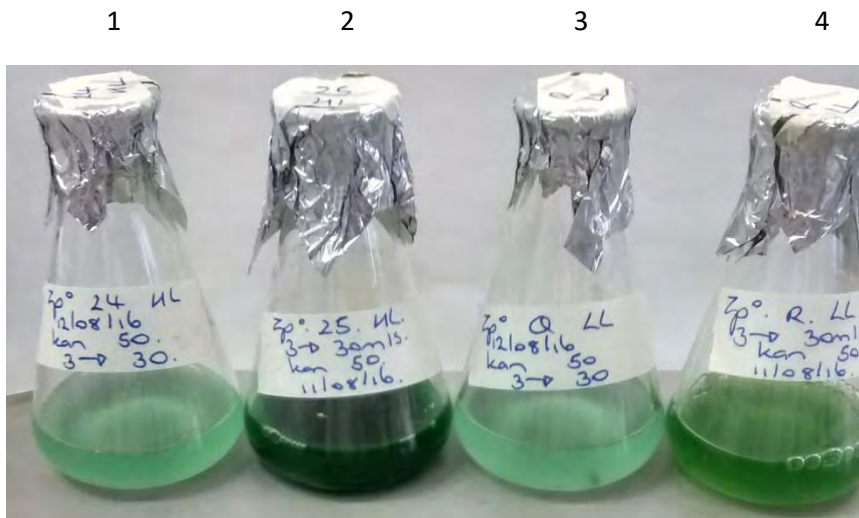
**Figure 3.32: Independent isolates of UL070 strains.** Re-created versions of UL004 to act as a control therefore these strains also contain pUL004 as described above in Figure 3.31.

Figure 3.33 shows some examples of UL071 cultures containing the *Zppdc*. Once again the colour variation is prominent with flask number 2 looking quite pale in colour in comparison to flask 1 and a vast difference can be seen against flask 3. These cultures below which were tested for ethanol were screened beforehand as mentioned above to confirm full segregation. For flask number 3 it is misleading that the culture looks relatively robust when the presence of ethanol would cause stress for the production of biomass, resulting in a similar appearance to flasks 1 or 2. In situations such as this it was questioned why there was no detectable ethanol production even with fully segregated and sequence verified strains. It is unlikely that during cultivation, the recombinant and segregated strains reverted back to wildtype status or were not as stable as previously thought. However, there are possibilities that the internal cytoplasmic conditions were incompatible with the functionality of the ZpPDC which operates best at an optimum pH of 5.5-6.0 (Raj *et al.* 2002) which is slightly more acidic than the preferred pH of *Synechocystis* 6803 which is between 7 and 8.5 (Heidorn *et al.* 2010), that its expression could have been reduced or that the availability of the ThDp cofactor may have been altered. Some sort of ThDp modification may also have been required as the ZpPDC has not been well studied. However, these potentialities were not examined.



**Figure 3.33: Independent isolates of UL071 strains.** These strains contain pUL101 which consists of the pPSBAII light promoter, the *Zppdc*, the native *slr1192 adh* and the *kanamycin* resistance gene in the PSBAII neutral site.

As mentioned above, some cultures appeared white or clear in colour which can be seen below in Figure 3.34, especially with flasks 1 and 3. These cultures are independent isolates of UL072 strains with the *Zppdc* which was codon optimised (*ZpOpdc*) for use in *Synechocystis* 6803. It was hypothesised that by taking this step, any issues which may arise with the strains containing the native version of the *Zppdc* may be resolved by simply adapting it to the organism in question. However, results will later show that this was not the case. Clumping of the cultures which contained the *ZpOpdc* did occur during growth (images not shown) which again is another sign of stress on the organism assumingly caused by high levels of ethanol in the environment, large amounts of pyruvate being diverted away from biomass production or a combination of both as previously mentioned.



**Figure 3.34: Independent isolates of UL072 strains.** These strains contain pUL102 which consists of the pPSBAII light promoter, the ZpOpdc, the native slr1192 *adh* and the *kanamycin* resistance gene in the PSBAII neutral site.

Figure 3.35 below also illustrates some extreme cases of bleaching as mentioned above. A slight tint of green is still visible for flasks 2 and 3 which began as healthy looking cultures but bleached out due to a stressful environment. Flask 1 is also quite a good example of the white/clear colour stated earlier.

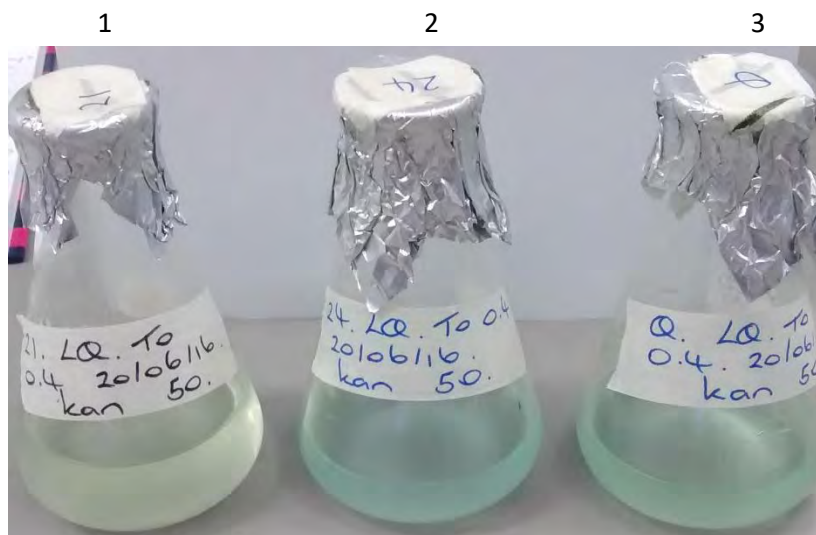


**Figure 3.35: Flask 1: Independent isolate of a UL070 strain. Flasks 2 and 3: Independent isolates of UL072 strains.** (UL070 strain described in Figure 3.31 and UL072 strain in Figure 3.34).

In order to overcome the problems with bleaching strains, some cultures were covered with one layer of tissue paper to reduce the light while others were given extra glucose. These actions however did not help with the growth of the cells.

### 3.6.2 OD<sub>730nm</sub> and ethanol results for tested strains

As described earlier, cultures were selected and tested for ethanol production over a period of 0, 3, 7 and 11 days. OD<sub>730nm</sub> and ethanol results over this time period were recorded and can be seen below.

**Table 3.10: OD<sub>730nm</sub> readings for wildtype *Synechocystis* 6803 on days 0, 3, 7 and 11.**

Time (days)	Wildtype
0	0.4
3	2.533
7	12.71
11	18.205

**Table 3.11: OD<sub>730nm</sub> readings for independent isolates of UL070 strains on days 0, 3, 7 and 11 as well as the average readings and standard deviation.**

Time (days)	UL070.2	UL070.4		Average	Standard Deviation
0	0.4	0.4		0.4	0
3	1.521	1.522		1.522	0
7	7.018	5.066		6.042	1.380
11	15.805	6.605		11.205	6.505

UL070 contains the *Zymomonas mobilis pdc*

**Table 3.12: OD<sub>730nm</sub> readings for independent isolates of UL071 strains on days 0, 3, 7 and 11 as well as the average readings and standard deviation.**

Time (days)	UL071.6	UL071.7	UL071.9	Average	Standard Deviation
0	0.4	0.4	0.4	0.4	0
3	1.615	0.391	0.38	0.795	0.710
7	4.88	1.682	1.732	2.765	1.832
11	7.825	4.89	4.72	5.812	1.746

UL071 contains the native *Zymobacter palmae pdc*

**Table 3.13: OD<sub>730nm</sub> readings for independent isolates of UL072 strains on days 0, 3, 7 and 11 as well as the average readings and standard deviation.**

Time (days)	UL072.6	UL072.7		Average	Standard Deviation
0	0.4	0.4		0.4	0
3	0.553	0.656		0.605	0.073
7	0.87	2.55		1.71	0.84
11	2.825	4.26		3.543	1.015

UL072 contains the codon optimised *Zymobacter palmae pdc*

**Table 3.14: Combined OD<sub>730nm</sub> readings for wildtype *Synechocystis* 6803 and UL070, UL071 and UL072 strains (average readings) as well as standard deviation.**

Time (days)	Wildtype	Average UL070	Average UL071	Average UL072
0	0.4	0.4	0.4	0.4
3	2.533	1.522	0.795	0.605
7	12.71	6.042	2.765	1.71
11	18.205	11.205	5.812	3.543
		<b>Standard Deviation</b>	<b>Standard Deviation</b>	<b>Standard Deviation</b>
		0	0	0
		0	0.710	0.073
		1.380	1.832	0.84
		6.505	1.746	1.015

UL070 contains the *Zymomonas mobilis pdc*, UL071 contains the native *Zymobacter palmae pdc* and UL072 contains the codon optimised *Zymobacter palmae pdc*

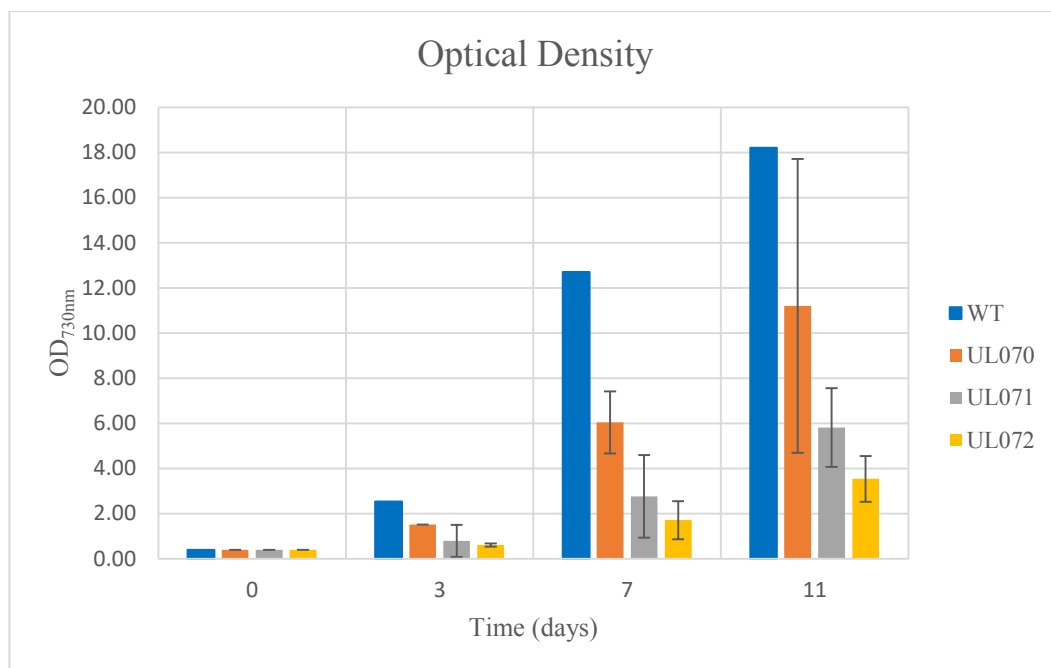


**Figure 3.36: Bar chart representation of the OD<sub>730nm</sub> readings of WT, UL070, UL071 and UL072 strains tested for ethanol production.** Produced from the data in Table 3.14. OD readings measured at 730nm on the y axis with time in days on the x axis. All cultures began at OD<sub>730nm</sub> of 0.4 on day 0.

In Figure 3.36 above by day 3 it can be seen that wildtype *Synechocystis* 6803 had the highest OD<sub>730nm</sub> out of all the strains (rather than it having the “fastest growth rate”). This is what was expected due to the inability to produce ethanol and hence no diversion of pyruvate away from biomass which resulted in a stress free environment (rephrased sentence). From day 3 to 7 its OD<sub>730nm</sub> jumps dramatically from 2.5 to 12.7 and steadily rises to 18.2 on day 11. For the modified strains, all OD<sub>730nm</sub> readings are clearly below wildtype which suggested some sort of metabolic stress which caused a decrease in cell mass with cultures struggling to grow. Strains UL071 and UL072 seemed to be struggling more so than UL070 which implied a greater burden had been placed on these cultures with the highest OD<sub>730nm</sub> for UL071 (5.8, day 11) and for UL072 (3.5, day 11) turning out to be less than half of the highest OD<sub>730nm</sub> for UL070 (11.2, day 11).

**Table 3.15: Ethanol levels in g/L/OD<sub>730nm</sub> for independent isolates of UL070 strains on days 0, 3, 7 and 11 as well as average levels, standard deviation and 90% confidence intervals (CI).**

Time (days)	UL070.2	UL070.4		Average	Standard Deviation	90% CI
0	0.00	0.00		0.00	0.00	0.00
3	0.1	0.1		0.1	0.00	+/-0
7	0.12	0.15		0.13	0.02	+/- 0.02
11	0.07	0.2		0.13	0.09	+/- 0.1

UL070 contains the *Zymomonas mobilis pdc*

**Table 3.16: Ethanol levels in g/L/OD<sub>730nm</sub> for independent isolates of UL071 strains on days 0, 3, 7 and 11 as well as average levels, standard deviation and 90% confidence intervals (CI).**

Time (days)	UL071.6	UL071.7	UL071.9	Average	Standard Deviation	90% CI
0	0.00	0.00	0.00	0.00	0.00	0.00
3	0.03	0.05	0.01	0.03	0.02	+/- 0.02
7	0.02	0.06	0.03	0.03	0.02	+/- 0.02
11	0.04	0.06	0.04	0.04	0.01	+/- 0.01

UL071 contains the native *Zymobacter palmae pdc*

**Table 3.17: Ethanol levels in g/L/OD<sub>730nm</sub> for independent isolates of UL072 strains on days 0, 3, 7 and 11 as well as average levels, standard deviation and 90% confidence intervals (CI).**

Time (days)	UL072.6	UL072.7		Average	Standard Deviation	90% CI
0	0.00	0.00		0.00	0.00	0.00
3	0.00	0.03		0.01	0.02	+/- 0.02
7	0.03	0.02		0.02	0.01	+/- 0.01
11	0.07	0.05		0.06	0.01	+/- 0.01

UL072 contains the codon optimised *Zymobacter palmae pdc*

**Table 3.18: Combined ethanol levels in g/L/OD<sub>730nm</sub> for wildtype *Synechocystis* 6803 and strains UL070, UL071 and UL072 (average readings) as well as standard deviation.**

		Average	Average	Average
Time (days)	<b>Wildtype</b>	<b>UL070</b>	<b>UL071</b>	<b>UL072</b>
0	0.00	0.00	0.00	0.00
3	0.00	0.1	0.03	0.01
7	0.00	0.13	0.03	0.02
11	0.00	0.13	0.04	0.06
		<b>Standard Deviation</b>	<b>Standard Deviation</b>	<b>Standard Deviation</b>
		0.00	0.00	0.00
		0.00	0.02	0.02
		0.02	0.02	0.01
		0.09	0.01	0.01

UL070 contains the *Zymomonas mobilis pdc*, UL071 contains the native *Zymobacter palmae pdc* and UL072 contains the codon optimised *Zymobacter palmae pdc*

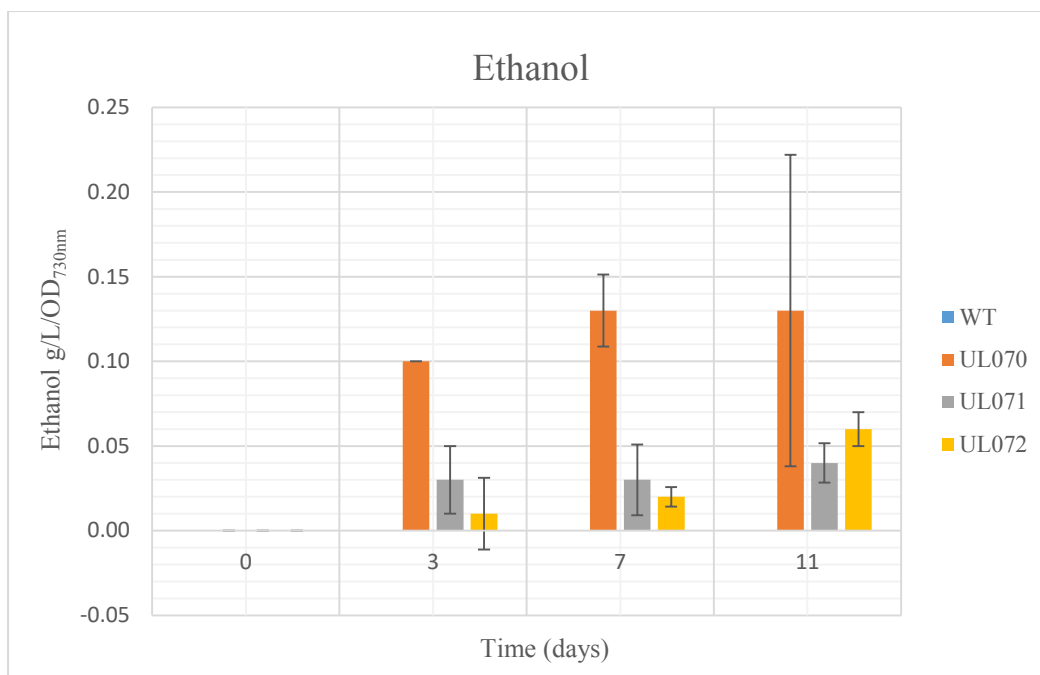


**Figure 3.37: Bar chart representation of ethanol levels in g/L/OD<sub>730nm</sub> for tested WT, UL070, UL071 and UL072 strains on days 0, 3, 7 and 11.** Produced from the data in Table 3.19. Time in days on the x axis and ethanol in g/L/OD<sub>730nm</sub> on the y axis.

The bar chart above in Figure 3.37 shows that all strains produced 0 g/L/OD<sub>730nm</sub> of ethanol on day 0 (removed Table 3.15 which showed ethanol levels produced by *Synechocystis* 6803 on days 0, 3, 7 and 11) and levels for each strain subsequently varied over the course of the 3, 7 and 11 days. The wildtype *Synechocystis* 6803 strain in Figure 3.36 above lies as a horizontal line along the x axis of the graph which implies no ethanol production during the test period. This correlates well with the wildtype OD<sub>730nm</sub> readings in Figures 3.34/3.35 as it was hypothesised that a high OD<sub>730nm</sub> indicated no ethanol production i.e. no stress. For UL070 (re-created version of UL004) which was used as a control, it can clearly be seen that it produced the largest amount of ethanol on each of the 3 days in comparison to the other strains. UL004 usually produces ~0.1 g/L/OD<sub>730nm</sub> after 3 days of cultivation and on day 3 for UL070, this was the amount produced by this strain with the levels rising to 0.13 g/L/OD<sub>730nm</sub> for days 7 and 11. This data is also in agreement with its above OD<sub>730nm</sub> values due to growing much less than wildtype *Synechocystis* 6803 which is indicative of a more stressful environment. So far, the data for both the wildtype and UL004 controls has reinforced what had been considered to be happening in these strains. However, looking at the ethanol levels

for the UL071 and UL072 strains, the same pattern was not followed. Both graphs show that these modified strains produced more ethanol than wildtype *Synechocystis* 6803 but much less than the best ethanol producing strain UL070 (re-created UL004). The OD<sub>730nm</sub> values in Figures 3.36 above for these strains are quite low and show poor growth which contradicts what was seen in the graphs for ethanol production. It was hypothesised from earlier findings with wildtype and UL070 that a decrease in growth would result in an increase in ethanol levels. If this was the case, then these modified strains should have produced even more ethanol than UL070 which is not what the results showed.

In reality, even though the OD<sub>730nm</sub> readings are low so too are the resulting ethanol levels which led us to believe that the ZpPDC was possibly converting a lot of pyruvate (directed away from biomass) to acetaldehyde but this may not have been coupled correctly to the ADH and so very low to no ethanol was produced. The over production of this toxic intermediate may also have contributed to the bleaching effect if the coupling mechanism was incorrect or if too much was present for the ADH to handle. It may also have been due to negative feedback or feedback inhibition which is a form of allosteric regulation. An increase in the production of the final product (ethanol) may have inhibited the activity of the ZpPDC enzyme by binding to its allosteric site and causing a conformational change. This may have halted the ethanol production and only when these levels fell under a certain threshold was the process started again due to the reactivation of the enzyme (Hearst Seattle Media LLC 2016). Could it be possible that the level of ethanol needed to cause this negative feedback was quite low and that any remaining ethanol (once the ZpPDC enzyme was inhibited) evaporated before the cultures could be tested? Another prospect that was considered was the pH of the environment that the ZpPDC was forced to operate in. *Zymobacter palmae* PDC has an optimum pH range of 5.5-6.0 (Table 1.3, Section 1.4.4). The internal pH of *Synechocystis* 6803 is ~8.2 which is considerably higher and a more alkaline pH than the optimal condition for ZpPDC. Therefore, the next step to investigate this further was to purify the *Zymobacter palmae* PDC and examine the activity via an enzymatic assay at various pH values.

### **3.7 Activity assay with *Synechocystis* sp. PCC 6803 CFE**

Once the above strains were tested for ethanol production and prior to assaying the purified ZpPDC at different pH values, it was decided to carry out an activity assay on each of the strains containing the Zm (UL070), Zp (UL071) and ZpOpdc (UL072) with wildtype *Synechocystis* 6803 used as a control. It was hypothesised that possibly little to no activity would be detected due to the lack of ethanol production which may also be due to problems associated with the ZpPDC protein itself, as well as the other possibilities mentioned above. Four strains in total were cultured and lysed according to a method kindly developed and provided by Davide Montesarchio (personal communication) from UvA, Amsterdam as per Section 2.9.3 with some modifications.

#### **3.7.1 Lysis analysis of *Synechocystis* sp. PCC 6803 cells prior to activity assay**

Prior to carrying out the activity assay, the lysis method was tested in order to guarantee correct lysis on the day of the assay. The same strains as above were selected, cultured and lysed as per Section 2.9.3.1 using heat and variation of the vortex time during the bead beating process. SDS-PAGE gels showing the results of each lysis method can be seen below.

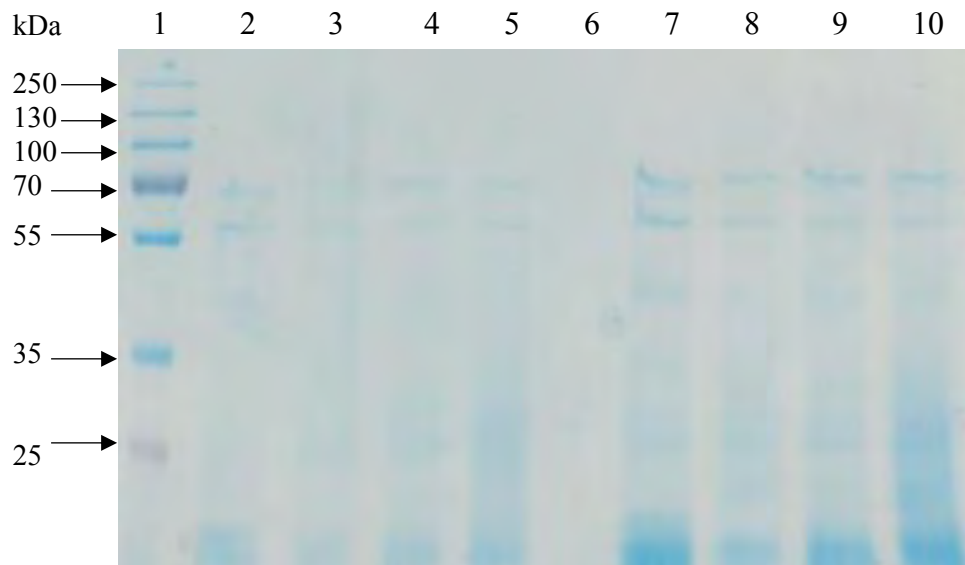


**Figure 3.38: 12% SDS-PAGE gel stained with Instant Blue showing samples of *Synechocystis* 6803 (WT, UL070, UL071 and UL072) lysed with heat.**

Lane 1: PageRuler™ plus pre-stained protein ladder.

Lane 2: 10 µl sample of WT *Synechocystis* 6803.

Lane 3: 10 µl sample of a UL070 strain (*Zmpdc*).

Lane 4: 10 µl sample of a UL071 strain (*Zppdc*).

Lane 5: 10 µl sample of a UL072 strain (*ZpOpdc*).

Lane 6: Empty.

Lane 7: 20 µl sample of WT *Synechocystis* 6803.

Lane 8: 20 µl sample of a UL070 strain (*Zmpdc*).

Lane 9: 20 µl sample of a UL071 strain (*Zppdc*).

Lane 10: 20 µl sample of a UL072 strain (*ZpOpdc*).

By looking at the gel above in Figure 3.38, it can be concluded that heat alone is not enough in order to successfully lyse *Synechocystis* 6803 cells. Only a small amount of protein is visible but this is an indication that some lysis did take place. Solely using this method would compromise the assay from the very beginning as even if the PDC enzymes were fully active, the release of such a small amount in the CFE could possibly lead to the detection of no activity.

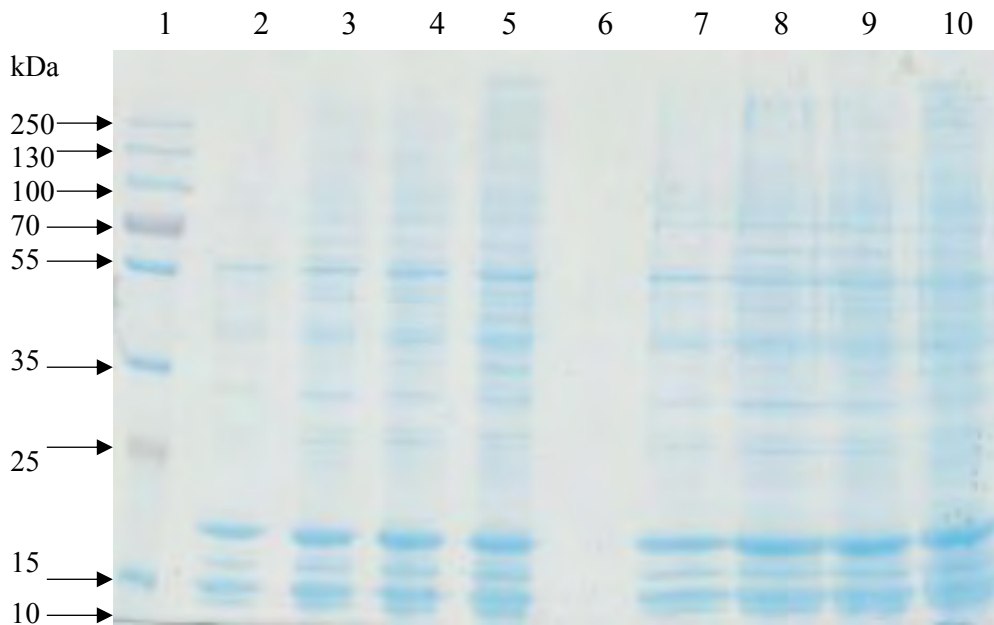


**Figure 3.39: 12% SDS-PAGE gel stained with Instant Blue showing samples of *Synechocystis* 6803 (WT, UL070, UL071 and UL072) lysed via bead beating (time variation) and freeze/thaw.**

Lane 1: PageRuler™ plus pre-stained protein ladder.

Lane 2: 10 µl sample of WT *Synechocystis* 6803, 30 minute bead beat.

Lane 3: 10 µl sample of a UL070 strain (*Zmpdc*), 1 hour bead beat.

Lane 4: 10 µl sample of a UL071 strain (*Zppdc*), 1.5 hour bead beat.

Lane 5: 10 µl sample of a UL072 strain (*ZpOpdc*), 2 hour bead beat.

Lane 6: Empty.

Lane 7: 20 µl sample of WT *Synechocystis* 6803, 30 minute bead beat.

Lane 8: 20 µl sample of a UL070 strain (*Zmpdc*), 1 hour bead beat.

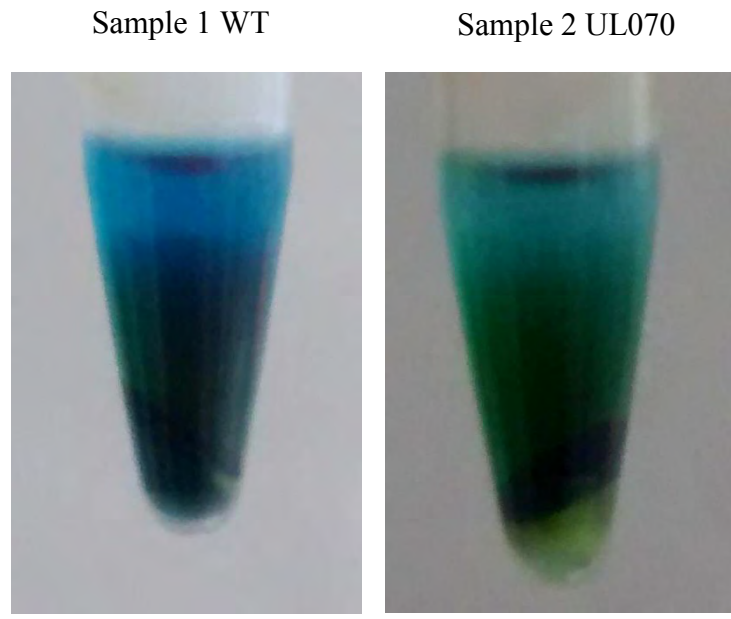
Lane 9: 20 µl sample of a UL071 strain (*Zppdc*), 1.5 hour bead beat.

Lane 10: 20 µl sample of a UL072 strain (*ZpOpdc*), 2 hour bead beat.

Using both the methods of bead beating and freeze thaw, it can be seen from the gel in Figure 3.39 that the lysis efficiency increased immensely from the gel in Figure 3.38. Many more proteins are visible throughout the gel for each time used to bead beat the cells. It can also be deduced that the effectiveness of the lysis did increase with time as slightly more blue bands can be seen after 1 hour in comparison to 30 minutes. The same can also be said when comparing the other time periods to one another. The lysate also appeared as a blue/purple colour which is a sign of successful lysis due to the release of the many pigments contained within cyanobacteria. However, even though the 2 hour bead beat time did show the best cell lysis, it gave very similar results to the 1.5 hour time period (lanes 4 and 5 and 9 and 10 respectively). Therefore, to save time and the use of

equipment, the 1.5 hour bead beat time was selected and was used in the activity assay.

The chosen strains (WT, UL070, UL071 and UL072) were therefore cultured and lysed by bead beating as per Section 2.9.3.



**Figures 3.40 and 3.41: Samples 1 and 2 showing lysed WT *Synechocystis* 6803 and a UL070 strain respectively.**

Sample 3 UL071



Sample 4 UL072



**Figures 3.42 and 3.43: Samples 3 and 4 showing lysed UL071 and UL072 strains respectively.**

The blue/purple colour indicative of a successful lysis can be seen very well in sample 1 (Figure 3.40) for the wildtype *Synechocystis* 6803 control. For samples 2 and 3 (Figures 3.41 and 3.42 respectively) it is also visible but to a lesser extent. For sample 4 (Figure 3.43) it's slightly more difficult to see which does imply that the lysis was not as successful as the others which is reflected in the concentration of protein in the CFE (see below). These observations also correlated well with the gel below in Figure 3.44 which shows the lysed samples used in the assay. The UL072 strain in lanes 5 and 10 do show less protein in comparison to the other lanes. However, the amount of protein present was still a sufficient amount to use in the activity assay.

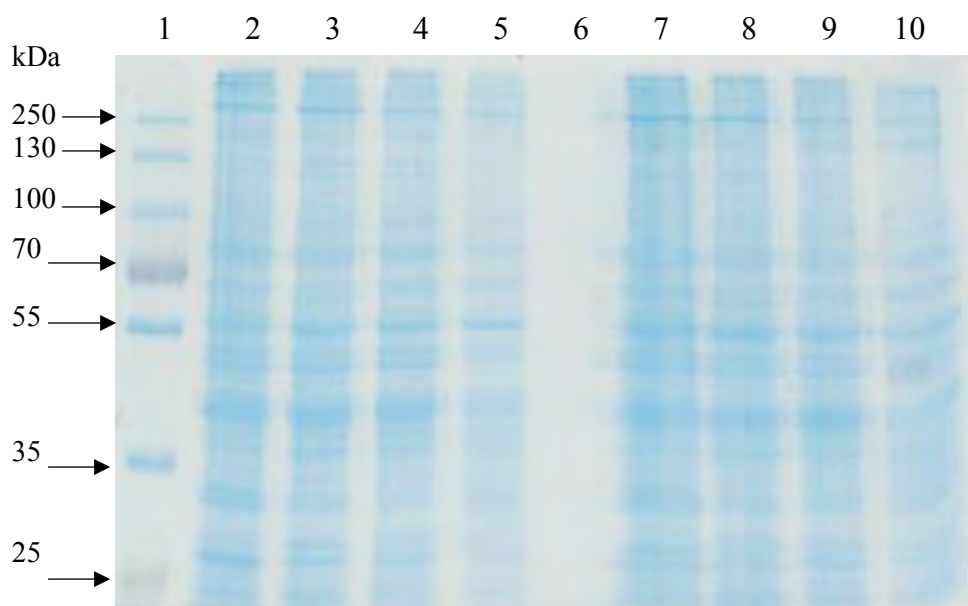


**Figure 3.44: 12% SDS-PAGE gel stained with Instant Blue showing samples of *Synechocystis* 6803 (WT, UL070, UL071 and UL072) lysed via bead beating for 1.5 hours and freeze/thaw for the activity assay.**

Lane 1: PageRuler™ plus pre-stained protein ladder.

Lane 2: 10 µl sample of WT *Synechocystis* 6803.

Lane 3: 10 µl sample of a UL070 strain (*Zmpdc*).

Lane 4: 10 µl sample of a UL071 strain (*Zppdc*).

Lane 5: 10 µl sample of a UL072 strain (*ZpOpdc*).

Lane 6: Empty.

Lane 7: 20 µl sample of WT *Synechocystis* 6803.

Lane 8: 20 µl sample of a UL070 strain (*Zmpdc*).

Lane 9: 20 µl sample of a UL071 strain (*Zppdc*).

Lane 10: 20 µl sample of a UL072 strain (*ZpOpdc*).

The CFE concentrations for each were checked as before using the Nanodrop spectrophotometer ND-1000 and were as follows:

Wildtype *Synechocystis* 6803: 8.88 mg.ml<sup>-1</sup>

UL070: 8.3 mg.ml<sup>-1</sup>

UL071: 6.98 mg.ml<sup>-1</sup>

UL072: 3.38 mg.ml<sup>-1</sup>

The assay was set up using the same reagents as per Section 2.9 and the same protocol as per Section 2.9.2.2 was followed for both the assay and data analysis.

Unfortunately upon analysis of the results, no sign of activity was detected. The absorbance readings for each substrate concentration remained more or less the same during the 5 minutes with no significant decrease. As predicted, this may have been due to inactive PDC protein or the lysis procedure may still not have been 100% efficient. This might have resulted in the release of too little protein or the pH of the assay environment may have been incorrect for the PDCs. The pH of the buffer used in these assays was at pH 7.8 which is close to the internal pH of *Synechocystis* 6803 (pH 8.2) and was therefore the ideal pH for the PDC to work at. An attempt was made to repeat this assay in the same way as before but to culture the strains in BG-11 buffer at different pH values: 6.0, 7.8 and 8.2 (standard BG-11 pH). These buffers were prepared as per Section 2.9.3.2. The cultures were allowed to grow for a few days and the pH was subsequently checked using pH indicator sticks from Thermo Fisher Scientific (Ballycoolin, Dublin 15, Ireland) in the laminar hood to keep the cultures sterile. However, upon doing so the cultures appeared at ~pH 8.0 which is the desired pH for *Synechocystis* 6803. It seemed that the strains buffered their environment back to their preferred pH and so as a result, it was decided not to proceed with this idea and chose to purify the ZpPDC and check its activity alone at the different pH values.

### **3.8 Purification of *Zymobacter palmae* PDC**

The ZpPDC protein was expressed and purified using the methods outlined in Gao *et al.* (2012) but with some modifications (Gao *et al.* 2012). Expression was carried out as per Section 2.6.1 using the *E.coli* BL21 (DE3)\* strain transformed with the pULLQ2 plasmid (Figure 3.6, Section 3.2.2). Purification was then performed as per Section 2.6.2 with an XK column and Akta prime™ plus purification system from GE healthcare.

### 3.8.1 Protein visualisation

Samples taken during the purification process were run on 12% SDS-PAGE gels and Western blots (Section 2.6.3), the results of which can be seen below.

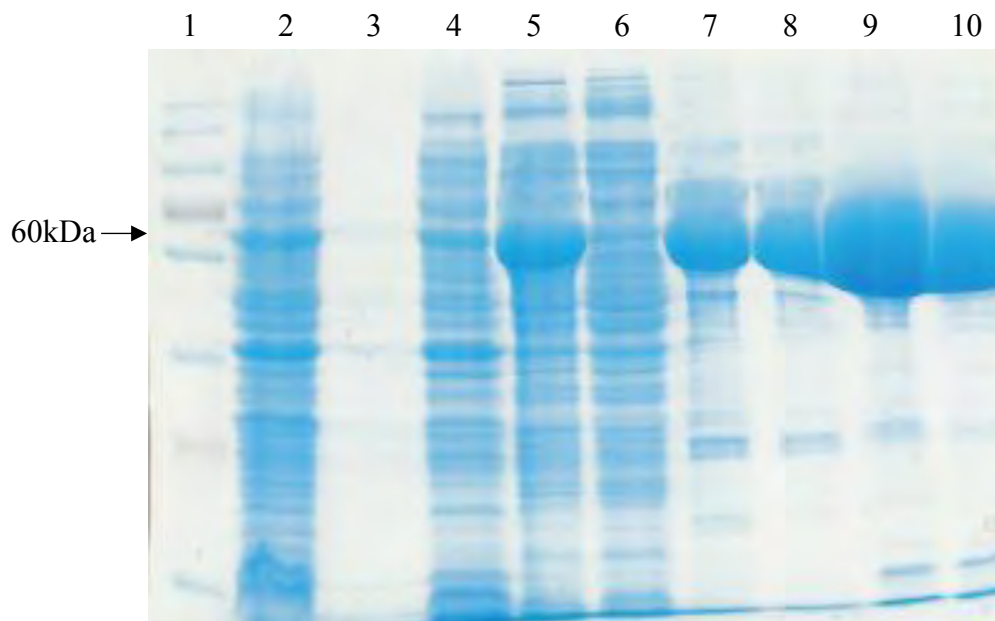


**Figure 3.45: Gel 1: 12% SDS-PAGE gel stained with Instant Blue showing fractions collected during the purification of the ZpPDC.**

- Lane 1: PageRuler™ plus pre-stained protein ladder.
- Lane 2: Cell pellet before sonication step.
- Lane 3: Supernatant before sonication step.
- Lane 4: Cell pellet after sonication step.
- Lane 5: Supernatant after sonication step.
- Lane 6: Flow through collected from the column.
- Lane 7: 150 mM elution fraction.
- Lane 8: 150 mM elution fraction.
- Lane 9: 250 mM elution fraction.
- Lane 10: 250 mM elution fraction.

The ZpPDC protein is a cytoplasmic protein of ~60 kDa. In lane 3 of gel number 1 above in Figure 3.45, no evidence of the protein can be seen prior to sonication but a large amount is visible in lane 5 at the 60 kDa mark once the cells were lysed. In lanes 2 and 4, trace amounts of the protein can be seen in the cell pellet. Lane 6 indicates the flow through collected from the column and even though a large quantity of proteins are evident, there is hardly any ZpPDC protein. Due to its 6X histidine tag, it is now bound to the nickel column while the majority of the unwanted proteins have simply flowed through and were collected. Lanes 7 and 8

show collected fractions once the 150 mM elution buffer was applied to the column. With such a high quantity of imidazole, the ZpPDC protein was knocked from the resin and was collected in 5 ml quantities. Some other proteins are visible here too but at a different size to the ZpPDC. These are other proteins which occasionally bind to the nickel resin possible due to a natural stretch of histidine residues in their amino acid sequence. Usually the majority of these proteins are knocked off at a lower imidazole concentration. In the final two lanes, large quantities of the desired protein can clearly be seen at the correct size as indicated by the two large blue bands.

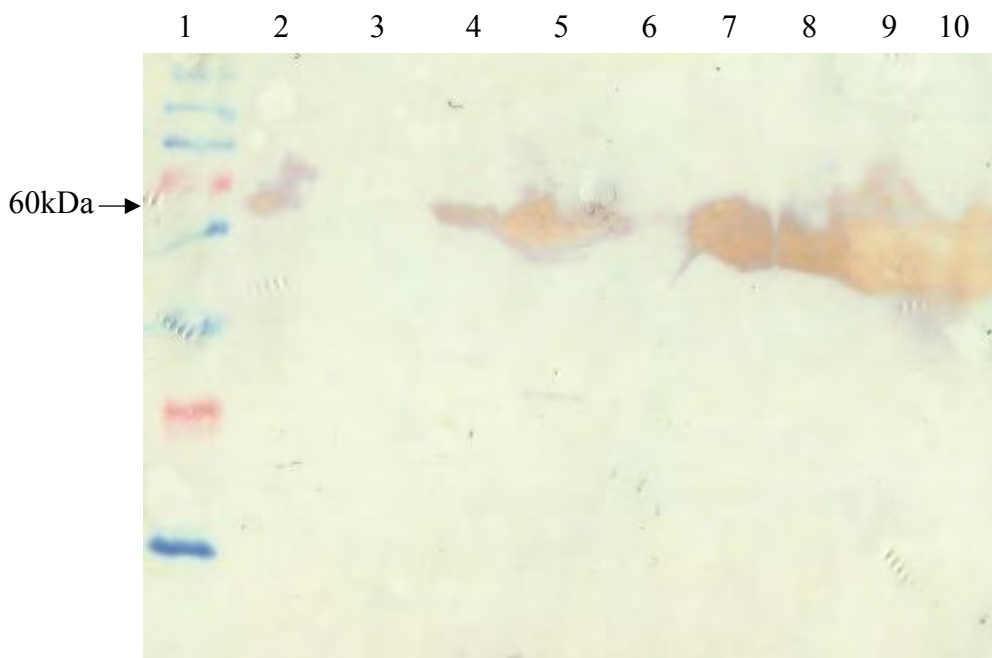


**Figure 3.46: Blot 1: Western blot showing fractions collected during the purification of ZpPDC.** Corresponds to the SDS-PAGE gel above in Figure 3.45.

Lane 1: PageRuler™ plus pre-stained protein ladder.

Lane 2: Cell pellet before sonication step.

Lane 3: Supernatant before sonication step.

Lane 4: Cell pellet after sonication step.

Lane 5: Supernatant after sonication step.

Lane 6: Flow through collected from the column.

Lane 7: 150 mM elution fraction.

Lane 8: 150 mM elution fraction.

Lane 9: 250 mM elution fraction.

Lane 10: 250 mM elution fraction.

Above is a Western blot which corresponds to the SDS-PAGE gel in Figure 3.45. Due to the 6X histidine tag on the ZpPDC, it was possible to visualise the protein on a blot to determine if the protein that was observed on the SDS-PAGE gels was indeed the correct protein. In Figure 3.46 above, a protein can be seen in lanes 2, 4, 5, 7, 8, 9 and 10 at ~60 kDa which corresponds to the position of the ZpPDC above in the gel. Therefore, it can be concluded that this protein is in fact the purified ZpPDC protein. In lanes 9 and 10 it can be observed that the protein has begun to flake away from the blot which usually happens when large amounts of protein are present. Again, this corresponds well to the quantity of protein visible in lanes 9 and 10 of the gel above.

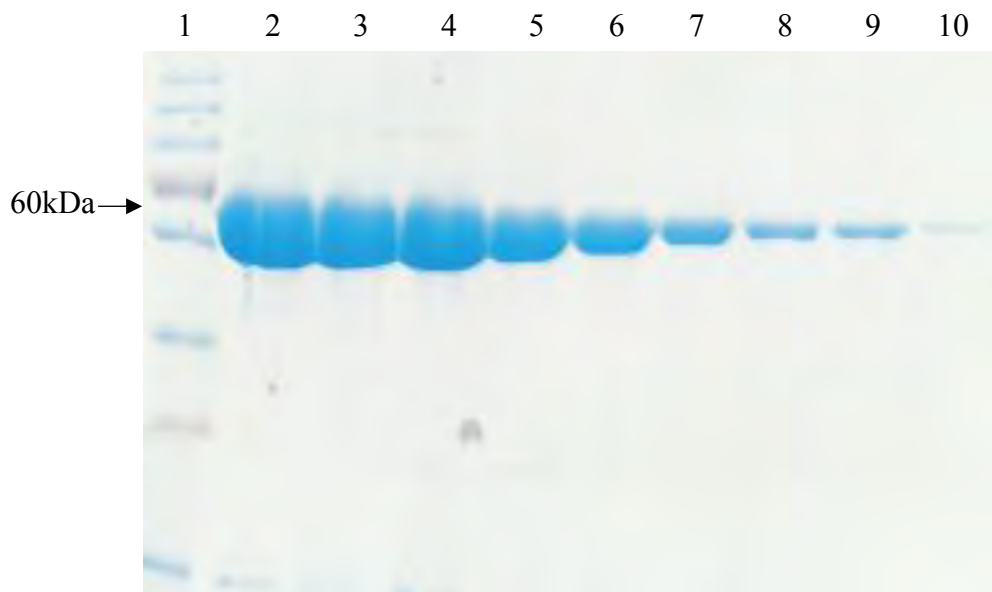


**Figure 3.47: Gel 2: 12% SDS-PAGE gel stained with Instant blue showing fractions collected during the purification of the ZpPDC.**

Lane 1: PageRuler™ Plus pre-stained protein ladder.

Lane 2: 250 mM elution fraction.

Lane 3: 350 mM elution fraction.

Lane 4: 350 mM elution fraction.

Lane 5: 350 mM elution fraction.

Lane 6: 500 mM elution fraction.

Lane 7: 500 mM elution fraction.

Lane 8: 1000 mM elution fraction.

Lane 9: 1000 mM elution fraction.

Lane 10: 1000 mM elution fraction.

In gel number 2 (Figure 3.47 above), a much more purified version of the ZpPDC protein can be seen in these collected fractions in comparison to those in gel 1 (Figure 3.45). The majority of the target protein was eluted from the column at the 250 mM and 350 mM imidazole concentrations as depicted by both gels. Some of the protein was still eluted at the higher imidazole concentrations of 500 and 1000 mM but only very small amounts. The gel also indicates that the majority of any non-specifically bound proteins were eluted earlier increasing the purity of the ZpPDC protein on this gel.

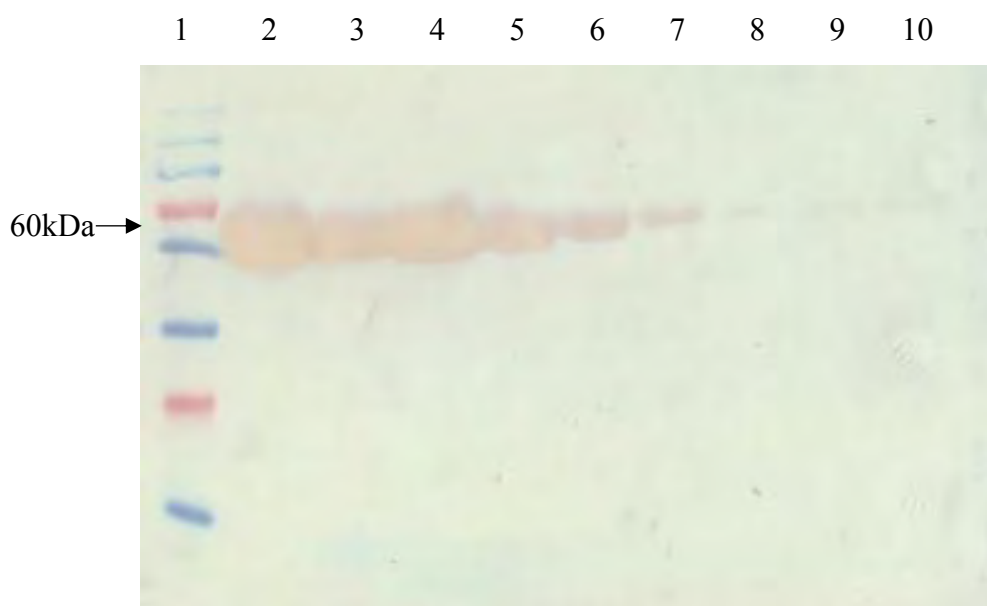


**Figure 3.48: Blot 2: Western blot showing fractions collected during the purification of the ZpPDC.** Corresponds to the SDS-PAGE gel above in Figure 3.47.

- Lane 1: PageRuler™ Plus pre-stained protein ladder.
- Lane 2: 250 mM elution fraction.
- Lane 3: 350 mM elution fraction.
- Lane 4: 350 mM elution fraction.
- Lane 5: 350 mM elution fraction.
- Lane 6: 500 mM elution fraction.
- Lane 7: 500 mM elution fraction.
- Lane 8: 1000 mM elution fraction.
- Lane 9: 1000 mM elution fraction.
- Lane 10: 1000 mM elution fraction.

The blot above in Figure 3.48 also supports what was concluded in blot 1 in Figure 3.46. Strong bands of the ZpPDC protein are visible at the 60 kDa mark for the 250

mM and 350 mM imidazole concentrations in lanes 2, 3, 4 and 5 which also correspond to what can be seen in the SDS-PAGE gel. Trace amounts of the target protein are visible in lanes 8, 9 and 10 eluted by the 1 M imidazole concentration. The peaks on the chromatogram below in Figure 3.49 provide a clear picture of the elution profile for the purification of the ZpPDC protein.

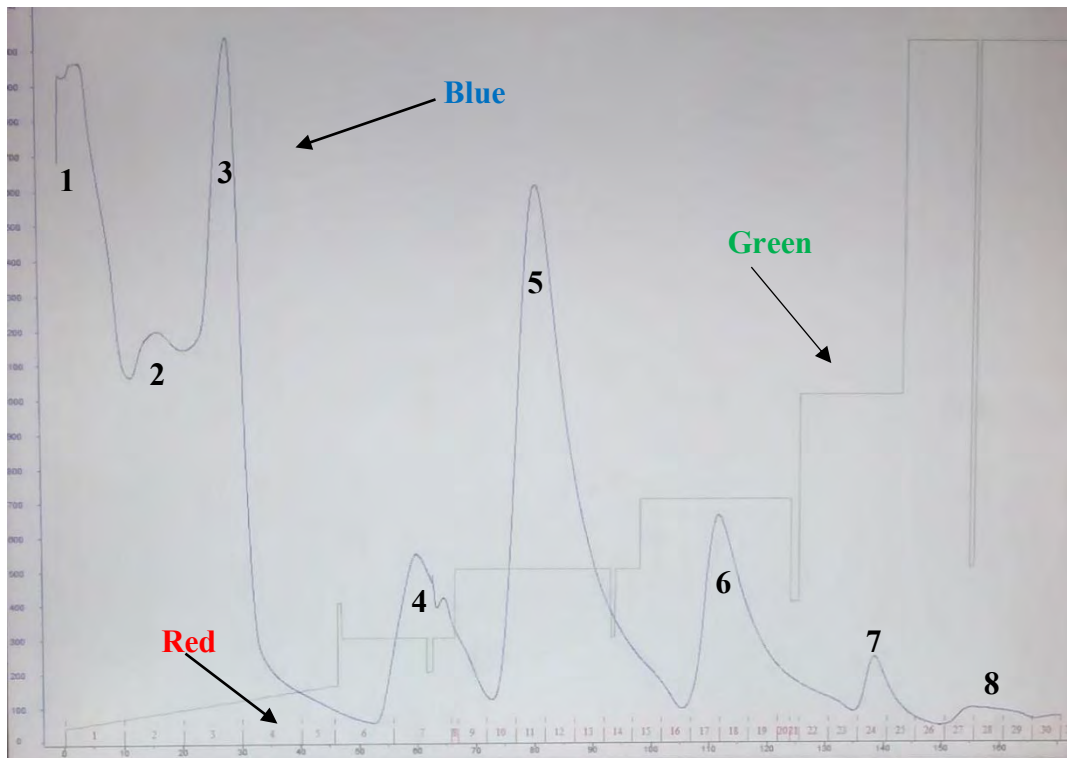


**Figure 3.49: Chromatogram of the purification process as shown by the Primeview software with the Akta™ prime plus purification system.** The peaks indicate the elution of a protein from the nickel column. Blue lines indicate the UV absorption of proteins, red indicates the fraction numbers and green indicates the concentration.

Peaks 1, 2 and 3: Tubes 1-5 with the 20, 60 and 100 mM wash fractions.

Peak 4: Tubes 6, 7 and 8 with the 150 mM wash fractions.

Peak 5: Tubes 9-14 with the 250 mM elution fractions.

Peak 6: Tubes 15-21 with the 350 mM elution fractions.

Peak 7: Tubes 22-25 with the 500 mM elution fractions.

Peak 8: Tubes 26-30 with the 1000 mM elution fractions.

### 3.8.2 Dialysis

The collected and pooled fractions containing the majority of the ZpPDC were dialysed as per Section 2.6.4. These fractions were the 250, 350, 500 and 1000 mM

fractions. In total there was ~100 ml of protein and so it was divided into two 50 ml volumes to make it easier to handle (50 ml number 1: the 250 mM and half of the 350 mM fraction, 50 ml number 2: remainder of the 350 mM fraction as well as the 500 mM and 1000 mM fractions). During the buffer exchange, it was noticed that tubing number two had taken on a white, cloudy appearance (see Figure 3.50 below) which was more than likely due to precipitated protein. The fractions in this tubing as described above certainly contained more of the ZpPDC protein than the others hence the reason it may have come out of solution. Prior to concentrating this volume, it was spun down to remove the precipitate as this could have blocked the filters in the concentrator.

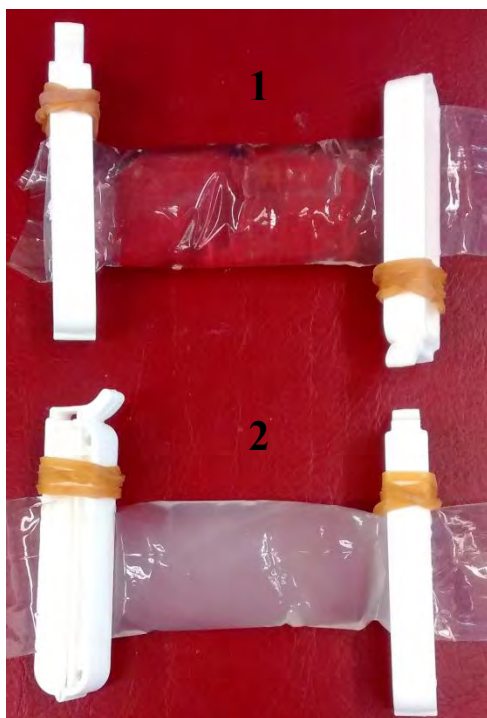


**Figure 3.50: Dialysis tubing sealed with dialysis tubing clips.** The first (1) and second (2) 50 ml volumes of collected protein are described above. Notice the different appearance of tubing number 2 due to the precipitated protein.

### 3.8.3 Concentration

Once dialysed, the two 50 ml volumes were concentrated and the concentration examined as per Section 2.6.5. This resulted in  $7.45 \text{ mg.ml}^{-1}$  for 50 ml number 1 and  $96.16 \text{ mg.ml}^{-1}$  for 50 ml number 2 which in total was  $\sim 100 \text{ mg.2ml}^{-1}$  or  $50 \text{ mg.ml}^{-1}$  of protein.

### 3.8.4 SEC

Usually the next step would be to purify the protein to homogeneity on a SEC (Size Exclusion Chromatography) column such as the Hiload™ 16/60 Superdex™ 200 prep grade column and concentrate it again in the same way as described earlier. However, based on the observed purity of the ZpPDC protein on the SDS-PAGE gel in Figure 3.47 above it was decided for this preparation to use the purified protein directly for crystallisation trials. The protein was therefore aliquoted to 20 µl amounts and stored in liquid nitrogen in the -80°C freezer.

## 3.9 Crystallisation trials

The crystallisation conditions used in Dobritsch *et al.* (1998) which crystallised the ZmPDC were used as a reference (Dobritsch *et al.* 1998). However at first, the Hampton Research Index Screen HR2-144 with 96 different conditions from Hampton Research (CA 92656-3317, USA) was used to attempt the crystallisation of the ZpPDC. This approach was taken as there was no guarantee that the conditions used to crystallise one protein would crystallise another, no matter what their similarity.

The kit used consisted of 96 reagents which are formulated to provide a rapid screening method for the crystallisation of various macromolecules such as nucleic acids, peptides and proteins. The screen contained various zones to cover a wide range of conditions that could potentially lead to crystal formation. These zones include classic salts such as sodium potassium phosphate or ammonium sulphate in a pH range of 3.5 to 8.5, high salt concentrations with low polymer concentrations and vice versa, neutralised organic acids such as succinate, sodium malonate, the pentaerythritols and tacsimate, low ionic strength and PEG (polyethylene glycol) with salt in the same pH range as above as well as PEG and salt at a set pH. Each of these zones are spread out amongst the 96 different conditions which aid to make the screening process somewhat easier and certainly faster. If some zones resulted in the formation of crystals, then the corresponding conditions were focused upon for optimisation of the crystal screen to enhance crystal growth (Hampton Research 2006b).

### 3.9.1 Initial trials

For the initial crystallisation attempt of the ZpPDC, the sitting drop vapour diffusion method was used even though it was noted that the ZmPDC was crystallised using the hanging drop method. Each crystallisation plate contained 24 wells therefore there were four in total each of which were filled as per Section 2.7.1 and labelled extensively. The four plates were left in a temperature controlled room at 20°C for a number of weeks and they were checked regularly using a Nikon SMZ1500 light microscope for crystal growth. Pictures of any crystals formed were taken and can be observed below in Figures 3.51 and 3.52.

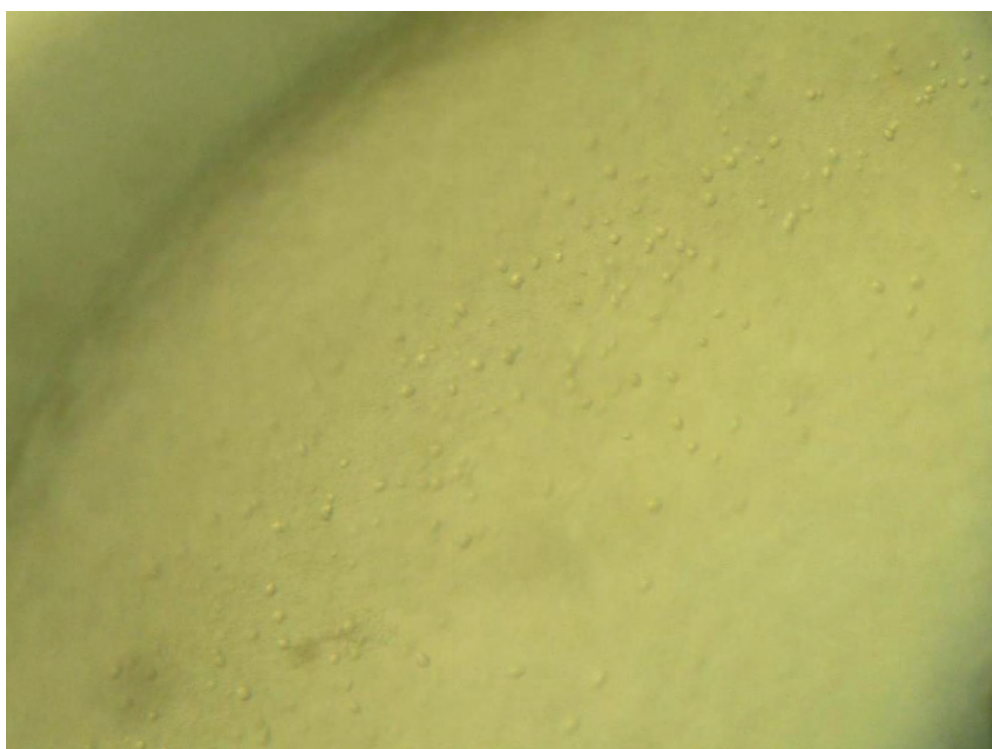


**Figure 3.51: Crystals obtained under index screen number 75 (attempt number 1, initial trials).** Similar crystals were obtained under screen number 88 but those in well 75 looked more promising.

### 3.9.2 Follow on trials

Following the results of the first screen, condition number 75 which contained 0.2 M lithium sulphate, 0.1 M BIS-TRIS pH 6.5 and 25% (w/v) PEG 3350 resulted in the growth of small crystals. Condition number 88 also gave similar results (0.2 M ammonium citrate tribasic pH 7.0, 20% PEG 3350) but screen number 75 was

pursued upon recommendation. Looking at the conditions used to crystallise the ZmPDC, more than double the protein concentration was used at  $13 \text{ mg.ml}^{-1}$  but the pH was the same at pH 6.5 albeit a different buffer. The PEG % was also close at 24% but PEG 1500 was used instead of 3350.

The PEG% of screen number 75 was varied at 15, 17, 20, 22.5 and 30% with screen number 75 used as a control (at 25%) while the protein concentration was varied from 1, 2, 5 and  $10 \text{ mg.ml}^{-1}$  by diluting the  $50 \text{ mg.ml}^{-1}$  stock. All other conditions remained the same. Reagents were prepared and the plate was filled as per Section 2.7.2. The same process as before was followed with regards to plate storage and checking for crystal growth.

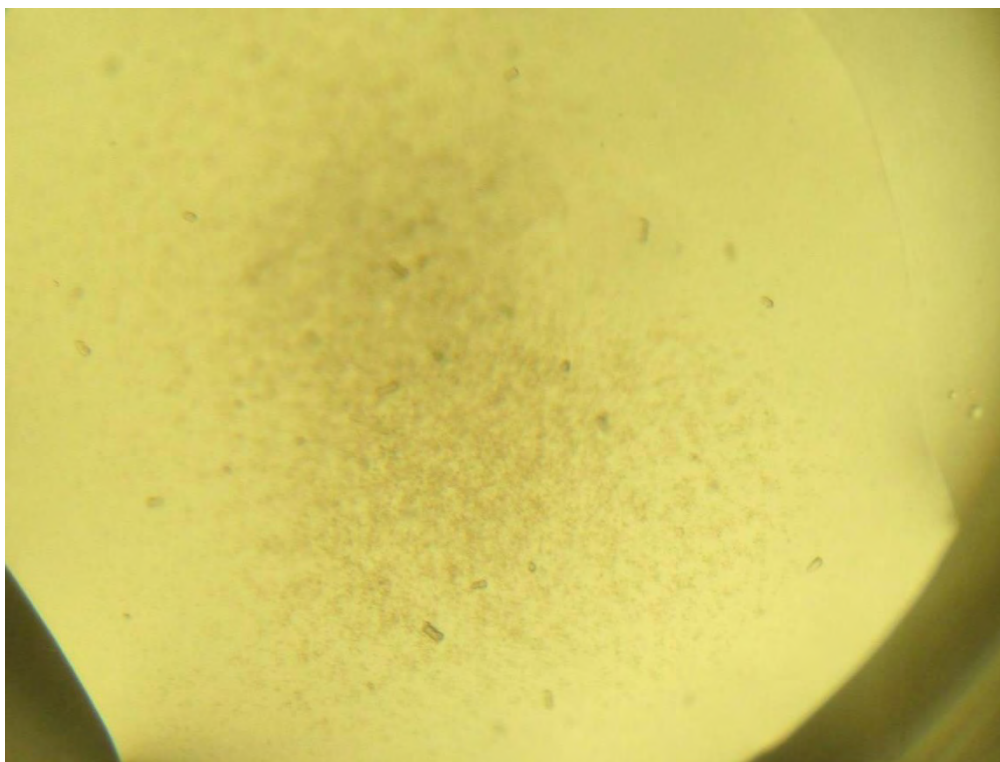


**Figure 3.52: Slightly larger crystals were seen at  $1 \text{ mg.ml}^{-1}$  ZpPDC and in the range of 20-25% PEG 3350 (attempt number two, follow on trials).**

### **3.9.3 Published data**

Crystallisation of ZmPDC by Dobritsch *et al.* (1998) indicated that their optimisation conditions consisted of a buffer at pH 6.0 and PEG in the range of 19-22% (Dobritsch *et al.* 1998) both of which were quite similar to the optimised

conditions used and observed for the ZpPDC in this study. The crystals however in Figure 3.52 above were obtained at a much lower protein concentration of 1 mg.ml<sup>-1</sup> in comparison to their 13 mg.ml<sup>-1</sup> in which they also had small amounts of the ThDp and Mg<sup>2+</sup> cofactors. Further optimisation was in progress, however unfortunately (removed “to our dismay”) during this study, the crystal structure of ZpPDC was published in August by Buddrus *et al.* 2016. The conditions used by Buddrus *et al.* (2016) to crystallise the ZpPDC were 0.15 M sodium citrate pH 5.5 so slightly lower than what was used for the ZmPDC in this study and what was used in both crystallisation trials. Also 14% PEG 3350 was used in comparison to 1550 but the percentage was again slightly lower than what was used before (Buddrus *et al.* 2016).

### **3.10 Homology Modelling**

Active site and surrounding amino acid residues of the Zm and ZpPDC enzymes from one monomer were grouped together from Dobritsch *et al.* (1998) and Buddrus *et al.* (2016) and can be viewed in Table 3.20 below (Dobritsch *et al.* 1998; Buddrus *et al.* 2016). From this Table it can be seen that all the active site and surrounding amino acid residues in both enzymes are the same except for a polar threonine (T) at position 471 in ZmPDC which is a non-polar aliphatic valine (V) at the corresponding position of 466 in ZpPDC. This is shown in Figures 3.53-3.55 below.

**Table 3.19: Active site and surrounding amino acid residues in one monomer of the Zm and ZpPDC enzymes.**

ZmPDC	ZpPDC	ZmPDC	ZpPDC
V24	V23	H414	H409
D27	D26	I415	I410
Y28	Y27	D440	D435
E50	E49	G441	G436
T72	T71	S442	S437
V75	V74	L445	L440
L112	L111	I465	I460
H113	H112	N467	N462
H114	H113	G469	G464
D289	D288	Y470	Y465
Y290	Y289	T471	V466
T388	T383	I472	I467
G389	G384	E473	E468
D390	D385	I476	I471
W392	W387	N483	N477
G413	G408		

The sole difference is highlighted in red: polar threonine (T) at position 471 in ZmPDC is a non-polar aliphatic valine (V) at the corresponding position of 466 in ZpPDC.

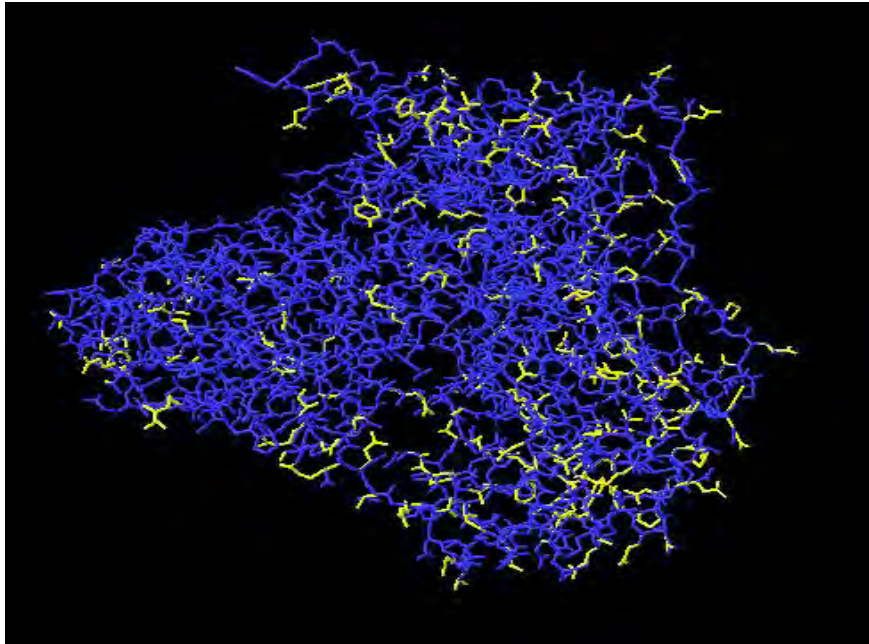


**Figure 3.53: A monomer from the Zm and ZpPDC enzymes superimposed on one another.** (Constructed in Swiss PDB viewer, see Section 2.7.3). ZmPDC in blue (PDB entry 1ZPD) and ZpPDC in yellow (PDB entry 5EUJ).

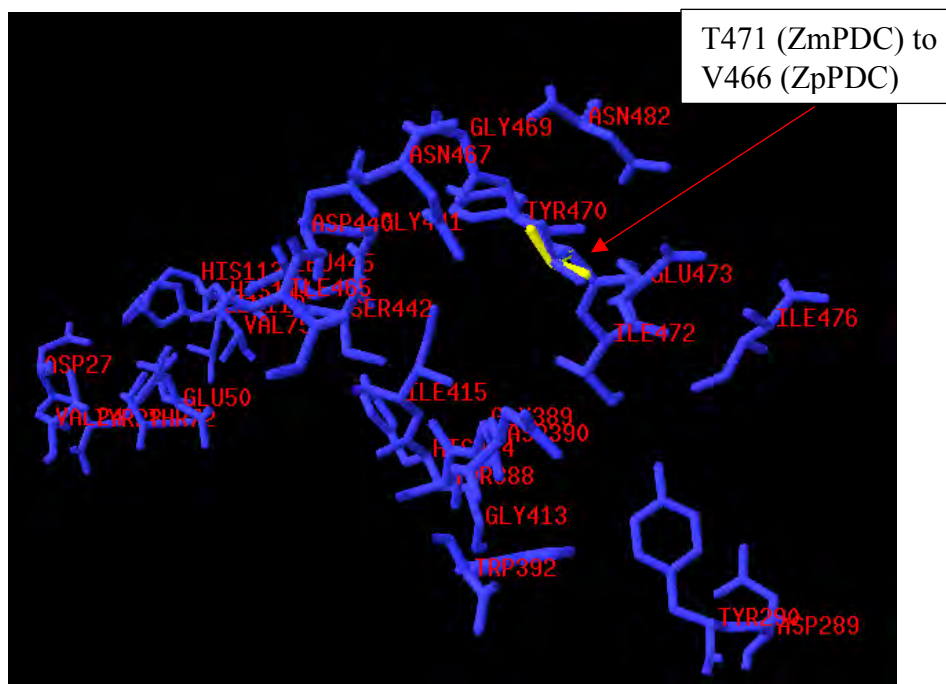


**Figure 3.54: Active site and surrounding amino acid residues (labelled according to the ZmPDC) in a monomer of the Zm and ZpPDC enzymes superimposed on one another.** (Constructed in Swiss PDB viewer, see Section 2.7.3). ZmPDC in blue (PDB entry 1ZPD) and ZpPDC in yellow (PDB entry 5EUJ). Sole difference: polar T471 in ZmPDC is a non-polar aliphatic V466 in ZpPDC as depicted by the visible yellow residue above. All other residues are the same in both enzymes.

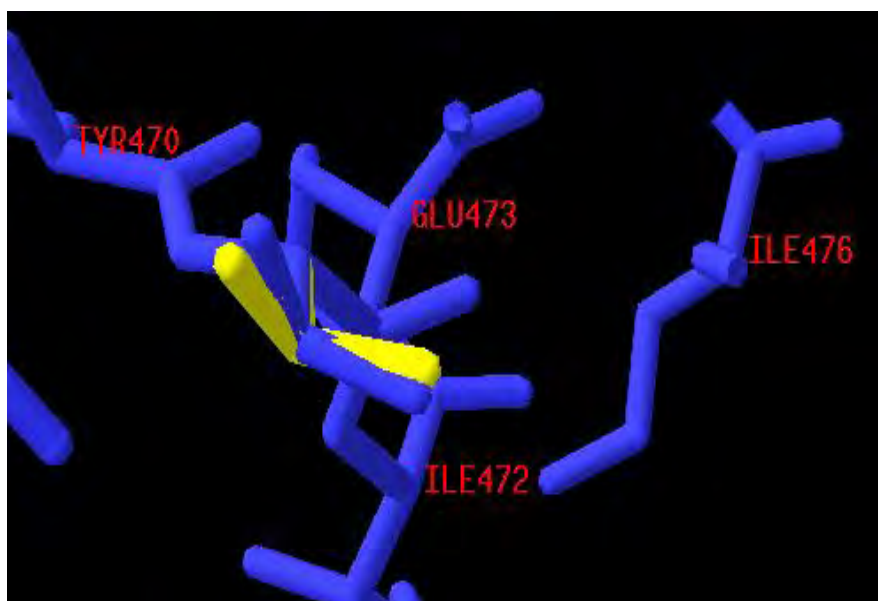


**Figure 3.55: Close up of the active site and surrounding amino acid residues (labelled according to the ZmPDC) in a monomer of the Zm and ZpPDC enzymes superimposed on one another.** (Constructed in Swiss PDB viewer, see Section 2.7.3). ZmPDC in blue (PDB entry 1ZPD) and ZpPDC in yellow (PDB entry 5EUJ). Sole difference as depicted above in Figure 3.54.

### **3.11 Activity assay with purified ZpPDC**

#### **3.11.1 Activity assay to determine a fixed [protein] of purified ZpPDC for future assays**

As with previous enzyme assays, it was necessary to determine the optimal amount of ZpPDC protein which would work best to measure activity. Therefore, an assay was carried out using the same reagents as per Section 2.9. The assay protocol and data analysis as per Section 2.9.2.2 were also followed. Protein was prepared as per Section 2.9.3.3. Upon analysis of the results, the 2  $\mu$ g protein concentration showed the most significant decrease in absorbance and so this amount was chosen for the assay with the variation in pH.

#### **3.11.2 Activity assay using a fixed [protein] of purified ZpPDC at different pH values**

This assay also followed the same protocols as above in Section 3.11.1 for reagents used, assay procedure and data analysis. However, the protein was diluted in Tris

buffer at either pH 6.0, 7.8 or 8.2. The buffers at these pH values used in the plate set up were also used in comparison to using a buffer at one pH.

Upon looking at the results (and the resulting Michaelis-Menten graphs in Figures 3.56, 3.57 and 3.58 below), a similar trend to what was witnessed earlier in Section 3.7 (the activity assay using *Synechocystis* 6803 CFE) was observed. No significant decrease was detected in the absorbance readings as well as no detectable change in the slope values which can be seen below in Table 3.21, possibly indicating no activity. This may have been due to the use of purified protein with a 6X histidine tag on the C terminus which could have possibly interfered with how the enzyme folded or with the interaction of the cofactors with the active site resulting in functional differences. Therefore, to rectify this it was decided to insert a TEV/thrombin cleavage site by re-cloning the *Zppdc* into the same pET22b (+) vector and then removing the 6X histidine tag from the C terminus once the protein had been purified again using IMAC. However, as with the crystallisation trials, during this process the paper by Buddrus *et al.* (2016) was published on the crystal structure of ZpPDC (Buddrus *et al.* 2016) and so it was decided to cease further work in this direction.

Despite the assay with the purified ZpPDC not giving any conclusive results on the hypothesis that the ZpPDC is pH dependent, it may still be valid as the optimum pH of ZpPDC is pH 6.0 rather than the more alkaline pH of 8.2 within *Synechocystis* 6803 which may be a possible reason for not producing an increased amount of ethanol. This may also imply that the *Zmpdc* used in the ethanol cassette may be only working to half its potential by operating at this much higher pH than its optimum value which is also pH 6.0. With regards to the ZpPDC, it cannot be compared directly to the PDC from *Zymomonas mobilis*. Simply because the ZpPDC is working well in *Synechocystis* 6803 to produce ethanol doesn't necessarily mean that the ZpPDC will behave in exactly the same way. It was hypothesised that it would enzymatically work better due to possessing a lower  $K_m$  but under the conditions used this was not the case.

**Table 3.20: Data gathered from the activity assay using a buffer at three different pH values: 6.0, 7.8 and 8.2.**

<b>pH 6.0</b>		<b>pH 7.8</b>		<b>pH 8.2</b>	
[S] mM	<b>Average slope (Vo) mM.sec<sup>-1</sup></b>	<b>Average slope (Vo) mM.sec<sup>-1</sup></b>	<b>Standard Deviation</b>	<b>Average slope (Vo) mM.sec<sup>-1</sup></b>	<b>Standard Deviation</b>
3.2	0.000005	0.0035	0.00069	0.003	0.00012
3.0	0.00000323	0.003167	0.00012	0.0029	0.00006
2.8	0.000005	0.003333	0.00012		
2.4	0.00012	0.0036	0.00017	0.00197	0.00006
2.0	0.0000073	0.003733	0.00023	0.00223	0.00012
1.6	0.000019	0.0036	0.00017	0.0021	0
1.2	0.0000073	0.003333	0.00006	0.0017	0
0.8	0.00028	0.003	0.0002	0.0013	0
0	0	0	0	0	0

The average slope (Vo) values in mM.sec<sup>-1</sup> are shown for each substrate concentration value in mM as well as the standard deviation. **Note:** A significant standard deviation could not be calculated for the pH 6.0 values due to them being so close to 0. Also, the values for the 2.8 mM [S] at pH 8.2 were outliers and so were omitted.

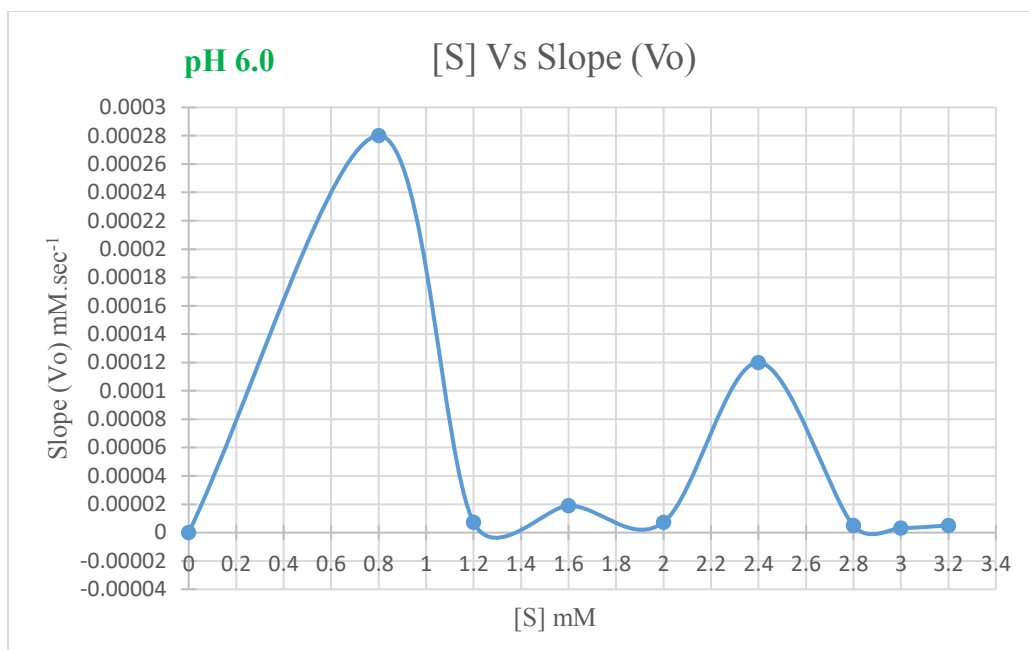


**Figure 3.56: Michaelis-Menten graph using purified ZpPDC at pH 6.0.** Produced from the data in Table 3.21 above using purified ZpPDC in Tris-HCl buffer pH 6.0 with substrate concentration in mM on the x axis and the average rate (slope Vo) for each substrate concentration value in mM.sec<sup>-1</sup> on the y axis.

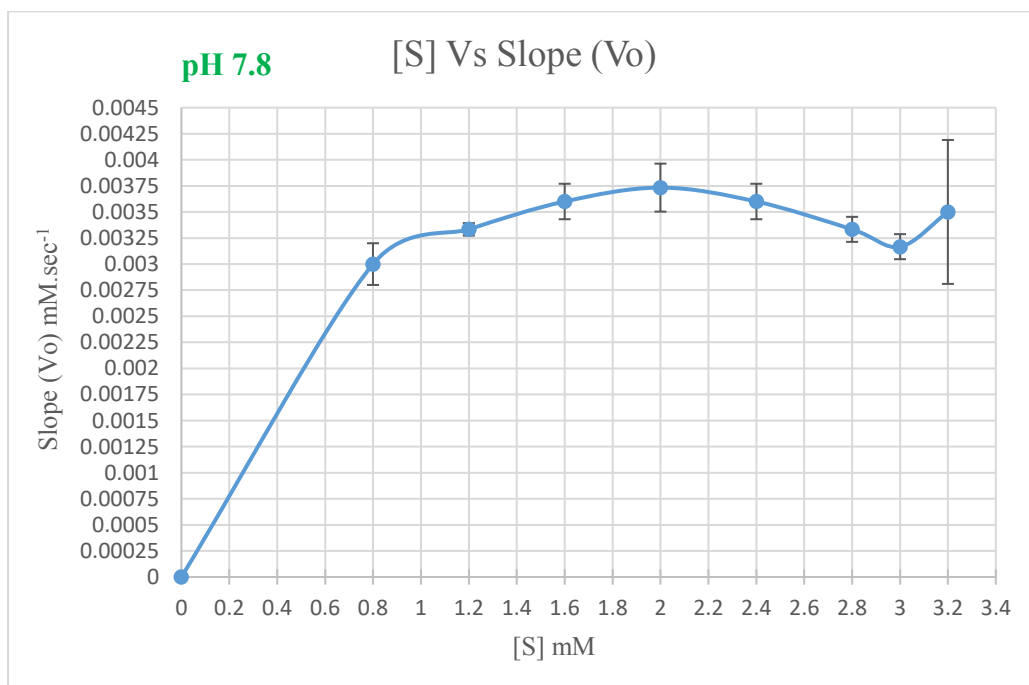


**Figure 3.57: Michaelis-Menten graph using purified ZpPDC at pH 7.8.** Produced from the data in Table 3.21 above using purified ZpPDC in Tris-HCl buffer pH 7.8 with substrate concentration in mM on the x axis and the average rate (slope Vo) for each substrate concentration value in mM.sec<sup>-1</sup> on the y axis along with the addition of error bars.

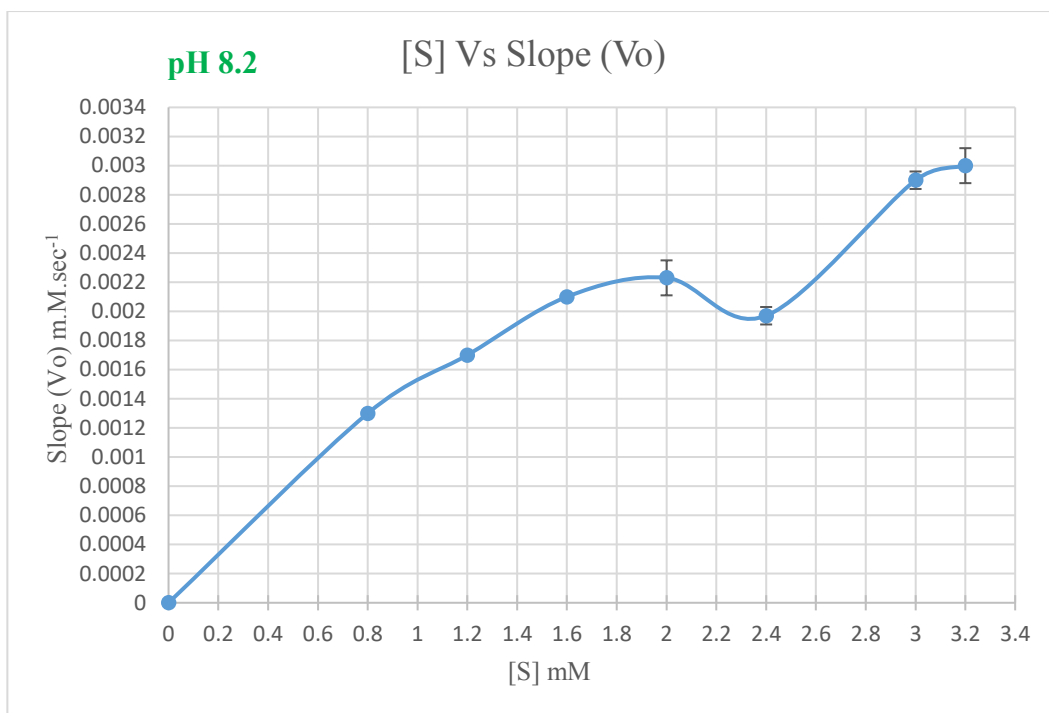


**Figure 3.58: Michaelis-Menten graph using purified ZpPDC at pH 8.2.** Produced from the data in Table 3.21 above using purified ZpPDC in Tris-HCl buffer pH 8.2 with substrate concentration in mM on the x axis and the average rate (slope Vo) for each substrate concentration value in mM.sec<sup>-1</sup> on the y axis along with the addition of error bars.

## Conclusion

Recently, much effort has been placed on the development of alternative sources of energy which are potentially more environmentally friendly and sustainable (Mabee *et al.* 2005) in comparison to fossil fuels such as coal, petroleum or natural gas (Bender 2000; Demirbas 2006). Renewable biofuels tackle the problems associated with dwindling stocks of fossil fuels and increased levels of CO<sub>2</sub> which is contributing to global warming (Naik *et al.* 2010; Shell 2016). Therefore attention has turned to third generation biofuels using metabolically engineered cyanobacteria to produce fuels such as ethanol (Osamu and Carl 1989).

These oxygenic photosynthetic organisms are model organisms which operate in a way similar to plants (Rippka *et al.* 1979). *Synechococcus elongatus* sp. PCC 7942 and *Synechocystis* sp. PCC 6803 are examples of organisms within this group which have been used to study the potential of ethanol production via these so called “cell factories” (Pembroke *et al.* 2017). During metabolism, pyruvate produced during the Calvin cycle can be used in many different ways (Dexter *et al.* 2015) but with the expression of heterologous *pdh* and *adhII* genes from *Zymomonas mobilis* it can be diverted to ethanol production within cyanobacteria.

As discussed earlier, ethanol production was seen in various organisms from *E.coli* in the late 1980s (Ingram *et al.* 1987), *Synechococcus elongatus* 7942 in the late 1990s (Deng and Coleman 1999) and in *Synechocystis* 6803 from 2009 to 2015 (Dexter and Fu 2009; Gao *et al.* 2012; Dexter *et al.* 2015). This was initially achieved using the *Zmpdh* and *adhII* genes (Ingram *et al.* 1987) followed by the use of a *rbcLS* promoter (Deng and Coleman 1999) and strong light driven promoter (Dexter and Fu 2009). US biofuel company Algenol then showed that ethanol levels could be further increased by using the *adh* (*slr1192*) gene native to *Synechocystis* 6803 in lieu of the *adhII* gene from *Zymomonas mobilis* (Dexter *et al.* 2015). Gao *et al.* (2012) also used gene dosage and PHB storage pathway knockouts to further enhance ethanol production (Gao *et al.* 2012). Other approaches which hold potential include the use of small native *Synechocystis* 6803 plasmids for the expression of the heterologous genes in the ethanol pathway (*pdh* and *adh*) (Armshaw *et al.* 2015), diversion of pyruvate via the over expression or

decreased expression of certain enzymes (like PK or PPC) involved in the Calvin cycle (Angermayr *et al.* 2012; Angermayr *et al.* 2014), the use of different promoters (Huang and Lindblad 2013), the fusion of the *pdh* and *adh* genes (Lewicka *et al.* 2014), the increase in carbon uptake by the cell (O’Riordan, personal communication, unpublished data) or the provision of another *adh* gene to deal with increased amounts of acetaldehyde (Liu *et al.* 2005). It may be useful in the future to consider using one of these methods with the *Zppdc* in order to investigate if merging a *pdh* which is reported to have a lower  $K_m$  (Raj *et al.* 2002) possibly with a different promoter (Huang and Lindblad 2013), providing it with more carbon (O’Riordan, personal communication, unpublished data) or an additional *adh* gene (Liu *et al.* 2005) which could make a difference in the ethanol levels produced.

In this study, the PDC enzyme was focused on by replacing the *pdh* currently in use from *Zymomonas mobilis* with a *pdh* from *Zymobacter palmae* which had a reported lower  $K_m$  (Raj *et al.* 2002) and could potentially improve enzyme kinetics and increase ethanol production if introduced into *Synechocystis* 6803. However, although recombinant constructs using native and codon optimised ZpPDC were diligently made and transformed and recombinant *Synechocystis* 6803 strains were selected, no increase in ethanol levels in comparison to the control strain was observed. This may have been due to many reasons which may include incorrect coupling between the *Zppdc* and *adh* or too much acetaldehyde may have been produced via the enzymatically improved *Zppdc* with the *adh* unable to cope and convert it to ethanol. This instance was previously seen in *Lactococcus lactis* where an increase in acetaldehyde levels by 8 fold in comparison to the control did not result in any increase in the production of ethanol. It was thought that the insertion of an *adh* gene after the *Zppdc* may aid in rectifying the problem (Liu *et al.* 2005). Another possible reason may be negative feedback where the production of ethanol (even at very low levels) may have inhibited the activity of the ZpPDC enzyme. There may also be issues with the environmental pH within *Synechocystis* 6803 transformants as ZmPDC has an optimum pH of 6.0 while the optimum pH for ZpPDC lies between 5.5 and 6.0 (Raj *et al.* 2002) which may imply that they are pH dependent and fail to function properly at the elevated pH within *Synechocystis* 6803 (which has a reported internal cytoplasmic pH of ~ 8.2). Studies have shown

that the  $K_m$  values for both Zm and ZpPDC for pyruvate are much lower at the optimum pH values which are slightly more acidic in comparison to the alkaline environment of *Synechocystis* 6803 (Bringer-Meyer *et al.* 1986; Raj *et al.* 2002; Meyer *et al.* 2010; Buddrus *et al.* 2016). A study by Meyer *et al.* (2010) also showed that the  $K_m$  constant for pyruvate increased at an alkaline pH for ZmPDC (Meyer *et al.* 2010). There may be reason to believe that the ZpPDC could behave in the same way due to a 62/63% identity with ZmPDC (Raj *et al.* 2002; Buddrus *et al.* 2016). To investigate this an activity assay at varied pH values of 6.0, 7.8 and 8.2 was carried out with engineered strains of *Synechocystis* 6803 with the ZpPDC. Unfortunately the strains buffered back to the pH of their preferred environment (~pH 8.0) and so it was decided to use purified ZpPDC instead which would also be used for some characterisation studies. Unfortunately, testing the activity of the purified ZpPDC at different pH values did not shed any further light on the hypothesis possibly due to the reasons mentioned above in Section 3.11.2. There may also be other functional reasons for incompatibility of the ZpPDC when expressed such as improper folding, modifications needed for ThDp cofactor use or some other heterologous recombinant protein incompatibility. Although somewhat disappointing, future work might focus on resolving these incompatibilities.

## Bibliography

- Agilent Technologies Inc. (2015) *pET System Vectors and Hosts*, California: Agilent Technologies Inc., available: <https://www.agilent.com/cs/library/usermanuals/Public/211521.pdf> [accessed 20 Nov 2016].
- Algar, E.M. and Scopes, R.K. (1985) 'Studies on cell-free metabolism: ethanol production by extracts of *Zymomonas mobilis*', *Journal of Biotechnology*, 2(5), 275-287.
- Angermayr, S.A., Hellingwerf, K.J., Lindblad, P. and de Mattos, M.J.T. (2009) 'Energy biotechnology with cyanobacteria', *Current opinion in biotechnology*, 20(3), 257-263.
- Angermayr, S.A., Paszota, M. and Hellingwerf, K.J. (2012) 'Engineering a cyanobacterial cell factory for production of lactic acid', *Appl Environ Microbiol*, 78(19), 7098-106, available: <http://dx.doi.org/10.1128/AEM.01587-12>.
- Angermayr, S.A., Van der Woude, A.D., Correddu, D., Vreugdenhil, A., Verrone, V. and Hellingwerf, K.J. (2014) 'Exploring metabolic engineering design principles for the photosynthetic production of lactic acid by *Synechocystis* sp. PCC 6803', *Biotechnology for biofuels*, 7(1), 1.
- Armshaw, P., Carey, D., Sheahan, C. and Pembroke, J.T. (2015) 'Utilising the native plasmid, pCA2. 4, from the cyanobacterium *Synechocystis* sp. strain PCC 6803 as a cloning site for enhanced product production', *Biotechnology for biofuels*, 8(1), 1.
- Armshaw, P. and Pembroke, J.T. (2013) 'Generation and analysis of an ICE R391 deletion library identifies genes involved in the element encoded UV-inducible cell-sensitising function', *FEMS Microbiology letters*, 342(1), 45-53.
- Atsumi, S., Higashide, W. and Liao, J.C. (2009) 'Direct photosynthetic recycling of carbon dioxide to isobutyraldehyde', *Nature biotechnology*, 27(12), 1177-1180.
- Balat, M. (2006) 'Sustainable transportation fuels from biomass materials', *Energy Education Science and Technology*, 17(1/2), 83.

- Bartsevich, V.V. and Pakrasi, H. (1995) 'Molecular identification of an ABC transporter complex for manganese: analysis of a cyanobacterial mutant strain impaired in the photosynthetic oxygen evolution process', *The EMBO journal*, 14(9), 1845.
- Battchikova, N., Vainonen, J.P., Vorontsova, N., Keränen, M., Carmel, D. and Aro, E.-M. (2010) 'Dynamic changes in the proteome of *Synechocystis* 6803 in response to CO<sub>2</sub> limitation revealed by quantitative proteomics', *Journal of proteome research*, 9(11), 5896-5912.
- Baykal, A.T., Kakalis, L. and Jordan, F. (2006) 'Electronic and nuclear magnetic resonance spectroscopic features of the 1', 4'-iminopyrimidine tautomeric form of thiamin diphosphate, a novel intermediate on enzymes requiring this coenzyme', *Biochemistry*, 45(24), 7522-7528.
- Beckmann, J., Lehr, F., Finazzi, G., Hankamer, B., Posten, C., Wobbe, L. and Kruse, O. (2009) 'Improvement of light to biomass conversion by de-regulation of light-harvesting protein translation in *Chlamydomonas reinhardtii*', *Journal of Biotechnology*, 142(1), 70-77.
- Bender, M.H. (2000) 'Potential conservation of biomass in the production of synthetic organics', *Resources, Conservation and Recycling*, 30(1), 49-58.
- Berla, B.M. and Pakrasi, H.B. (2012) 'Upregulation of plasmid genes during stationary phase in *Synechocystis* sp. strain PCC 6803, a cyanobacterium', *Applied and Environmental Microbiology*, 78(15), 5448-5451.
- Bio-Rad (2016) *Hand Casting Polyacrylamide Gels*, available: <http://www.bio-rad.com/en-uk/applications-technologies/hand-casting-polyacrylamide-gels> [accessed 15 Nov 2016].
- Boiteux, A. and Hess, B. (1970) 'Allosteric properties of yeast pyruvate decarboxylase', *Febs Letters*, 9(5), 293-296.
- Borirak, O., de Koning, L.J., van der Woude, A.D., Hoefsloot, H.C.J., Dekker, H.L., Roseboom, W., de Koster, C.G. and Hellingwerf, K.J. (2015) 'Quantitative proteomics analysis of an ethanol- and a lactate-producing mutant strain of *Synechocystis* sp. PCC6803', *Biotechnology for biofuels*, 8, 111-111, available: <http://dx.doi.org/10.1186/s13068-015-0294-z>.
- Bräu, B. and Sahm, H. (1986) 'Cloning and expression of the structural gene for pyruvate decarboxylase of *Zymomonas mobilis* in *Escherichia coli*', *Archives of microbiology*, 144(3), 296-301.

- Brennan, L. and Owende, P. (2010) 'Biofuels from microalgae—a review of technologies for production, processing, and extractions of biofuels and co-products', *Renewable and Sustainable Energy Reviews*, 14(2), 557-577.
- Briggs, L.M., Pecoraro, V.L. and McIntosh, L. (1990) 'Copper-induced expression, cloning, and regulatory studies of the plastocyanin gene from the cyanobacterium *Synechocystis* sp. PCC 6803', *Plant molecular biology*, 15(4), 633-642.
- Bringer-Meyer, S. (1988) 'Acetoin and phenylacetylcarbinol formation by the pyruvate decarboxyase of *Zymomonas mobilis* and *Saccharomyces carlsbergensis*', *Biocatalysis*, 1, 321-331.
- Bringer-Meyer, S., Schimz, K.-L. and Sahm, H. (1986) 'Pyruvate decarboxylase from *Zymomonas mobilis*. Isolation and partial characterization', *Archives of microbiology*, 146(2), 105-110.
- Bruhn, H., Pohl, M., Grötzinger, J. and Kula, M.R. (1995) 'The replacement of Trp392 by alanine influences the decarboxylase/carboligase activity and stability of pyruvate decarboxylase from *Zymomonas mobilis*', *European Journal of Biochemistry*, 234(2), 650-655.
- Buddrus, L., Andrews, E.S., Leak, D.J., Danson, M.J., Arcus, V.L. and Crennell, S.J. (2016) 'Crystal structure of pyruvate decarboxylase from *Zymobacter palmae*', *Acta Crystallographica Section F: Structural Biology Communications*, 72(9), 700-706.
- Budny, D. and Sotero, P. (2007) 'The global dynamics of biofuels', *Brazil Institute Special Report*, 4(3), 8.
- Cao, Y.-X., Xiao, W.-H., Liu, D., Zhang, J.-L., Ding, M.-Z. and Yuan, Y.-J. (2015) 'Biosynthesis of odd-chain fatty alcohols in *Escherichia coli*', *Metabolic engineering*, 29, 113-123.
- Chisti, Y. (2007) 'Biodiesel from microalgae', *Biotechnology advances*, 25(3), 294-306.
- Ciriacy, M. (1975) 'Genetics of alcohol dehydrogenase in *Saccharomyces cerevisiae*: I. Isolation and genetic analysis of adh mutants', *Mutation Research/Fundamental and Molecular Mechanisms of Mutagenesis*, 29(3), 315-325.
- Clontech Laboratories Inc. (2014) *In-Fusion HD Cloning Kit User Manual* California: Clontech Laboratories Inc., available:

[http://www.clontech.com/FR/Products/Cloning\\_and\\_Compentent\\_Cells/Cloning\\_Resources/Cloning\\_Resource\\_Portal?gclid=ClrBg7Kz9tACFeW97QodRJwLgA](http://www.clontech.com/FR/Products/Cloning_and_Compentent_Cells/Cloning_Resources/Cloning_Resource_Portal?gclid=ClrBg7Kz9tACFeW97QodRJwLgA) [accessed 15 Nov 2016].

Collier, J.L. and Grossman, A. (1992) 'Chlorosis induced by nutrient deprivation in *Synechococcus* sp. strain PCC 7942: not all bleaching is the same', *Journal of Bacteriology*, 174(14), 4718-4726.

Conway, T., Osman, Y.A., Konnan, J.I., Hoffmann, E.M. and Ingram, L.O. (1987) 'Promoter and nucleotide sequences of the *Zymomonas mobilis* pyruvate decarboxylase', *Journal of Bacteriology*, 169(3), 949-954.

Conway, T., Sewell, G., Osman, Y. and Ingram, L. (1987) 'Cloning and sequencing of the alcohol dehydrogenase II gene from *Zymomonas mobilis*', *Journal of Bacteriology*, 169(6), 2591-2597.

Daley, S.M., Kappell, A.D., Carrick, M.J. and Burnap, R.L. (2012) 'Regulation of the cyanobacterial CO<sub>2</sub>-concentrating mechanism involves internal sensing of NADP<sup>+</sup> and  $\alpha$ -ketogutarate levels by transcription factor CcmR', *PloS one*, 7(7), e41286.

Dehring, U., Kramer, D. and Ziegler, K., Algenol Biofuels Inc (2012) *Selection of ADH in genetically modified cyanobacteria for the production of ethanol* US8163516B2.

Demirbas, M.F. (2006) 'Current technologies for biomass conversion into chemicals and fuels', *Energy Sources, Part A: Recovery, Utilization, and Environmental Effects*, 28(13), 1181-1188.

Deng, M.D. and Coleman, J.R. (1999) 'Ethanol synthesis by genetic engineering in cyanobacteria', *Applied and Environmental Microbiology*, 65(2), 523-528.

Dexter, J., Armshaw, P., Sheahan, C. and Pembroke, J. (2015) 'The state of autotrophic ethanol production in Cyanobacteria', *Journal of Applied Microbiology*, 119(1), 11-24.

Dexter, J. and Fu, P. (2009) 'Metabolic engineering of cyanobacteria for ethanol production', *Energy & Environmental Science*, 2(8), 857-864, available: <http://dx.doi.org/10.1039/B811937F>.

Diefenbach, R.J. and Duggleby, R.G. (1991) 'Pyruvate decarboxylase from *Zymomonas mobilis*. Structure and re-activation of apoenzyme by the cofactors thiamin diphosphate and magnesium ion', *Biochemical Journal*, 276(2), 439-445.

- Dien, B.S., Nichols, N.N., O'bryan, P.J. and Bothast, R.J. (2000) 'Development of new ethanologenic *Escherichia coli* strains for fermentation of lignocellulosic biomass', *Applied Biochemistry and Biotechnology*, 84(1), 181-196.
- Dobritzsch, D., Konig, S., Schneider, G. and Lu, G.G. (1998) 'High resolution crystal structure of pyruvate decarboxylase from *Zymomonas mobilis* - Implications for substrate activation in pyruvate decarboxylases', *Journal of Biological Chemistry*, 273(32), 20196-20204, available: <http://dx.doi.org/10.1074/jbc.273.32.20196>.
- Ducat, D.C., Way, J.C. and Silver, P.A. (2011) 'Engineering cyanobacteria to generate high-value products', *Trends in biotechnology*, 29(2), 95-103.
- Dyda, F., Furey, W., Swaminathan, S., Sax, M., Farrenkopf, B. and Jordan, F. (1993) 'Catalytic centers in the thiamin diphosphate dependent enzyme pyruvate decarboxylase at 2.4- Å resolution', *Biochemistry*, 32(24), 6165-6170.
- Englund, E., Andersen-Ranberg, J., Miao, R., Hamberger, B.r. and Lindberg, P. (2015) 'Metabolic engineering of *Synechocystis* sp. PCC 6803 for production of the plant diterpenoid manoyl oxide', *Acs Synthetic Biology*, 4(12), 1270-1278.
- Eriksson, J., Salih, G.F., Ghebramedhin, H. and Jansson, C. (2000) 'Deletion mutagenesis of the 5' psbA2 region in *Synechocystis* 6803: identification of a putative cis element involved in photoregulation', *Molecular Cell Biology Research Communications*, 3(5), 292-298.
- Eurofins Genomics (2016) *Sample Submission Guide:Value Read*, available: [https://www.eurofinsgenomics.eu/media/892645/samplesubmissionguide\\_valuereadtubes\\_update\\_296x105\\_4c.pdf](https://www.eurofinsgenomics.eu/media/892645/samplesubmissionguide_valuereadtubes_update_296x105_4c.pdf) [accessed 10 Dec 2016].
- Finn, R.K., Bringer, S. and Sahm, H. (1984) 'Fermentation of arabinose to ethanol by *Sarcina ventriculi*', *Applied microbiology and biotechnology*, 19(3), 161-166.
- Fu, P.P. and Dexter, J., Algenol Biofuels Canada Inc (2013) *Methods and compositions for ethanol producing cyanobacteria*, US8372613B2, active.
- Fuszard, M.A., Ow, S.Y., Gan, C.S., Noirel, J., Ternan, N.G., McMullan, G., Biggs, C.A., Reardon, K.F. and Wright, P.C. (2013) 'The quantitative proteomic response of *Synechocystis* sp. PCC 6803 to phosphate acclimation', *Aquatic biosystems*, 9(1), 1.

- Gao, Z., Zhao, H., Li, Z., Tan, X. and Lu, X. (2012) 'Photosynthetic production of ethanol from carbon dioxide in genetically engineered cyanobacteria', *Energy & Environmental Science*, 5(12), 9857-9865.
- Gocke, D., Berthold, C.L., Schneider, G. and Pohl, M. (2008) *Holostructure of pyruvate decarboxylase from Acetobacter pasteurianus*, Internal Report, unpublished.
- Gold, R.S., Meagher, M.M., Tong, S., Hutkins, R.W. and Conway, T. (1996) 'Cloning and expression of the *Zymomonas mobilis* "production of ethanol" genes in *Lactobacillus casei*', *Current Microbiology*, 33(4), 256-260.
- Gomez, L.D., Steele-King, C.G. and McQueen-Mason, S.J. (2008) 'Sustainable liquid biofuels from biomass: the writing's on the walls', *New Phytologist*, 178(3), 473-485.
- Griese, M., Lange, C. and Soppa, J. (2011) 'Ploidy in cyanobacteria', *FEMS Microbiology letters*, 323(2), 124-131.
- Hampton Research (2006a) *Index TM Index Fundamentals* California: Hampton Research, available: [https://hamptonresearch.com/documents/product/hr006670\\_2-144\\_fundamentals.pdf](https://hamptonresearch.com/documents/product/hr006670_2-144_fundamentals.pdf) [accessed 29 Oct 2016].
- Hampton Research (2006b) *Index TM User Guide* California: Hampton Research, available: [https://www.hamptonresearch.com/documents/product/hr007379\\_index\\_documents.pdf](https://www.hamptonresearch.com/documents/product/hr007379_index_documents.pdf) [accessed 12 Nov 2016].
- Hearst Seattle Media LLC (2016) *What is feedback inhibition and why is it important in regulating enzyme activity?*, available: <http://education.seattlepi.com/feedback-inhibition-important-regulating-enzyme-activity-3665.html> [accessed 09 Nov 2016].
- Heidorn, T., Camsund, D., Huang, H.-H., Lindberg, P., Oliveira, P., Stensjö, K. and Lindblad, P. (2010) 'Synthetic biology in cyanobacteria engineering and analyzing novel functions', *Methods in enzymology*, 497, 539-579.
- Heyer, H. and Krumbein, W.E. (1991) 'Excretion of fermentation products in dark and anaerobically incubated cyanobacteria', *Archives of microbiology*, 155(3), 284-287.

- Hildenbrand, C., Stock, T., Lange, C., Rother, M. and Soppa, J. (2011) 'Genome copy numbers and gene conversion in methanogenic archaea', *Journal of Bacteriology*, 193(3), 734-743.
- Hoppner, T.C. and Doelle, H.W. (1983) 'Purification and kinetic characteristics of pyruvate decarboxylase and ethanol dehydrogenase from *Zymomonas mobilis* in relation to ethanol production', *European journal of applied microbiology and biotechnology*, 17(3), 152-157.
- Huang, H.-H., Camsund, D., Lindblad, P. and Heidorn, T. (2010) 'Design and characterization of molecular tools for a synthetic biology approach towards developing cyanobacterial biotechnology', *Nucleic acids research*, 38(8), 2577-2593.
- Huang, H.-H. and Lindblad, P. (2013) 'Wide-dynamic-range promoters engineered for cyanobacteria', *Journal of biological engineering*, 7(1), 1.
- Hübner, G., Weidhase, R. and Schellenberger, A. (1978) 'The mechanism of substrate activation of pyruvate decarboxylase: a first approach', *European Journal of Biochemistry*, 92(1), 175-181.
- Ikeuchi, M. and Tabata, S. (2001) '*Synechocystis* sp. PCC 6803—a useful tool in the study of the genetics of cyanobacteria', *Photosynthesis research*, 70(1), 73-83.
- Imamura, S. and Asayama, M. (2009) 'Sigma factors for cyanobacterial transcription', *Gene regulation and systems biology*, 3, 65.
- Imamura, S., Asayama, M. and Shirai, M. (2004) 'In vitro transcription analysis by reconstituted cyanobacterial RNA polymerase: roles of group 1 and 2 sigma factors and a core subunit, RpoC2', *Genes to Cells*, 9(12), 1175-1187.
- Ingram, L.O., Conway, T., Clark, D.P., Sewell, G.W. and Preston, J.F. (1987) 'Genetic engineering of ethanol production in *Escherichia coli*', *Applied and Environmental Microbiology*, 53(10), 2420-2425.
- Ivanikova, N.V., McKay, R.M.L. and Bullerjahn, G.S. (2005) 'Construction and characterization of a cyanobacterial bioreporter capable of assessing nitrate assimilatory capacity in freshwaters', *Limnol. Oceanogr.: Methods*, 3, 86-93.
- Jornvall, H., Persson, B. and Jeffery, J. (1987) 'Characteristics of alcohol/polyol dehydrogenases', *European Journal of Biochemistry*, 167(2), 195-201.

- Kamennaya, N.A., Ahn, S., Park, H., Bartal, R., Sasaki, K.A., Holman, H.-Y. and Jansson, C. (2015) 'Installing extra bicarbonate transporters in the cyanobacterium *Synechocystis* sp. PCC6803 enhances biomass production', *Metabolic engineering*, 29, 76-85.
- Kaneko, T., Nakamura, Y., Sasamoto, S., Watanabe, A., Kohara, M., Matsumoto, M., Shimpo, S., Yamada, M. and Tabata, S. (2003) 'Structural analysis of four large plasmids harboring in a unicellular cyanobacterium, *Synechocystis* sp. PCC 6803', *DNA research*, 10(5), 221-228.
- Kaneko, T., Sato, S., Kotani, H., Tanaka, A., Asamizu, E., Nakamura, Y., Miyajima, N., Hirosawa, M., Sugiura, M. and Sasamoto, S. (1996) 'Sequence analysis of the genome of the unicellular cyanobacterium *Synechocystis* sp. strain PCC6803. II. Sequence determination of the entire genome and assignment of potential protein-coding regions', *DNA research*, 3(3), 109-136.
- KEGG genome (2016) *Synechocystis* sp. PCC 6803, available: [http://www.genome.jp/kegg-bin/show\\_organism?org=syn](http://www.genome.jp/kegg-bin/show_organism?org=syn) [accessed 20 Nov 2016].
- Kern, D., Kern, G., Neef, H., Tittmann, K., Killenberg-Jabs, M., Wikner, C., Schneider, G. and Hübner, G. (1997) 'How thiamine diphosphate is activated in enzymes', *Science*, 275(5296), 67-70.
- Kim, E.-J., Kim, J.-S., Rhee, H.J. and Lee, J.K. (2009) 'Growth arrest of *Synechocystis* sp. PCC6803 by superoxide generated from heterologously expressed *Rhodospirillum rubrum* sphaeroides chlorophyllide a reductase', *Febs Letters*, 583(1), 219-223.
- Kim, H.W., Vannela, R., Zhou, C. and Rittmann, B.E. (2011) 'Nutrient acquisition and limitation for the photoautotrophic growth of *Synechocystis* sp. PCC6803 as a renewable biomass source', *Biotechnology and bioengineering*, 108(2), 277-285.
- Kinoshita, S., Kakizono, T., Kadota, K., Das, K. and Taguchi, H. (1985) 'Purification of two alcohol dehydrogenases from *Zymomonas mobilis* and their properties', *Applied microbiology and biotechnology*, 22(4), 249-254.
- Koenig, S., Svergun, D., Koch, M.H., Huebner, G. and Schellenberger, A. (1992) 'Synchrotron radiation solution x-ray scattering study of the pH-dependence of the quaternary structure of yeast pyruvate decarboxylase', *Biochemistry*, 31(37), 8726-8731.

- Konig, S., Svergun, D., Koch, M.H.J. (1998) *Angle x-ray scattering studies*, Internal Report, unpublished.
- Labarre, J., Chauvat, F. and Thuriaux, P. (1989) 'Insertional mutagenesis by random cloning of antibiotic resistance genes into the genome of the cyanobacterium *Synechocystis* strain PCC 6803', *Journal of Bacteriology*, 171(6), 3449-3457.
- Lagarde, D., Beuf, L. and Vermaas, W. (2000) 'Increased production of zeaxanthin and other pigments by application of genetic engineering techniques to *Synechocystis* sp. strain PCC 6803', *Applied and Environmental Microbiology*, 66(1), 64-72.
- Lan, E.I. and Liao, J.C. (2011) 'Metabolic engineering of cyanobacteria for 1-butanol production from carbon dioxide', *Metabolic engineering*, 13(4), 353-363.
- Laursen, W. (2005) 'Students take a green initiative', *Chemical engineer*, (774-75), 32-34.
- Lewicka, A.J., Lyczakowski, J.J., Blackhurst, G., Pashkuleva, C., Rothschild-Mancinelli, K., Tautvaisas, D., Thornton, H., Villanueva, H., Xiao, W., Slikas, J., Horsfall, L., Elfick, A. and French, C. (2014) 'Fusion of pyruvate decarboxylase and alcohol dehydrogenase increases ethanol production in *Escherichia coli*', *ACS Synth Biol*, 3(12), 976-8, available: <http://dx.doi.org/10.1021/sb500020g>.
- Lindberg, P., Park, S. and Melis, A. (2010) 'Engineering a platform for photosynthetic isoprene production in cyanobacteria, using *Synechocystis* as the model organism', *Metabolic engineering*, 12(1), 70-79.
- Liu, S.Q., Dien, B.S. and Cotta, M.A. (2005) 'Functional expression of bacterial *Zymobacter palmae* pyruvate decarboxylase gene in *Lactococcus lactis*', *Current Microbiology*, 50(6), 324-328, available: <http://dx.doi.org/10.1007/s00284-005-4485-x>.
- Liu, X., Sheng, J. and Curtiss III, R. (2011) 'Fatty acid production in genetically modified cyanobacteria', *Proceedings of the National Academy of Sciences*, 108(17), 6899-6904.
- Lobell, M. and Crout, D.H. (1996) 'Pyruvate decarboxylase: a molecular modeling study of pyruvate decarboxylation and acyloin formation', *Journal of the American Chemical Society*, 118(8), 1867-1873.

- Lowe, S.E. and Zeikus, J.G. (1992) 'Purification and characterisation of pyruvate decarboxylase from *Sarcina ventriculi*', *Journal of General Microbiology*, 138, 803-807.
- Lutstorf, U. and Megnet, R. (1968) 'Multiple forms of alcohol dehydrogenase in *Saccharomyces cerevisiae*: I. Physiological control of ADH-2 and properties of ADH-2 and ADH-4', *Archives of biochemistry and biophysics*, 126(3), 933-944.
- Mabee, W.E., Gregg, D.J. and Saddler, J.N. (2005) 'Assessing the emerging biorefinery sector in Canada', in *Twenty-Sixth Symposium on Biotechnology for Fuels and Chemicals*, Springer, 765-778.
- Mackenzie, K., Eddy, C. and Ingram, L. (1989) 'Modulation of alcohol dehydrogenase isoenzyme levels in *Zymomonas mobilis* by iron and zinc', *Journal of Bacteriology*, 171(2), 1063-1067.
- Marcus, Y., Altman-Gueta, H., Wolff, Y. and Gurevitz, M. (2011) 'Rubisco mutagenesis provides new insight into limitations on photosynthesis and growth in *Synechocystis* PCC6803', *Journal of experimental botany*, err116.
- Mazouni, K., Bulteau, S., Cassier-Chauvat, C. and Chauvat, F. (1998) 'Promoter element spacing controls basal expression and light inducibility of the cyanobacterial *secA* gene', *Molecular microbiology*, 30(5), 1113-1122.
- Meyer, D., Neumann, P., Ficner, R. and Tittmann, K. (2013) 'Observation of a stable carbene at the active site of a thiamin enzyme', *Nature chemical biology*, 9(8), 488-490.
- Meyer, D., Neumann, P., Parthier, C., Friedemann, R., Nemeria, N., Jordan, F. and Tittmann, K. (2010) 'Double duty for a conserved glutamate in pyruvate decarboxylase: evidence of the participation in stereoelectronically controlled decarboxylation and in protonation of the nascent carbanion/enamine intermediate', *Biochemistry*, 49(37), 8197.
- Mikami, K., Kanesaki, Y., Suzuki, I. and Murata, N. (2002) 'The histidine kinase Hik33 perceives osmotic stress and cold stress in *Synechocystis* sp. PCC 6803', *Molecular microbiology*, 46(4), 905-915.
- Minteer, S. (2016) *Alcoholic fuels*, CRC Press.
- Mohamed, A. and Jansson, C. (1989) 'Influence of light on accumulation of photosynthesis-specific transcripts in the cyanobacterium *Synechocystis* 6803', *Plant molecular biology*, 13(6), 693-700.

- Montenecourt, B. (1986) 'Zymomonas, a unique genus of bacteria', *Biotechnology Series[BIOTECHNOL. SER.]*, 1986.
- Moon, J.H., Lee, H.J., Song, J.M., Park, S.Y., Park, M.Y., Park, H.M., Sun, J., Park, J.H. and Kim, J.S. (2011) 'PDB ID: 3OWO/3OX4, Structures of iron-dependent alcohol dehydrogenase 2 from *Zymomonas mobilis* ZM4 with and without NAD cofactor', *Journal of Molecular Biology*, 407, 413-424.
- Mori, T., Binder, B. and Johnson, C.H. (1996) 'Circadian gating of cell division in cyanobacteria growing with average doubling times of less than 24 hours', *Proceedings of the National Academy of Sciences*, 93(19), 10183-10188.
- Muramatsu, M. and Hihara, Y. (2007) 'Coordinated high-light response of genes encoding subunits of photosystem I is achieved by AT-rich upstream sequences in the cyanobacterium *Synechocystis* sp. strain PCC 6803', *Journal of Bacteriology*, 189(7), 2750-2758.
- Murata, N. and Suzuki, I. (2006) 'Exploitation of genomic sequences in a systematic analysis to access how cyanobacteria sense environmental stress', *Journal of experimental botany*, 57(2), 235-247.
- Murphy, K.C. (1998) 'Use of bacteriophage  $\lambda$  recombination functions to promote gene replacement in *Escherichia coli*', *Journal of Bacteriology*, 180(8), 2063-2071.
- Mutsuda, M., Michel, K.-P., Zhang, X., Montgomery, B.L. and Golden, S.S. (2003) 'Biochemical properties of CikA, an unusual phytochrome-like histidine protein kinase that resets the circadian clock in *Synechococcus elongatus* PCC 7942', *Journal of Biological Chemistry*, 278(21), 19102-19110.
- Naik, S., Goud, V.V., Rout, P.K. and Dalai, A.K. (2010) 'Production of first and second generation biofuels: a comprehensive review', *Renewable and Sustainable Energy Reviews*, 14(2), 578-597.
- Nair, U., Ditty, J.L., Min, H. and Golden, S.S. (2002) 'Roles for sigma factors in global circadian regulation of the cyanobacterial genome', *Journal of Bacteriology*, 184(13), 3530-3538.
- Naveena, B., Armshaw, P. and Pembroke, J.T. (2015) 'Ultrasonic intensification as a tool for enhanced microbial biofuel yields', *Biotechnology for biofuels*, 8(1), 1.

- Neale, A.D., Scopes, R.K., Kelly, J.M. and Wettenhall, R.E. (1986) 'The two alcohol dehydrogenases of *Zymomonas mobilis*', *European Journal of Biochemistry*, 154(1), 119-124.
- Neale, A.D., Scopes, R.K., Wettenhall, R. and Hoogenraad, N.J. (1987a) 'Pyruvate decarboxylase of *Zymomonas mobilis*: isolation, properties, and genetic expression in *Escherichia coli*', *Journal of Bacteriology*, 169(3), 1024-1028.
- Neale, A.D., Scopes, R.K., Wettenhall, R.E. and Hoogenraad, N.J. (1987b) 'Nucleotide sequence of the pyruvate decarboxylase gene from *Zymomonas mobilis*', *Nucleic acids research*, 15(4), 1753-1761.
- Ng, W.-O., Zentella, R., Wang, Y., Taylor, J.-S.A. and Pakrasi, H.B. (2000) 'PhrA, the major photoreactivating factor in the cyanobacterium *Synechocystis* sp. strain PCC 6803 codes for a cyclobutane-pyrimidine-dimer-specific DNA photolyase', *Archives of microbiology*, 173(5-6), 412-417.
- Nichols, N.N., Dien, B.S. and Bothast, R.J. (2003) 'Engineering lactic acid bacteria with pyruvate decarboxylase and alcohol dehydrogenase genes for ethanol production from *Zymomonas mobilis*', *Journal of Industrial Microbiology and Biotechnology*, 30(5), 315-321.
- Niederholtmeyer, H., Wolfstädter, B.T., Savage, D.F., Silver, P.A. and Way, J.C. (2010) 'Engineering cyanobacteria to synthesize and export hydrophilic products', *Applied and Environmental Microbiology*, 76(11), 3462-3466.
- Nordling, E., Jörnvall, H. and Persson, B. (2002) 'Medium-chain dehydrogenases/reductases (MDR)', *European Journal of Biochemistry*, 269(17), 4267-4276.
- Osamu, K. and Carl, H. (1989) 'Biomass handbook', *Gordon Breach Science Publisher*.
- Osman, Y., Conway, T., Bonetti, S. and Ingram, L. (1987) 'Glycolytic flux in *Zymomonas mobilis*: enzyme and metabolite levels during batch fermentation', *Journal of Bacteriology*, 169(8), 3726-3736.
- Page, L.E., Liberton, M. and Pakrasi, H.B. (2012) 'Reduction of photoautotrophic productivity in the cyanobacterium *Synechocystis* sp. strain PCC 6803 by phycobilisome antenna truncation', *Applied and Environmental Microbiology*, 78(17), 6349-6351.

- Pawluk, A., Scopes, R.K. and Griffiths-Smith, K. (1986) 'Isolation and properties of the glycolytic enzymes from *Zymomonas mobilis*. The five enzymes from glyceraldehyde-3-phosphate dehydrogenase through to pyruvate kinase', *Biochemical Journal*, 238(1), 275-281.
- Peca, L., Kós, P.B., Máté, Z., Farsang, A. and Vass, I. (2008) 'Construction of bioluminescent cyanobacterial reporter strains for detection of nickel, cobalt and zinc', *FEMS Microbiology letters*, 289(2), 258-264.
- Pecoraro, V., Zerulla, K., Lange, C. and Soppa, J. (2011) 'Quantification of ploidy in proteobacteria revealed the existence of monoploid,(mero-) oligoploid and polyploid species', *PloS one*, 6(1), e16392.
- Pei, X.Y., Erixon, K.M., Luisi, B.F. and Leeper, F.J. (2010) 'Structural insights into the prereaction state of pyruvate decarboxylase from *Zymomonas mobilis*', *Biochemistry*, 49(8), 1727-36, available: <http://dx.doi.org/10.1021/bi901864j>.
- Pembroke, J.T., Quinn, L., O' Riordan, H. and Armshaw, P. (2017) 'Ethanol Production in Cyanobacteria: Impact of Omics of the Model Organism *Synechocystis* on Yield Enhancement' in Los, D. A., ed., *Cyanobacteria: Omics and Manipulation*, Norfolk, UK: Caister Academic Press, 200-217.
- Pepper, E.D., Farrell, M.J., Nord, G. and Finkel, S.E. (2010) 'Antiglycation effects of carnosine and other compounds on the long-term survival of *Escherichia coli*', *Applied and Environmental Microbiology*, 76(24), 7925-7930.
- Persson, B., Zigler, J.S. and Jörnvall, H. (1994) 'A Super-Family of Medium-Chain Dehydrogenases/Reductases (MDR)', *European Journal of Biochemistry*, 226(1), 15-22.
- Pierce, J., Carlson, T. and Williams, J. (1989) 'A cyanobacterial mutant requiring the expression of ribulose biphosphate carboxylase from a photosynthetic anaerobe', *Proceedings of the National Academy of Sciences*, 86(15), 5753-5757.
- Pohl, M., Mesch, K., Rodenbrock, A. and Kula, M. (1995) 'Stability investigations on the pyruvate decarboxylases from *Zymomonas mobilis*', *Biotechnology and applied biochemistry*, 22(1), 95-105.
- Price, G.D. (2011) 'Inorganic carbon transporters of the cyanobacterial CO<sub>2</sub> concentrating mechanism', *Photosynthesis research*, 109(1-3), 47-57.

- Price, G.D. and Howitt, S.M. (2010) 'The cyanobacterial bicarbonate transporter BicA: its physiological role and the implications of structural similarities with human SLC26 transporters ', *Biochemistry and Cell Biology*, 89(2), 178-188.
- Promega Corporation (2016) *Wizard SV Gel and PCR Clean-up System Technical Bulletin*, Wisconsin: Promega Corporation, available: <https://worldwide.promega.com/-/media/files/resources/protocols/technical-bulletins/101/wizard-sv-gel-and-pcr-clean-up-system-protocol.pdf> [accessed 15 Dec 2016].
- Qiagen (2013) *QIAprep Miniprep Handbook-Qiagen*, Hilden: Qiagen.
- Qiagen (2016) *Protein Analysis: SDS-PAGE* available: <https://www.qiagen.com/ie/resources/molecular-biology-methods/protein/> [accessed 12 Dec 2016].
- Qiao, J., Wang, J., Chen, L., Tian, X., Huang, S., Ren, X. and Zhang, W. (2012) 'Quantitative iTRAQ LC-MS/MS proteomics reveals metabolic responses to biofuel ethanol in cyanobacterial *Synechocystis* sp. PCC 6803', *Journal of proteome research*, 11(11), 5286-5300.
- R-Biopharm AG (2014) *Ethanol: UV-method for the determination of ethanol in foodstuffs and other materials*, Darmstadt: R-Biopharm AG, available: [http://www.r-biopharm.com/wp-content/uploads/4056/Roche\\_IFU\\_Ethanol\\_EN\\_10176290035\\_2014-06.pdf](http://www.r-biopharm.com/wp-content/uploads/4056/Roche_IFU_Ethanol_EN_10176290035_2014-06.pdf) [accessed 01 Nov 2016].
- Radmer, R.J. (1996) 'Algal diversity and commercial algal products', *Bioscience*, 46(4), 263-270.
- Raj, K.C., Ingram, L.O. and Maupin-Furlow, J.A. (2001) 'Pyruvate decarboxylase: a key enzyme for the oxidative metabolism of lactic acid by *Acetobacter pasteurianus*', *Archives of microbiology*, 176(6), 443-451.
- Raj, K.C., Talarico, L.A., Ingram, L.O. and Maupin-Furlow, J.A. (2002) 'Cloning and Characterization of the *Zymobacter palmae* Pyruvate Decarboxylase Gene (pdc) and Comparison to Bacterial Homologues', *Applied and Environmental Microbiology*, 68(6), 2869-2876, available: <http://dx.doi.org/10.1128/aem.68.6.2869-2876.2002>.
- Ramanan, R., Vinayagamoorthy, N., Sivanesan, S.D., Kannan, K. and Chakrabarti, T. (2012) 'Influence of CO<sub>2</sub> concentration on carbon concentrating mechanisms in cyanobacteria and green algae: a proteomic approach', *Algae*, 27(4), 295-301.

- Reid, M.F. and Fewson, C.A. (1994) 'Molecular characterization of microbial alcohol dehydrogenases', *Critical reviews in microbiology*, 20(1), 13-56.
- Richter, R., Hejazi, M., Kraft, R., Ziegler, K. and Lockau, W. (1999) 'Cyanophycinase, a peptidase degrading the cyanobacterial reserve material multi-L-arginyl-poly-L-aspartic acid (cyanophycin)', *European Journal of Biochemistry*, 263(1), 163-169.
- Rippka, R., Deruelles, J., Waterbury, J.B., Herdman, M. and Stanier, R.Y. (1979) 'Generic assignments, strain histories and properties of pure cultures of cyanobacteria', *Microbiology*, 111(1), 1-61.
- Riveros-Rosas, H., Julián-Sánchez, A., Villalobos-Molina, R., Pardo, J.P. and Piña, E. (2003) 'Diversity, taxonomy and evolution of medium-chain dehydrogenase/reductase superfamily', *European Journal of Biochemistry*, 270(16), 3309-3334.
- Sakai, M., Ogawa, T., Matsuoka, M. and Fukuda, H. (1997) 'Photosynthetic conversion of carbon dioxide to ethylene by the recombinant cyanobacterium, *Synechococcus* sp. PCC 7942, which harbors a gene for the ethylene-forming enzyme of *Pseudomonas syringae*', *Journal of fermentation and bioengineering*, 84(5), 434-443.
- Sanderson, K. (2006) 'US biofuels: A field in ferment', *Nature*, 444(7120), 673-676.
- Schenk, G., Leeper, F.J., England, R., Nixon, P.F. and Duggleby, R.G. (1997) 'The role of His113 and His114 in pyruvate decarboxylase from *Zymomonas mobilis*', *European Journal of Biochemistry*, 248(1), 63-71, available: <http://dx.doi.org/10.1111/j.1432-1033.1997.t01-1-00063.x>.
- Scopes, R. (1983) 'An iron-activated alcohol dehydrogenase', *Febs Letters*, 156(2), 303-306.
- Scrutton, M.C. (1971) 'Chapter XII Assay of Enzymes of CO<sub>2</sub> Metabolism', *Methods in microbiology*, 6, 479-541.
- Shell (2016) *Climate Change and Energy Transitions/Renewable Energy*, available: <http://www.shell.com/sustainability/environment/climate-change.html> [accessed 01 Dec 2016].

- Shi, X.-M., Zhang, X.-W. and Chen, F. (2000) 'Heterotrophic production of biomass and lutein by *Chlorella protothecoides* on various nitrogen sources', *Enzyme and Microbial Technology*, 27(3), 312-318.
- Shimakawa, G., Suzuki, M., Yamamoto, E., Saito, R., Iwamoto, T., Nishi, A. and Miyake, C. (2014) 'Why don't plants have diabetes? Systems for scavenging reactive carbonyls in photosynthetic organisms', *Biochemical Society Transactions*, 42(2), 543-547.
- Shoumskaya, M.A., Paithoonrangsarid, K., Kanesaki, Y., Los, D.A., Zinchenko, V.V., Tanticharoen, M., Suzuki, I. and Murata, N. (2005) 'Identical Hik-Rre systems are involved in perception and transduction of salt signals and hyperosmotic signals but regulate the expression of individual genes to different extents in *Synechocystis*', *Journal of Biological Chemistry*.
- Sigma-Aldrich (2010) *Specification comparison, Tris base*, Missouri: Sigma-Aldrich.
- Sigma-Aldrich (2012) *Safety Data Sheet, beta-Nicotinamide adenine dinucleotide, reduced disodium salt hydrate*, Missouri: Sigma-Aldrich.
- Sigma-Aldrich (2015a) *Safety Data Sheet, Alcohol dehydrogenase from *Saccharomyces cerevisiae**, Missouri: Sigma-Aldrich.
- Sigma-Aldrich (2015b) *Safety Data Sheet, Pyruvate decarboxylase from baker's yeast (*S.cerevisiae*)*, Missouri: Sigma-Aldrich.
- Sigma-Aldrich (2015c) *Safety Data Sheet, Thiamine pyrophosphate*, Missouri: Sigma-Aldrich.
- Sigma-Aldrich (2016) *Product specification, Magnesium chloride hexahydrate*, Missouri: Sigma-Aldrich.
- Source Bioscience (2016) *Sample Requirements and Sample Analysis*, available: <http://www.lifesciences.sourcebioscience.com/genomic-services/sanger-sequencing-service/information/sample-requirements/> [accessed 10 Dec 2016].
- Speight, J.G. (2007) 'Handbook of Alternative Fuel Technologies'.
- Stanier, R., Kunisawa, R., Mandel, M. and Cohen-Bazire, G. (1971) 'Purification and properties of unicellular blue-green algae (order Chroococcales)', *Bacteriological reviews*, 35(2), 171.

- Sun, S., Duggleby, R.G. and Schowen, R.L. (1995) 'Linkage of catalysis and regulation in enzyme action. Carbon isotope effects, solvent isotope effects, and proton inventories for the unregulated pyruvate decarboxylase of *Zymomonas mobilis*', *Journal of the American Chemical Society*, 117(28), 7317-7322.
- Sunda, W.G., Price, N.M. and Morel, F.M. (2005) 'Trace metal ion buffers and their use in culture studies', *Algal culturing techniques*, 35-63.
- Tajima, N., Sato, S., Maruyama, F., Kaneko, T., Sasaki, N.V., Kurokawa, K., Ohta, H., Kanesaki, Y., Yoshikawa, H. and Tabata, S. (2011) 'Genomic structure of the cyanobacterium *Synechocystis* sp. PCC 6803 strain GT-S', *DNA research*, 18(5), 393-399.
- Takahama, K., Matsuoka, M., Nagahama, K. and Ogawa, T. (2003) 'Construction and analysis of a recombinant cyanobacterium expressing a chromosomally inserted gene for an ethylene-forming enzyme at the psbAI locus', *Journal of bioscience and bioengineering*, 95(3), 302-305.
- Takara Bio USA (2016) *In-Fusion Cloning FAQs: How does In-Fusion Cloning work?*, available: [http://www.clontech.com/US/Products/Cloning\\_and\\_Compentent\\_Cells/Cloning\\_Resources/FAQs/In-Fusion\\_Cloning](http://www.clontech.com/US/Products/Cloning_and_Compentent_Cells/Cloning_Resources/FAQs/In-Fusion_Cloning) [accessed 10 Nov 2016].
- Talarico, L.A., Ingram, L.O. and Maupin-Furlow, J.A. (2001) 'Production of the Gram-positive *Sarcina ventriculi* pyruvate decarboxylase in *Escherichia coli*', *Microbiology*, 147(9), 2425-2435.
- Thermo Fisher Scientific (2015) *Western Blot Transfer Methods*, available: <https://www.thermofisher.com/ie/en/home/life-science/protein-biology/protein-biology-learning-center/protein-biology-resource-library/pierce-protein-methods/western-blot-transfer-methods.html> [accessed 14 Oct 2016].
- Thermo Fisher Scientific (2013) *Safety Data Sheet, Sodium pyruvate*, Massachusetts: Thermo Fisher Scientific.
- Thermo Fisher Scientific (2015) *T7 Expression System* available: <https://www.thermofisher.com/ie/en/home/life-science/protein-biology/protein-expression/bacterial-protein-expression/t7-expression-system.html> [accessed 25 Oct 2016].
- Tse, P., Scopes, R.K., Wedd, A.G., Bakshi, E. and Murray, K.S. (1988) 'An iron-activated alcohol dehydrogenase: metal dissociation constants and magnetic

- and spectroscopic properties', *Journal of the American Chemical Society*, 110(4), 1295-1297.
- Ullrich, J. (1982) 'Structure-function relationships in pyruvate decarboxylase of yeast and wheat germ ', *Annals of the New York Academy of Sciences*, 378(1), 287-305.
- US Environmental Protection Agency (2016) *Cyanobacteria/Cyanotoxins*, available: <https://www.epa.gov/nutrient-policy-data/cyanobacteriacyanotoxins> [accessed 15 Oct 2016].
- Van Zyl, L.J., Schubert, W.-D., Tuffin, M.I. and Cowan, D.A. (2014) 'Structure and functional characterization of pyruvate decarboxylase from *Gluconacetobacter diazotrophicus*', *BMC structural biology*, 14(1), 21.
- Varman, A.M., Xiao, Y., Pakrasi, H.B. and Tang, Y.J. (2013a) 'Metabolic engineering of *Synechocystis* sp. strain PCC 6803 for isobutanol production', *Applied and Environmental Microbiology*, 79(3), 908-914.
- Varman, A.M., Yu, Y., You, L. and Tang, Y.J. (2013b) 'Photoautotrophic production of D-lactic acid in an engineered cyanobacterium', *Microbial cell factories*, 12(1), 1.
- Vermaas, W.F. (1998) '[20] Gene modifications and mutation mapping to study the function of photosystem II', *Methods in enzymology*, 297, 293-310.
- Vidal, R., López-Maury, L., Guerrero, M.G. and Florencio, F.J. (2009) 'Characterization of an alcohol dehydrogenase from the Cyanobacterium *Synechocystis* sp. strain PCC 6803 that responds to environmental stress conditions via the Hik34-Rre1 two-component system', *Journal of Bacteriology*, 191(13), 4383-4391.
- Williams, J.G. (1988) '[85] Construction of specific mutations in photosystem II photosynthetic reaction center by genetic engineering methods in *Synechocystis* 6803', *Methods in enzymology*, 167, 766-778.
- Wills, C., Kratochil, P., Londo, D. and Martin, T. (1981) 'Characterization of the two alcohol dehydrogenases of *Zymomonas mobilis*', *Archives of biochemistry and biophysics*, 210(2), 775-785.
- Woods, R.P., Coleman, J.R. and De Deng, M., Algenol Biofuels Canada Inc (2001) *Genetically modified cyanobacteria for the production of ethanol, the constructs and method thereof*, US6306639B1, active.

- Xu, W. and McFadden, B.A. (1997) 'Sequence Analysis of Plasmid pCC5. 2 from Cyanobacterium *Synechocystis* PCC 6803 That Replicates by a Rolling Circle Mechanism', *Plasmid*, 37(2), 95-104.
- Yang, X. and McFadden, B. (1993) 'A small plasmid, pCA2. 4, from the cyanobacterium *Synechocystis* sp. strain PCC 6803 encodes a rep protein and replicates by a rolling circle mechanism', *Journal of Bacteriology*, 175(13), 3981-3991.
- Yang, X. and McFadden, B.A. (1994) 'The complete DNA sequence and replication analysis of the plasmid pCB2. 4 from the cyanobacterium *Synechocystis* PCC 6803', *Plasmid*, 31(2), 131-137.
- Yoshikawa, K., Hirasawa, T., Ogawa, K., Hidaka, Y., Nakajima, T., Furusawa, C. and Shimizu, H. (2013) 'Integrated transcriptomic and metabolomic analysis of the central metabolism of *Synechocystis* sp. PCC 6803 under different trophic conditions', *Biotechnology journal*, 8(5), 571-580.
- Young, J.D., Shastri, A.A., Stephanopoulos, G. and Morgan, J.A. (2011) 'Mapping photoautotrophic metabolism with isotopically nonstationary  $^{13}\text{C}$  flux analysis', *Metabolic engineering*, 13(6), 656-665.
- Yu, Y., You, L., Liu, D., Hollinshead, W., Tang, Y.J. and Zhang, F. (2013) 'Development of *Synechocystis* sp PCC 6803 as a Phototrophic Cell Factory', *Marine Drugs*, 11(8), 2894-2916, available: <http://dx.doi.org/10.3390/md11082894>.
- Zabaniotou, A., Ioannidou, O. and Skoulou, V. (2008) 'Rapeseed residues utilization for energy and 2nd generation biofuels', *Fuel*, 87(8), 1492-1502.
- Zang, X., Liu, B., Liu, S., Arunakumara, K. and Zhang, X. (2007) 'Optimum conditions for transformation of *Synechocystis* sp. PCC 6803', *Journal of microbiology-Seoul*, 45(3), 241.
- Zhang, S., Liu, M., Yan, Y., Zhang, Z. and Jordan, F. (2004) 'C2- $\alpha$ -Lactylthiamin Diphosphate Is an Intermediate on the Pathway of Thiamin Diphosphate-dependent Pyruvate Decarboxylation-Evidence on enzymes and models', *Journal of Biological Chemistry*, 279(52), 54312-54318.

## Appendices

### Appendix I

#### Appendix I A

##### Restriction enzymes + primer design and preparation

Restriction enzymes:

SacII:

5' C C G C G G 3'

3' G G C G C C 5'

NdeI:

5' C A T A T G 3'

3' G T A T A C 5'

NotI:

5' G C G G C C G C 3'

3' C G C C G G C G 5'

Primers were ordered from IDT and reconstituted with DNase/RNase free water to 100 picomole/ $\mu$ l for the main primer stock which was then diluted 1/20 to give working primer stocks at a concentration of 5 picomole/ $\mu$ l unless otherwise stated or recommended. When designing primers, properties such as length, GC content and T<sub>m</sub> temperature were checked using oligo calc, an online oligonucleotide properties calculator.

#### Appendix I B

##### Media details

Specified media for culturing *Zymobacter palmae*:

753 MY broth

100 ml:

1 g yeast extract, 2 g maltose (20% solution made, filter sterilised, 10 ml added for 2% after autoclaving), 0.2 g  $\text{KH}_2\text{PO}_4$ , 0.5 g NaCl.

753 MY agar

As above but with 1.5 g of agar for 100 ml.

Media for culturing *Synechocystis* sp. PCC 6803:

BG-11 liquid media:

For 1 litre:

10 ml 100X BG11

1 ml 1000X Ferric ammonium citrate

1 ml 1000X  $\text{Na}_2\text{CO}_3$

1 ml 1000X  $\text{K}_2\text{HPO}_4$

Filled to 1 litre with distilled water, autoclaved and stored at 4°C. 20 ml of filter sterilised 50X HEPES buffer pH 8.9 was added before use.

**100X BG-11**

1 litre:

149.60 g  $\text{NaNO}_3$

7.49 g  $\text{MgSO}_4 \cdot 7\text{H}_2\text{O}$

3.60 g  $\text{CaCl}_2 \cdot 2\text{H}_2\text{O}$

0.60 g Citric acid (or 0.89 g Na-citrate, dihydrate)

1.12 ml NaEDTA, pH 8.0, 0.25 M

100 ml Trace Minerals

**Trace Minerals**

For 1 litre:

2.86 g  $\text{H}_3\text{BO}_3$

1.81 g  $\text{MnCl}_2 \cdot 4\text{H}_2\text{O}$

0.222 g  $\text{ZnSO}_4 \cdot 7\text{H}_2\text{O}$

0.39 g  $\text{Na}_2\text{MoO}_4 \cdot 2\text{H}_2\text{O}$

0.079 g CuSO<sub>4</sub>.5H<sub>2</sub>O

0.0494 g Co(NO<sub>3</sub>)<sub>2</sub>.6H<sub>2</sub>O

**Ferric ammonium citrate (1000X)**

600 mg per 100 ml H<sub>2</sub>O

**Na<sub>2</sub>CO<sub>3</sub> (1000X)**

2 g Na<sub>2</sub>CO<sub>3</sub> per 100 ml H<sub>2</sub>O

**K<sub>2</sub>HPO<sub>4</sub> (1000X)**

3.05 g K<sub>2</sub>HPO<sub>4</sub> per 100 ml H<sub>2</sub>O

**50X HEPES**

50 g of HEPES was added to 1 litre of distilled water. The pH was adjusted to 8.9 with 5 M NaOH and filter sterilised before use.

**BG-11 agar:**

10 ml of 1M TES/NaOH pH 8.2, 4.7 g of sodium thiosulphate pentahydrate and 15 g of Difco Bacto agar were added to 1 litre of BG-11 liquid media, divided into 300 ml, 300 ml and 400 ml amounts and autoclaved before use.

## **Appendix II**

### **PCR and sequencing primers**

-To amplify the *Zymomonas mobilis pdc* from pUL004 to create pULLQ1:

Forward LQ1: ATATACATATGAGTTATACTGTCGGTACCTATTTAGC

Reverse LQ2:

**6X histidine tag**

TATATGCGGCCGCCTA**GTGGTGATGGTGATG**GAGGAGCTTGTTA  
ACAGGCT

-To linearise pET22b (+) by inverse PCR to create ULLQ2 and ULLQ3:

Forward 262F: CATCATCACCATCACCAC

Reverse 263R: ATGTATATCTCCTTCTTAAAGTTAAAC

-To amplify the native *Zymobacter palmae pdc* for insertion into pET22b (+) to create pULLQ2:

Forward 264F:

GAAGGAGATATACATATGTATAACCGTTGGTATGTACTTGGCAG

Reverse 265 R: GTGATGGTGATGATGCGCTTGTGGTTTTCGAGAGTTGG

-Sequencing primers for inserts in the pET22b (+) vector:

Forward T7F: TAATACGACTCACTATAGGG

Reverse T7R: GCTAGTTATTGCTCAGCGG

-To amplify the codon optimised *Zymobacter palmae pdc* for insertion into pET22b (+) to create pULLQ3:

Forward 04F:

GAAGGAGATATACATATGTATAACCGTTGGTATGTATTTGGCTG

Reverse 04R: GTGATGGTGATGATGTGCCTGGGGCTTCCGGGAATTGG

-To linearise the PSBII vector to create pUL101 and pUL102:

Forward 01F: TAGTTTTTGGGGATCAATTC

Reverse 01R: ATGGTTATAATTCCTTATGTATTTG

-To amplify the native *Zymobacter palmae pdc* for the PSBII vector to create pUL101:

Forward 02F: AGGAATTATAACCATATGTATAACCGTTGGTATGTACTTGG

Reverse 02R: GATCCCCAAAACACTACGCTTGTGGTTTTCGAGAGTTGG

-To amplify the codon optimised *Zymobacter palmae pdc* for the PSBII vector to create pUL102:

Forward 03F: AGGAATTATAACCATATGTATAACCGTTGGTATGTATTTGG

Reverse 03R: GATCCCCAAAACACTATGCCTGGGGCTTCCGGGAATTGG

-Sequencing and screening primers for the ethanol cassette (pPSBII promoter, *pdc*, *slr1192 adh*, *kan*) in the PSBII vector:

Forward P35: CTCTACACAGCCCAGAACTATGG

Reverse P13: CAATTTGCAGATTATTCAGTTGGCAT

Forward P9: GTCAGTTCCAATCTGAACATCGA

-Sequencing primer for the *Zymomonas mobilis*, native and codon optimised *Zymobacter palmae pdc* in PSBAII, pUL004, pUL101 and pUL102:

Reverse 05Rbc: GGAGTTTTCCGTTGGCTTCCAG

-Internal sequencing primer for the *Zymomonas mobilis pdc* in PSBAII, pUL004:  
CAAGCGCATTGTTCAATGACGAAG

-Internal sequencing primer for the native *Zymobacter palmae pdc* in PSBAII, pUL101:

Forward 07Rb: ATCAATAGCCTGCTGCGTGAAGTC

Forward 08Rb: TTCTCGCCCGGCAACGACTCAAG

Reverse 06Rb: GACTGGATCTGACGCGTCATTTTCG

-Internal sequencing primer for the codon optimised *Zymobacter palmae pdc* in PSBAII, pUL102:

Reverse 06Rc: GACTGAATTTGGCGTGTCATCTC

## Appendix III

### Gene and amino acid sequences

#### Appendix III A

##### Gene sequence of *Zymomonas mobilis pdc*: 1707 bps

atgagttatactgtcggtaacctatttagcggagcggctgtccagattggtctcaagcatcacttcgcagtcgcgggcg  
actacaacctcgtccttctgacaacctgctttgaacaaaaacatggagcaggtttattgctgtaacgaactgaactgc  
ggtttcagtcgagaaggttatgctcgtgcaaaaggcgcagcagcagccgtcgttacctacagcgtcggcgttc  
cgcaattgatgctatcggcggcctatgcagaaaacctccggttatcctgatcctccggcgtcctcgaacaacaatgat  
cacgctgctggtcacgtgttcacacgctcttgcaaaaccgactatcactatcagttgaaatggccaagaacatc  
acggccgccgctgaagcgattacaccccggaagaagctccggctaaaatcgatcacgtgataaaactgctcttcgt  
gagaagaagccggtttatctcgaatcgttgcaacattgcttccatgccctgcgccgctcctggaccgcaagcgc  
attgttcaatgacgaagccagcgcgaagcttcttgaatgcagcgggtgaagaaacctgaaattcatcgccaaccg  
cgacaaaattgccgctcctcgtcggcagcaagctgcgcgcagctggtgctgaagaagctgctgcaatttgctgatg  
ctcctggcggcagttgctaccatggctgctgcaaaaagcttctccagaagaaaaccgcattacatcggcact  
catggggtgaagtcagctatccggcggtgaaaagacgatgaaagaagccgatcggttatcgtctggctcctgctc  
ttcaacgactactccaccactggttgacggatattcctgatcctaagaaactggttctcgtgaaccgcttctgctc

cgtaacggcattcgcttccccagcgtccatctgaaagactatctgaccggttggtcagaaaagttccaagaaaacc  
ggtgcattggacttctcaaatccctcaatgcaggtgaactgaagaaagccgctccggctgatccgagtgctccggtg  
gtcaacgcagaaatcggcgtcaggtcgaagctcttctgacccgaacacgacggttattgtgaaaccggtgactc  
ttggttcaatgctcagcgcgatgaagctcccgaacgggtgctcgcgttgaatatgaaatgcagtggggtcacattggtg  
gtccgttctgccgcttccggttatgccgtcgggtcctccggaacgtcgcaacatcctcatggttggtgatggttcttcc  
agctgacggctcaggaagtcgctcagatggttcgctgaaactgccggttatcattcttctgatcaataactatggttac  
accatcgaagttatgatccatgatggtccgtacaacaacatcaagaactgggattatgccggtctgatggaagtgtca  
acggtaacgggtggttatgacagcgggtgctgtaaaaggcctgaaggctaaaaccgggtggcgaactggcagaagctat  
caaggttctctggcaaacaccgacggcccaacctgatcgaatgcttcatcggtcgtgaagactgcactgaagaat  
tggtcaaatggggtgaagcgcgttgctgccccaacagccgtaagcctgtaacaagctcctctag

## Appendix III B

### Amino acid sequence of *Zymomonas mobilis* PDC: 568aas

MSYTVGTYLAERLVQIGLKHHFAVAGDYNLVLLDNLLLKNMEQVYCC  
NELNCGFSAEGYARAKGAAA VVTYSVGALS AFDAIGGAYAENLPVILIS  
GAPNNNDHAAGHVLHHALGKTDYHYQLEMAKNITAAAEAIYTPPEAPA  
KIDHVIKTALREKKPVYLEIACNIASMPCAAPGPASALFNDEASDEASLNA  
AVEETLKFIANRDKVAVLVGSKLRAAGAEAAVKFADALGGAVATMAA  
AKSFFPEENPHYIGTSWGEVSYPGVEKTMKEADAVIALAPVFNDYSTTG  
WTDIPDPKLLVLAEPRSVVVNGIRFPSVHLKDYLTRLAQKVSKKTGALDF  
FKSLNAGELKKAAPADPSAPLVNAEIARQVEALLTPNTTVIAETGDSWFN  
AQRMKLPNGARVEYEMQWGHIGWSVPAAFGYAVGAPERRNILMVG DG  
SFQLTAQEVAQMVR LKLPVII FLINNYGYTIEVMIH DGPYNNIKNWDYA  
GLMEVFNGNGGYDSGAGKGLKAKTGGELAEAIKVALANTDGPTLIECFI  
GREDCTEELVKWGKRVA AANS RKPVNKLL

## Appendix III C

### Gene sequence of *Zymobacter palmae* pdc: 1670 bps

atgtataccggttggtatgtacttggcagaacgcctagcccagatcggcctgaaacaccacttggcgtggccggtgac  
tacaacctggtgttgcttgcagctcctgtgaacaaagacatggagcaggtctactgctgtaacgaacttaactcgcg  
gcttagcggcgaaggttacgctcgtgcacgtggtgcccgcctgcatcgtcacgttcagcgtaggtgctatctctg  
caatgaacgccatcgggtggcgcctatgcagaaaacctgccggtatcctgatctctggctcaccgaacaccaatgac  
tacggcacaggccacatcctgcaccacaccattggtactactgactataactatcagctggaaatggtaaaacacggt  
acctgcgca **cg**tgaagcatcgtttctgccgaagaagcaccggcaaaaatcaccacgtatccgttacggctctac  
gtgaacgcaaaccggcttatctgaaatcgcacgtcgcacgtcgtggcgtgaaatgtgttcgtccggccgatcaat  
agcctgctgctgtaactcgaagttgaccagaccagtgctactgccgctgtagatgccgccgtagaatggctgcagg  
accgccagaacgtcgtcatgctggtcggtagcaaacgcgtgccgctgcccgtgaaaaacaggctgttgccctagc  
ggaccgctgggctgctgctgacgatcgtgctgccc **gaa**aaagcttcttcccggaagatcatccgaacttccc  
ggcctgactggggtgaagtcagctccgaaggtgcacaggaactggtgaaaacgccgatccatcctgtgtctgg  
caccggtattcaacgactatgctaccgttggtggaactcctggccgaaaggcgacaatgcatggtcatggacacc  
gaccgcgtcacttctgcaggacagtccttgaaggtctgctttagacaccttcccgcagcactggctgagaaagc  
acctctcggccgcaacgactcaaggcactcaagcaccggtactgggtattgaggccgcagagcccaatgcacc

gctgaccaatgacgaaatgacgcgtcagatccagtcgctgatcacttccgacactactctgacagcagaaacaggtg  
actcttggttcaacgcttctcgcattcggcattcctggcggtgctcgtcgaactggaaatgcaatggggcctatcgg  
ttggtcctgacattctgcatcggtaacgccgttggttctccggagcgtcgcacatcatgatggtcggtgatggctttt  
ccagctgactgctcaagaagttgctcagatgatccgctatgaaatcccggtcacatcttctgatcaacaaccgcggt  
tacgtcatgaaatcgctatccatgacggccttacaactacatcaaaaactggaactacgtggcctgatcagctct  
tcaatgacgaagatggatggcctgggtctgaaagcttactggcagaactagaaggcgctatcaagaaagca  
ctcgacaatcgctcgggtccgacgctgatcgaatgtaacatcgctcaggacgactgcactgaaacctgattgcttgg  
ggtaaactgtagcagctaccaactctcgcaaccacaagcgtaa

The regions highlighted in **red** above are incorrect.

CGT at base pairs 400-402 should be GCT

GAA at base pairs 733-735 should be GCA

## Appendix III D

### Amino acid sequence of *Zymobacter palmae* PDC: 556aas

MYTVGMYLAERLAQIGLKHFFAVAGDYNLVLLDQLLLNKDMEQVYCC  
NELNCGFSAEGYARARGAAAAIVTFSVGAISAMNAIGGAYAENLPVILISG  
SPNTNDYGTGHILHHTIGTTDYNQLEMVKHVTCAR**ES**IVSAEEAPAKID  
HVIRTUALRERKPAYLEIACNVAGAECV R**P**GPIN**S**LLRELEVDQTSVTA**A**V  
DAAVEWLQDRQNVVMLVGSKLRAAAAEKQ**A**VALADRLGCAVTIMAA**E**  
KGFFPEDHPNFRGLYWGEVSSEGAQELVENADAILCLAPVFNDYATVGW  
NSWPKGDNMVMDTDRVTFAGQSFEGLSLSTFAAALAEKAPSRPATTQG  
TQAPVLGIEAAEPNAPLTNDEMTRQIQSLITSDTTLTAETGDSWFNASRMP  
IPGGARVELEMQWGHIGWSVPSAFGNAV**G**SPERRHIMMVGDGSFQLTAQ  
EVAQMIRYEIPVIIFLINNRGYVIEIAIHDGPYNYIKNWN**Y**AGLIDVFND**E**D  
GHGLGLKASTGAELEGAIKKALDNRRGPTLIECNIAQDDCTETLIAWGKR  
VAATNSRKPQA

The regions highlighted in **green** above are incorrect.

R arginine at position 134 should be A alanine due to the change in the gene sequence above.

E glutamic acid at position 245 should also be A alanine due to the change in the gene sequence above.

## Appendix III E

**Codon optimised gene sequence of *Zymobacter palmae* *pdc* for *Synechocystis* sp. PCC 6803: 1670 bps**

ATGTATACCGTTGGTATGTATTTGGCTGAACGGCTCGCTCAGATTGGC  
CTAAGCATCATTTTGCTGTGGCCGGTGATTATAACTTGGTGCTATTGGA  
TCAACTGTTGTTAAACAAAGATATGGAGCAAGTGTACTGTTGTAACGA  
GTAAATTGTGGTTTTTCCGCTGAGGGTTATGCCCGGGCCCGTGGAGC  
CGCCGCCGCTATTGTGACTTTCAGCGTCGGAGCAATTTCCGCTATGAA  
TGCCATCGGTGGTGCATACGCAGAAAACCTCCCGGTAATCCTAATTAG  
CGGCTCCCCAAATACGAACGACTATGGTACCGGGCACATTTTACATCA  
TACTATTGGAACCACTGACTATAATTATCAATTGGAAATGGTGAAACA  
TGTTACCTGTGCCCGTGAGAGCATTGTGTCCGCCGAAGAAGCTCCCGC  
CAAGATCGATCACGTCATCCGGACCGCCCTGCGCGAACGGAAACCCG  
CCTACTTGGAATCGCCTGCAACGTGGCAGGGGCAGAGTGTGTGCGCC  
CCGGCCCCATCAATAGTTTATTGCGGGAAGTGGAAAGTGGATCAAACGT  
CTGTCACCGCCGCCGTTGATGCCGCTGTTGAATGGCTACAGGATCGGC  
AAAATGTGGTAATGTTAGTGGGCAGCAAGCTACGCGCTGCGGCCGCT  
GAGAAACAAGCCGTCGCCTTAGCTGATCGCCTGGGATGTGCGGTAACT  
ATCATGGCCGCTGAAAAAGGCTTTTTTCCCGAAGACCATCCTAACTTT  
CGGGGGTTGTATTGGGGCGAAGTTTCTAGCGAAGGTGCCCAGGAACT  
GGTCGAAAATGCAGACGCGATTTTGTGCCTCGCCCCGTTTTCAACGA  
TTACGCGACCGTGGGCTGGAATAGCTGGCCCAAAGGAGATAACGTGA  
TGGTTATGGATACCGATCGAGTGACCTTTGCCGGACAATCCTTTGAAG  
GGTTGTCCTTGTCTACCTTTGCGGCCGCCCTAGCTGAAAAAGCCCCCT  
CCCGCCCCGCAACCACGCAAGGCACCCAAGCCCCAGTGTGGGTATTG  
AGGCTGCGGAACCTAATGCTCCCTAACGAATGATGAGATGACACGCC  
AAATTCAGTCTTTAATTACTAGTGACACCACGTTGACAGCCGAAACCG  
GAGATTCCTGGTTCAACGCCTCTCGTATGCCAATCCCTGGGGGGGCTC  
GTGTAGAACTAGAAATGCAATGGGGCCACATCGGCTGGAGCGTACCG  
AGCGCGTTTGGCAACGCCGTTGGCTCTCCCGAACGGCGTCACATTATG  
ATGGTTGGTGACGGGAGCTTTCAACTAACCGCGCAAGAAGTTGCCAG  
ATGATCCGCTATGAAATTCCTGTTATTATTTTTTTGATCAATAATCGCG  
GATATGTGATTGAGATCGCAATCCACGATGGGCCCTATAATTATATTA  
AAAATTGGAATTACGCCGGGCTAATTGATGTCTTTAATGATGAAGACG  
GACACGGGCTAGGTTTGAAGGCTTCCACCGGTGCCGAATTAGAAGGC  
GCCATTA AAAAAGGCATTGGATAATCGTCGAGGGCCTACCTTGATCGAA  
TGTAACATTGCACAAGATGATTGTACAGAAACACTAATTGCCTGGGGT  
AAACGTGTAGCTGCCACCAATTC CGGAAGCCCCAGGCATGA

## Appendix IV

### Constructs and Strains

#### Appendix IV A

##### Constructs

pUL004: pUC18 backbone, PSBAII neutral site, pPSBAII light promoter, *Zymomonas mobilis pdc*, slr1192 *Synechocystis* 6803 *adh*, *kanamycin* resistance gene from ICE R391.

pUL030: pUC18 backbone, position of genes *phaAB*, pPSBAII light promoter, *Zymomonas mobilis pdc*, slr1192 *Synechocystis* 6803 *adh*, *zeocin* resistance gene.

pULLQ1: pET22b (+) vector, T7 promoter, *Zymomonas mobilis pdc*, *ampicillin* resistance gene.

pULLQ2: pET22b (+) vector, T7 promoter, native *Zymobacter palmae pdc*, *ampicillin* resistance gene.

pULLQ3: pET22b (+) vector, T7 promoter, codon optimised *Zymobacter palmae pdc*, *ampicillin* resistance gene.

pUL101: pUC18 backbone, PSBAII neutral site, pPSBAII light promoter, native *Zymobacter palmae pdc*, slr1192 *Synechocystis* 6803 *adh*, *kanamycin* resistance gene from ICE R391.

pUL102: pUC18 backbone, PSBAII neutral site, pPSBAII light promoter, codon optimised *Zymobacter palmae pdc*, slr1192 *Synechocystis* 6803 *adh*, *kanamycin* resistance gene from ICE R391.

## **Appendix IV B**

### **Strains**

UL004: pUL004 construct transformed into *Synechocystis* sp. PCC 6803.

UL030: pUL030 construct transformed into strain UL004.

ULLQ1: pULLQ1 construct transformed into BL21 (DE3)\*.

ULLQ2: pULLQ2 construct transformed into BL21 (DE3)\*.

ULLQ3: pULLQ3 construct transformed into BL21 (DE3)\*.

UL070: pUL004 construct transformed into *Synechocystis* sp. PCC 6803 (recreated UL004 to act as a control).

UL071: pUL101 construct transformed into *Synechocystis* sp. PCC 6803.

UL072: pUL102 construct transformed into *Synechocystis* sp. PCC 6803.

